SYNTHESIS AND BIOLOGICAL ACTIVITY OF CHLOROQUINE FERROCENYL CONJUGATES FOR THE TREATMENT OF MALARIA

by

PALOMA SALAS FERNANDEZ

Hons. B. Sc. Pontificia Universidad Catolica del Peru, 2005

A THESIS SUBMITTED IN PARTIAL FULFILLMENT OF
THE REQUIREMENTS FOR THE DEGREE OF

DOCTOR OF PHILOSOPHY

in

THE FACULTY OF GRADUATE STUDIES

(Chemistry)

THE UNIVERSITY OF BRITISH COLUMBIA

(Vancouver)

August 2012

ABSTRACT

Malaria is one of the main causes of mortality and morbidity in the world, endangering billions and affecting millions of people each year. Resistance to common antimalarial drugs has proven to be a challenging problem in malaria control. In an attempt to develop an effective and affordable treatment for malaria, ferrocenyl conjugates incorporating a common antimalarial drug such as chloroquine have been developed.

Based on the previous successes of organometallic derivatives of classical pharmacophores, a series of chloroquine-bridged ferrocenyl derivatives was synthesized. These novel compounds present an unprecedented binding mode of chloroquine to the ferrocene moiety, through the bridging of the two Cp rings. The structural effects of this type of conjugation of chloroquine and ferrocene were studied by NMR spectroscopy and crystal structure determination.

These compounds were studied along with the monosubstituted ferrocenyl analogs and the organic components in order to compare the effects of the substitution on their biological response. The antiplasmodial activity of these sets of compounds was evaluated against the chloroquine-sensitive (D10) and the chloroquine-resistant (D2d and K1) malaria parasite (*Plasmodium falciparum*) strains. Additionally, their biological activity was assessed using a number of *in vitro* assays. Biological and physical properties were correlated to the antimalarial activity.

All compounds were active against the tested parasite strains. The presence of the ferrocene significantly improved the antiplasmodial action, when compared to chloroquine, against the drug-resistant parasite strains. While the chloroquine-bridged ferrocenyl derivatives were in general less active than the monosubstituted ferrocenyl analogs, they

retained activity in the drug-resistant strain to a greater extent. Their particular conformation, compact size and lipophilicity/hydrophilicity balance could be providing them with the structural characteristics needed to escape the mechanisms responsible for resistance.

Additionally, two strategies for drug design were applied: multiple-loading and multifunctional therapy approaches. Ferrocenyl compounds loaded with two molecules of chloroquine and mefloquine were synthesized and characterized. Similarly, ferrocenyl derivatives of chloroquine and mefloquine were further derivatized with a monossacharide molecule. The double-loaded compounds are the first few examples of their kind. The multifunctional conjugates improved the antimalarial action of the ferrocenyl quinoline derivatives.

PREFACE

The majority of the material in Chapter 1 has been submitted for publication: P. F. Salas, C. Herrmann, C. Orvig. *Metalloantimalarials*. Portions of the introductory part of Chapters 2 and 3 are also part of this manuscript. I was responsible for the researching and writing of this review article. Preparation of figures and tables and formatting of the manuscript was done by me and Dr. Herrmann. Editing was performed by me, Dr. Herrmann and Dr. Orvig.

Portions of the content in Chapter 2 pertaining to the antimalarial activity of compounds **4a**, **4b** and **4e** have been published: C. Herrmann, P. F. Salas, B. O. Patrick, C. de Kock, P. J. Smith, M. Adam, C. Orvig. *1,2-Disubstituted Ferrocenyl Carbohydrate Chloroquine Conjugates as Potential Antimalarial Agents*. Dalton Transactions, 2012, 41, 6431-6442.

The majority of the content in Chapters 2 and 3 will be submitted for publication: P. F. Salas, C. Herrmann, J. Cawthray, C. de Kock, P. J. Smith, J. Chen, E. Polishchuk, B. O. Patrick, M. J. Adam, C. Orvig. *Synthesis and Biological Activity Evaluation of Chloroquine-Bridged Ferrocenyl Conjugates as Potential Antimalarial Agents*. I was responsible for the outline and design of this project. I performed all synthetic experiments and structural characterization, with the help of Dr. Herrmann. All solid-state structures were obtained by X-ray diffraction by Dr. Patrick at UBC X-Ray Crystallography services. The *in vitro* antiplasmodial activity assay was performed by Dr. De Kock and Dr. Smith at the University of Cape Town. The *in vitro* antitumor and cytotoxicity assays were performed by me, Dr. Herrmann and Jessie Chen from the Biological Services Laboratory at the UBC. The qualitative evaluation of inhibition of β-hematin formation was performed by Dr. Cawthray with my help. The electron density surface maps and polar surface area values were obtained

by Dr. Cawthray. I was solely responsible for the rest of the assays performed and for the structure-activity correlations established.

The work in Chapter 4 will be submitted for publication: P. F. Salas, C. Herrmann, C. Nimphius, A. Kenkel, M. J. Adam, C. Orvig. *Synthesis and Characterization of Bischloroquine and Bismefloquine Ferrocenyl Derivatives as Potential Antimalarials*. I was responsible for the outline and design of this project. C. Nimphius and A. Kenkel (under my instruction and supervision) performed part of the synthetic experiments. I was responsible for the remaining synthetic work and structural characterization.

The work in Chapter 5 will be submitted for publication: P. F. Salas, C. Herrmann, B. O. Patrick, M. J. Adam, C. Orvig. *Synthesis and Characterization of Ferrocenyl Carbohydrate Conjugates of Chloroquine and Mefloquine.* I was responsible for the outline and design of this project. I performed all synthetic experiments and structural characterization, with the help of Dr. Herrmann. All solid state structures were obtained by X-ray diffraction by Dr. Patrick UBC X-Ray Crystallography services. The *in vitro* antitumor and cytotoxicity assays were performed by me, Dr. Herrmann and Jessie Chen from the Biological Services Laboratory at the UBC.

This work is covered under an international patent: Adam, M. J., Orvig, C., Salas, P., Herrmann, C. *Carbohydrate-metallocene-antimalarial conjugates*. U.S. Pat. Appl. US2010216727, 2010.

TABLE OF CONTENTS

LIST OF TABLES

LIST OF FIGURES

LIST OF SCHEMES

LIST OF ABBREVIATIONS

ACT	artemisinin-based combined therapy
ADME	absorption, distribution, metabolism and excretion
AF	Auranofin
ATP	adenosine-5'-triphosphate
AuCQ	gold(I) chloroquine complex $[Au(PPh_3)(CQ)]PF_6$
AuCyclam	gold(III) cyclam
BAT	ethane-1,2-bis(*N*-l-amino-3-ethylbutyl-3-thiol
CD	chlorproguanil-dapsone
CDC	Centre for Disease Control
Cp	cyclopentadienyl
CQ	chloroquine
CQDP	chloroquine diphosphate
CQS	chloroquine-resistant
CQS	chloroquine-sensitive
DDT	dichlorodiphenyltrichloroethane
DFO	desferrioxamine
DFT	desferrithiocin
DFT	density functional theory
DHFR	dihydrofolate reductase
DHPS	dihydropteroate synthetase
DMSO	dimethylsulfoxide
DNA	deoxyribonucleic acid
ENBPA	ethylenediamine-*N*,*N*'-bis[propyl(2-hydroxy-(*R*)- benzylamino)
ENBPI	ethylenediamine-*N*,*N*'-bis[propyl(2-hydroxy-(*R*)-benzylimino)
EPR	electron paramagnetic resonance
$[Fe\text{-}3\text{-}Eadd]^+$	$[\{1,12\text{-bis}(2\text{-hydroxy-}3\text{-ethyl-benzyl})\text{-}1,5,8,12\text{-tetraazadodecane}\}\text{iron(III)}]^+$
Fe(III)PPIX	ferriprotoporphyrin IX
FQ	ferroquine
FTIR	Fourier transform infrared spectroscopy

G6PD	glucose-6-phosphate dehydrogenase
GR	gluthatione reductase
GSH	gluthatione
GSSG	glutathione disulfide dimer
HAP	histoaspartic protease
HCl	hydrochloric acid
HEPES	4-(2-hydroxyethyl)-1-piperazineethanesulfonic acid
HFQ	hydroxyferroquine
HNFBH	2-hydroxyl-1-naphthylaldehyde *m*-fluorobenzoyl hydrazone
HPOs	3-hydroxypyridin-4-ones
IC_{50}	half maximum inhibitory concentration
ICL670	4-[(3,5-bis-(2-hydroxyphenyl)-1,24)triazol-1-yl]-benzoic acid
IPT	intermittent preventive treatment
IPTp	intermittent preventive treatment for pregnant women
IRS	indoor residual spraying
ITN	insecticide-treated net
LLIN	long-lasting insecticide-treated mosquito net
log *P*	partition coefficient
MA-DFO	*N*-methylanthranilic desferrioxamine
MEP	molecular electrostatic potential
MFA	molecular field analysis
MIC	minimum inhibitory concentration
MPPIX	metalloporphyrins
MQ	mefloquine
MS	mass spectrometry
MSA	molecular shape analysis
NaH	sodium hydride
NaOH	sodium hydroxide
*n*BuLi	*n*-Butyllithium
NMR	nuclear magnetic resonance
PfCRT	*P. falciparum* chloroquine-resistant transporter

PfHT	*P. falciparum* hexose transporter
PfMDR1	*P. falciparum* multi drug resistance gene
Pgh1	P-glycoprotein
PIH	pyridoxal isonicotinoyl hydrazone
pKa	acid dissociation constant
PSA	polar surface area
3D-QSAR	3D quantitative structural-activity relationship
RDT	rapid diagnostic test
RI	resistance index
RNA	ribonucleic acid
ROS	reactive oxygen species
RQ	ruthenoquine
SAR	structure activity relationship
SD	sulfadiazine
SIH	salicylaldehyde isonicotinoyl hydrazone
SP	sulfadoxine/pyrimethamine
TAT	*N*',*N*',*N*'-tris(2-methyl-2-mercaptopropyl)-1,4,7-triazacyclononane
TCTP	translationally controlled tumor protein
TI	therapeutic index
TMEDA	N,N,N',N'-tetramethylethylenediamine
TMPS	tetramesitylporphyrin
TPPS	tetraphenylporphyrin
TrxR	thioredoxin reductase
TSCs	thiosemicarbazones
WHO	World Health Organization
Zn-DFO	zinc desferrioxamine

ACKNOWLEDGEMENTS

I would like to thank my supervisor, Chris Orvig, for giving me the opportunity to work for him in the field of medicinal inorganic chemistry, fulfilling a dream of mine. It has been a privilege; you have been supportive and encouraging throughout this journey not only as an advisor but as a mentor, I will take the lessons learnt with me. I will also like to thank my other supervisor, Dr. Mike Adam, for his support and encouragement over the years. I will also like to thank Dr. Katherine H. Thompson who was the first person I met from the Orvig group and I am sure was responsible for my acceptance into this group.

I was very fortunate to work alongside Dr. Christoph Hermann who taught me possibly everything I know about synthetic chemistry and whose broad knowledge and vision were an invaluable contribution to the project. I am also lucky he is such a wonderful friend. It was my pleasure to supervise the work of two amazingly bright summer students, Corinna Nimphius and Alexander Kenkel, and I thank the three of them.

Thanks to Jessie Chen and Dr. Elena Polishchuk from the Biological Services laboratory at UBC for their guidance and insightful contributions. Thanks to Dr. Peter Smith from the University of Cape Town for allowing us to test our compounds in his laboratory. Thanks to Dr. Brian Patrick for collecting and solving the crystal structures presented in this thesis. Thanks to Elizabeth Varty and Cristina Rodriguez Rodriguez for their help with the figures included in this thesis.

I will like to thank all past and present members of the Orvig group, especially Maria who always believed in me without a shadow of doubt and whose support along this process was at times all I had to keep me going. Thanks Jacquie for your work done on this project, for all the support and for always having your door open. Thanks Yasmin for all these years of

friendship. Thanks to Lisa, Cristina and Katja for your sweet words of encouragement and for your lovely attitude. Thanks to Drs. Lauren Scott and Meryn Bowen for all their help when I was getting settled into grad school and into the lab.

I would like to thank so many friends in the UBC Chemistry Department that I will run short of paper if I were to mention everyone. I would like though to give a special mention to Paul, Sammy, Alberto, Emmanuel, Montse, Brent, Jennifer, Gab, Glen, Stephanie, Alex, Kyle, Insun, Tulin and Danielle. Thanks for making this such an amazing experience.

Finally, I want to thank my parents, Felipe and Friedda, my brother Andres, my sister Paula, my grandmother Laura and all my pets, for their constant love and support that, despite the distance, never fell short and kept me strong at my weakest.

To my parents,
Felipe and Friedda,
who taught me the greatest love of all.

CHAPTER 1 INTRODUCTION

1.1 Malaria

Malaria is an infectious disease that, despite decades of research invested in its prevention and treatment, remains one of the main causes of mortality and morbidity in the world. As reported by the WHO (the World Health Organization) in 2011, 3.3 billion people were at risk of malaria, mainly in the 106 malaria-endemic countries located in the tropical and sub-tropical zones of the globe.[1] Nearly half of the world's population lives under the constant threat of malaria, with the heaviest toll borne by the poorest and most vulnerable.

Malaria is caused by protozoan parasites of the genus *Plasmodium*. From over 300 known species of *Plasmodium*, only five infect humans and cause the distinct disease patterns of malaria: *P. falciparum* (malaria tropica), *P. vivax* (malaria tertiana), *P. malariae* (malaria tertiana), *P. ovale* (malaria quartana) and *P. knowlesi*. *P. falciparum* is the most lethal of these four and considered responsible for approximately 90% of all reported cases. *P. vivax* is not nearly as lethal as is *P. falciparum* but persists for years in the dormant stage in the liver and can cause clinical relapses at regular intervals. Parasites of the species *P. malariae* and *P. ovale* are less common. Generally, the parasites are transmitted by certain species of the female *Anopheles* mosquito. The complex life cycle of the malaria parasite involves different developmental stages taking place in different tissues of both human and mosquito hosts. A simplified schematic representation of the malaria cycle is depicted in Figure 1.1

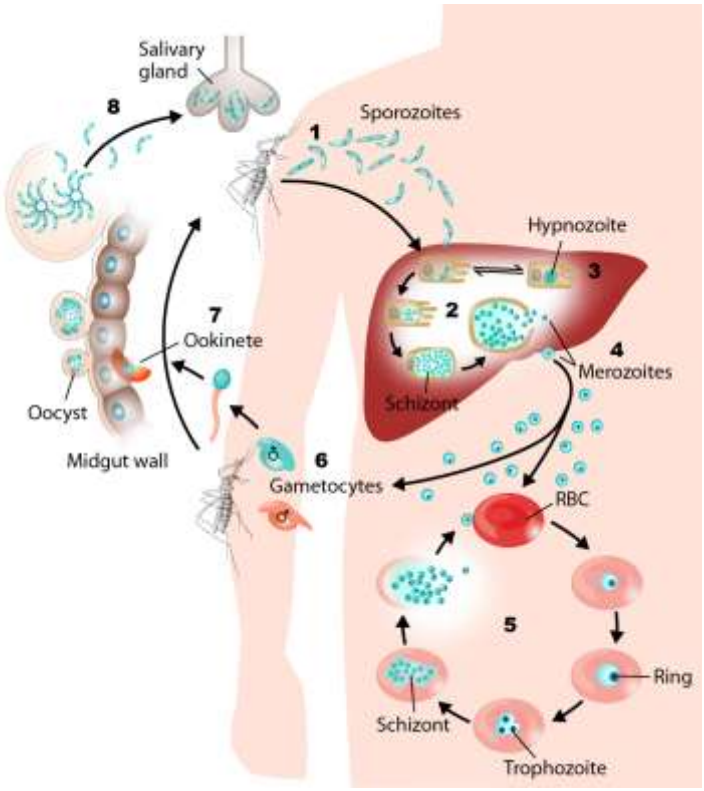

Figure 1.1. Life cycle of malaria cycle infection.

When an infected mosquito stings a human host, it injects saliva containing sporozoites of the *Plasmodium* parasite into the blood stream (**1**). The sporozoites first invade the host liver where they mature and multiply (**2**). In *P. vivax* and *P. ovale*, part of the liver-stage parasites stay dormant in the liver as hypnozoites (**3**). Infected liver cells eventually burst, releasing *Plasmodium* merozoites back into the blood stream, where they invade the red blood cells (**4**). Merozoites reproduce asexually inside the red blood cells (erythrocytes) developing through the stages of rings, trophozoites and schizonts. Each schizont typically divides into merozoites which are released by lysis of the erythrocyte immediately invading new erythrocytes (**5**). Symptoms of uncomplicated malaria such as fever, headaches, diarrhea, vomiting and anaemia develop at this stage. If malaria remains untreated, erythrocytes filled

with mature stages of the parasite can adhere to the walls of capillary veins, causing vascular occlusion and cerebral death (cerebral malaria). Some merozoites develop into male and female gametocytes (**6**). If at this erythrocytic stage an uninfected mosquito bites the host, it will pick up *Plasmodium* gamete cells. The sexual phase of the *Plasmodium* life cycle takes place inside the mosquito through fusion of male and female gametes, producing ookinetes that migrate to the midgut of the insect. The oocyst that is formed will reside and mature in the external membrane of the mosquito midgut (**7**). Division and rupture of the oocysts result in the release of thousands of sporozoites that will travel to the insect salivary glands (**8**), closing the cycle.

Malaria, as a human disease, evolved with mankind through history.[2] From its origin in West and Central Africa more than 10,000 years ago, malaria spread to other areas through the journey of man, following human migrations to the Mediterranean, Mesopotamia, the Indian peninsula, South-East Asia, Northern Europe and the Americas.[2,3] By the end of the 18th century, malaria had spread across North America, and during the 19th century it was present almost all over the globe, resulting in millions succumbing to the disease.[3]

The first record of malaria treatment dates back to the 1600s, when the natives of South America used the bark of the *Cinchona* tree (originally from the high altitudes of South America) to treat the symptoms of malaria.[4] But significant progress in malaria treatment was not achieved until the late 19th century, when physicians Alphonse Laveran and Ronald Ross identified the *Plasmodium* parasite as the agent that causes malaria and the *Anopheles* mosquito as the vector of the disease, discoveries that granted each of them the Nobel Prize in Physiology or Medicine in 1907 and 1902, respectively.[5] Since then, malaria has become one of the best-studied diseases in Western medicine until eclipsed in the mid 20th century.

By the 1950s, as a result of the combined action of the now-banned pesticide DDT (dichlorodiphenyltrichloroethane) on vector control and the effectiveness of antimalarial treatments, malaria was almost eradicated from North America and from almost all of Europe, but persisted in the tropics, especially in Africa where the intensity of the transmission was and still is the highest.[3]

Despite the initial success, the emergence of drug-resistant strains of the parasite, the ban on DDT, the appearance of mosquito resistance to insecticides and climate changes, in addition to other social and political factors, led to a collapse of the eradication campaign.[6] From the early 1970s onward, the situation progressively deteriorated, leading to a 2-3-fold increase in malaria cases globally.[6] By the 1980s, the situation reached endemicity levels in 108 countries.[7,8] Three billion people were at risk of contracting malaria, resulting in an estimated 300-500 million new cases annually.[7,8]A recent study shows that global malaria casualties increased from 995,000 in 1980 to a peak of 1,817,000 in 2004.[9] Malaria also contributes to other health-related issues and to a halt of the economic growth of those countries with the highest burden.[10]

Only in recent years, after decades of neglect, growing international awareness and funding has led to new efforts towards controlling the disease. The 2010 and 2011 World Malaria Reports document the prevention efforts in fighting this disease, showing a measurable public health impact.[1,11] Approximately 600 million people have received vector protection and 11 African countries have cut cases and casualties from malaria by half.[1,11] The annual number of malaria cases has decreased to an estimated 216 million and the number of malaria-endemic countries has been reduced to 106 from 108 in 2004.[1,11] Even though the WHO reports a total number of 655,000 casualties in 2010,[1] a recent study reports

1,238,000 malaria-related casualities in 2010, still representing a decrease of 32% since 2004.[9] In its own efforts to raise awareness and promote research for the cure of this disease, UBC started the Neglected Global Diseases Initiative (NGDI) in 2009.

However, this progress remains fragile, as the malaria parasite proves to be very adaptable to inclement conditions while funding remains short and political resolution and financial commitments diminish. It is estimated that comprehensive coverage of the resources required for malaria control and eradication would cost $5 billion per year over the next few years; however, the budget in 2011 was only $2 billion.[1] The current global economic crisis also represents a threat to the malaria program. With the announcement of the cancellation of funding by the Global Fund (one of the major supporters of this program),[12,13] the sustainable growth of the malaria health plan falls into question. In addition, resistance of the parasite to drugs is a permanent threat that might lead to a resurgence of malaria in already epidemically controlled countries. Therefore, sustained funding and constant research in the treatment and prevention of this disease is necessary to prevent it from bouncing back.

1.2 Prevention, diagnosis and treatment of malaria

Malaria is preventable through methods of malaria vector control.[14] The two most important vector control methods recommended by the WHO are long lasting insecticide-treated mosquito nets (LLINs) and indoor residual spraying (IRS).[15] These interventions work by reducing both human-vector contact and the lifespan of female mosquitoes.[15] Indoor residual spraying (IRS) with WHO-approved chemicals consists of the application of

residual insecticides to the inner surfaces of dwellings where many vector species of the *Anopheles* mosquito tend to rest after ingesting blood. Currently, 12 insecticides belonging to 4 different chemical classes are recommended by the WHO for IRS.[15] Long lasting insecticide-treated mosquito nets (LLINs or ITNs), also known as "bed nets", protect individuals against bites at night when the mosquitoes are most active and their prey is not. ITNs are currently treated with pyrethroids only.[15]

Malaria can also be prevented by drugs (chemoprophylaxis).[14,15] In most endemic areas, pregnant women and infants are at the highest risk of contracting this disease.[16] For this very vulnerable population, the WHO has established the Intermittent Preventive Treatment (IPT) program, consisting of the periodic administration of an antimalarial drug, regardless of the presence of *Plasmodium* parasites.[16]

Malaria prevention for individuals travelling from malaria-risk free zones to malaria-endemic zones is strongly suggested.[17,18] Individual risk assessment through a health care provider is recommended for the traveler.[18] It will likely include basic preventative measures such as the use of insect repellent, long-sleeved clothing, bed nets and the administration of antimalarial drugs.[17] The Centre for Disease Control (CDC) recommends the use of specific medicines for malaria prevention depending on the visited country.[19]

Certainly, the best long-term prevention of this disease would be a malaria vaccine. Several candidates for a vaccine have been investigated in the past decades, but the realization of this has proven elusive. Only recently, some promising malaria vaccine candidates are being developed at the pre-clinical phase,[20] but only one, the GlaxoSmithKline Biologicals' RTS,S malaria vaccine candidate is currently in Phase III clinical trials at 11 sites in Africa.[21] This is the only candidate to have reached this stage.[21]

Unfortunately, the development of many promising vaccine candidates already failed due to difficulties resulting from the complex life cycle of the malaria parasite and the parasite's potent adaptability to generate resistance against an immune response in the host.

Malaria can be treated and cured if diagnosed promptly and accurately. The WHO recommends a parasitological confirmation by microscopy or a rapid diagnostic test (RDT) for all patients with a suspected case of malaria, before commencing treatment, in order to avoid the spread of resistance by administrating medicines to treat non-malaria-related fever.[22] Nevertheless, it has proven a challenge to establish these diagnostic policies in the most affected areas such as the majority of the African countries. In the early 2000s, only 5% of suspected malaria cases reported in Africa were properly confirmed via diagnostic testing and by 2009, this number increased to only 35%.[11]

The standard treatment recommended by the WHO as the first-line therapy for uncomplicated *P. falciparum* malaria worldwide consists of artemisinin-based combined therapy (ACT).[22] Chloroquine (CQ), a well-known antimalarial drug, is only effective to treat *P. falciparum* malaria in Egypt, and in a few countries in Central America and the Middle East.[23] The recommended treatment for *P. vivax* malaria consists of a chloroquine-based therapy where effective, or ACT in areas of resistance to chloroquine.[22] Artemisinin and derivatives (Figure 1.2) are fast acting and highly effective drugs, capable of rapid elimination of malaria parasites. ACT is best described as a combination of artemisinin or an artemisinin-derivative and a second drug with a different mechanism of action to enhance efficacy while diminishing the risk of resistance development.[24] The five ACTs currently recommended for treatment are: Artemether/lumefantrine (*Coartem*® and *Riamet*®), artesunate/amodiaquine (*Winthrop*® and *Coarsucam*®), artesunate/mefloquine (*Artequin*®),

artesunate/sulfadoxine pyrimethamine (*Gen-Art SP*® and *Artecospe*®) and dihydroartemisinin/piperaquine (*Artekin*® and *Eurartesim*®).[24] The choice of the ACT would depend on the efficacy of the combination in the country or area of intended use.[24]

In 2007, the WHO officially banned oral artemisinin monotherapies and recommended them to be replaced by ACTs.[25] Based on previous experience with antimalarial drugs, the WHO concluded that misuse and/or overuse of oral artemisinin-based monotherapies represented a threat to the therapeutic life of ACTs by fostering the spread of resistance to artemisinins.[25] By recommending ACTs as the only alternative for malaria therapy, the WHO hopes to reduce the chances of developing resistance to artemisinin and its derivatives by administering the artemisinin derivative that will exterminate most of the parasites with its potent action first and second by administering the partner drug, that has a longer retention time in the body, terminating the remaining parasites within the host.[25] This would limit the exposure of the parasite to larger doses of artemisinin which would reduce the parasite time to adapt and develop resistance.

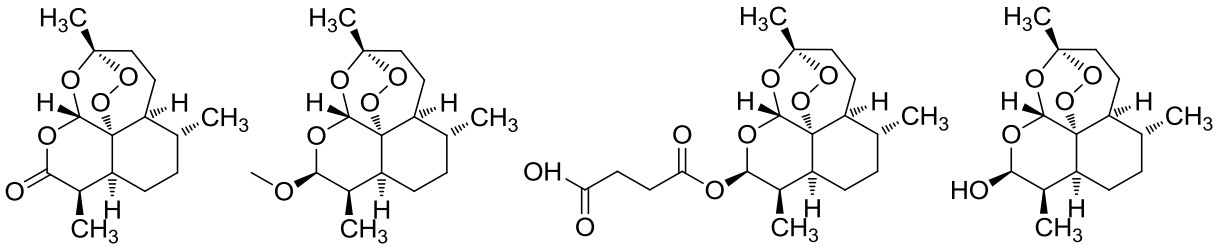

Figure 1.2. Artemisinin and derivatives.

The spread of resistance to antimalarial medicines over the past decades has led to an intensification of efficacy-monitoring to allow for an early detection of resistance.[22] Yet even in their combination, the highly effective artemisinin derivatives and their partner drugs are susceptible to the development of resistance. In 2009, resistance of *P. falciparum* parasites to artemisinins was confirmed at the Cambodia-Thailand border.[26] Suspected resistance to artemisinins has now been identified in Cambodia, Vietnam, Myanmar and Thailand.[27] As of today, the drugs still work but take more time to be effective.[1,24] Measures have been taken to limit the spread of the artemisinin-resistant parasites.[27] But if the current generation of ACTs were to fail, there would be no alternative treatment available on the market, because currently developed drugs in the pipeline are mostly artemisinin-derivatives that would likely present the same type of resistance.

1.3 Traditional antimalarial therapy

Of all factors that have contributed to the recrudescence of malaria in the last 50 years, increasing antimalarial drug resistance is probably the major contributor. This phenomenon, that rapidly depleted the therapies available to fight malaria, has led to intensive research carried out for decades that produced a large pool of antimalarial drugs. Yet, as a consequence of the eradication of malaria from North America and most of Europe and the end of social conflicts in malaria-risk zones, governmental and military research in antimalarial therapy slowed down significantly.[28] Additionally, drug development has also suffered a lack of interest from the pharmaceutical industry in investing in the development

of drugs for disadvantaged markets and from the limited understanding of the complex biochemistry of the malaria parasite that ultimately hinders rational approaches to new drug targets.[29]

Nevertheless, over the course of the last five decades, different types of antimalarial drug families were developed addressing the necessity to attack not one but multiple mechanisms of survival of the parasite (preferably in a parallel manner).[28,29] A well-established method for the development of drug targets is the identification of biologically relevant pathways that are either unique to the parasite or have sufficient differences from the host so that the drugs have little or no effect on the host.[30]

The biological targets of the many families of antimalarial drugs range from cell functions such as the detoxification of toxic metabolites and folate metabolism to the more recently discovered biochemical pathways like fatty acid synthesis or protein farnesylation.[31] Based on their role in parasite growth and survival, the parasite food vacuole, apicoplast and mitochondrion have been identified as the major organelles for drug targeting.[30] Figure 1.3 gives an overview of old and new antimalarial targets and their localization during the different stages of the malaria infection.

At present, a number of antimalarial drugs are available, but high cost, toxicity and, most importantly, slowly originating or already widespread parasitic resistance, limit their use. Thus, it is imperative to continue the development of new treatment options and to improve the current therapeutics if the progress in malaria control is to be sustained. For that purpose it is important to understand the mechanisms through which the drugs act and resistance is generated. In the following sub-sections, the best-known quinoline-based antimalarial drug

class will be described, along with the current knowledge of mechanism of action and parasite resistance.

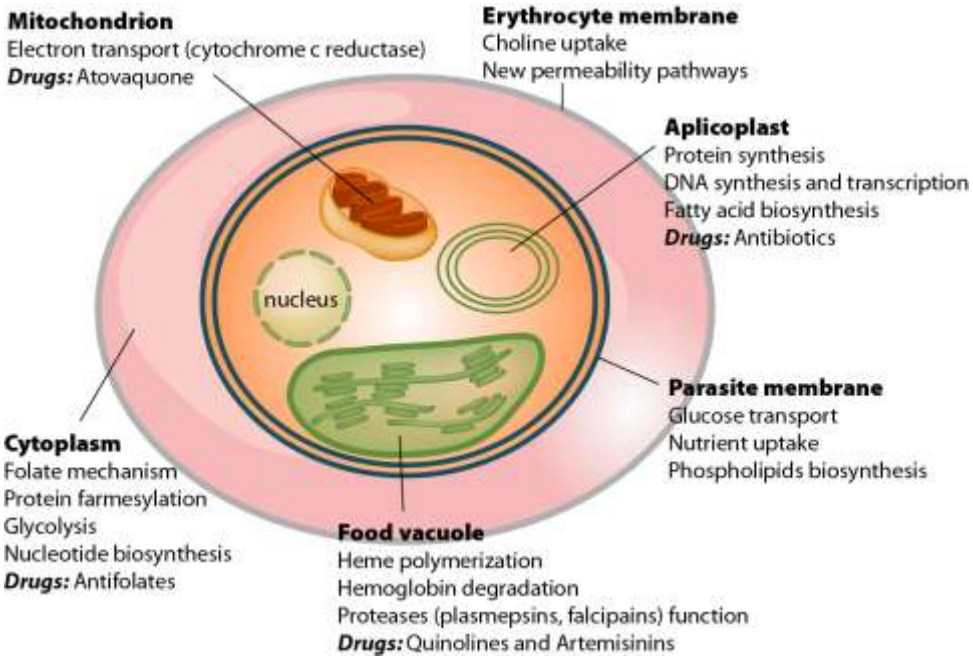

Figure 1.3. Schematic representation of a *P. falciparum* infected red blood cell and the localization of the different drug targets.

1.3.1 Quinoline-containing antimalarial drugs

This family of antimalarials is formed by organic compounds containing a heterocyclic aromatic quinoline group. This is the oldest class of antimalarial drug and it is found in some of the most commonly used antimalarial drugs. Figure 1.4 shows the main quinoline-based antimalarial drugs that are either commercially available or in clinical development.

This class of drugs can be divided into three general sub-groups: (i) 4-amino quinolines including chloroquine (**3**), amodiaquine (**4**), piperaquine (**5**) and pyronaridine (**6**), (ii) quinoline methanols including quinine (**1**), quinidine (**2**) and mefloquine (**7**) and (iii) 8-aminoquinolines that include primaquine (**8**), pamaquine (**9**) and tafenoquine (**10**).[32] Chloroquine (**3**), amodiaquine (**4**) and pyronaridine (**6**) are weak bases that are di-protonated and hydrophilic at neutral pH. Quinine (**1**), quinidine (**2**), mefloquine (**7**) are weaker bases and lipid-soluble at neutral pH.[33]

This family is structurally derived from quinine (**1**), the active ingredient found in the bark of the *Cinchona* tree, used for centuries to treat malaria. In 1820, quinine (**1**) was the first antimalarial drug to be identified and isolated.[28] Despite its relatively low efficacy and tolerability, quinine (**1**) still plays an important role in the treatment of multidrug-resistant malaria. [32,34] Quinidine (**2**), a stereoisomer of **1,** has been used previously for the treatment of cardiac arrhythmia and later was shown to be suitable for the treatment of malaria.[32]

Nevertheless, without a doubt, the most popular representative of this family is chloroquine (**3**). Once known as the most effective, most frequently used and most important antimalarial in the world, **3** now has been rendered inactive in most parts of the world, remaining 100% effective against *P. falciparum* in only two countries in the Americas.[24] Chloroquine (**3**) still remains effective against *P. ovale, P. malariae* and most cases of *P. vivax* malaria. [32,34] It was first synthesized in 1934 but it was not until 1946 that it was made commercially available. Chloroquine (**3**) was used widely after World War II and was the drug of choice and first line of treatment for treating malaria worldwide for about five decades.[28]

This synthetic 4-amino quinoline (**3**) showed high effectiveness against many parasite strains.[32,34] Well-defined pharmaceutical properties of this drug include good tolerance in the patient, better effectiveness and reduced toxicity compared to quinine (**1** - its predecessor), and low cost of production.[32,34,35]

While attempting a global eradication of malaria, in a widespread distribution of the drug, **3** was included even in table salt supplies all over the world, as a prophylactic.[35] Possibly as a result of this medicated salt program, the first cases of chloroquine resistance appeared at the end of the 1950s in East Africa.[33,35] The extensive and quick spread of resistance literally destroyed the therapeutic efficacy of this drug. As chloroquine-resistant parasites started appearing, efforts were initiated to develop new antimalarial drugs. Synthetic derivatives included new antimalarial drugs such as the 4-aminoquinoline amodiaquine (**4**), and the quinoline methanol mefloquine (**7**), among others. Several of these derivatives, designed in the 1970s and 1980s, have subsequently decreased in efficacy due to developing resistances.

Amodiaquine (**4**) was one of the first chloroquine derivatives synthesised to replace chloroquine (**3**) but has been used less extensively.[32] Although there is significant cross-resistance between amodiaquine (**4**) and chloroquine (**3**), many of the chloroquine-resistant strains of *P. falciparum* remain sensitive to this drug and it is still used in ACT as one of the drugs in combination with artesunate (**19**). Piperaquine (**5**) is a bisquinoline antimalarial drug introduced in the 1960s as a replacement for chloroquine.[30] Unfortunately, its extensive usage led to the development of resistance, but due to its good tolerability it is now being used as part of an ACT together with dihydroartemisinin.[30]

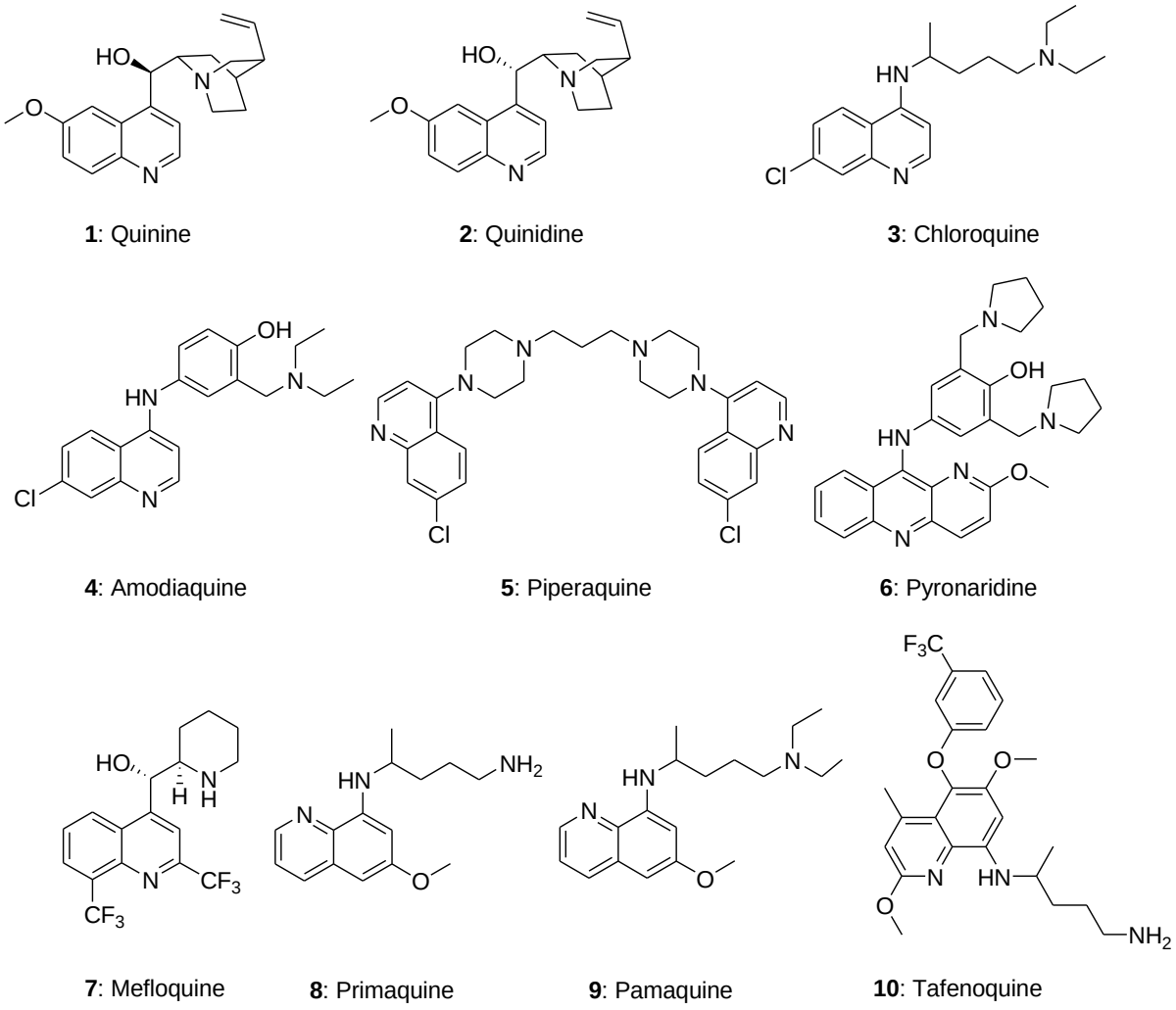

Figure 1.4. Some traditional and novel quinoline-based antimalarial drugs.

Pyronaridine (**6**) is a synthetic 1-aza-9-anilino-acridine and one of the newest members of this family. It is generally active against chloroquine-resistant parasite strains[36,37] and is to be included as an ACT agent in combination with artesunate in the future.[30] Mefloquine (**7**) is a 4-quinoline methanol that was introduced in the mid-1980s to treat patients suffering from chloroquine-resistant malaria. Mefloquine (**7**) is administered orally and used in prophylaxis. In different parts of the world, it is sold under the commercial names of *Lariam*®, *Mefliam*™ or *Mephaquine*®. Used for treatment of uncomplicated multidrug-resistant *P. falciparum*

malaria,[38] mefloquine (**7**) is also one of the drugs administrated in combination with artesunate as one of the recommended ACTs.

Structurally related to the 4-aminoquinolines and quinoline methanols are the 8-aminoquinolines that include primaquine (**8**), pamaquine (**9**) and tafenoquine (**10**). Since they are structurally related to the 4-amino quinolines, they are suspected to have similar targets and mechanism of action; however, the exact mode of action remains unknown.[38,39] 8-Aminoquinolines (**8**-**10**) are extremely effective against the hypnozoite stage of *P. vivax* and *P. ovale* (before the erythrocytic infection), a latent form of liver-stage parasite commonly seen in *P. vivax* infections.[39] Tafenoquine (**10**) is a newer drug that offers improved activity, less toxic side effects and a longer acting time in comparison to primaquine (**8**).[40] In addition, tafenoquine (**10**) is also active against the blood stages in chloroquine- and multidrug-resistant strains of the parasite.[40]

All these quinoline-based drugs offer both advantages and disadvantages either due to reduced activity, as a consequence of the development of resistance, or due to detrimental toxic side effects. Nowadays, the disadvantages are usually compensated for by pairing these drugs and others with artemisinin or its derivatives.

1.3.2 Mode of action of quinoline-containing drugs

Most of the quinoline-containing drugs are active only against the intraerythrocytic stages of the parasite infection and are used to rapidly clear parasites from the blood.[39] While inhabiting the red blood cells, the parasite is surrounded by the single major cytosolic protein in that media, human hemoglobin. During the trophozoite form and at the early stages of the schizonts (Figure 1.1), the parasite ingests 60% to 80% of the hemoglobin present in the red

blood cell along with the cytoplasm by a phagocytosis-like mechanism and transports the hemoglobin into its digestive vacuole.[41,42]

Inside the vacuole, hemoglobin is digested into small peptides, which are subsequently transported to the cytoplasm of the parasite.[41,42] The degradation of hemoglobin occurs in a systematic pathway that involves a series of proteases operating in a highly specific pathway for hemoglobin proteolysis.[43,44,45] Because the parasite has a limited capacity to synthesize amino acids,[44] hemoglobin is thought to be broken down to provide essential amino acids for growth and maturation, making hemoglobin catabolism essential for parasite survival.[41,42] For this reason, targeting hemoglobin metabolism appeared as a strategy for antimalarial drugs.

Proteolysis of hemoglobin leaves free heme as a waste product, the iron in which is rapidly oxidized from Fe^{2+} to Fe^{3+} to give ferriprotoporphyrin IX (PPIX) (presumably present as H_2O–Fe(III)PPIX) (Figure 1.5) as a toxic by-product of this catabolism. Free heme can cause enzyme inhibition, peroxidation of membranes, production of oxygen free radicals, and impaired leukocyte function.[46] Heme oxygenase, used by vertebrates to catabolize heme is absent or occurs in neglectable concentrations within *P. falciparum*.[46]

Plasmodium species have developed different pathways to detoxify heme. The most important and predominant mechanism is the sequestration of heme and its crystallization into an insoluble and chemically-inert crystalline structure called hemozoin or malaria pigment, which accumulates within the parasite food vacuole.[43] The pigment is visible under the microscope (black opaque crystals) in parasite stages that are actively degrading hemoglobin, such as trophozoites, schizonts, and gametocytes.[43]

Hemozoin was formerly considered to be a polymeric chain of heme in the form of β-hematin, a non-covalent coordination complex with the ferric iron of each heme moiety bound to a carboxyl side chain of the adjacent heme.[47] A ground-breaking discovery was the report on the crystal structure of β-hematin that confirmed hemozoin as a crystalline arrangement of dimers of five-coordinated Fe(III)PPIXs linked by reciprocal iron-carboxylate bonds to one of the propionate side chains of each porphyrin macrocycle and the dimers forming chains, linked by hydrogen bonds in the crystal (Figures 1.5 and 1.6).[48,49,50] The process of hemozoin formation is regarded as a non-enzymatic autocatalytic biocrystallization process.[51,52,53]

Despite decades of use of the above-mentioned drugs, the mechanism of action is not completely understood. Many different theories were studied in the past but nowadays it has been widely accepted that the mechanism of action of these drugs involves the interruption of the formation of hemozoin.[39,54] Quinoline-containing drugs such as chloroquine (**3**) and quinine (**1**) accumulate in the acid food vacuoles of the intraerythrocytic stage of the malaria parasite and are selectively trapped inside the food vacuole in an ion-trapping mechanism.[33,39,54] Chloroquine (**3**) can accumulate to a large extent inside the vacuole, with a gradient ranging from nanomolar concentrations on the outside to millimolar concentrations inside the digestive vacuole of the intra erythrocytic trophozoite.[55]

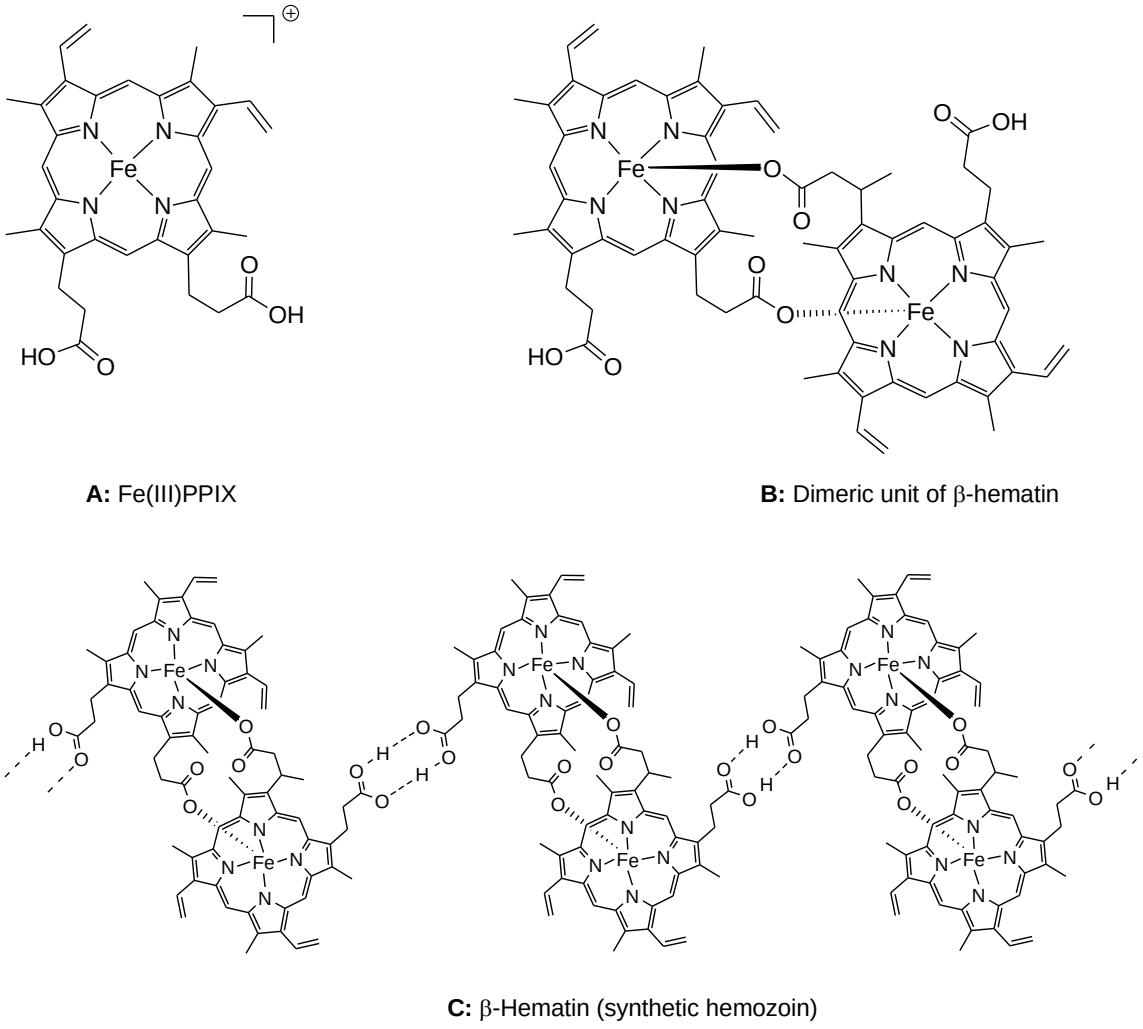

Figure 1.5. Structures of Fe(III)PPIX (A), dimeric unit of β-hematin (B) and β-hematin (synthetic hemozoin, C).

There is extensive evidence indicating that chloroquine (**3**) exerts its antiplasmodial activity by interfering with the sequestration of toxic heme. The drug interferes with the formation of hemozoin by direct interaction and binding to free hematin that ultimately prevents the incorporation of the latter into hemozoin.[56] Additionally, chemisorption of the drug onto crystallized hemozoin, capping the fast growing faces of crystalline hemozoin through the formation of very strong lipophilic and cytotoxic heme-chloroquine coordination complexes, is also a proposed mechanism of action.[57,58] Either mechanism results in the

build-up of large concentrations of free heme, perturbing the barrier properties of cellular membranes irreversibly, causing electronic and membrane stress, disturbing ion homeostasis and eventually causing the destruction of membranes and parasite death.[33]

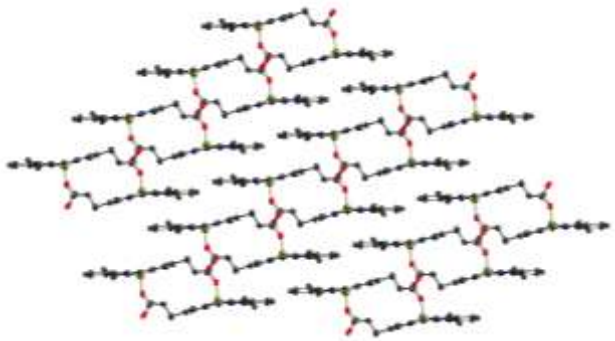

Figure 1.6. Solid state structure of β-hematin (synthetic hemozoin).

Beside interference with hemozoin formation, other pathways of action for quinoline antimalarial drugs involve the disruption of the degradation of heme (a second mechanism of detoxification of heme),[59,60,61] and the alteration of the parasite DNA conformation by intercalation of the quinoline drug into the double helix of DNA.[62,63,64]

Quinoline-containing drugs have been shown to be capable of both inhibiting formation of hemozoin and degradation of heme,[65,66] following of course certain differences in their paths of action that could explain the differences in therapeutic responses. Thus, the mechanism of action of all quinoline-containing drugs may not be identical to that of chloroquine (**3**), although they may share some biological effects. Figure 1.7 shows a schematic representation of the mechanism of formation of hemozoin and the proposed mechanisms of action of quinoline-containing drugs on the hemozoin.

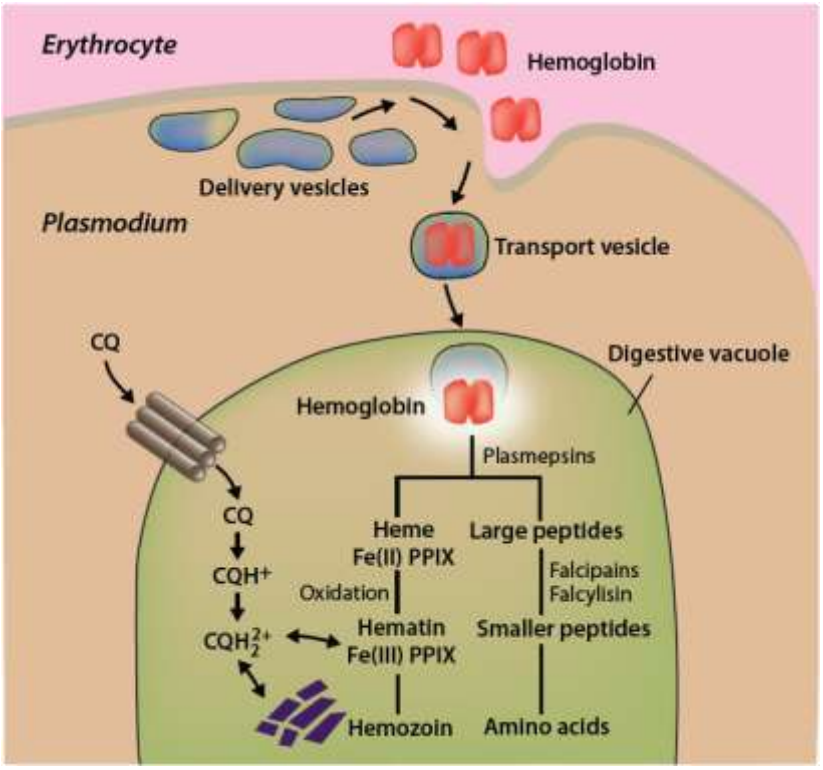

Figure 1.7. Schematic representation of the mechanism of formation of hemozoin inside the parasite digestive vacuole. Once chloroquine (CQ) has entered the digestive vacuole, it becomes protonated and it is believed to interact with free Fe(III)PPIX.

1.3.3 Resistance

Parasite resistance has rendered many antimalarials ineffective. Chloroquine (**3**) began to fail only 10 years after being put into use. By 2000, the drug was virtually useless in most parts of the world.[24] As is the case for the mechanism of action, the mechanism for the development of resistance against quinoline-containing drugs is not well characterized. What is known though is that the mechanisms by which the parasite turns chemoresistant to antimalarials generally involve chromosomal mutations.[67]

In numerous chloroquine-resistant parasite strains one characteristic recurs: when compared to chloroquine-sensitive strains, parasites would accumulate much lower (four to ten times) levels of drug inside their digestive vacuoles.[68] From this, it was concluded that resistance to chloroquine in *P. falciparum* is not due to a change in heme processing but to an alteration in the chloroquine accumulation in the digestive vacuole.[69] This could be caused by lower rates of drug influx, higher rates of drug efflux, or a combination of both.[69] While a higher rate of efflux was originally proposed to be the major contributing factor,[70] it is now generally accepted that a mechanism of reduced accumulation of drug better explains the observed differences between resistant and sensitive strains of the parasite.[71]

Changes in the transmembrane proteins of the food vacuole in resistant strains of *P. falciparum* cause a reduced accumulation of the drug in the parasitic food vacuole and, therefore, reduced accumulation of the toxic heme by-product.[72,73] How these changes affect the mechanisms of drug uptake are still vague. The observed resistance is probably conferred by mutations in multiple genes encoding transmembrane proteins that are necessary for the transport of drug into the food vacuole of the parasite.[74]

There are at least two documented types of transporter proteins that have been mutated in the case of chloroquine-resistant *Plasmodium falciparum*. The *PfCRT* gene located on chromosome 7 codes one of these transporter proteins, termed *PfCRT* (*P. falciparum* Chloroquine-Resistant Transporter) that could either be a channel or a carrier in the membrane of the food vacuole.[74] A mutation in the *PfMDR1* gene (*Plasmodium falciparum Multi Drug Resistance* gene) from chromosome 5 that codes the transmembrane transporter protein P-glycoprotein *Pgh1*, is also suspected to be responsible for chloroquine resistance by altering the membrane permeability due to an accelerated drug efflux mechanism.[75,76]

Much evidence suggests that the *PfCRT* mutation is more strongly associated with chloroquine resistance than is the *PfMDR1* mutation. It has been considered that the latter mutation plays a secondary role in chloroquine resistance.[77] Such pronounced resistance response is ultimately believed to be caused by more than two mutations of the *PfCRT* that are able to promote important physiological changes in the digestive vacuole; several resistant strains show closely related *PfCRT* alleles that differ from those of sensitive strains in seven or eight point mutations.[77]

Given the similarities in molecular structure, some of these processes confer resistance to other quinoline-containing drugs such as mefloquine (**7**) and quinine (**1**) as well, generating cross-resistance to other, structurally different, antimalarials with similar mechanisms of action like the artemisinins.[78] Nevertheless, the mechanisms of resistance against this family of antimalarials and others are still an active area of research.

1.4 Metalloantimalarials

The incorporation of metals into medicines dates back centuries. Metal-containing drugs offer a wide range of fine tuning of either the metal or ligand, to achieve or improve an observed efficacy. This approach also offers the advantage of possible metal/organic fragment synergisms. Many successful examples of bioinorganic compounds currently used in therapy such as the platinum anticancer therapy agent *Cisplatin* and its successors, as well as the technetium- and gadolinium-based diagnostic agents *Cardiolite*® and *Magnevist*®

have demonstrated that the application of metal-containing compounds in medicine can be beneficial and successful in both therapy and diagnosis.[79,80]

Encouraged by the success of many metal compounds as antitumor and antiarthritic agents and the pronounced selectivity that certain metal-containing compounds show for biomolecules exclusively found in parasites,[81] diverse metallic compounds, that had already been extensively applied in the treatment of other parasitic diseases in the past, were re-evaluated for antiplasmodial properties. As an example, various inorganic salts of bismuth were previously administered against major tropical diseases such as leishmaniasis as well as malaria itself.[79]

This trend has led to many metal compounds that have shown promising efficacy as antimalarials, described in this section. These compounds have been divided in three categories: metal chelators used as scavengers for metal ions essential for the parasite survival, intact metal coordination complexes of known antimalarial agents, and bioorganometallic compounds.

1.4.1 Metal chelators

These therapeutic agents are administered in the form of free ligands to scavenge and chelate free metabolically active metal ions causing the death of the parasite due to deprivation.[82] Iron deprivation caused by iron chelation therapy proved to be an option in malaria treatment. Withholding iron results in the inhibition of the growth of *P. falciparum* by either depletion of iron from its metabolic pathways or by *in situ* formation of toxic iron complexes.[82] Some antimalarial metal chelators are represented in Figure 1.8.

Desferrioxamine (DFO, **11**), a siderophore useful in the management of transfusion-related iron overload, is the first example of a vast family of iron chelators used for the therapy of malaria. DFO (**11**) is pharmaceutically well-known and widely used in experimental studies and clinical applications.[83] It inhibits malaria *in vitro* and *in vivo*[84] and has been used clinically to treat malaria in humans.[85,86] MA-DFO (**12**), with an *N*-methylanthranilic acid attached to the *N*-terminus of **11**, is more lipophilic and has shown considerably higher antimalarial activity compared to **11**.[87] Another derivatization approach was the synthesis of a zinc-desferrioxamine (Zn-DFO) complex (not pictured).[88] This pre-formed complex penetrates infected erythrocytes and exchanges Zn(II) for Fe(III) in a transmetallation reaction, forming a more stable complex. Zn-DFO seemed to be superior to metal free DFO, improving the inhibitory potency against parasite growth to concentrations below 20 mM.[88]

In addition to DFO and its derivatives, several other classes of Fe(III) chelators have been considered for malaria chemotherapy: catecholate siderophores, aminothiols, 3-hydroxypyridin-4-ones, bis-hydroxyphenyl-triazoles, acylhydrazones, thiosemicarbazones, dihydroxycoumarins, polyanionic amines, aminophenols, bicyclic imides, 2,2'-bipyridyl and 8-hydroxyquinolines.[89]

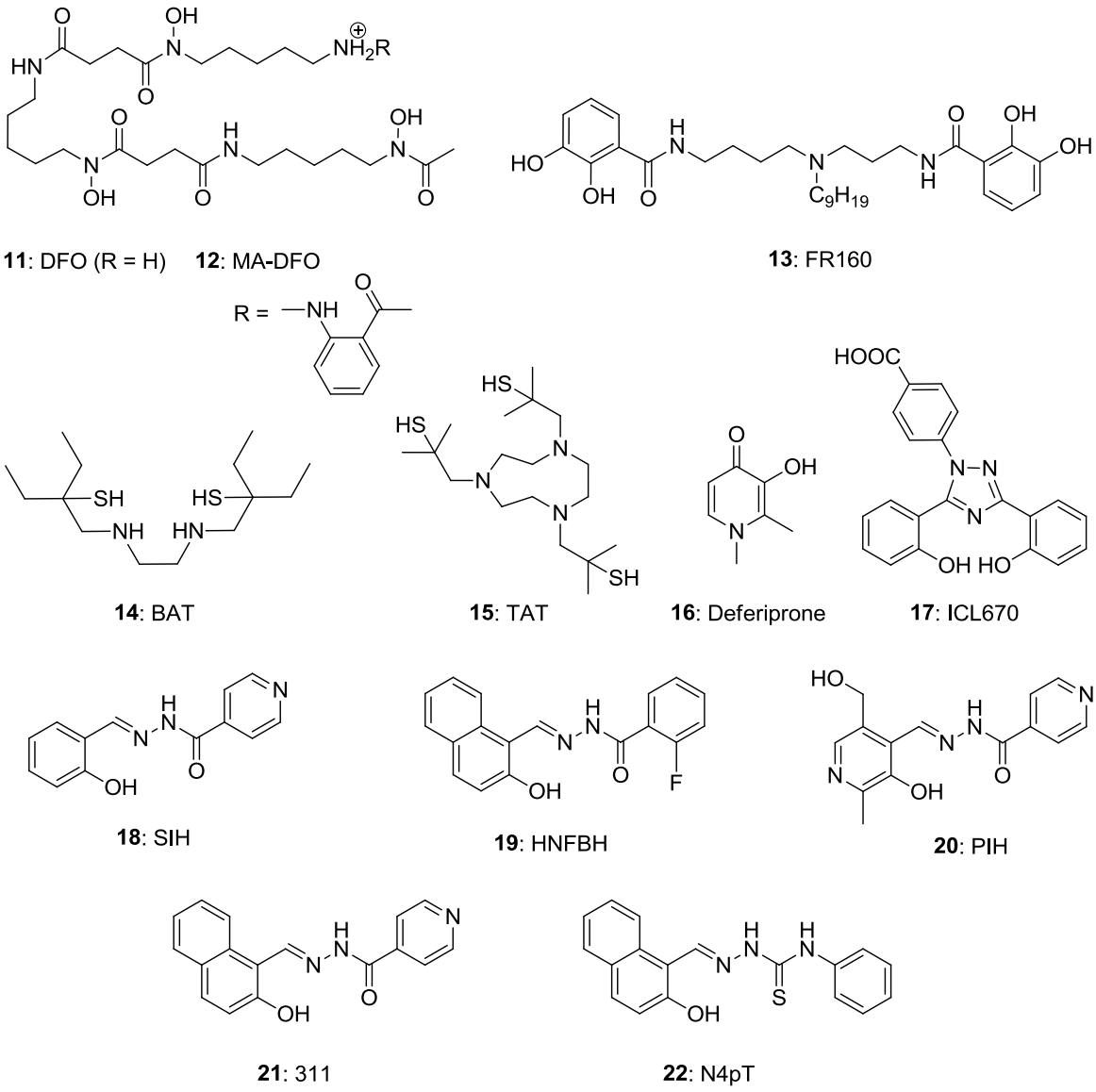

Figure 1.8. Metal chelators used for antimalarial therapy.

FR160 (**13**) is a catechol iron chelator siderophore with remarkable antimalarial activity.[90] It is 7 to 60 times more active than **11** against chloroquine-sensitive and chloroquine-resistant strains of *P. falciparum* with average inhibitory concentrations (IC_{50}) of 170 nM and 1 mM, respectively.[91,92]

Within the family of aminothiol multidentate chelators two remarkable examples are the ethane-1,2-bis(*N*-l-amino-3-ethylbutyl-3-thiol) (BAT, **14**) and *N*',*N*',*N*'-tris(2-methyl-2-mercaptopropyl)-1,4,7-triazacyclononane (TAT, **15**) that showed IC_{50} values of 7.6 and 3.3 μM, respectively, against a chloroquine-sensitive *P. falciparum* strain.[93] These two compounds were 5-10 times more potent than was DFO (**11**).[93] The bidentate 3-hydroxypyridin-4-ones (HPOs) have been extensively studied as orally active Fe(III) chelating agents and have been investigated for antimalarial activity.[94,95] The best representative of this family is deferiprone (1,2-dimethyl-3-hydroxypyridin-4-one, **16**) that, when administered in combination with other antimalarial drugs such as quinine (**1**) or doxycycline, resolves fever and coma faster and better than does DFO alone.[95]

The tridentate chelator 4-[(3,5-bis-(2-hydroxyphenyl)-1,24)triazol-1-yl]-benzoic acid (ICL670) (**17**) showed significantly lower malarial growth when compared to DFO (**11**).[96] Compound **17** was 4 times more active in growth control (at 48 h, growth relative to control was 53% with **17** and 83% with **11** at concentrations of 30 mM, and 20% with **17** compared to 26% with **11** at concentrations of 60 mM) but with IC_{50} values in the same range.[97] The acylhydrazones salicylaldehyde isonicotinoyl hydrazone (SIH, **18**), 2-hydroxyl-1-naphthylaldehyde *m*-fluorobenzoyl hydrazone (HNFBH, **19**) and pyridoxal isonicotinoyl hydrazone (PIH, **20**) were found to be orally effective and inexpensive antimalarials when used individually, and with potentiated action when used in combination with DFO (**11**), extending their action longer, potentially due to synergistic action.[98] Structure activity relationship (SAR) studies in a series of derivatives indicated that, regardless of the group attached to the aromatic ring, the hydrazide derivative determines the action, with

methylhydrazide and benzylhydrazide being the most active in inhibition of parasite growth.[99]

Structurally related to acylhydrazones, the thiosemicarbazones are another promising class of iron chelators. Aroylhydrazones and thiosemicarbazone iron chelators have shown antimalarial activity *in vitro* against chloroquine-sensitive and chloroquine-resistant strains of *P. falciparum*, being significantly more active than DFO (**11**).[100] Two of the most successful examples are 2-hydroxy-1-naphthylaldehyde isonicotinoyl hydrazone (311, **21**) and 2-hydroxy-1-naphthylaldehyde-4-phenyl-3-thiosemicarbazone (N4pT, **22**) with IC_{50} values of 4.5 μM and 3.0 μM, respectively, for a chloroquine-sensitive strain and of 4.75 μM and 2.5 μM, respectively, for a chloroquine-resistant strain.[101] These values were significantly lower than those of DFO (**11**) and SIH (**18**) and these compounds appear to be the most effective of the analogs, having IC_{50} values four times lower than the parent compound PIH (**20**).[101]

The mechanism by which these compounds act, be it either by causing iron deficiency by chelation or by direct interference with the acquisition of intracellular iron, is still a matter of discussion. The direct relation between lipophilicity and antiplasmodial activity supports direct intracellular iron chelation as the mode of action: the higher the affinity to cross lipid membranes, the higher the antimalarial activity.[83] This would suggest the entry of these compounds into the erythrocytes and the subsequent sequestration of Fe(III) from this environment. Also, incubation of these compounds with other sources of Fe(III) suppressed or decreased the *in vitro* antimalarial activity. On the other hand, no decrease of activity was detected when incubated with free Cu^{2+} and Zn^{2+}.[83] This suggests that the antiplasmodial action stems mainly from complexation of free intracellular iron.

The use of free ligands for antimalarial applications may result in formation of complexes with other essential metal cations resulting in undesired side effects for the patient. In addition, the antimalarial activity of these compounds, in the milli-to micromolar range, is not competitive with the nanomolar activities observed for other antimalarial drugs. But the large advantage resides in the fact that no resistance or signs of potential cross resistance have been found, either as standalone compounds or in combination with other known antimalarials and, given the large structural differences with other antimalarials, the development of cross resistance at a later stage seems unlikely.

1.4.2 Metal complexes

One of the most successful approaches in the field of metalloantimalarials so far is the modification of the chloroquine structure with metal-containing fragments. A number of transition metal ions have been used to form coordination complexes with chloroquine.[81,102,103,104] Complexes of chloroquine and chloroquine derivatives (Figure 1.9) have been shown to exhibit improved efficacy in both chloroquine-sensitive and resistant strains of *P. falciparum*, compared to the parent drug. Although the mechanism of action of these metal-based agents is unknown, the presence of the metal ion results in an enhanced activity, notably against chloroquine-resistant strains.

Ruthenium complexes of chloroquine were the first coordination complexes to be documented in this field.[105] The dinuclear Ru(II) chloroquine $[RuCQCl_2]_2$ complex (**23**) showed a marked inhibition of *P. berghei* and *P. falciparum* strains.[105] Compound **23** is five times more potent than is chloroquine against strains of *P. berghei* (IC_{50} = 18 nM).[105] *In vivo*

experiments in a rodent malarial model of *P. berghei* demonstrated **23** to be more potent than the parent drug **3**, reducing the parasitemia levels by 94% in comparison to 55% for **3** at an equivalent concentration without producing acute toxicity.[105]

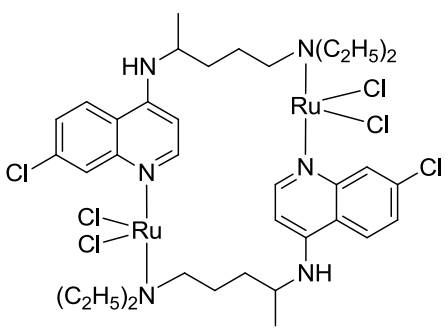

23: $[Ru(II)CQCl_2]_2$

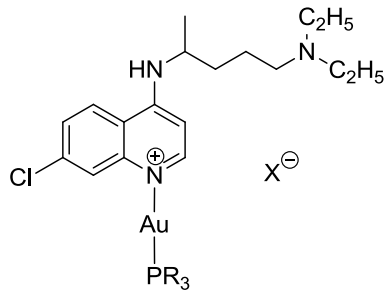

24: R = C_6H_5, X = PF_6 (AuCQ)
25: R = CH_3, X = PF_6
26: R = C_2H_5, X = PF_6
27: R = C_6H_5, X = NO_3

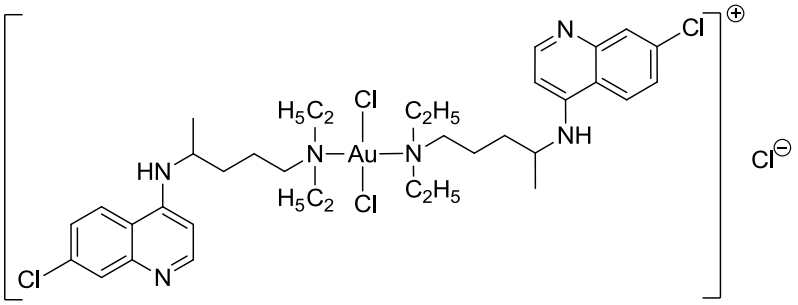

28

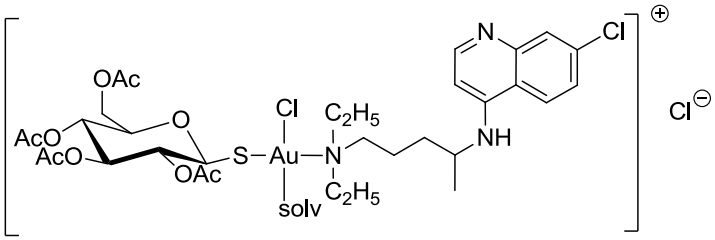

29

Figure 1.9. Metal complexes of chloroquine and chloroquine derivatives.

The mechanism of action of this compound has been described as the post-hydrolytic binding of **23** to hematin in solution, inhibiting its aggregation to β-hematin.[106] This inhibitory activity is significantly better than for chloroquine (**3**). Partition coefficients indicate that **23** is significantly more lipophilic than is **3** and therefore more likely to accumulate near the water-lipid regions of the parasite digestive vacuole leading to a higher efficiency both *in vitro* and *in vivo*.[106]

Gold(I) antimalarial chemistry has produced several coordination complexes, most through the attachment of a gold phosphine fragment to chloroquine. These compounds performed better than CQ (**3**) and were generally more potent than ruthenium and rhodium chloroquine complexes against both *P. berghei* and *P. falciparum* parasite strains. The most representative example is the gold(I) chloroquine complex $[Au(PPh_3)(CQ)]PF_6$ (AuCQ) (**24**). This complex caused marked inhibition *in vitro* and *in vivo* in models of *P. falciparum* and *P. berghei*.[107] In an *in vitro* model of rodent malaria parasite *P. berghei* **24** demonstrated an IC_{50} value of 3 nM, 22 times more potent than the parent drug CQ (**3**, IC_{50} = 67 nM).[107] The same was observed in *in vitro* cultures of chloroquine-resistant parasite strains of *P. falciparum* (FcB1, FcB2) where **24** displays IC_{50} values of 5.1 nM and 23 nM, respectively.[107,108] The mechanism of action of **24** has been investigated and it was determined that it interacts, similarly to **23**, with heme and inhibits β-hematin formation to a greater extent than do CQ or other known metal-based antimalarial agents.[109] The higher inhibition activity is probably related to higher lipophilicity of **24** compared to CQ.[109]

A second generation of gold chloroquine complexes (**25**-**29**, Figure 1.9) was synthesized to induce changes in electronic and steric properties of the complexes.[108,110] *In vitro* studies on the activity of these chloroquine gold compounds were carried out against several strains

of *P. falciparum* of different chloroquine sensitivity, with all compounds displaying similar or superior activity than CQ, especially in chloroquine-resistant strains.[108] Neither the nature of the anion nor the substituent of the phosphine ligand proved to be relevant for the activity of the complexes.[108] However, one of the highest activities within this group of derivatives was found for $[Au(PEt_3)(CQ)]PF_6$ (**26**) which was 5-fold more effective than chloroquine and 4-fold more effective than the parent complex $[Au(PPh_3)(CQ)]PF_6$ (**24**) against the chloroquine-resistant strain FcB1.[109]

Metal complexes of other antimalarial drugs are shown in Figure 1.10. Complexes of amodiaquine (**4**) and primaquine (**8**) with a selection of metal ions that included VO(II), Cr(III), Fe(III), Cu(II), Co(II), Ni(II), Zn(II), Cd(II), Hg(II), Rh(III), Pd(II), Au(III), Ag(I), Mn(II), Sn(II) and Pt(II) of the general formula $[M^{2+}(amodiaquine)(Cl)_2]$ (**30**) and $[M^{n+}(primaquine)_2(X)_n(H_2O)_y]$ (**31**) were screened *in vitro* against the FAN-5 strain of *P. falciparum*.[111] The complexation of either primaquine or amodiaquine did not represent any increase in potency since the activities of the complexes were identical to the parent drugs.[111]

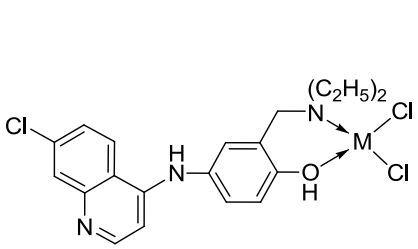

30: M = Cu(II), Co(II), Zn(II), Sn(II), Cd(II), Hg(II), Pd(II), Pt(II)

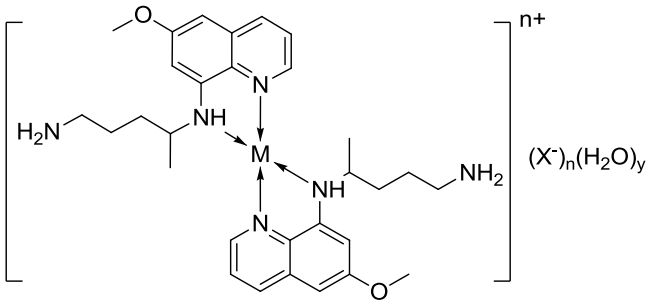

31: M = Cu(II), Co(II), Zn(II), Sn(II), Cd(II), Hg(II), Pd(II), Ag(I)
X^- = Halide
y = 2 (Zn), 5 (Co), 0 (Cu,Sn,Cd,Hg,Pd,Ag)

Figure 1.10. Metal complexes of other antimalarial drugs.

Metal coordination complexes of other ligands also demonstrated antiplasmodial activity. A selection of the most representative examples is shown in Figure 1.11. Several gold(I) thiolate and phosphine complexes ([Au(PEt_3)Cl] (**32**), sodium aurothiomalate (**33**), gold(III) cyclam (AuCyclam) (**34**) and auranofin (**35**)) *in vitro* inhibit the growth of *P. falciparum*. Sodium aurothiomalate (**33**) decreased the *in vitro* parasitemia of *P. falciparum*-infected human erythrocytes and delayed the lethal course of *P. berghei* malaria in an *in vivo* murine model, leading to survival of more than 50% of the mice 30 days after infection.[112] Auranofin (AF, **35**), a clinically established antiarthritic drug, caused a strong and nearly complete inhibition of *P. falciparum* growth at very low concentrations (IC_{50} = 142 nM), outperforming the mentioned gold complexes and other complexes.[110,113,114] Furthermore, there is evidence (isobolographic analysis) that **35** has a synergistic role with artemisinin. Compared to artemisinin (16 nM), auranofin is less potent, but when tested for synergistic action, the combination of artemisinin/50 nM auranofin and artemisinin/100 nM auranofin had IC_{50} values of 12 nM and 9 nM, respectively, improving the action of artemisinin alone.[110,113]

Complexes of Al(III), Fe(III), Ga(III) and In(III) with Schiff-base phenol and amine-phenol ligands proved to have antimalarial properties. The most representative example is [{1,12-bis(2-hydroxy-3-methoxybenzyl)-1,5,8,12-tetraazadodecane}gallium(III)]$^+$, [Ga-3-Madd]$^+$ (**36**) (Figure 1.11), that exhibited potent activity against several chloroquine-resistant parasite strains despite poor antimalarial activity in the chloroquine-sensitive clones.[115] In its ability to inhibit β-hematin formation, **36** also proved to be a potent inhibitor (IC_{50} = 1.2 μM), with 2-3-fold higher activity than chloroquine.[115] Susceptibility to this compound, mapped in a genetic cross, had a perfect correlation with the chloroquine resistance

phenotype, suggesting that a locus for **36** susceptibility would be located in the same segment of chromosome 7 as for the chloroquine resistance determinant.[115] From the results of structural studies, both in the solid and solution state, the authors were able to confirm that the selective biotransport and localization properties of this compound reside in the spatial orientation of the peripheral regions of the aromatic moieties rather than the central core.[116] Further studies demonstrated that the overall charge of the complex is also critical to the drug's ability to inhibit hemozoin formation and that this process is possible because of the formation of a drug-hematin propionate salt.[117]

Other examples of amino-phenol complexes are **37** and **38** (Figure 1.10). Screened for antiplasmodial activity, **37** showed modest IC_{50} values of ~ 2μM and >15μM against the chloroquine-sensitive HB3 and the chloroquine-resistant Dd2 parasite strains, respectively.[118] The inversion of trend in **37,** whose only structural difference to **36** is the position of the methoxy-group, indirectly confirms the hypothesis that the high activity observed for **36** is strongly related to the spatial orientation of the peripheral regions of the aromatic parts of the complex.[118] The Ga(III) aminophenol complex **38** was synthesized and screened for antimalarial activity against chloroquine-sensitive (HB3, IC_{50} = 0.6 μM) and chloroquine-resistant (Dd2, IC_{50} = 1.4 μM) parasite strains of *P. falciparum*.[119] For HB3, the obtained activity constitutes an improvement by a factor of 33, compared to **36**, whereas the activity against Dd2 is not significantly different from that of **36** (IC_{50} = 1.8 μM).[119]

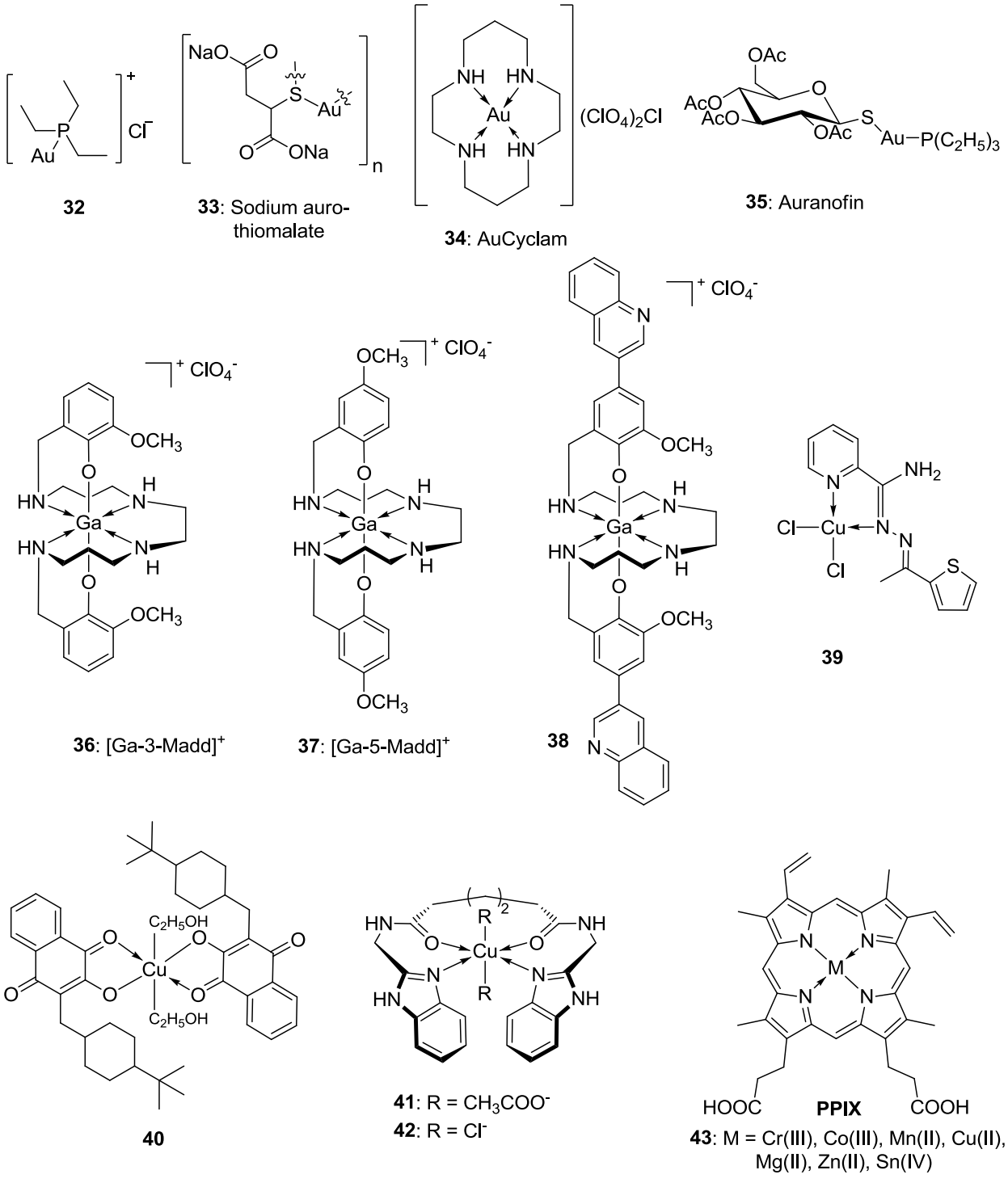

Figure 1.11. Metal complexes of other ligands.

Various Cu(II) coordination compounds also exhibited notable antimalarial activity - some examples are displayed in Figure 1.11. The copper(II) complex of pyridine-2-carboxamidrazone (**39**) has a 360-fold increase in activity over the ligand upon copper complexation when tested against the chloroquine-sensitive *P. falciparum* 3D7 strain.[120] This high activity seems to be associated with the four-coordinate planar geometry, whose planarity is suggested to promote its facile internalization.[120] A second factor proposed to contribute to the enhanced antimalarial activity of the copper compound is the positive reduction potential that facilitates intracellular reduction to Cu(I) species, which are detrimental to parasite growth.[120] Coordination complexes of buparvaquone (3-*trans*(4-*tert*-butylcyclohexyl)methyl-2-hydroxy-1,4-naphthoquinone) with diverse metal ions such as Cu(II) (**40**), Ni(II), Co(II), Fe(II), and Mn(II) were studied for their *in vitro* antimalarial activity.[121] All synthesized metal complexes except for Ni(II) showed enhanced activities, [Cu(buparvaquone)$_2$(C_2H_5OH)$_2$] (**40**) being the most active compound, showing a thousand-fold enhancement of activity compared to the parent quinone against 3D7 and a three-fold improvement against the chloroquine-resistant K1 strain.[121]

A series of copper(II) nanohybrid solids LCu(CH_3COO)$_2$ (**41**) and $LCuCl_2$ (**42**) with particle sizes of 5-10 nm and 60-70 nm, respectively, were synthesized using bis(benzimidazole) diamide as the capping ligand L.[122] When evaluated for their *in vitro* antimalarial activity against a chloroquine-sensitive MCR2 isolate of *P. falciparum*, IC_{50} values of 0.059 and 0.048 μM for **41** and **42** were reported, respectively.[122] These are the first literature-described examples of copper complexes with IC_{50} values comparable to that of chloroquine (**3**, IC_{50} = 0.039 μM vs. MCR2). These benzimidazole copper derivatives are expected to function as inhibitors of plasmepsins, the aspartic proteases involved in the

catabolism of hemoglobin inside the parasite digestive vacuole. A study on the interaction between these nanohybrid solids and the protease Plasmepsin II by UV-vis spectroscopy and inhibition kinetics indicated that both **41** and **42** inhibit Plasmepsin II competitively with regard to substrate.[122]

Metalloporphyrins MPPIX of metals ions such as Fe(II), Cr(III), Co(III), Mn(II), Cu(II), Mg(II), Zn(II) and Sn(IV) (**43**) (Figure 1.11) also demonstrated antimalarial properties.[123,124] The central metal ion played an important role in the efficacy of the metalloporphyrins. The metalloporphyrins MPPIX (**43**) of Mg(II), Zn(II) and Sn(IV) were found to be as effective as Fe(II)PPIX and up to six- and four-fold more effective than the metal-free porphyrin and chloroquine (**3**), respectively, in the inhibition of β-hematin formation.[124] Less active were the MPPIX complexes **43** of Cu(II) and Mn(II), followed by the MPPIX complexes **43** of Cr(III) and Co(III), which did not present an advantage over metal-free PPIX.[124] The efficacy of these compounds was found to correlate well with the exchange rate of water at the central metal ion of the octahedral porphyrin aqua complexes.[124] Aggregation studies supported the occurrence of acid-triggered π-stacking of heme-MPPIX assemblies, responsible for hemozoin inhibition by disrupting interactions critical to the stability of the hemozoin.[124]

Metal coordination compounds of antimalarial drugs represent in most cases an improvement compared to the activity of the parent drugs against chloroquine-sensitive and resistant parasite strains, with activities that remained for the most part in the micromolar range, with a few exceptions in the nanomolar range. Even though these compounds are far better than the metal chelator in terms of activity, their close resemblance to the parent antimalarial drugs presents the potential for developing cross-resistance.

1.4.3 Bioorganometallic compounds

Organometallic compounds have played an important role in biology and medicine in the last decades, even though they are better known for their use in catalysis and other applications.[125,126] In contrast to coordination compounds of transition metals, organometallic complexes are thought to be unstable or insoluble, or both, in aqueous media and not well-adapted for biological systems. Whilst certainly accurate for many organometallic compounds, many others are suitable for biological applications. Among those, a selection of metallocenes and organometallic complexes has proven their potential as pharmaceutical agents experimentally and clinically. One well-known example is Ferrocifen, a ferrocene derivative of tamoxifen, a chemotherapeutic agent for the treatment of breast cancer that demonstrated not only greater potency than the parent drug, but was also the first chemotherapeutic agent to be active in both hormone-dependent and hormone-independent breast cancer tissue.[127,128]

Thus, the biological activity of certain organometallic compounds attracted the attention that fostered the development in this field. During the last 15 years, significant progress on the treatment of malaria with bioorganometallic compounds, with special emphasis on ferrocene compounds, has been achieved. Results showed in several cases that the presence of ferrocene improves antiplasmodial activity in the parent structure and in some cases can even overcome drug-resistance in parasite strains.

Ferroquine or ferrochloroquine (FQ, **44**) (Figure 1.12) was the first derivative of chloroquine containing a ferrocene molecule to be reported and it is undoubtedly the most successful of all metallo-antimalarials synthesized and tested to date. FQ (**44**) shares

structural and biological features with chloroquine (**3**), but their individual responses against several *P. falciparum* strains tend to be very different. FQ (**44**) is highly active in chloroquine-sensitive and chloroquine-resistant *P. falciparum* parasite strains *in vitro*.[129,130] Against chloroquine-sensitive parasite strains, **44** was as effective as the parent **3** with IC_{50} values that ranged from 3.5 to 218 nM. Against chloroquine-resistant parasite strains, **44** was up to 20 times more effective than was chloroquine, with IC_{50} values that ranged from 5 to 241 nM, maintaining the high observed activity from the drug-sensitive strains.[131,132,133] The antimalarial activity of ferroquine (**44**) has been demonstrated extensively against several strains of *P. falciparum* from both laboratory clones and clinically-isolated clones, obtaining an IC_{50} mean of 10.8 nM from 103 isolates of chloroquine-sensitive and resistant *P. falciparum*.[134] It also exhibited remarkably high antimalarial activity *in vivo* in mice infected with *P. berghei*, *P. yoeli* and *P. vinckei vinckei*.[135,136] Furthermore, studies of **44** with other quinoline-based drugs demonstrated that **44** is unlikely to develop cross-resistance among multiple field isolates.[134,137,138] Ferroquine (**44** - SSR97193) is now in phase IIb clinical trials under the aegis of Sanofi-Aventis.[139] To the best of our knowledge, clinical trials were to be carried out examining the efficacy of an ACT based on artesunate and ferroquine (**44**) in malaria patients.[140]

Following the success of ferroquine, other structural analogs were synthesised in order to delineate structure–activity relationships.[130,131,132,141,142,143,144] These analogs will be further described in the following chapters. Most of these derivatives show better activities than does the parent drug chloroquine **3** and were, in the most successful cases, as good as ferroquine (**44**). Despite the effort invested to further improve the activity of FQ, none of them to the date has out-performed ferroquine in antimalarial potency and pharmacological properties.

Other derivatives implemented the masked pro-drugs or "dual drugs" approach, for example, the series of hybrid compounds consisting of a 1,2,4-trioxane fragment and ferroquine, coined "trioxaferroquines" (**45-48**, Figure 1.12). These compounds combine the ferroquine moiety and the main feature of the group of artemisinins, the endo-peroxide bridge-fragment essential for artemisinin activity. These hybrids have the possibility of a dual or a synergistic antimalarial action. Trioxaferroquines exhibit potent antimalarial action with IC_{50} values in the range 16-71 nM for both chloroquine-sensitive and resistant parasite strains.[145] Trioxaferrocenes (not containing the quinoline fragment) were much less active inhibitors with IC_{50} values in the rage of 145-1697 nM. Despite their good activity, the organometallic trioxaferroquines do not represent an advantage over their organic trioxaquine counterparts (no ferrocene).[145] Another example is the 4-aminoquinoline **49** bearing an amino side-chain substituted by an aliphatic Mannich base (Figure 1.12).[146] This drug was designed so that the quinoline part facilitates recognition and accumulation inside the digestive vacuole meanwhile, once inside the parasite, oxidative *N*-dealkylation (catalyzed by cytP450 enzymes or other oxidative conditions found inside the parasite) will release the 4-aminoquinoline, whose function will be to inhibit hemozoin formation and produce oxidative stress (through the thiol-reactive Mannich bases). Compound **49** proved to be a potent inhibitor of parasite growth, nearly as potent as is ferroquine.[146] However, **49** is also six-times more toxic than FQ to both the human lung MRC-5 and the glioblastoma carmustine-resistant NCH89 cell lines.[146]

A "double-load" approach was followed in the synthesis of ferrocene quinoline derivatives of triazacyclonane (**50-51**, Figure 1.12), containing two units of a chloroquine derivative or two units of ferrocene.[147] *In vitro* testing revealed that the the bisquinoline 7-

chloro-4-[4-(7-chloro-4-quinolyl)-7-ferrocenylmethyl-1,4,7- triazacyclononan-1-yl]quinoline (**50**) proved to be more potent than **51** (a bisferrocenyl derivative).[147] Compound **50** is 5.5 times less active than CQ in HB3 (drug-resistant) but 1.5 times more active than CQ in the Dd2 strain (drug-sensitive).[147] The authors proposed that for **50** the redox behaviour of ferrocene as a one-electron system and its high lipophilicity may partially explain the increased activity, whereas for **51** the even higher lipophilicity, high molecular weight and steric hindrance may contribute to its lower potency by perturbing its transport to the parasitic food vacuole of the parasite and/or destabilizing the interaction of the quinoline-fragment with hematin.[147]

Heterobimetallic compounds incorporating ferroquine and a second metal center were also studied. Derivatives of ferrocenyl-4-aminoquinoline acted as coordinating ligands (L) to form complexes of the general formula $[Au(L)(PPh_3)]NO_3$, $[Au(C_6F_5)(L)]$ and [Rh(Cl)(COD)(L)] (**52-54a-c**, Figure 1.12).[148] The coordination of the second metal ion did not lead to a significant improvement.[148] On the contrary, for most compounds a decrease in activity was observed. The most active compounds were the gold complexes of the general formula $[Au(C_6F_5)(L)]$ (**53**). It was noted that the presence of the second metal, specifically gold, made the ferrocenyl moiety far more difficult to oxidise and the authors postulated this could explain some of the loss in efficacy.[148]

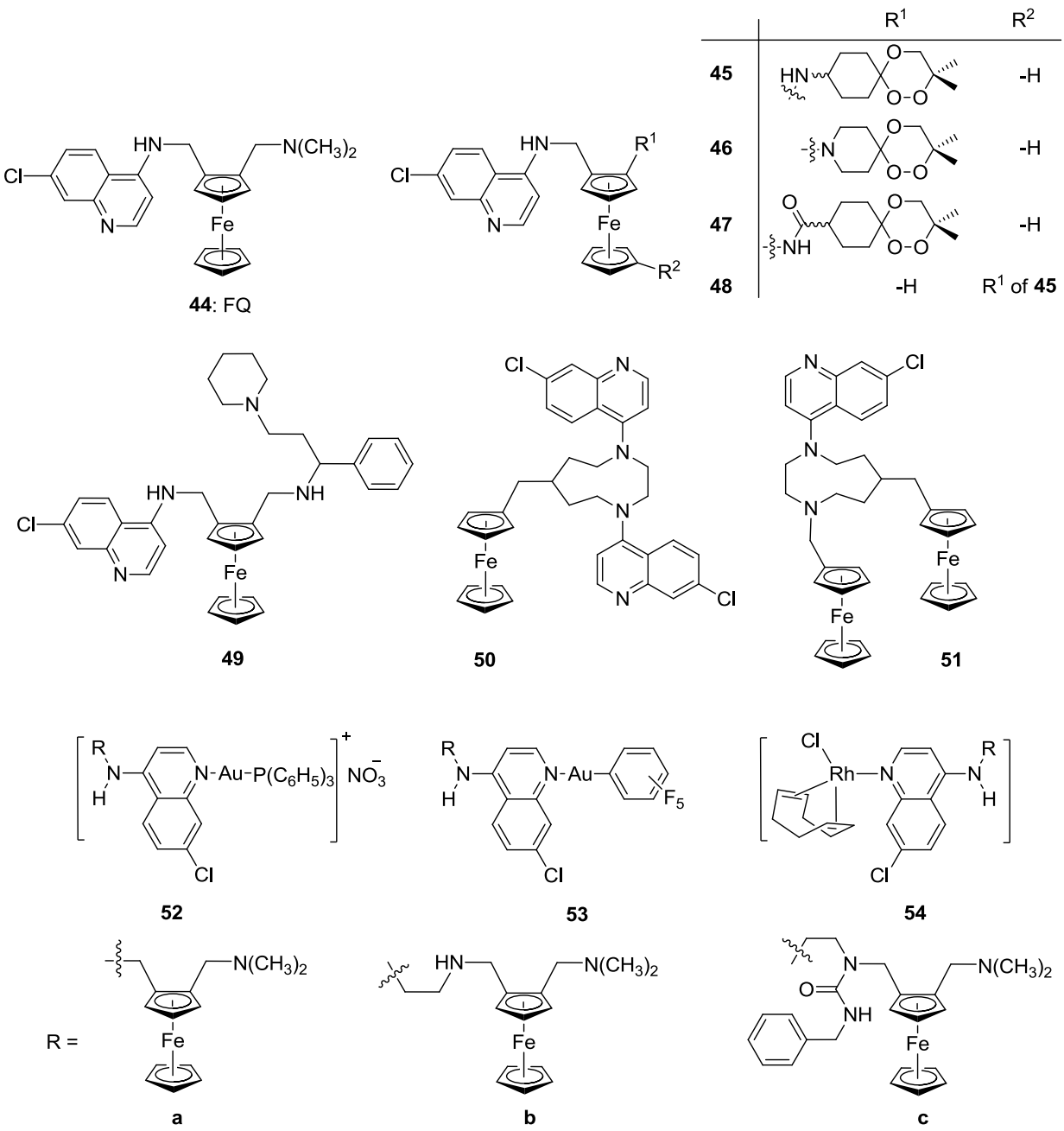

Figure 1.12. Ferrocene chloroquine derivatives showing antimalarial action.

Ferrocene was also conjugated to other antimalarial drugs. Two series of artemisinin derivatives bearing a ferrocene-pendant at the core (through the use of a variety of linkers) were tested *in vitro* against strains of *P. falciparum*. Series 1 (**55**-**56**, Figure 1.13) was functionalized at the C-16 position of artemisinin and the Fc-derivatives were found to be 2.5 to 5-fold more active than the parent artemisinin.[149] The second series of derivatives, represented by **57** and **58** (Figure 1.13), was functionalized at the carbonyl functionality of artemisinin *via* an ether or ester bond and did not perform better when compared to artemisinin.[150] A series of ferrocene aminohydroxynaphthoquinones (**59**, Figure 1.13), analogs of the antimalarial drug atovaquone, were found to be 4 to 10-fold less active than the parent drug atovaquone.[151] Ferrocenyl derivatives of mefloquine **60** and quinine **61** (Figure 1.12) exhibited lower antimalarial activity than did the parent drugs mefloquine (**7**) and quinine (**1**), indicating no activity enhancement attributable to the ferrocene unit.[152]

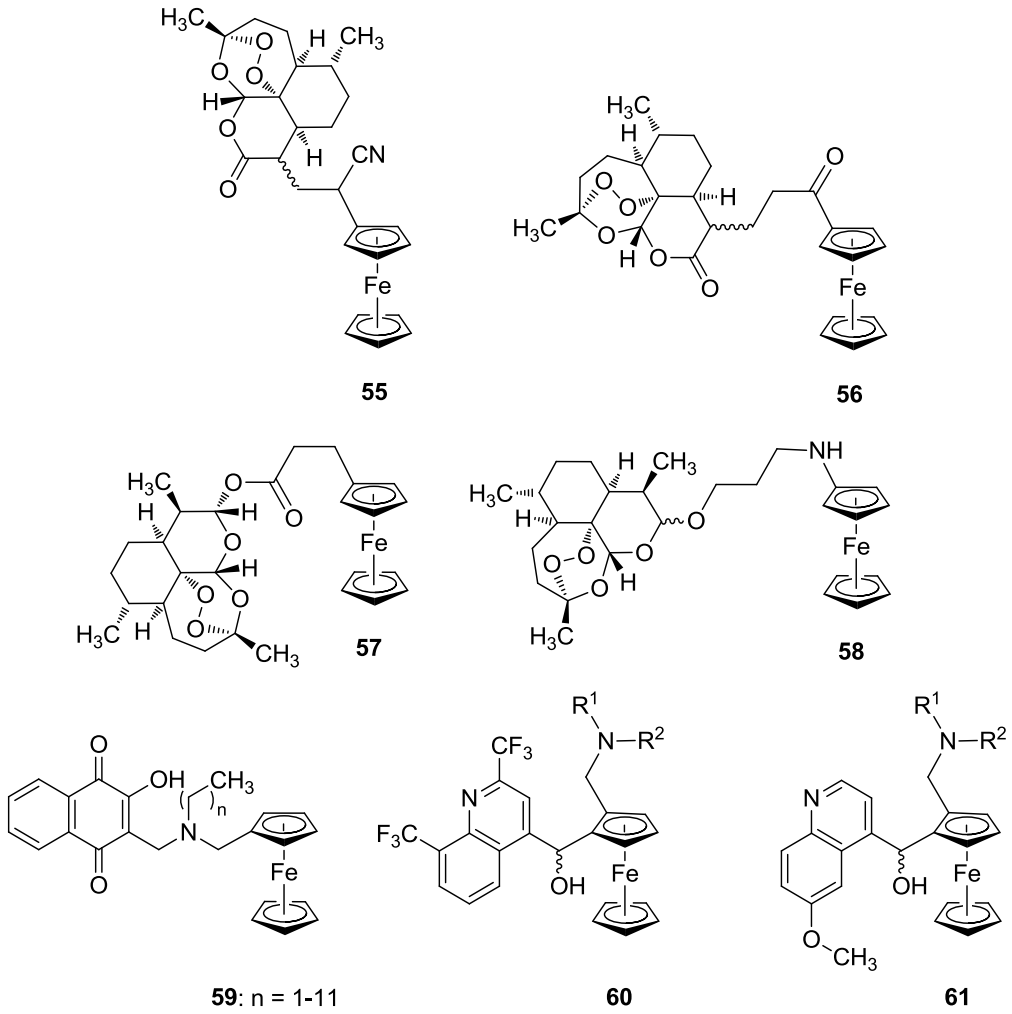

Figure 1.13. Ferrocene derivatives of other antimalarial drugs.

Ferrocene derivatives of other non-antimalarial drugs also demonstrated antiplasmodial activity. Conjugates of ferroquine and thiosemicarbazones (TSC) (**62**, Figure 1.14), when evaluated *in vitro* against four strains of *P. falciparum* with different levels of drug resistance, were more active than the TSC alone, displaying activity in the micromolar range with IC_{50} values of 0.2-16.2 μM; however, activity was comparable with the purely organic derivatives of TSC and 4-aminoquinoline, indicating that the ferrocene does not increase

antimalarial activity.[153] Ferrocenylthiosemicarbazone metallodendrimers (**63**, **64**, Figure 1.14) were synthesized in the hope of increasing the antimalarial activity by increasing bioavailability through the peripheral amine groups of the dendrimer. Compounds **63** and **64** displayed moderate antimalarial activity *in vitro* with IC_{50} values of 6.59 and 1.79 μM against the chloroquine-resistant W2 strain, respectively.[154] These activities are far better than those displayed by the non-dendritic ferrocenylthiosemicarbazones with 3- to 11-fold increases in activity.[154]

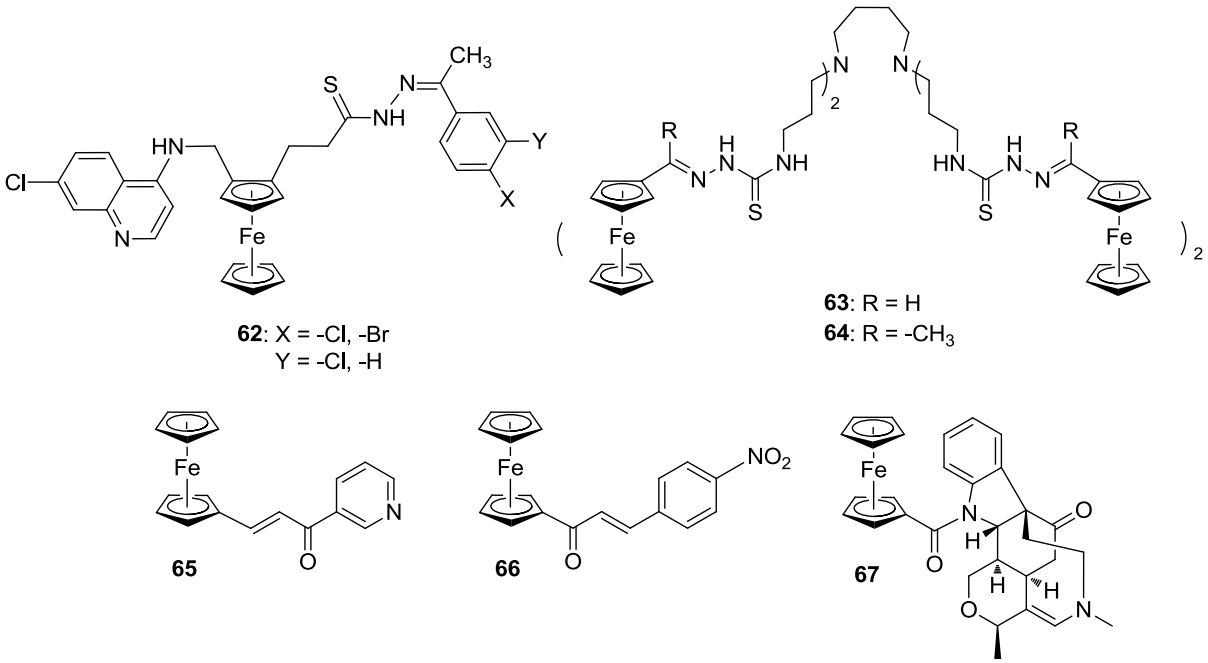

Figure 1.14. Ferrocene conjugates of other compounds with antiplasmodial action.

Ferrocenyl chalcones (**65** and **66**, Figure 1.14) were evaluated *in vitro* for antimalarial activity. Against the chloroquine-resistant K1 *P. falciparum* strain, **65** and **66** exhibited moderate antimalarial activity (IC_{50} 4.5 and 5.1 μM, respectively), but still were less active than the parent chalcones.[155] When evaluated for size, electronic, lipophilic and

electrochemical character, it was discovered that the location of the ferrocene influences both the redox potential of the central Fe^{2+} and the polarity of the carbonyl linkage, and these in turn influence the antiplasmodial activity.[156] Hence, it was noted that compounds that are more resistant to oxidation and bear the ferrocene moiety adjacent to the carbonyl linkage (**66**) were more selective and potent antiplasmodial agents.[156] Based on these results, ferrocene was dismissed as having a purely structural role as a hydrophobic spacer.

Conjugates of a chemosensitizer (improves the action of chloroquine in drug-resistant parasite strains) like strychnobrasiline and ferrocenyl derivatives were designed in hopes of overcoming the lack of *in vivo* activity of strychnobrasiline.[157] N_a-Deacetyl-ferrocenoyl-strychnobrasiline (**67**) showed *in vitro* activity 15 times higher than the parent strychnobrasiline and significant synergistic effects (with chloroquine) against the chloroquine-resistant strain FCM29;[157] however, the compound lacked any *in vivo* potentiating effect and an antagonistic effect was even observed at higher doses.[157]

Ferrocenyl conjugates with compounds that did not display antimalarial properties also exhibited the ability to inhibit the growth of the malaria parasite.[158,159,160] Among these serendipitous discoveries are, for example, the ferrocenyl ellagitannin derivatives.[158] Compound **68** (Figure 1.15) with an IC_{50} value of 0.6 μM, shows an inhibitory activity similar to quinine (0.11 μM) against the FCR3 chloroquine-sensitive strain while the parent compound ellagitannin, a trideca-*O*-methyl-α-pedunculagin, displayed no antimalarial activity whatsoever.[158] Another example is the group of ferrocenyl carbohydrate compounds with ferrocene substituted with either one or two monosaccharides *via* different linkers (amide, ester, thioester) (**69-71**, Figure 1.15).[159,161] Compound **69** was active in the chloroquine-sensitive D10 strain (IC_{50} = 12.5 μM) but lost activity by a factor of 4 against

the chloroquine-resistant K1 strain. Compound **70**, the disubstituted analog of **69**, showed similar behaviour but was 3 times more active with IC_{50} values of 6.7 to 16.4 μM against the chloroquine-sensitive and resistant strains. Compound **71** was the most active of the derivatives with IC_{50} values of 4.9 and 6.1 μM for 3D7 and K1, respectively.[159] Notably, for compounds showing activity, disubstituted conjugates were generally more active than their monosubstituted analogs.[159]

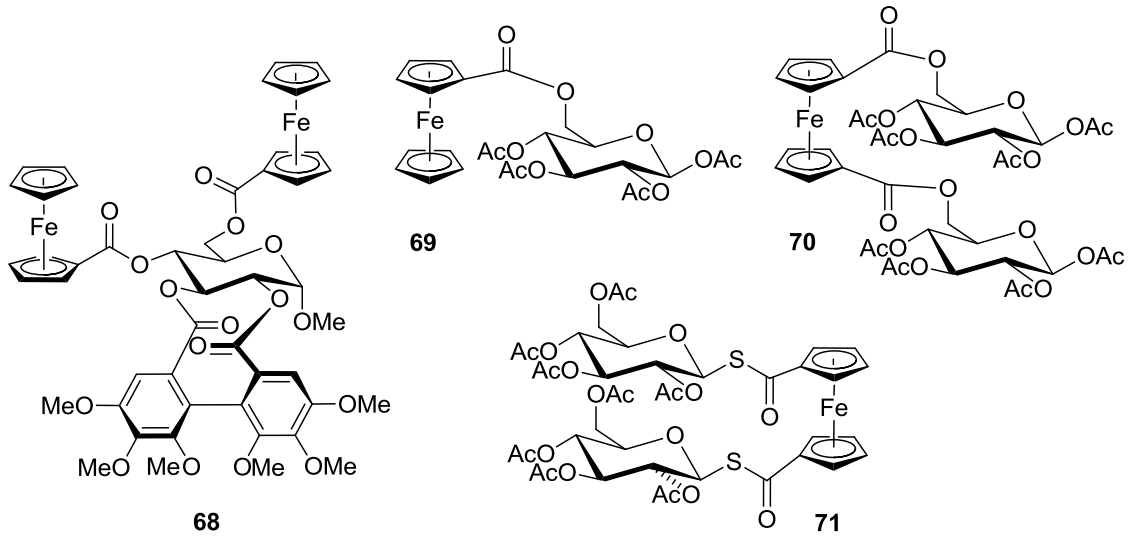

Figure 1.15. Ferrocene conjugates of other compounds with antiplasmodial action.

As iron and ruthenium are both group 8 transition metals, ruthenocene analogues of ferroquine were the logical choice of analogs to be developed. Slight modifications to the synthetic methodology yielded ruthenoquine (RQ) (**72**) and its structural derivatives (**73**-**75**, Figure 1.16).[133,141,142] These compounds exhibited good efficacy in both chloroquine-sensitive (D10) and chloroquine-resistant (K1) strains and, as observed for ferroquine, addition of the ruthenocene was key for overcoming chloroquine resistance.[133,141,142] Ruthenoquine (**72**) was found to be slightly less active than ferroquine (**44**) in both parasite strains with IC_{50} values

of 23.8 and 6.3 nM for D10 and K1, respectively.[133] Nonetheless, this compound was still as effective as chloroquine in D10 and 53-times more potent than CQ in K1, generally showing the same efficacy as ferroquine (**44**) against both types of parasite strains.[133,141,142] In further studies in several strains of *P. falciparum* of different drug-sensitivity, it was shown that activity of FQ and RQ is correlated with each other but not with CQ, confirming a similar mode of action for these metallocenes and a lack of cross resistance.[162]

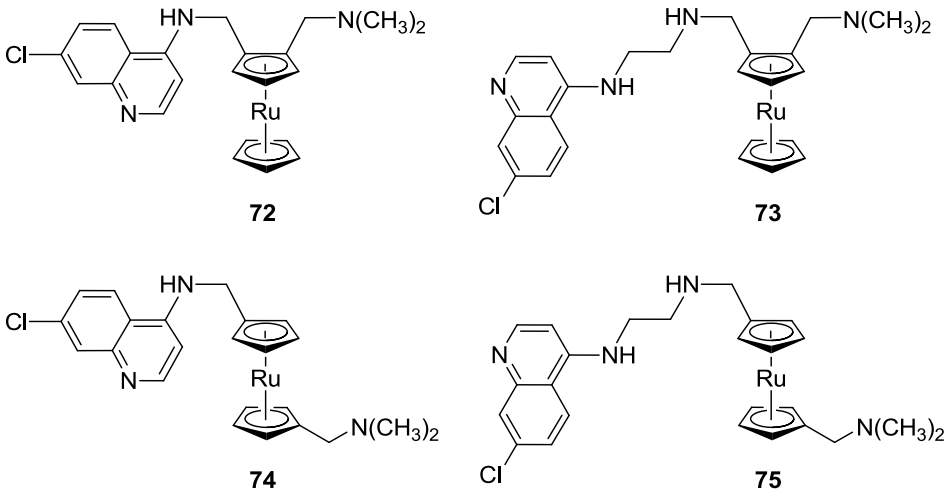

Figure 1.16. Ruthenocene chloroquine derivatives with antimalarial action.

One of the main goals of synthesizing the ruthenium analogs was to establish the role and importance of iron in the improved action observed for ferrocenyl complexes such as ferroquine. It was suggested that the redox contribution of the ferrocene/ferrocenium couple can be crucial in explaining the antimalarial activity of ferroquine.[162,163] For the redox-pair $Ru^{2+/}Ru^{3+}$ a much higher potential is expected and oxidation is therefore less likely to occur compared to ferroquine. It was shown that **72** and derivatives **73-75** are not able to facilitate the formation of OH radicals, which *in vitro* and *in vivo* would create oxidative stress and

contribute to the death of the parasite.[162,163] This difference in electrochemical behaviour between **44** and **72** is, nevertheless, not reflected in a strong difference in antimalarial potency, which would suggest that any redox contribution from the Fe^{2+}/Fe^{3+} pair may contribute to the overall antimalarial action but not be the determining factor.

Even though metallocene compounds of ferrocene make up most of the bioorganometallic antimalarials, due to their stability *in vivo* and beneficial redox properties, other organometallic classes of compounds have been envisioned and described as antimalarials. Selected organo-ruthenium compounds have been evaluated for their antiplasmodial activity.[164] A series of organo-Ru(II)-CQ half-sandwich complexes of the general formula [Ru(II)(η^6-arene)(CQ)]L_2 (**76-80**, Figure 1.17) were found to display different binding modes of chloroquine, including the first example of a η^6-chloroquine binding mode through the carbocyclic ring.[164] Compounds **76-79** have a conventional half-sandwich structure motif while compound **80** has chloroquine coordinated as the chloroquine diphosphate salt (CQDP) in an unprecedented π-coordination through the aromatic ring of quinoline side chain to Ru(II).[164]

These compounds proved to be less active than the parent drug chloroquine in all tested drug-sensitive strains except for 3D7, for which the compounds were twice as active as chloroquine.[164] Against the chloroquine-resistant parasite strains, **76-78** and **80** were more potent than chloroquine, successfully overcoming resistance in these strains, the exception being **80** showing slightly lower activity than CQDP against the highly resistant W2 strain.[164] The authors have proposed that a balance of physicochemical properties, particularly the lipophilicity and structural features of the drug, play a determining role in their increased capacity for heme aggregation inhibition.[165]

Growth inhibition studies of the air-stable [Rh(CQ)(COD)Cl] (**81**, Figure 1.17) carried out *in vitro* against *P. berghei* indicated the rhodium complex as equipotent to CQDP, representing no advantage over the action of chloroquine.[105] *In vivo* experiments in a rodent malarial model of *P. berghei* demonstrated, though, that **81** was more potent than chloroquine leading to a reduction of parasitemia levels by 73% compared to 55% with chloroquine, using equivalent concentrations of 1mg /kg CQ.[105] Iridium-CQ complexes were also evaluated for antimalarial activity in *in vitro* cultures of *P. berghei*.[166] The only compound seemingly improving the action of the parent drug was **82** (Figure 1.17) with an IC_{50} value of 59 nM.[166]

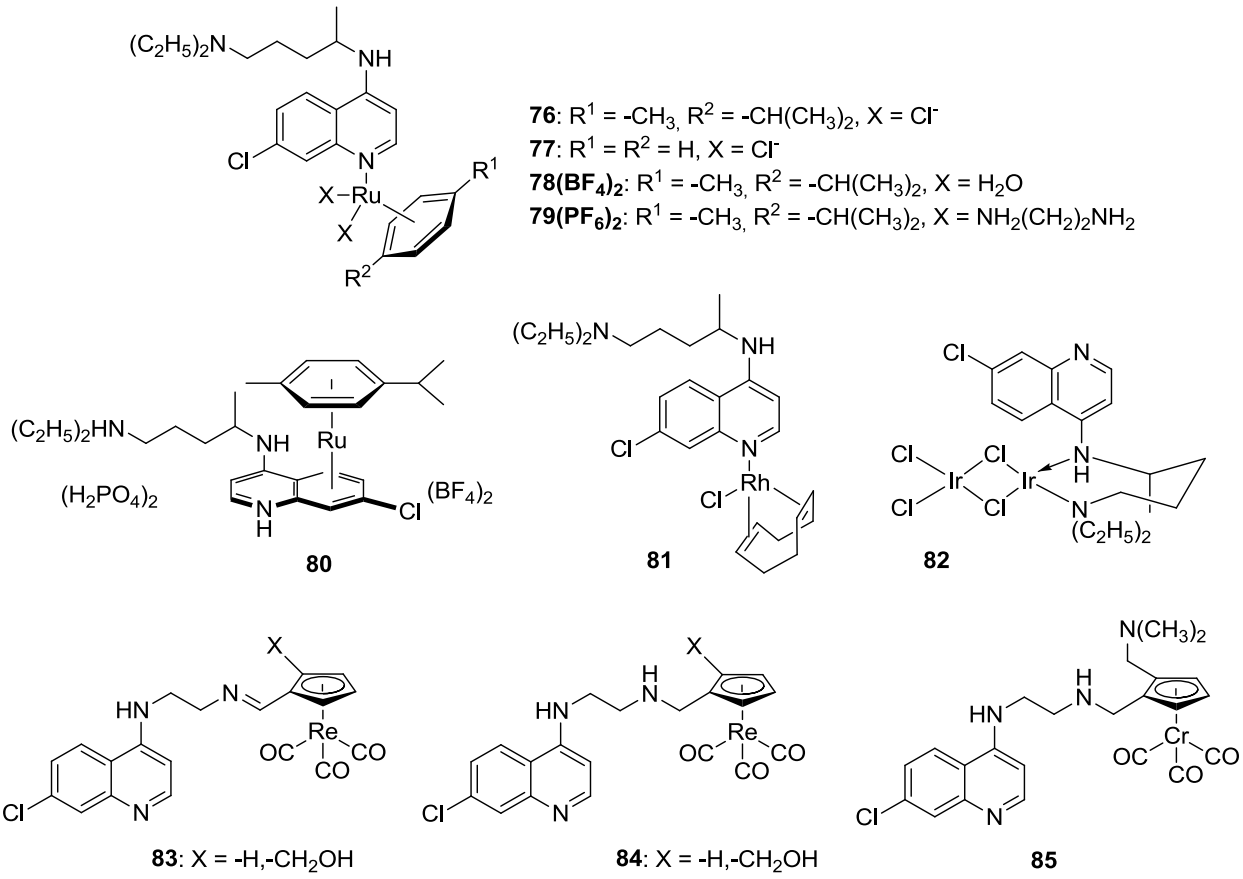

Figure 1.17. Other organometallic compounds containing chloroquine.

Cyclopentadienyl tricarbonylrhenium derivatives of chloroquine (**83**-**84**, Figure 1.17) were evaluated *in vitro* against *P. falciparum* strains.[167] Against the chloroquine-sensitive 3D7 strain, the cyrhetrenylimines (**83**) were the most active with IC_{50} values of 64-85 nM; however, against the chloroquine-resistant W2 strain they showed reduced activity, the exception being the amine analogue of **84** that exhibited a significant activity against W2 (IC_{50} = 267 nM) but was relatively inactive against 3D7. This compound is another example of selected susceptibility towards drug-resistant strains.[167] The lipophilicity of these compounds was studied with respect to the parasite vacuolar and cytosolic pH.[167] The introduction of the cyrhetrenyl moiety at the end of the lateral chain of the 4-aminoquinoline scaffold dramatically increased lipophilicity at the pH of the parasite digestive vacuole (pH = 5.2); however, no direct correlation could be observed between the *P. falciparum* culture growth inhibition and lipophilicity of the compounds.[167]

A series of chromium η^6-arene-tricarbonyl CQ analogs was synthesized and evaluated.[168] Compound **85** (Figure 1.17), studied *in vitro* against the chloroquine-sensitive D10 and the chloroquine-resistant Dd2 strains of *P. falciparum*, exhibits IC_{50} values of 3.8 and 33.9 nM, respectively. In these strains, **85** was 3 to 6 times more active than was chloroquine, far more active than the chromium η^6-arene-tricarbonyl alone, as effective as the organic quinoline part against the chloroquine-sensitive strain, and twice as effective as the same organic core against the resistant strain.[168] Compared to ferrocene analogs, the nature of the metal ion and the electron-withdrawing effect of the single cyclopentadienyl moiety in the last three examples (versus the electron donating properties of ferrocene) have a significant effect on the antimalarial properties of the compounds.[167]

Finally, organometallic compounds not containing chloroquine were also evaluated in their antiplasmodial properties. A series of mononuclear salicylaldiminato (thiosemicarbazone) Pd(II) compounds (**86**, Figure 1.18) showed superior *in vitro* activity in comparison with their thiosemicarbazone ligand precursors, by approximately a factor of 2, with IC_{50} values ranging between 1.38 and 9.02 μM for the drug-sensitive D10 and 8.87-13.74 μM for the resistant W2 parasite strains.[169] Recently, a new series of mono-, di- and tetranuclear organo Pd(II) complexes of thiosemicarbazones ligands (**87**-**89**, Figure 1.18) was found to display antiplasmodial activity with IC_{50} values in the range of 3.19-7.2 μM for the chloroquine-sensitive 3D7 and 2.27-5.10 μM for the chloroquine-resistant K1 parasite strains.[170] These improved activities, compared to those of their free ligands, illustrate that coordination to palladium enhances the inhibitory effects of the coordinated thiosemicarbazones. On average, mononuclear complex **87** was the best inhibitor showing almost identical IC_{50} values (4.71/4.81 μM) in both strains. No direct relationship could be found for the number of metal centers and antiplasmodial activity.[170]

Bioorganometallic compounds comprise the biggest successes in antimalarial metallotherapy to date. Some of these compounds are exceedingly more active than the classic antimalarial drug chloroquine in chloroquine-resistant strains. The cooperative effects between the metal and the organic antimalarial portion of the molecule are beneficial for overall activity. The toxicity of the metal and the discovered ability to avoid detection by the transmembrane proteins, being a cause of resistance, led to an increased accumulation of drug inside the parasite food vacuole. Represented by the benchmark compound ferroquine (**44**) as the only metallodrug that has entered clinical trials as an antimalarial, organometallic antimalarial drugs have proven to be a promising field for investigation. Modification of an

existing drug such as chloroquine would offer a second mainstay for drug developers in their search for new remedies of disease, benefiting from the previously gathered knowledge-base. Most of these compounds offer diverse scaffolds for the potential exploitation of activity and the study of their properties. Even if not suitable as a stand-alone drug, most of these compounds are potential partners for a combination therapy approach with other antimalarials.

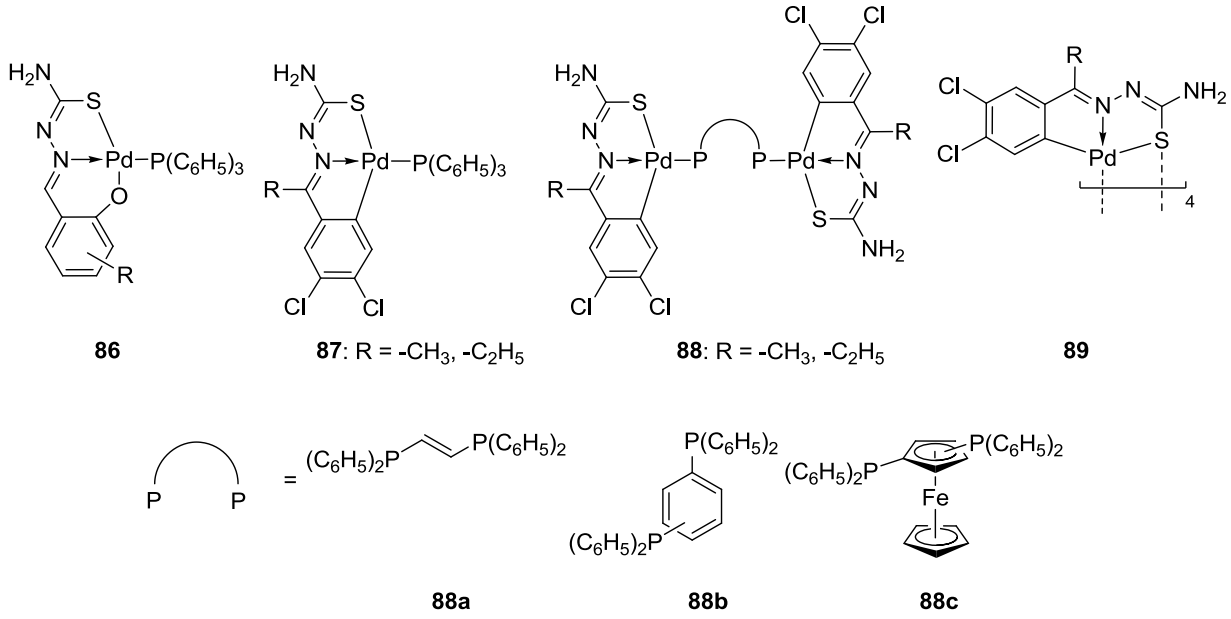

Figure 1.18. Organometallic compounds with antimalarial action, not containing chloroquine.

1.5 Thesis overview

This thesis explores the synthesis and biological evaluation of conjugates of ferrocene and quinoline antimalarial drugs. Since the discovery of ferroquine, several ferrocenyl analogs of chloroquine have been synthesized and studied; however, to date, none of them has been able to outdo ferroquine in performance and, possibly more importantly, studies have not been able to explain unequivocally the role of the iron and how does it contributes to the overcoming of resistance when ferrocene is bound to chloroquine. We consider the continuation of this exploration of utmost importance since more rational designs will be needed soon if resistance to current antimalarials continues to grow worldwide.

The specific goals of this thesis comprised the synthesis of a set of ferrocene chloroquine derivatives with a previously unexplored form of derivatization and the structure activity relationship study of this specific conformation by correlation of its antiplasmodial activity with other biological and physicochemical properties. Other specific goals were the synthesis of compounds based on different therapeutic approaches such as multiple loading and multifunctional therapy. We consider important that having discovered the potential of ferrocene chloroquine compounds as antimalarials, all possible uses and applications must be investigated since a direct application of this type of metallocene drug could be needed in the near future.

Chapter 2 focuses on the synthesis and characterization of a set of ferrocene chloroquine derivatives showcasing a previously-unexplored mode of substitution with the chloroquine derivative bridging both cyclopentadienyl rings of the ferrocene. The corresponding literature-known organic fractions and monosubstituted ferrocenyl analogs were also synthesized.

Chapter 3 focuses on the structural activity relationship study of the sets of compounds described in Chapter 2. The different modes of substitution on ferrocene have a significant effect in the biological activity and the physicochemical properties of the final products. Antiplasmodial activity against drug-sensitive and drug-resistant *P.falciparum* strains is correlated to physical properties such as lipophilicity, capacity to undergo hydrogen bonding and association with hematin. This correlation sheds light into the elucidation of the structural factors that determine the antimalarial action of these biorganometallic compounds.

Chapter 4 focuses on the synthesis and characterization of other ferrocene derivatives of quinoline antimalarial drugs, chloroquine and mefloquine, following the therapeutic approach of multiple loading of drugs.

Chapter 5 explores one final drug design approach, the multifunctional therapy. Ferrocenyl conjugates of chloroquine and mefloquine and glucosamine were synthesized in the hopes that glucose would improve the targeting of the drug to the parasites present in the red blood cells.

Finally, Chapter 6 contains the summary and conclusion of the work presented in this thesis, outlining potential avenues for future work.

CHAPTER 2 SYNTHESIS AND CHARACTERIZATION OF CHLOROQUINE-BRIDGED FERROCENYL CONJUGATES

2.1 Introduction

As mentioned in the previous chapter, among all the organometallic compounds synthesized and tested for antimalarial activity, ferrocene antimalarial drug conjugates demonstrated the most promising activity. Ferrocene has particular properties such as stability under both aqueous and aerobic conditions, non-toxicity, high lipophilicity, small size, accessible redox potential and ease of derivatization which make it highly attractive for biological applications.[171,172] Ferrocene derivatives of chloroquine are by far the most successful drug candidates.

Ferroquine (FQ, Figure 2.1), the benchmark compound, emerged from a collaborative drug discovery project in which more than 50 ferrocene compounds were synthesized.[100] It was first synthesized in 1997 and incorporates ferrocene into the lateral side chain of chloroquine, between the two exocyclic nitrogens substituting two alkyl carbons by two Cp-carbons of ferrocene, maintaining the 1-4 relative position of the two exocyclic nitrogens.[129]

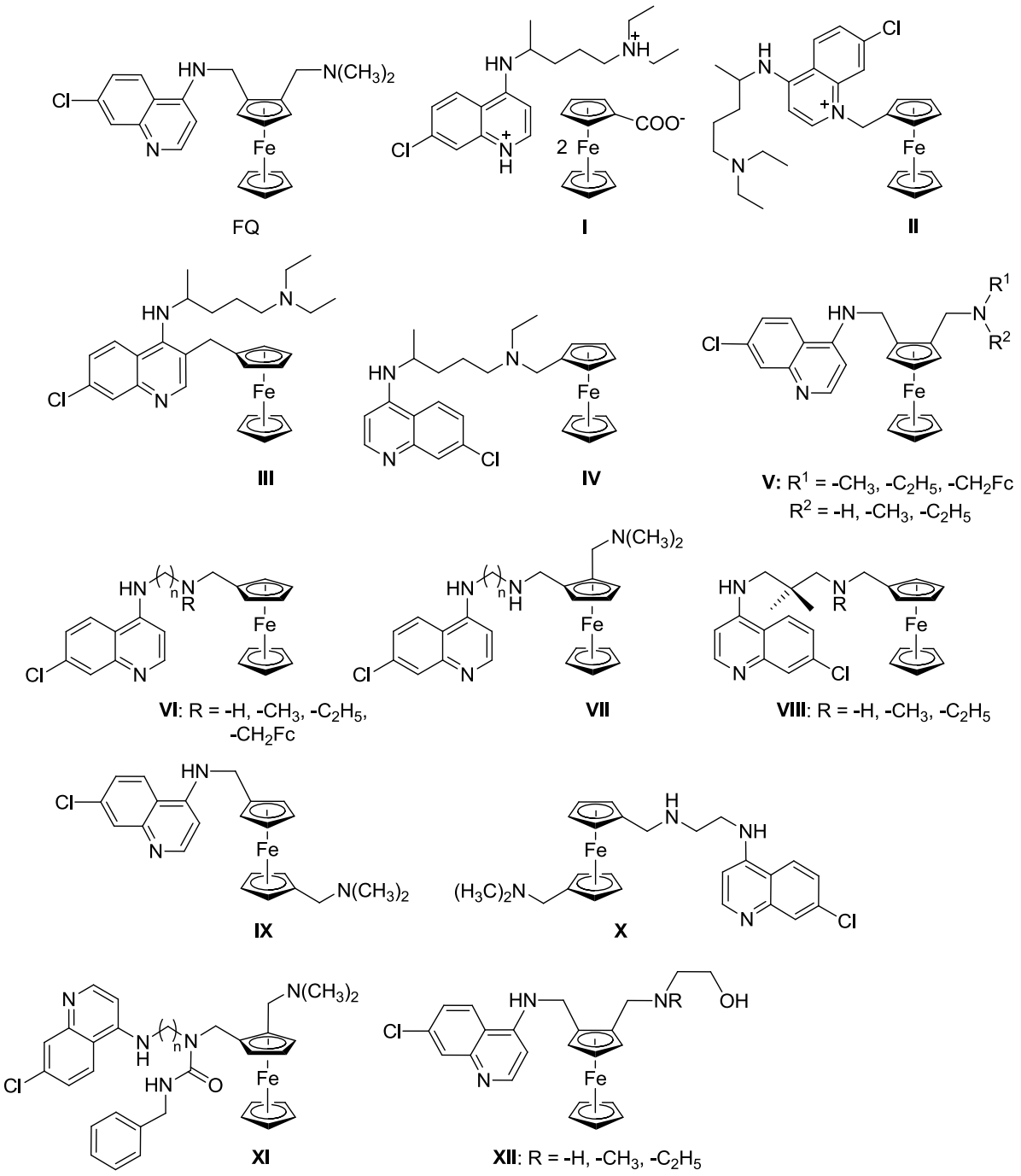

Figure 2.1. Ferroquine and known structural analogs.[130,131,132,141,142,143,144]

Ferroquine, or 7-chloro-4-[[[2-[(*N*,*N*-dimethylamino)methyl] ferrocenyl]methyl]amino] quinoline, was synthesized in a 5-step synthesis with a total yield of approximately 50%.[129] The product called ferroquine is normally the tartrate salt of the free base ferroquine. According to Lipinski's rules,[173] the free base will be more suitable for pharmaceutical purposes but the tartrate salt seems to be much more water-soluble, which is also considered in the famous set of rules for drug-likeness.[173] Regardless of the difference, ferroquine and its tartrate salt have the same level of activity, the latter being more useful for its increased water solubility.

Ferroquine was remarkably active against *Plasmodium falciparum*, regardless of the level of susceptibility to chloroquine, *in vitro* and *in vivo*.[129,130,131,132,133,135,136] Ferroquine has the same IC_{50} range as does chloroquine in chloroquine-susceptible parasites but is approximately 30 times more active than chloroquine in chloroquine-resistant parasites.[130] FQ is also more active than the commercially available chloroquine diphosphate (CQDP) (35-times higher against chloroquine-resistant isolates) and many other commonly used antimalarial drugs.[102,125]

Furthermore, the positive significant correlations[134] (as a measure of linear dependence: a positive correlation (r^2) between the IC_{50} values of two drugs indicates the possibility of cross-resistance or the capacity to develop resistance to the "new" drug, if there is resistance for the "old" drug) observed between the responses of ferroquine and drugs such as chloroquine, amodiaquine, quinine, mefloquine, halofantrine, artesunate, atovaquone, cycloguanil and pyrimethamine were too low to suggest cross-resistance among multiple field isolates.[134,137,138] Also, susceptibility of *P. falciparum* field isolates to ferroquine is not associated with a specific polymorphism or a modulation of expression of the *PfCRT* gene.[174]

Ferroquine, in summary, offers (i) activity at nanomolar concentrations,[134] greater potency than any quinoline-containing antimalarial drug and potency comparable to artemisinins against chloroquine-sensitive and resistant *P. falciparum* strains *in vitro*; (ii) activity *in vivo* against strains of *P. berghei*, *P. yoeli* and *P. vinckei*;[102] (iii) inhibition of the *in vivo* development of both chloroquine-sensitive and resistant *P. vinckei* strains and protection of mice from lethal infection with a curative effect that was 5-20 times more potent than chloroquine;[135,136] (iv) high selectivity and therapeutic indices;[175,176] and (v) unlikely development of resistance so it can be used as monotherapy or in combination with existing therapies.[177]

Several structural analogs of ferroquine were synthesized during the last 15 years.[130,131,132,141,142,143,144] A selection of them is shown in Figure 2.1. FQ analogs explored different connectivity between the ferrocene and the chloroquine moiety. These include an ionic pair chloroquine-ferrocene (I),[130] ferrocene attached to different positions on chloroquine such as directly connected to the quinoline ring (III),[140] to the quinoline nitrogen (II)[131] or to the terminal position of chloroquine (IV, VI, VIII).[144] While maintaining the internal position of ferrocene in FQ, homo- and heteroannular substitution was studied (VII and IX,X, respectively).[142] Substitution on the alkyl amino position on chloroquine was also explored (VIII, XI, XII).[132,141]

Structure-activity relationship studies showed that incorporation of a ferrocenyl moiety as an integral part of the side chain of chloroquine between the two exocyclic nitrogens of a chloroquine derivative has superior efficacy to other analogs in which the moiety is attached terminally on the side chain (IV)[144] or bound to the quinoline nitrogen (II).[131,132] In order to have antiplasmodial activity, ferrocene requires covalent linkage to the 4-aminoquinoline and

the alkyl amine moieties.[130] Thus, while ferrocene alone does not show any efficacy, ferrocene incorporation enhanced the potency of chloroquine when enclosed within the molecule.[132] The pattern of substitution of the ferrocene, as either 1,2- (FQ) or 1,1'-disubstituted (IX) ferrocene, seems to have little effect on the activity. The 1,1'-disubstituted analogs presented only a slightly lower activity in the examined chloroquine-resistant strains.[142] Also, each pure enantiomer of the 1,2-ferrocene derivative (FQ) that possesses planar chirality is equally active, yet slightly less potent than the racemic mixture.[178]

Recent publications have reviewed in great detail the diverse list of ferrochloroquine analogs.[140,175,179] Unfortunately, none of these ferroquine derivatives has out-performed FQ in antimalarial potency and pharmacological properties, thus demonstrating, indirectly, the structural specificity of the antimalarial action of FQ.

One pattern of substitution on ferrocenyl chloroquine that was never explored consists of the 1,1'-disubstitution of the Cp rings of ferrocene by a molecule of chloroquine that works as a bridge (Figure 2.2). Since antimalarial activity seems to be strongly structurally dependant, it is worthwhile to study this new class of ferrocene-chloroquine connectivity and explore its effects in the antiplasmodial activity. This chapter describes the synthesis and characterization of a series of ferroquine derivatives that incorporate this connectivity pattern (**5a-e**), along with the synthesis and characterization of the respective mono-substituted ferrocenyl chloroquine derivatives (**4a-e**) and organic quinoline fragments (**3a-e**).

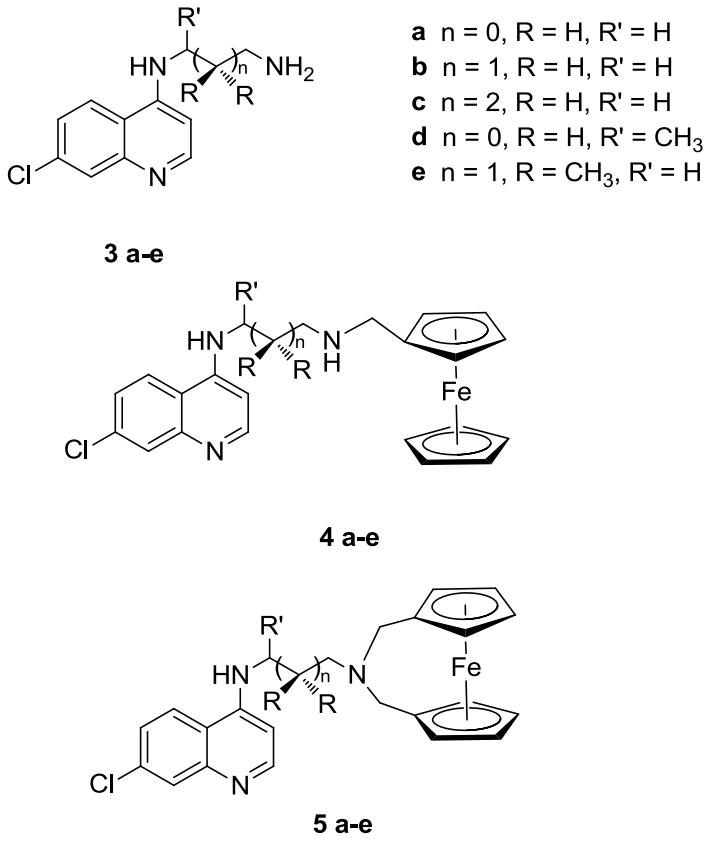

Figure 2.2. Chloroquine derivatives (**3**), monosubstituted chloroquine ferrocenyl compounds (**4**) and 1,1'-disubstituted bridged chloroquine ferrocenyl conjugates (**5**).

2.2 Experimental

2.2.1 Materials and instrumentation

All syntheses were performed using dried solvents under an inert atmosphere (nitrogen or argon) using *Schlenk*-type glassware unless otherwise indicated. Solvents were dried and distilled prior to use. All other chemicals were purchased from Sigma Aldrich or Acros Organics and used without further purification. Selected syntheses were carried using a

microwave reactor Initiator 2.5 (Biotage). Column chromatography was performed using ultra pure silica gel (230-400 mesh) (Silicycle) or alumina neutral (60-325 mesh) (Fisher Scientific). An automated column system CombiFlashRf (Teledyne ISCO, Inc.) was also employed using RediSepRf gold silica high performance columns.

^{1}H and ^{13}C NMR spectra were recorded at room temperature on Bruker AV-300, AV-400dir, AV-400inv and AV-600 instruments at 300, 400, 400 and 600 MHz, respectively. The NMR spectra are expressed on the δ (ppm) scale and referenced to residual solvent peaks or internal tetramethylsilane. The NMR assignments were supported by additional 2D experiments ($^{1}H/^{1}H$-COSY, $^{1}H/^{13}C$-HSQC, $^{1}H/^{13}C$-HMBC). High resolution mass spectra and elemental analyses were performed at the UBC Chemistry Mass Spectrometry and Microanalysis Services. Low resolution mass spectra were obtained using a Bruker Esquire Ion Trap ESI-MS spectrometer. High resolution mass spectra were obtained on a Waters/Micromass LCT spectrometer. Elemental analyses were performed on a *Carlo Erba* Elemental Analyzer EA 1108. X-ray data were collected and processed by Dr. B. O. Patrick at UBC using a Bruker X8 APEX II diffractometer with graphite monochromated Mo-Kα radiation. The structures were solved using the Bruker SAINT software package (SAINT. Version 7.60A. Bruker AXS Inc., Madison, Wisconsin, USA. 1997-2009). All non-hydrogen atoms were refined anisotropically. All hydrogen atoms were placed in calculated positions. All N-H hydrogen atoms were located in difference maps and refined isotropically. All other hydrogen atoms were included in calculated positions but not refined. Further crystal structure exploration and analysis was conducted using the Mercury software package (Version.2.3, CCDC, Cambridge, UK.).

2.2.2 Synthesis

1,1'-Bis(*N,N'*-dimethylaminomethyl)ferrocene (1).

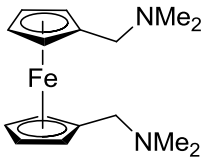

This compound was prepared as previously reported[180] with slight modifications. *n*-Butyllithium (1.6 M in hexanes, 32.8 mL, 52.5 mmol, 2.1 equiv) was added dropwise to a stirred solution of freshly distilled TMEDA (7.83 mL, 52.5 mmol, 2.1 equiv) in hexanes (10 mL). Ferrocene (4.65 g, 25.0 mmol, 1.0 equiv) was dissolved in hexanes (180 mL) and added dropwise by syringe over a period of an hour. The reaction mixture was stirred under inert atmosphere at RT for 12 hours. The solution was further diluted with THF (200 mL) and (*N,N'*-dimethyl)methyleneammonium iodide (9.7 g, 52.5 mmol, 2.1 equiv) was added in one portion. The reaction mixture was heated under reflux for ten minutes and then allowed to cool to room temperature and stirred under inert atmosphere for 24 hours. Water (30 mL) was added to terminate the reaction. The organic layer was separated and the aqueous layer was extracted with portions of diethyl ether (3 x 25 mL). The combined organic fractions were dried over anhydrous $MgSO_4$ and the solvent was removed under reduced pressure to afford an orange-brown oil. Purification of the desired product was done by flash column chromatography on neutral alumina Brockman activity V. Elution was achieved with petroleum ether to obtain unreacted ferrocene, diethyl ether/petroleum ether (3:7) to obtain the mono-dimethylaminomethyl derivative and methanol/diethylether (3:97) to obtain product **1** as an orange-brown oil (2.64 g, 8.79 mmol, 35%). ^{1}H NMR (400 MHz, $CDCl_3$) δ (ppm) 4.10 (t, ^3J = 1.71 Hz, 4H), 4.07 (t, ^3J = 1.71 Hz, 4H), 3.27 (s, 4H), 2.17 (s, 12H).

1,1'-Bis(*N,N'*-trimethylaminomethyl)ferrocene iodide (2).

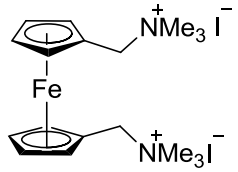

Based on a previously published method,[180] iodomethane (1.4 mL, 22.4 mmol, 3 equiv) was added slowly to a solution of 1,1'-bis(*N,N*-dimethylaminomethyl)ferrocene (**1**, 2.24 g, 7.47 mmol, 1 equiv) in methanol (40 mL) under inert atmosphere. The resulting solution was heated at reflux for 10 minutes before cooling to RT. Diethyl ether (150 mL) was then added and the product precipitated as a pale yellow solid, which was collected by filtration, washed with dichloromethane (30 mL) and diethyl ether (2x 25 mL) before being dried under vacuum to yield 1,1'-bis(*N,N'*-trimethylaminomethyl)ferrocene iodide **2** as a yellow powder (3.0 g, 6.2 mmol, 83%). ^{1}H NMR (300 MHz, CD_3OD): δ (ppm) 4.69 (s, 4H), 4.66 (t, ^{3}J = 1.83 Hz, 4H), 4.56 (t, ^{3}J = 1.96 Hz, 4H), 3.07 (s, 18H). ESI-MS(+): 457.1 $[M\text{-}I]^{+}$. Anal. Calc. for $C_{18}H_{30}FeI_2N_2$: C, 37.01; H, 5.18; N, 4.08. Found: C, 37.34; H, 5.13; N, 4.58.

General procedure for the synthesis of 4-aminoquinoline derivatives (3a-e).

N-(7-Chloroquinolin-4-yl)-ethane-1,2-diamine (**3a**), *N*-(7-chloroquinolin-4-yl)-propane-1,3-diamine (**3b**), N-(7-chloroquinolin-4-yl)-butane-1,4-diamine (**3c**), N-(7-chloroquinolin-4-yl)-propane-1,2-diamine (**3d**) and N-(7-chloroquinolin-4-yl)-2,2-dimethylpropane-1,3-diamine (**3e**) were prepared by following modifications from literature procedures.[132,181,182,183] 4,7-Dichloroquinoline (1 g, 5.04 mmol, 1 equiv) was dissolved in the respective diamine (approx. 50.4 mmol, 10 equiv) in a 20 mL microwave vial. The mixture was heated using a heat gun until complete dissolution. The reaction was carried out in a microwave reactor for 30 min at 165 °C. After cooling the vial to room temperature, aqueous NaOH (1N, 10 mL) was added and the mixture was extracted with methylene chloride (3 x 15 mL). The organic

fractions were combined and successively washed with water (3 x 10 mL) and brine (3 x 10 mL). The organic layer was dried over anhydrous $MgSO_4$ and the solvent was removed under reduced pressure. The respective products (**3a-e**) were obtained by precipitation after the addition of a 8:2 hexane/methylene chloride solution.

***N*-(7-Chloroquinolin-4-yl)-ethane-1,2-diamine (3a).**

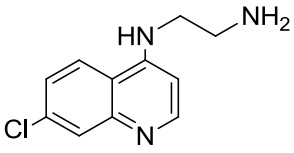

This compound was obtained as a yellow solid (0.74 g, 3.33 mmol, 65%). ^{1}H NMR (300 MHz, $CDCl_3$): δ (ppm) 8.52 (d, ^3J = 5.5 Hz, 1H), 7.95 (d, ^4J = 2.1 Hz, 1H), 7.74 (d, ^3J = 9.1 Hz, 1H), 7.35 (dd, ^3J = 9.1 Hz, ^4J = 2.1 Hz, 1H), 6.40 (d, ^3J = 5.5 Hz, 1H), 5.82 (br. s., 1H), 3.32 (m, 2H), 3.12 (m, 2H), 1.48 (br. s., 2H). ^{13}C NMR (75 MHz, $CDCl_3$): δ (ppm) 152.2, 150.1, 149.3, 135.0, 128.9, 125.4, 121.4, 117.6, 99.4, 44.9, 40.4. Anal. Calc. for $C_{11}H_{12}ClN_3$: C, 59.60, H, 5.46, N, 18.95; found: C, 59.34, H, 5.42, N, 18.87. ESI-MS (HR) calculated for $C_{11}H_{13}ClN_3^+$: 222.0798, found: 222.0793 $[M + H]^+$.

***N*-(7-Chloroquinolin-4-yl)-propane-1,3-diamine (3b).**

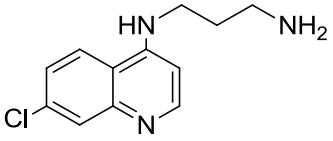

This compound was obtained as a beige solid (1.08 g, 4.55 mmol, 89%). ^{1}H NMR (300 MHz, $CDCl_3$): δ (ppm) 8.50 (d, ^3J = 5.3 Hz, 1H), 7.93 (d, ^4J = 1.9 Hz, 1H), 7.72 (d, ^3J = 9.0 Hz, 1H), 7.44 (br. s., 1H), 7.31 (dd, ^3J = 9.0 Hz, ^4J = 1.9 Hz, 1H), 6.33 (d, ^3J = 5.3 Hz, 1H), 3.42 (m, 2H), 2.87 (t, ^3J = 5.7 Hz, 2H), 1.90 (m, ^3J = 5.7 Hz, 2H), 1.65 (br. s., 2H). ^{13}C NMR (75 MHz, $CDCl_3$): δ (ppm) 152.3, 150.6, 149.4, 134.8, 128.7, 125.1, 122.2, 117.7, 98.4, 43.9, 41.7, 30.1. ESI-MS (HR) calculated for $C_{12}H_{15}ClN_3^+$: 236.0955, found: 236.0953 $[M + H]^+$.

***N*-(7-Chloroquinolin-4-yl)-butane-1,4-diamine (3c).**

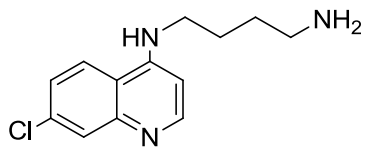

This compound was obtained as an off-white solid (0.62 g, 2.48 mmol, 48%). ^{1}H NMR (400 MHz, $CDCl_3$): δ (ppm) 8.53 (d,^{3}J = 5.5 Hz, 1H), 7.95 (d, ^{4}J = 2.1 Hz, 1H), 7.74 (d, ^{3}J = 8.8 Hz, 1H), 7.34 (dd, ^{3}J = 8.8, ^{4}J = 2.1 Hz, 1H), 6.39 (d, ^{3}J = 5.5 Hz, 1H), 6.00 (br. s., 1H), 3.32 (m, 2H), 2.84 (t, ^{3}J = 6.5 Hz, 2H), 1.88 (quin, ^{3}J = 6.9 Hz, 2H), 1.67 (quin, ^{3}J = 6.9 Hz, 2H), 1.44 (br. s., 2H). ^{13}C NMR (101 MHz, $CDCl_3$): δ (ppm) 152.1, 149.2, 144.1, 134.7, 128.8, 125.0, 121.4, 117.3, 98.8, 43.2, 41.5, 30.8, 26.1. ESI-MS (HR) calculated for $C_{13}H_{17}ClN_3^+$: 250.1111, found: 250.1114 $[M + H]^+$.

***N*-(7-Chloroquinolin-4-yl)-propane-1,2-diamine (3d).**

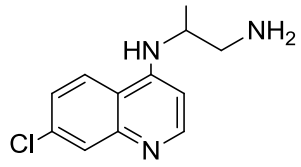

This compound was obtained as an off-white solid (0.68 g, 2.88 mmol, 56%). ^{1}H NMR (400 MHz, $CDCl_3$): δ (ppm) 8.53 (d, ^{3}J = 5.5 Hz, 1H), 7.96 (d, ^{4}J = 2.0 Hz, 1H), 7.75 (d, ^{3}J = 8.9 Hz, 1H), 7.38 (dd, ^{3}J = 8.9 Hz, ^{4}J = 2.0 Hz, 1H), 6.40 (d, ^{3}J = 5.5 Hz, 1H), 5.85 (br. s., 1H), 3.32 (m, 2H), 3.00 (m, 1H), 1.64 (s, 2H), 1.27 (d, ^{3}J = 6.1 Hz, 3H). ^{13}C NMR (101 MHz, $CDCl_3$): δ (ppm) 152.4, 150.2, 149.5, 135.1, 129.1, 125.6, 121.5, 117.7, 99.5, 50.3, 46.1, 23.3. Anal. Calc. for $C_{12}H_{14}ClN_3$: C, 61.15, H, 5.99, N, 17.83, found: C, 61.22, H, 5.96, N, 17.76. ESI-MS (HR) calculated for $C_{12}H_{15}ClN_3^+$: 236.0955, found: 236.0948 $[M + H]^+$.

***N*-(7-Chloroquinolin-4-yl)-2,2-dimethylpropane-1,3-diamine (3e).**

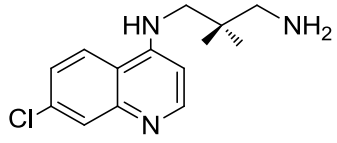

This compound was obtained as a yellowish solid (0.70 g, 2.62 mmol, 52%). ^{1}H NMR (300 MHz, $CDCl_3$): δ (ppm) 8.48 (br. s.,

1H), 8.47 (d, ^{3}J = 5.4 Hz, 1H), 7.91 (d, ^{4}J = 2.2 Hz, 1H), 7.72 (d, ^{3}J = 9.0 Hz, 1H), 7.29 (dd, ^{3}J = 9.0 Hz, ^{4}J = 2.2 Hz, 1H), 6.27 (d, ^{3}J = 5.4 Hz, 1H), 3.18 (br. s., 2H), 2.87 (br. s., 2H), 1.68 (br. s., 2H), 1.08 (s, 6H). ^{13}C NMR (75 MHz, $CDCl_3$): δ (ppm) 152.3, 151.1, 149.4, 134.7, 128.6, 124.9, 122.5, 117.9, 98.0, 55.9, 52.9, 34.0, 24.7. Anal. Calc. for $C_{14}H_{18}ClN_3$: C, 63.75, H, 6.88, N, 15.93; found: C, 63.16, H, 6.83, N, 15.85. ESI-MS (HR) calculated for $C_{14}H_{19}ClN_3^+$: 264.1268, found: 264.1270 $[M + H]^+$.

General procedure for the synthesis of mono-substituted ferrocenyl 4-aminoquinoline derivatives (4a-e).

These compounds were prepared as previously reported (with the exception of **4d**)[132] with modifications. Ferrocenecarboxaldehyde (0.214 g, 1.0 mmol, 1 equiv) and the corresponding 4-aminoquinoline derivative **3a-e** (1.10 mmol, 1.1 equiv) were dissolved in dry methanol (20 mL). The mixture was stirred at room temperature overnight. Sodium borohydride (0.114 g, 3.0 mmol, 3 equiv) was added and the resulting mixture was stirred for an additional 2 hours. The reaction mixture was quenched with the addition of 5% $NaHCO_3$ solution (10 mL) and the resulting mixture was extracted with diethyl ether (3 x 20 mL). The combined organic fractions were dried over anhydrous Na_2SO_4 and solvent was removed under reduced pressure. Purification of the desired product was done by flash column chromatography on silica with a mixture of ethyl acetate/methanol/TEA in increasing polarity 94:4:2 to 75:15:10 ratios.

***N*-(7-Chloro-4-quinolyl)-*N*'-ferrocenyl ethane-1,2-diamine (4a).**

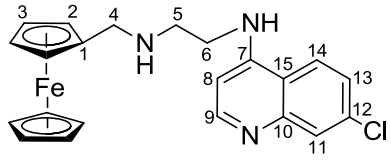

This product was obtained as an orange solid (0.254 g, 0.61 mmol, 61%). ^{1}H NMR (300 MHz, $CDCl_3$): δ (ppm) 8.52 (d, ^{3}J = 5.4 Hz, 1H, 9-H), 7.95 (d, ^{4}J = 2.1 Hz, 1H, 11-H), 7.70 (d, ^{3}J = 8.9 Hz, 1H, 14-H), 7.35 (dd, ^{3}J = 8.9 Hz, ^{4}J = 2.1 Hz, 1H, 13-H), 6.38 (d, ^{3}J = 5.4 Hz, 1H, 8-H), 5.91 (br, 1H, Ar-N*H*-), 4.19 (m, 2H, 2-H), 4.14 (m, 2H, 3-H), 4.13 (s, 5H, Cp-H), 3.59 (s, 2H, 4-H), 3.31 (m, 2H, 6-H), 3.05 (m, 2H, 5-H), 1.92 (vb, 1H, CH_2NHCH_2). ^{13}C NMR (75 MHz, $CDCl_3$): δ (ppm) 152.3 (C9), 150.1 (C7), 149.3 (C10), 135.0 (C12), 128.8 (C11), 125.4 (C13), 121.6 (C14), 117.6 (C15), 99.4 (C8), 86.5 (C1), 68.7 (*Cp*), 68.6 (C2), 68.2 (C3), 48.5 (C4), 47.0 (C6), 42.1 (C5). Anal. Calc. for $C_{22}H_{22}ClFeN_3$: C, 62.95, H, 5.28, N, 10.01; found: C, 61.72, H, 5.38, N, 9.82. ESI-MS (HR) calculated for $C_{22}H_{23}ClFeN_3^+$: 420.0930, found: 420.0931 $[M + H]^+$.

***N*-(7-Chloro-4-quinolyl)-*N*'-ferrocenyl propane-1,3-diamine (4b).**

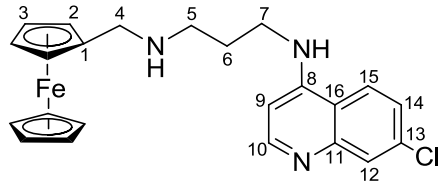

This product was obtained as a yellow solid (0.356 g, 0.82 mmol, 82%). ^{1}H NMR (300 MHz, $CDCl_3$): δ (ppm) 8.50 (d, ^{3}J = 5.4 Hz, 1H, 10-H), 7.96 (br, 1H, Ar-N*H*-), 7.93 (d, ^{4}J = 2.0 Hz, 1H, 12-H), 7.62 (d, ^{3}J = 8.9 Hz, 1H, 15-H), 7.27 (dd, ^{3}J = 8.9 Hz, ^{4}J = 2.0 Hz, 1H, 14-H), 6.29 (d, ^{3}J = 5.4 Hz, 1H, 9-H), 4.24 (m, 2H, 2-H), 4.22 (m, 2H, 3-H), 4.17 (s, 5H, Cp-H), 3.62 (s, 2H, 4-H), 3.38 (m, 2H, 7-H), 2.98 (m, 2H, 5-H), 1.92 (m, 2H, 6-H), 1.80 (vb, 1H, CH_2NHCH_2). ^{13}C NMR (75 MHz, $CDCl_3$): δ (ppm) 152.4 (C10), 150.8 (C8), 149.4 (C11), 134.7 (C13), 128.7 (C12), 125.1 (C14), 122.7 (C15), 117.8 (C16), 98.3 (C9), 86.0 (C1), 68.9 (C2), 68.7 (Cp), 68.4 (C3), 49.8 (C4), 49.7 (C7), 44.5 (C5), 27.4 (C6).

Anal. Calc. for $C_{23}H_{24}ClFeN_3$: C, 63.69, H, 5.58, N, 9.69; found: C, 63.67, H, 5.59, N, 9.62. ESI-MS (HR) calculated for $C_{23}H_{25}ClFeN_3^+$: 434.1086, found: 434.1089 $[M + H]^+$.

***N*-(7-Chloro-4-quinolyl)-*N*'-ferrocenyl butane-1,4-diamine (4c).**

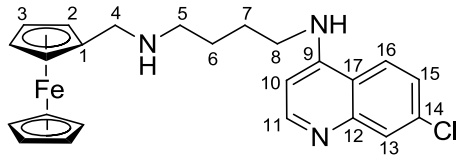

This product was obtained as a light yellow solid (0.323 g, 0.72 mmol, 72%). ^{1}H NMR (300 MHz, $CDCl_3$): δ (ppm) 8.52 (d, ^3J = 5.5 Hz, 1H, 11-H), 7.95 (d, ^4J = 2.1 Hz, 1H, 13-H), 7.74 (d, ^3J = 8.9 Hz, 1H, 16-H), 7.31 (dd, ^3J = 8.9 Hz, ^4J=2.1 Hz, 1H, 15-H), 6.37 (d, ^3J = 5.5 Hz, 1H, 10-H), 6.07 (br, 1H, Ar-N*H*-), 4.20 (d, ^3J = 1.8 Hz, 2H, 2,3-H), 4.14 (s, 5H, Cp-H), 3.59 (s, 2H, 4-H), 3.30 (m, 2H, 8-H), 2.76 (m, 2H, 5-H), 2.32 (br. s., 1H, CH_2NHCH_2), 1.86 (m, 2H, 7-H), 1.72 (m, 2H, 6-H). ^{13}C NMR (75 MHz, $CDCl_3$): δ (ppm) 155.5 (C11), 155.1 (C9), 151.9 (C12), 134.8 (C14), 128.5 (C13), 125.1 (C15), 121.6 (C16), 117.3 (C17), 98.8 (C10), 85.3 (C1), 68.6 (C2), 68.5 (Cp), 68.1 (C3), 48.8 (C4), 48.1 (C8), 43.1 (C5), 27.3 (C7), 26.1 (C6). Anal. Calc. for $C_{24}H_{26}ClFeN_3$: C, 64.37, H, 5.85, N, 9.38; found: C, 64.01, H, 6.11, N, 8.98. ESI-MS (HR) calculated for $C_{24}H_{27}ClFeN_3^+$: 448.1243, found: 448.1249 $[M + H]^+$.

***N*-(7-Chloro-4-quinolyl)-*N*'-ferrocenyl propane-1,2-diamine (4d).**

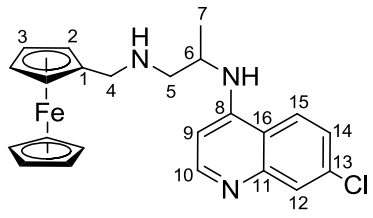

This product was obtained as a yellow solid (0.366 g, 0.84 mmol, 84%). ^{1}H NMR (300 MHz, $CDCl_3$): δ (ppm) 8.53 (d, ^3J = 5.3 Hz, 1H, 10-H), 7.96 (d, ^4J = 2.0 Hz, 1H, 12-H), 7.66 (d, ^3J = 8.9 Hz, 1H, 15-H), 7.36 (dd, ^3J = 8.9 Hz, ^4J = 2.0 Hz, 1H, 14-H), 6.37 (d, ^3J = 5.5 Hz, 1H, 9-H), 5.94 (br. s., 1H, Ar-N*H*-), 4.21 (s, 1H, 2-H), 4.18 (s,

1H, 3-H), 4.14 (s, 2H, 2',3'-H), 4.13 (s, 5H, Cp-H), 3.59 (m, 2H, 4-H), 3.32 (m, 1H, 5-H), 3.15 (m, 1H, 5'-H), 3.02 (m, 1H, 6-H), 1.58 (br. s., 1H, CH_2NHCH_2), 1.27 (d, ^3J = 6.1 Hz, 3H, 7-H). ^{13}C NMR (75 MHz, $CDCl_3$): δ (ppm) 150.8 (C10), 150.3 (C8), 141.9 (C11), 135.6 (C13), 126.9 (C12), 125.6 (C14), 122.2 (C15), 117.1 (C16), 98.6 (C9), 89.9 (C1), 68.8 (C2), 68.6 (Cp), 68.4 (C3), 50.5 (C4), 46.7 (C6), 45.4 (C5), 17.5 (C7). Anal. Calc. for $C_{23}H_{24}ClFeN_3$: C, 63.69, H, 5.58, N, 9.69; found: C, 63.69, H, 5.94, N, 9.55. ESI-MS (HR) calculated for $C_{23}H_{25}ClFeN_3^+$: 434.1086, found: 434.1090 $[M + H]^+$.

***N*-(7-Chloro-4-quinolyl)-*N*'-ferrocenyl 2,2-dimethyl-propane-1,3-diamine (4e).**

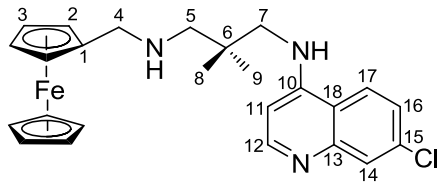

This product was obtained as a light yellow solid (0.313 g, 0.68 mmol, 68%). ^{1}H NMR (300 MHz, $CDCl_3$): δ (ppm) 8.56 (br, 1H, Ar-N*H*-), 8.47 (d, ^3J = 5.4 Hz, 1H, 12-H), 7.90 (d, ^4J = 2.0 Hz, 1H, 14-H), 7.60 (d, ^3J = 8.9 Hz, 1H, 17-H), 7.19 (dd, ^3J = 8.9 Hz, ^4J = 2.0 Hz, 1H, 16-H), 6.25 (d, ^3J = 5.4 Hz, 1H, 11-H), 4.24 (m, 2H, 2-H), 4.23 (m, 2H, 3-H), 4.15 (s, 5H, Cp-H), 3.58 (br, 2H, 4-H), 3.14 (m, 2H, 7-H), 2.77 (br, 2H, 5-H), 1.50 (vb, 1H, CH_2NHCH_2), 1.09 (s, 6H, 8,9-H). ^{13}C NMR (75 MHz, $CDCl_3$): δ (ppm) 152.4 (C12), 151.1 (C10), 149.4 (C13), 134.6 (C15), 128.6 (C14), 125.0 (C16), 123.0 (C17), 117.0 (C18), 97.9 (C11), 85.9 (C1), 69.1 (C2), 68.7 (Cp), 68.5 (C3), 61.3 (C7), 56.1 (C4), 50.4 (C5), 33.8 (C6), 25.2 (C8-9). Anal. Calc. for $C_{25}H_{28}ClFeN_3$: C, 65.02, H, 6.11, N, 9.10; found: C, 64.91, H, 6.38, N, 8.62. ESI-MS (HR) calculated for $C_{25}H_{29}ClFeN_3^+$: 462.1399, found: 462.1413 $[M + H]^+$.

General procedure for the synthesis of bridged ferrocenyl 4-aminoquinoline derivatives (5a-e).

Method A: 1,1'-bis(*N,N'*-trimethylaminomethyl)ferrocene iodide **2** (0.10 g, 0.17 mmol, 1 equiv), the corresponding 4-aminoquinoline derivative **3a-e** (0.34 mmol, 2 equiv) and NaOH (0.04 g, 1 mmol, 6 equiv) were combined with 20 mL of acetonitrile in a 20 mL microwave vial. The reaction was carried out in a microwave reactor for 6 h at 110 °C. The solvent was removed under reduced pressure. Purification of the desired product was done by flash column chromatography on silica (**5a, b, d, e**) or on preparative TLC silica gel plate (**5c**) with a acetone/dichloromethane/triethylamine (5:4:1) mixture as eluent.

Method B: 1,1'-bis(*N,N'*-trimethylaminomethyl)ferrocene iodide **2** (0.10 g, 0.17 mmol, 1 equiv), the corresponding 4-aminoquinoline derivative **3a-e** (0.34 mmol, 2 equiv) and NaOH (0.04 g, 1 mmol, 6 equiv) were refluxed in acetonitrile (20 mL) for 48 h. Purification of the desired product was as specified above.

***N*-{[*N'*-(7-Chloroquinolin-4-yl)]-ethane-1,2-diamine}-1,1'-(*N*,*N*-dimethane-yl)ferrocene (5a).**

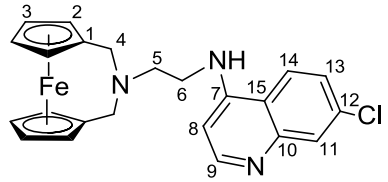

This product was obtained as a yellow solid (0.016 g, 0.037 mmol, 22%). ^{1}H NMR (600 MHz, CD_3OD): δ (ppm) 8.41 (d, ^{3}J = 5.6 Hz, 1H, 9-H), 8.13 (d, 3*J* = 8.7 Hz, 1H, 14-H), 7.82 (d, ^{4}J = 2.0 Hz, 1H, 11-H), 7.49 (dd, ^{3}J = 8.7, ^{4}J = 2.0 Hz, 1H, 13-H), 6.66 (d, ^{3}J = 5.6 Hz, 1H, 8-H), 4.10 (t, 4H, 2-H), 4.07 (t, 4H, 3-H), 3.65 (t, ^{3}J = 6.4 Hz, 2H, 6-H), 3.13 (t, ^{3}J = 6.7 Hz, 2H, 5-H), 3.06 (br. s., 4H, 4-H). ^{13}C NMR (151 MHz, CD_3OD): δ (ppm) 158.4 (C7), 149.4 (C9), 148.8 (C15), 133.4 (C10), 124.0 (C11), 123.0 (C13), 120.6 (C14), 115. 4 (C12),

96.6 (C8), 80.7 (C1), 67.5 (C3), 66.8 (C2), 52.8 (C5), 49.7 (C4), 38.5 (C6). ESI-MS (HR) calculated for $C_{23}H_{23}ClFeN_3^+$: 432.0930, found: 432.0927 $[M + H]^+$.

_N_-{[_N'_-(7-Chloroquinolin-4-yl)]-propane-1,3-diamine}-1,1'-(_N_,_N_-dimethane-yl)ferrocene (5b).

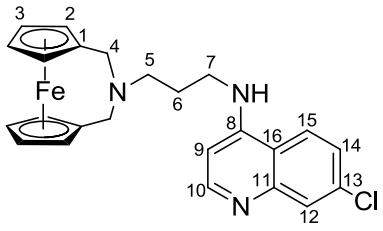

This compound can be further purified by recrystallization in an acetone/dichloromethane (1:1) mixture, yielding orange crystals (0.015 g, 0.03 mmol, 20%). ^{1}H NMR (600 MHz, CD_3OD): δ (ppm) 8.37 (d, ^3J = 5.6 Hz, 1H, 10-H), 8.14 (d, ^3J = 8.7 Hz, 1H, 15-H), 7.78 (d, ^4J = 2.0 Hz, 1H, 12-H), 7.42 (dd, ^3J = 8.7 Hz, ^{4}J = 2.0 Hz, 1H, 14-H), 6.63 (d, ^3J = 5.6 Hz, 1H, 9-H), 4.10 (t, 4H, 2-H), 4.05 (t, 4H, 3-H), 3.54 (t, 2H, 5-H), 2.96 (br. s., 4H, 4-H), 2.87 (t, 2H, 7-H), 2.09 (m, 2H, 6-H). ^{13}C NMR (151 MHz, CD_3OD): δ (ppm) 153.4 (C8), 152.4 (C10), 149.7 (C16), 136.8 (C11), 127.6 (C12), 126.4 (C14), 124.7 (C15), 119.0 (C13), 100.0 (C9), 84.3 (C1), 71.2 (C2), 70.5 (C3), 56.5 (C7), 53.5 (C4), 42.6 (C5), 27.7 (C6). ESI-MS (HR) calculated for $C_{24}H_{25}ClFeN_3^+$: 446.1086, found: 446.1093 $[M + H]^+$.

_N_-{[_N'_-(7-chloroquinolin-4-yl)]-butane-1,4-diamine}-1,1'-(_N_,_N_-dimethane-yl)ferrocene (5c).

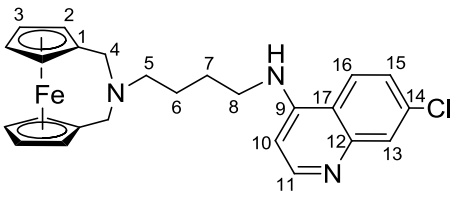

This product was obtained as a yellow solid (0.015 g, 0.033 mmol, 19%). ^{1}H NMR (400 MHz, CD_3OD): δ (ppm) 8.38 (d, ^3J = 6.0 Hz, 1H, 11-H), 8.19 (d, ^3J = 8.8 Hz, 1H, 16-H), 7.80 (d, ^4J = 2.2 Hz, 1H, 13-H), 7.48 (dd, ^3J = 9.1, ^4J = 2.2 Hz, 1H, 15-H),

6.67 (d, ^{3}J = 6.2 Hz, 1H, 10-H), 4.10 (m, 4H, 2-H), 4.07 (m, 4H, 3-H), 3.53 (m, 2H, 8-H), 3.04 (br. s., 4H, 4-H), 2.89 (m, 2H, 5-H), 1.94 (s, 2H, 7-H), 1.88 (m, 2H, 6-H). ^{13}C NMR (101 MHz, CD_3OD): δ (ppm) 152.6 (C9), 149.2 (C11), 146.5 (C17), 136.1 (C14), 125.4 (C15), 124.8 (C13), 123.4 (C16), 117.5 (C12), 98.5 (C10), 81.8 (C1), 69.7 (C2), 69.2 (C3), 57.1 (C5), 51.7 (C4), 42.8 (C8), 26.0 (C7), 24.3 (C6). ESI-MS (HR) calculated for $C_{25}H_{27}ClFeN_3^+$: 460.1243, found: 460.1255 $[M + H]^+$.

***N*-{[*N'*-(7-Chloroquinolin-4-yl)]-propane-1,2-diamine}-1,1'-(*N*,*N*-dimethane-yl)ferrocene (5d).**

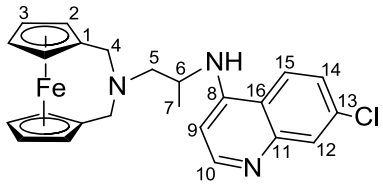

This product was obtained as a yellow solid (0.018 g, 0.04 mmol, 23%). ^{1}H NMR (600 MHz, CD_3OD): δ (ppm) 8.41 (d, ^{3}J = 5.4 Hz, 1H, 10-H), 8.13 (d, ^{3}J = 8.9 Hz, 1H, 15-H), 7.84 (d, ^{4}J = 2.3 Hz, 1H, 12-H), 7.53 (dd, ^{3}J = 8.9, ^{4}J = 1.9 Hz, 1H, 14-H), 6.61 (d, ^{3}J = 5.4 Hz, 1H, 9-H), 4.17 (m, 2H, 2-H), 4.07 (m, 2H, 2'-H), 4.02 (m, 2H, 3-H), 3.99 (m, 2H, 3'-H), 3.57 (m, 1H, 6-H), 3.46 (m, 2H, 5-H), 3.20 (m, 2H, 4-H), 2.99 (m, 2H, 4'-H), 1.26 (d, ^{2}J = 6.6 Hz, 3H, 7-H). ^{13}C NMR (151 MHz, CD_3OD): δ (ppm) 157.9 (C8), 152.8 (C10), 150.0 (C16), 136.9 (C11), 128.1 (C12), 126.6 (C14), 123.9 (C15), 118.8 (C13), 100.5 (C9), 84.5 (C1), 71.2 (C2), 71.0 (C2'), 70.4 (C3, C3'), 59.7 (C4), 47.5 (C5), 31.2 (C6), 12.5 (C7). ESI-MS (HR) calculated for $C_{24}H_{25}ClFeN_3^+$: 446.1086, found: 446.1075 $[M + H]^+$.

***N*-{[*N'*-(7-Chloroquinolin-4-yl)]-2,2-dimethylpropane-1,3-diamine}-1,1'-(*N*,*N*-dimethane-yl)ferrocene (5e).**

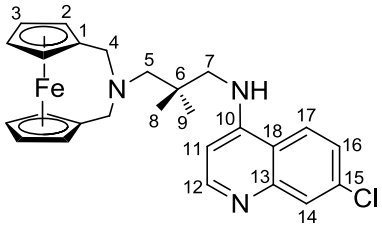

This product was obtained as a yellow solid (0.004 g, 0.009 mmol, 5%). ^{1}H NMR (400 MHz, CD_3OD): δ (ppm) 8.39 (d, ^{3}J = 6.1 Hz, 1H, 12-H), 8.25 (d, ^{3}J = 8.9 Hz, 1H, 17-H), 7.82 (d, ^{4}J = 2.4 Hz, 1H, 14-H), 7.50 (dd, ^{3}J = 8.9, ^{4}J = 2.0 Hz, 1H, 16-H), 6.76 (d, ^{3}J = 6.1 Hz, 1H, 11-H), 4.13 (m, 4H, 2-H), 4.08 (m, 4H, 3-H), 3.46 (m, 2H, 5-H), 3.04 (m, 2H, 7-H), 2.69 (m,4H, 4-H), 1.16 (s, 6H, 8,9-H). ^{13}C NMR (101 MHz, CD_3OD): δ (ppm) 161.8 (C10), 156.3 (C12), 148.4 (C18), 136.8 (C13), 129.0 (C14), 126.6 (C16), 124.6 (C17), 122.1 (C15), 100.3 (C9), 85.6 (C1), 70.7 (C2), 70.2 (C3), 61.7 (C4), 52.7 (C7), 39.9 (C5), 32.2 (C6), 14.6 (C8,9). ESI-MS (HR) calculated for $C_{26}H_{29}ClFeN_3^+$: 474.1399, found: 474.1398 $[M + H]^+$.

2.3 Results and discussion

2.3.1 Design

Malaria's resistance to chloroquine (CQ, Figure 1.4) can be circumvented by structural modifications to the parent drug. Prior work has demonstrated that 4-aminoquinolines containing modified side alkyl chains of altered lengths can retain the antiplasmodial activity of the parent drug against certain chloroquine-resistant strains of *Plasmodium falciparum*.[184,185,186] Studies on the shortening (to 2-3 carbon atoms) or the lengthening (to

10-12 carbon atoms) of this diamine alkane exocyclic linker can be determinant in overcoming the resistance to chloroquine. Other modification patterns such as the replacement of the substituents on the distal amine with bulky groups[187] and electronic changes of the aromatic ring both with electron-donating and electron-withdrawing groups were not found to cause a significant effect on the activity.[188,189]

These findings led to the conclusion that the number of carbon atoms between the two nitrogens in the diamine alkane side chain is a major factor for activity against chloroquine-resistant parasite strains.[190,191] A number of studies found that compounds presenting a shorter rather than longer side chain were among the most active, especially those with propyl[187,190] and butyl[182,189] alkyl chains.

Although these modifications represented an alternative to retain activity against resistant parasites, some disadvantages of these purely organic derivatives of chloroquine were observed. Early N-dealkylation of the side chain (during *in vivo* metabolism)[184,185,190] lowered the lipid solubility of the compounds and the antiplasmodial capacity against chloroquine-resistant parasites.[186,192] In addition, these derivatives showed a high correlation or a high index of cross-resistance with chloroquine,[184] and had increased toxicity when administered in the same doses as chloroquine.[184]

In our attempt to overcome these disadvantages associated with these chloroquine derivatives, we have synthesized ferrocenyl chloroquine conjugates with two distinct substitution patterns (**4** and **5**). We used 4-amino quinolines with an alkyl side chain of four or less carbon atoms, both linear and branched, **3**.

The first series of chloroquine analogs, the mono-substituted ferrocenyl 4-aminoquinoline derivatives (**4a-e**), presents a ferrocene moiety covalently attached at the end of the N-alkyl

amino side chain in the 4-aminoquinoline moiety. Some elements of this series of compounds have been partially studied in the past[132] and were taken here as a point of reference to develop a strong comparison with the second series of compounds.

The second series of chloroquine analogs, the bridged ferrocenyl 4-aminoquinoline derivatives (**5a-e**), was designed to incorporate the same elements of the first series, a ferrocenyl unit and the 4-aminoquinoline scaffold. Instead of the linear conformation, they present a closed conformation with the alkyl nitrogen bridging both cyclopentadienyl rings in the ferrocene, forming a ferrocenophane.

Both series of ferrocenyl compounds (**4a-e** and **5a-e**) are also structural analogs of ferroquine. These compounds were synthesized, characterized and evaluated for their antimalarial properties and their physicochemical properties studied in order to further assess the importance of the linkage of the 4-aminoquinoline scaffold to the ferrocenyl unit, the presence of the hydrogen bonding acceptor atom, and the conformation and lipophilicity of the final metallocene conjugate.

2.3.2 Synthesis

The 4-aminoquinoline chloroquine derivatives employed (**3a-e**) differ from chloroquine in the nature of the side chain attached to the quinoline moiety. These compounds have ethyl, propyl, and butyl chains, unbranched or methyl branched, and the syntheses of **3a-e** are outlined in Scheme 2.1.

The syntheses of these and other 4-aminoquinoline derivatives have been previously described in the literature.[181,182] Compounds **3a-d** were synthesized by variations of

previously mentioned methods.[181,182] In the literature these syntheses are carried out using traditional bench methods but they can also be conducted in a microwave reactor (Scheme 2.1). Both methods are comparable and our approach utilizing the microwave reactor is advantageous since it reduces considerably the reaction time.

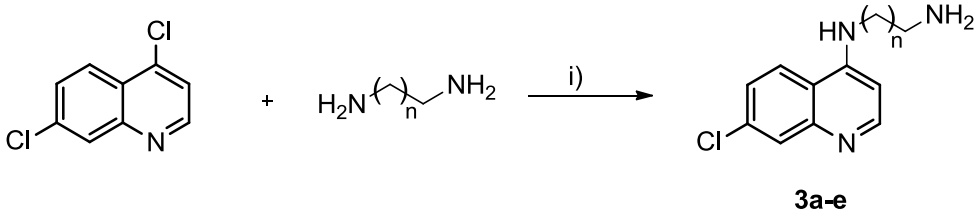

Scheme 2.1. General synthetic route for the synthesis of 4-aminoquinoline components (**3a-e**): i) 30 min 165 °C; **3a** (n=1, ethyl), **3b** (n=2, propyl), **3c** (n=3, butyl), **3d** (2-propyl), **3e** (2,2'-dimethylpropyl).

Compounds **3a-e** were formed by the condensation reaction of commercially available 4,7-dichloroquinoline with the corresponding alkyl diamine. A nucleophilic aromatic substitution by the corresponding amine takes place at the 4-Cl position of the 4,7-dichloroquinoline. This is carried out in the presence of a large excess of the diamine that acts as both the base and the solvent, helping to avoid the formation of terminally di-substituted diamines.[193] After heating the mixture in the microwave reactor for 30 minutes, the work-up consisted of dilution with 1.0 M NaOH and subsequent extraction with methylene chloride. Even though the reaction is estimated to go to completion, the yields are dependent on the solubility of the products in methylene chloride during the extraction process. After reducing the solution to a small volume, the products were precipitated with the addition of excess hexanes. The pure compounds were characterized by ^{1}H NMR and ^{13}C NMR spectroscopy, HR-MS and, in some cases, elemental analysis.

The synthesis of the mono-substituted ferrocenyl 4-aminoquinoline derivatives (**4a-e**) is described in Scheme 2.2. These compounds were formed via a reductive amination between commercially available ferrocenecarboxaldehyde and the corresponding 4-aminoquinoline derivative **3a-e**. These compounds were prepared following a general methodology previously reported[132] with slight modifications. Ferrocenecarboxaldehyde was reacted with the 4-aminoquinoline derivative in an overnight reaction to form an imine intermediate that was then reduced to the amine form by the subsequent addition of sodium borohydride. It was observed that the latter reductive step takes place almost immediately, with results that are independent of the reaction time. The workup with a basic aqueous solution and extraction with diethyl ether afforded the crude product containing unreacted ferrocenecarboxaldehyde and other unidentified byproducts. The desired products were purified by column chromatography and characterized by ^{1}H NMR and ^{13}C NMR spectroscopy as well as HR-MS and elemental analysis.

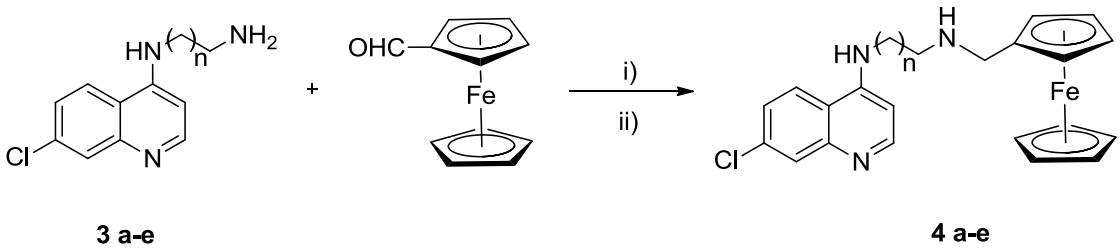

Scheme 2.2. General synthetic route for the synthesis of mono-substituted ferrocenyl 4-aminoquinoline derivatives (**4a-e**): i) MeOH, 12 h, RT; ii) $NaBH_4$, 2 h, RT; **4a** (n=1, ethyl), **4b** (n=2, propyl), **4c** (n=3, butyl), **4d** (2-propyl), **4e** (2,2'-dimethylpropyl).

The synthesis of the bridged ferrocenyl 4-aminoquinoline derivatives (**5a-e**) is outlined in Scheme 2.3. The starting material 1,1'-bis(*N,N'*-dimethylaminomethyl)ferrocene (**1**) was

prepared as previously reported[180] with slight modifications. Ferrocene was doubly deprotonated at the 1- and 1'-positions by the action of *n*-butyllithium, previously activated by a solution of N,N,N',N'-tetramethylethylenediamine (TMEDA) in hexanes. The 1,1'-dilithio ferrocene was then reacted with Eschenmoser's salt or (*N,N'*-dimethyl)methyleneammonium iodide in THF to afford the crude product containing unreacted ferrocene, N-(dimethylaminomethyl)ferrocene and 1,1'-bis(*N,N'*-dimethylaminomethyl)ferrocene (**1**). Starting material (**1**) was purified by column chromatography on neutral alumina. The structure and purity of **1** was verified by ^{1}H NMR spectroscopy and LR-MS. The addition of diethyl ether or THF is absolutely required since hexanes alone would not dissolve the solid *N,N'*-dimethylmethylene ammonium iodide and the latter would react with the dilithioferrocene intermediate. It was also observed that better dissolution of the iodide salt and thus better yields were obtained when THF was used. Purification of **1** by column chromatography from a mixture that contained the disubstituted product **1**, the monosubstituted product and the unreacted ferrocene was rather complicated. Different polarities of neutral alumina (from activity I to V on the Brockman scale, I being the most polar and V the least polar) were employed. Crude quantities of less than 1 g could be separated with alumina of activity V whereas crude amounts larger than 1 g, in addition to requiring bigger columns, also needed alumina of increased polarity (Brockman activity III, II or I).

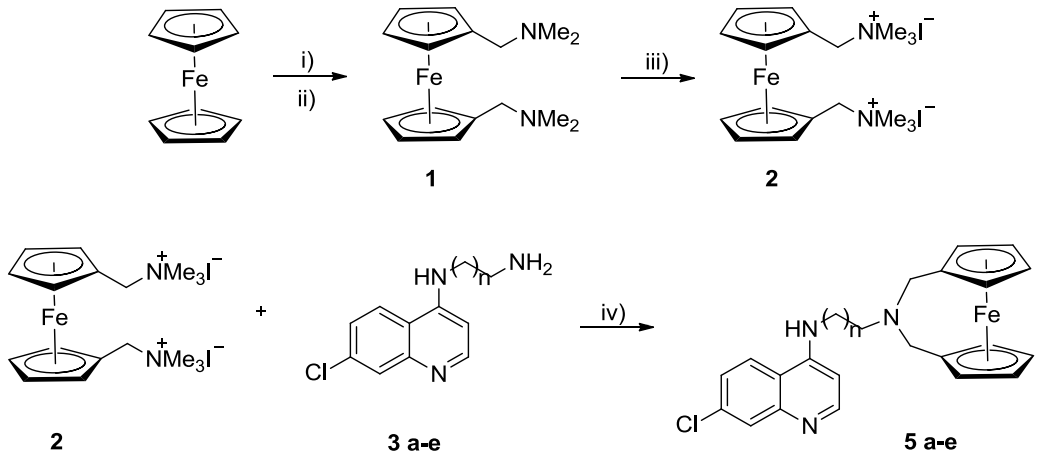

Scheme 2.3. General synthetic route for the synthesis of bridged ferrocenyl 4-aminoquinoline derivatives (**5a-e**): i) nBuLi, TMEDA, hexanes, 12 h, RT; ii) $CH_2=N(CH_3)_2^+I^-$, THF, 10 min reflux, 24 h RT; iii) MeI, MeOH, 10 min reflux; iv) NaOH, CH_3CN, 6h 110 °C; **5a** (n=1, ethyl), **5b** (n=2, propyl), **5c** (n=3, butyl), **5d** (2-propyl), **5e** (2,2'-dimethylpropyl).

The synthesis of 1,1'-bis(*N,N'*-trimethylaminomethyl)ferrocene iodide (**2**) was carried out as described originally in the literature.[180] The tertiary amino groups on 1,1'-bis(*N,N'*-dimethylaminomethyl)ferrocene (**1**) were quaternized by reaction with iodomethane. The original paper[180] suggests to heat at reflux for ten minutes; stirring at room temperature overnight, instead, afforded the desired product in a lower yield. The ferrocene trimethylammonium iodide salt was precipitated by the addition of a large excess of diethyl ether and was collected pure by vacuum filtration. The structure and purity of **2** was verified by ^{1}H NMR spectroscopy, LR-MS and elemental analysis.

The bridged ferrocenyl 4-aminoquinoline derivatives (**5a-e**) were formed by the condensation reaction of 1,1'-bis(*N,N'*-trimethylaminomethyl)ferrocene iodide (**2**) and the corresponding 4-aminoquinoline derivative **3a-e** (Scheme 2.3). The nucleophilic displacement of the trimethylammonium group using the 4-aminoquinoline in the presence of a base is a known reaction for ferrocene substrates[194] with yields of up to 80% when

employing conditions similar to those used here.[195,196] The trimethylammonium methylferrocene iodide is known to be an excellent electrophile due to the good leaving group property of the trimethylamine.

Acetonitrile was used as the solvent and sodium hydroxide was used as the deprotonating base. Two methodologies were developed for the synthesis of these compounds, one using conventional bench methods and a second using the microwave reactor. Again, both methods were comparable but the latter method was advantageous since it reduces the reaction time by 8-fold. These compounds were characterized by ^{1}H NMR, ^{13}C NMR, 2D NMR spectroscopic techniques (COSY, HMBC, HSQC) and HR-MS.

The average yield obtained was 20% (except for **5e**). Up to 10 equivalents of softer bases such as pyridine and sodium carbonate yielded approximately half the amount of product when 6 equivalents of NaOH was used. When a stronger base such as NaH was employed no product was obtained; instead an unidentified ferrocenyl product (not containing the quinoline fragment) was observed on the column, possibly a product of decomposition during the reaction. When the reaction was undertaken in a protic solvent such as methanol, no product was observed by LR-MS.

All the syntheses followed the same procedure except for that of **5e**. This product is obtained in a 3-5% yield compared to the 20% for **5a-d**. Unlike the other syntheses, the crude product contains more side products, thus the need for preparative TLC to purify **5e**. An explanation for this lower yield has been attempted in the X-ray crystallography analysis section (section 2.3.4).

In order to make these compounds more water-soluble, the syntheses of the tartrate salts of **5a-e** were attempted unsuccessfully. Mixing of a solution of L-(+)-tartaric acid in acetone

with a solution of **5a-e** in acetone yielded immediately a pale yellow compound that seemed to incorporate tartaric acid by ^{1}H NMR spectroscopy and elemental analysis. The formation of the tartrate salt proved successful for other compounds such as ferroquine and the monosubstituted **4a-e** (data not included) but did not yield the expected products for **5a-e**. We hypothesize that, in the case of **5a-e**, the bridging nitrogen is more sterically hindered and buried in the structure, and thus more difficult to protonate.

Another research group, intending to produce a double 4-aminoquinoline substituted ferrocene started with 1,1'-ferrocenedicarboxyaldehyde and the 4-aminoquinoline derivatives to accidentally obtain some of these bridged products (**5b** was fully characterized, **5a** and **5c** were also allegedly synthesized but data was not reported).[197] The reductive amination of the free base 4-aminoquinoline **3b** and 1,1'-ferrocenedicarboxyaldehyde took place over 12 days refluxing in methanol at 85 °C in the presence of $NaBH_3CN$ to yield the product **5b** in 34% yield.[197] Compared to the previously reported method, we offer a simpler and more general methodology to produce these rare chloroquine ferrocenyl derivatives, as well as their full characterization and detailed study of physical and biological properties.

2.3.3 NMR structural analysis

The influence of the two different bonding modes of chloroquine to the ferrocene moiety (in the compound series **4** and **5**) was explored by ^{1}H and ^{13}C NMR spectroscopy. The data presented in Table 2.1 show the ^{1}H NMR chemical shifts of the 4-aminoquinoline hydrogens upon derivatization with ferrocene. The consideration of these shifts is important since they represent an alteration of the structural environment of the chloroquine-like molecule and

therefore a potential alteration in the interaction (i.e. binding affinity) between the drug and the drug target, hematin. Other ^{1}H NMR signals that suffered less shifting upon derivatization have been excluded from Table 2.1.

Small shifting can be observed across the table for H_3, H_6 and H_7; however, these are minor compared to the NH aromatic proton displacement. The same small effect is observed for the alkyl protons in the side chain attached to the quinoline moiety (data not included in Table 2.1).

Table 2.1. ^{1}H NMR chemical shifts* of selected 4-aminoquinoline signals.

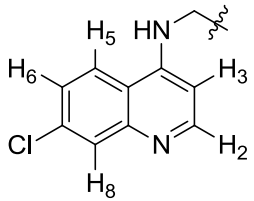

δ	3a	4a	5a	3b	4b	5b	3c	4c	5c	3d	4d	5d	3e	4e	5e
H_2	8.52	8.52	8.58	8.50	8.50	8.57	8.53	8.52	8.56	8.53	8.53	8.57	8.47	8.47	8.55
H_3	6.40	6.38	6.44	6.33	6.29	6.49	6.39	6.37	6.47	6.40	6.37	6.41	6.27	6.25	6.49
H_5	7.74	7.70	7.79	7.72	7.62	7.80	7.74	7.74	7.74	7.75	7.66	7.86	7.72	7.60	7.76
H_6	7.35	7.35	7.50	7.31	7.27	7.40	7.34	7.31	7.39	7.38	7.36	7.51	7.29	7.19	7.40
H_8	7.95	7.95	8.01	7.93	7.93	7.98	7.95	7.95	7.99	7.96	7.96	8.01	7.91	7.90	7.99
NH_{Ar}	5.82	5.91	6.20	7.44	7.96	5.76	6.00	6.07	5.22	5.85	5.94	6.38	8.48	8.56	5.13

* δ is given in ppm, measured in $CDCl_3$, 400 MHz

The biggest deviation, by far, is observed for the secondary amine hydrogen at the aromatic heterocycle (^{1}H-N$_{Ar}$). This could potentially be related to the formation or removal of intramolecular hydrogen bonds between the NH-proton in the 4-position of the quinoline ring and the N-atom in the β-position to the cyclopentadienyl ring. Table 2.2 shows the ^{1}H NMR chemical shifts of the NH protons (^{1}H-N$_{Ar}$) expressed as Δ (δ [ppm]) for the mono-substituted (**4a-e**) and the disubstituted (**5a-e**) compounds from the respective quinoline derivative **3**. A positive Δ indicates the shifting of the ^{1}H-N$_{Ar}$ to higher frequencies (lower field) upon coupling to ferrocene and a negative Δ indicates the shifting of the ^{1}H-N$_{Ar}$ to lower frequencies (higher field).

Table 2.2. Comparison of the ^{1}H NMR chemical shift of the NH$_{Ar}$ signals in the quinoline (**3a-e**) upon coordination to ferrocene (**4a-e** and **5a-e**).

	3a	**3b**	**3c**	**3d**	**3e**
Δδ (4)	0.09	0.52	0.07	0.09	0.08
Δδ (5)	0.38	- 1.68	- 0.78	0.53	- 3.35

* Δδ is given in ppm, measured in $CDCl_3$, 400 MHz

The first set of compounds to be discussed are those with an ethyl alkyl chain (**a** and **d**). For both sets of compounds it can be observed that when present in the monosubstituted ferrocene (**4a** and **4d**), the NH ^{1}H NMR signals shift slightly to higher frequencies; however, upon formation of the bridging unit in **5**, the shift to higher frequencies is even more pronounced as shown in Table 2.2. This significant shift can be attributed to the deshielding effect of the formation of an intramolecular hydrogen bond between the aromatic NH and the alkyl N. The difference in intensity of this deshielding effect can be explained as a consequence of the alkyl nitrogen being a secondary amine (in **4**) and a tertiary amine (in **5**).

For the second set of compounds, those with a propyl chain (**b** and **e**), a shifting to higher frequency is observed upon monocoordination of the quinoline derivative to ferrocene (**4**) (more pronounced for compounds **b** than for compounds **e**), again indicating the formation of a similar hydrogen bond. However, when these chloroquine-like derivatives are coordinated in the bridging fashion to ferrocene (**5**), a very pronounced shifting to lower frequencies is observed, more pronounced for **e** than for **b**. This could indicate that, compared to the chloroquine derivative (**3**) and mono substituted derivative (**4**), the hydrogen bonding between the aromatic NH and the alkyl N is lost, possibly due to conformational restrictions in the geometry of **5b** and **5e**.

Finally, compounds **c** with a butyl alkyl chain follow the same trend for compounds **b** and **e** but with the shifting of peaks less pronounced. It could be speculated that the hydrogen bonding in the original chloroquine derivative **3c** is not very strong so it is not very affected by the changes in conformation in **4c** and **5c**.

In general, it can be observed that the H-bonding under the conformation of **5** is maintained and even intensified when the length of the alkyl chain is n=2 (branched or unbranched - **5a** and **5d**) but it is lost when the length of the alkyl chain is n=3 or higher (**5b**, **5c**, **5e**). A similar type of intramolecular hydrogen bonding between two amine groups has been described for ferroquine, with an increase in lipophilicity that is attributed to this back-bonding.[162] Intramolecular hydrogen bonding has been associated with antimalarial activity in the past.[162,198] It is believed that intramolecular H-bonding will give a closed conformation that could penetrate more efficiently the parasite membranes to reach the drug site of action.[162]

For the ferrocene signals, we can observe the typical displacement for both types of substituted ferrocene. In monosubstituted products (**4a-e**) one singlet is observed for the unsubstituted Cp ring, normally at δ 4.14-4.18 (ppm) and an AA'BB'-type spectrum with two triplets is observed for the $H_{\alpha,\alpha'}$ and $H_{\beta,\beta'}$ hydrogens in the substituted Cp ring. The hydrogens of the singly substituted cyclopentadienyl are located at lower field (compared to the Cp singlet) due to the electronic withdrawal effect of the chloroquine-derivative. As is expected for the disubstituted products (**5a-e**) two sets of triplets/multiplets are observed for the $H_{\alpha,\alpha'}$ and $H_{\beta,\beta'}$ hydrogens and the Cp singlet is absent. The only exception in the group is compound **5d**, whose non symmetric branched alkyl chain gives four different triplets for the substituted Cp rings. These peaks appear at higher field (4.02-4.20 ppm) in an opposite effect to that observed for the previous series (**4**). This might be related to an electron donating effect of the nitrogen bridging both Cp rings. A comparison of the ^{1}H NMR spectra of a disubstituted ferrocenyl derivative, a monosubstituted ferrocenyl derivative and the organic fragment (**5a**/**4a**/**3a** in this case) can be appreciated in Figure 2.3.

Spectroscopic characterization with ^{13}C NMR spectroscopy is consistent with the ^{1}H NMR. In the case of **5a-e**, the hydrogen and carbon connected to the bridging nitrogen appear as singlets (although broad for H) in the ^{1}H and ^{13}C NMR spectra, respectively, indicating that the nitrogen undergoes rapid inversion to render these hydrogens and carbons magnetically equivalent. All the products are air and thermally stable.

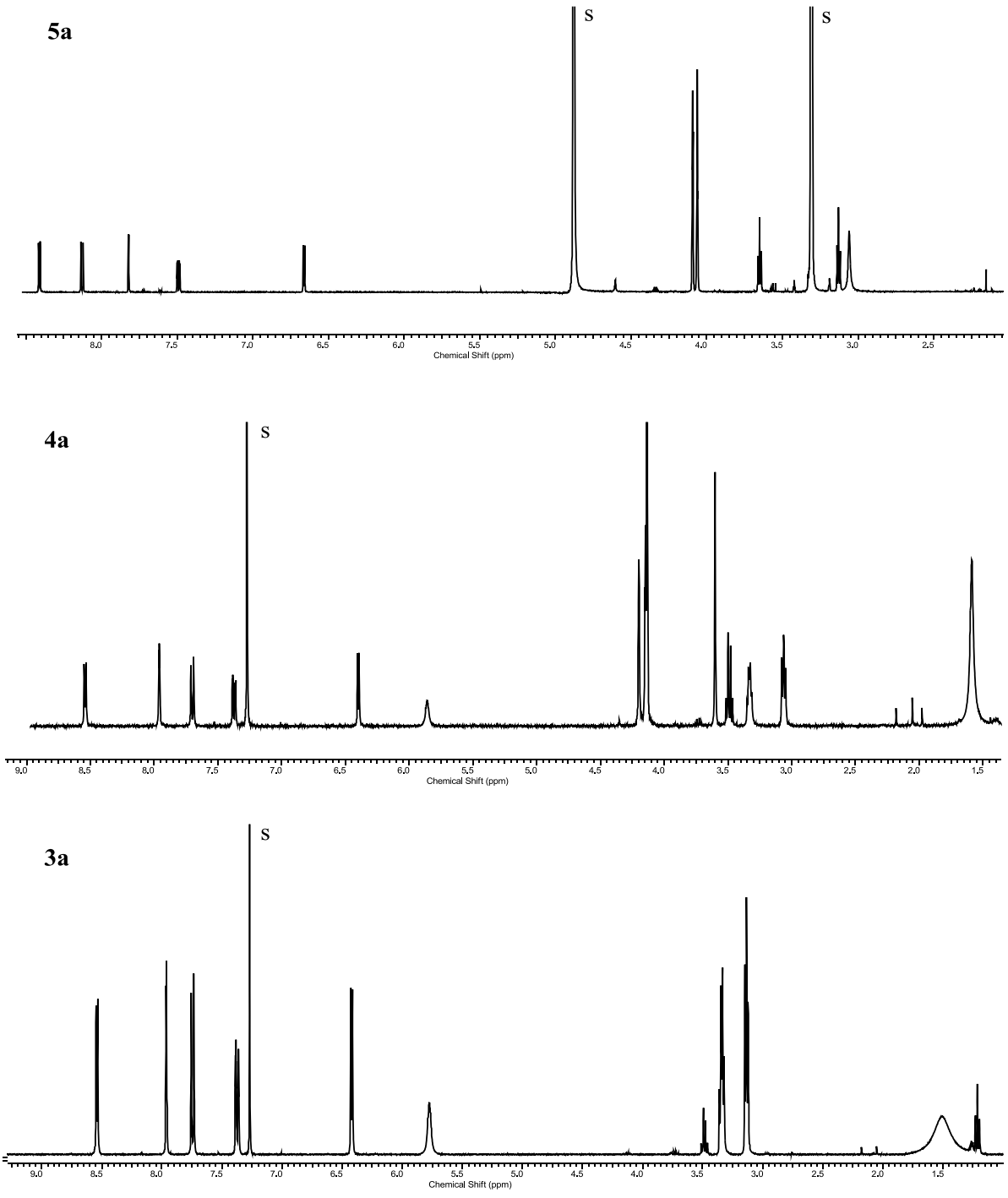

Figure 2.3. From top to bottom (at RT): ^{1}H NMR (CD_3OD, 600 MHz) spectrum of **5a**, ^{1}H NMR ($CDCl_3$, 400 MHz) spectrum of **4a** and ^{1}H NMR ($CDCl_3$, 400 MHz) spectrum of **3a**; s indicates solvent peaks.

2.3.4 X-Ray crystal structure characterization

Single crystals of compounds **4b**, **4e** and **5b** suitable for X-ray diffraction were obtained. Characteristic bond lengths and angles for these structures are summarized in Table 2.3 and Table 2.4.

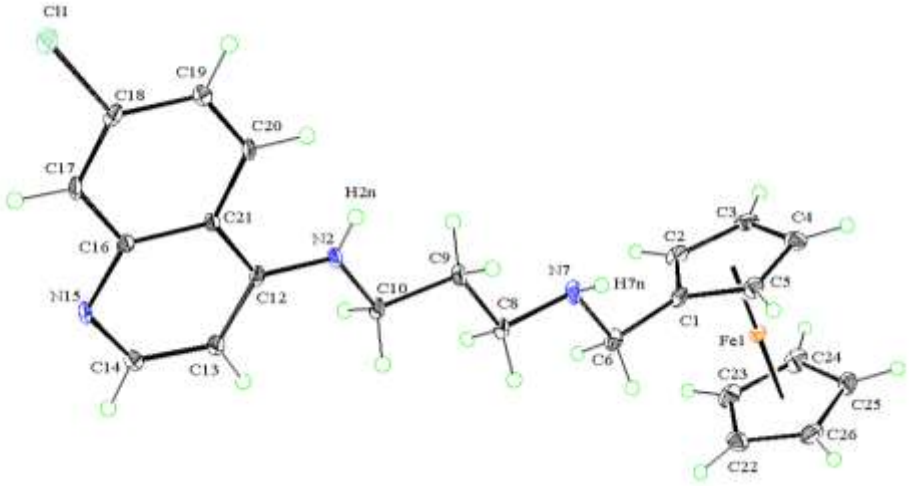

Figure 2.4. ORTEP diagram for compound **4b** with 50% thermal ellipsoid level.

Table 2.3. Selected bond distances (Å) and angles (°) in **4b** and **4e**.

	4b	**4e**
C6-N7	1.463(3)	1.474(2)
N7-C8	1.459(3)	1.470(2)
N11-C12	1.353(3) (N2-C12)	1.345(2)
N11-C10	1.454(3) (N2-C12)	1.455(2)
N11-$H11_N$	0.77(3) (N2-$H2_N$)	0.79(2)
N7-$H7_N$	0.79(3)	0.85(2)
$H11_N$-N11-C12	120(2) ($H2_N$-N2-C12)	120.5(15)
C12-N11-C10	121.8(2) (C12-N2-C10)	125.10(14)
C10-N11-$H11_N$	118(2) (C10-N2-$H2_N$)	113.2(15)
$H7_N$-N7-C6	109(2)	106.8(14)
C6-N7-C8	112.7(2)	111.59(13)
C8-N7-$H7_N$	107(2)	110.3(14)
N7-C6-C1-C2	-95.2(3)	-115.54(17)

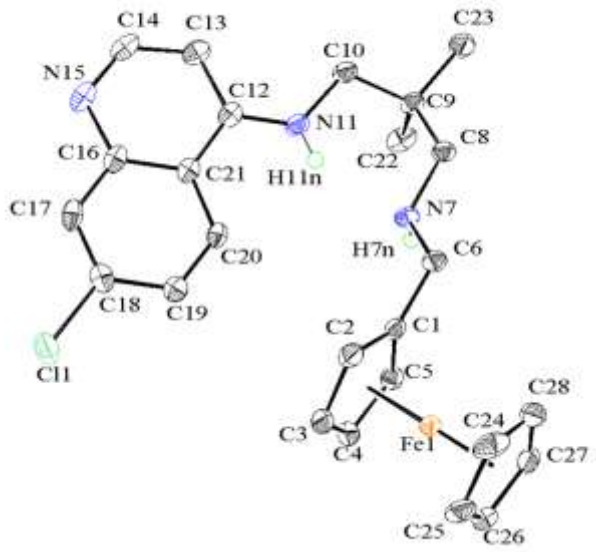

Figure 2.5. ORTEP diagram for compound **4e** with 50% thermal ellipsoid level.

The crystal structures of compounds **4b** (Figure 2.4) and **4e** (Figure 2.5) show the ferrocene scaffold with eclipsed cyclopentadienyl rings monosubstituted by the corresponding chloroquine derivative at the terminal amine functionality. The carbon nitrogen bonds incorporating N7 are in the typical range for C-N single bonds. Due to the quinoline ring, C12-N11 is shortened; the electronic influence of the aromatic quinoline on the N11 nitrogen atom is further demonstrated by bond angles indicating a planar sp^2 arrangement, which stands in contrast to the sp^3-hybridized character of N7 and suggests conjugation of N7 with the quinoline ring. The propyl side chain of **4b** is oriented perpendicular to the cyclopentadienyl ring and is fully staggered. The quinoline substituent falls into the same staggered pattern and is therefore almost perpendicularly oriented to the cyclopentadienyl ring of the ferrocene.

The side chain of **4e** is twisted out of the perpendicular plane of the cyclopentadienyl ring, turning back on itself with C9 as the center. The non-staggered geometry of the side chain orients the quinoline substituent above the plane of the cyclopentadienyl ring. The two methyl substituents differ in their orientation towards the propyl chain.

It is this conformation that we hypothesize is responsible for the low yield of formation of the bridged disubstituted analogue **5e**. We hypothesize that formation of **5** takes place by the stepwise attack of the primary terminal amine of the chloroquine derivative **3** on the trimethylammonium groups of **2**. We propose that after the first attack of **3e** to form a closed analog of **4e**, a strong hydrogen bonding interaction turns the quinoline away from the other trimethylammonium group and that will impede the second attack and displacement of the latter, resulting in lower yields for its formation.

It is noteworthy in the crystal structure of **4e** that the side chain orientation brings the two secondary amines in close proximity to one another, so hydrogen bonding can occur between N7 and H11N. The distance measured between N7-H11N is 2.11(2) Å, consistent with a hydrogen bonding interaction.[199] The distance observable between the corresponding N7-H2N in **4b** is much larger (4.86 Å) and it is clear from Figure 2.4 that intramolecular hydrogen bonding does not occur in the solid state. What can be observed, though, is an intermolecular hydrogen bond H2N-N15 with a bond distance of 2.42(3) Å.

The single crystal structure of compound **5b** is shown in Figure 2.6 and the characteristic bond lengths and angles for this structure are summarized in Table 2.4.

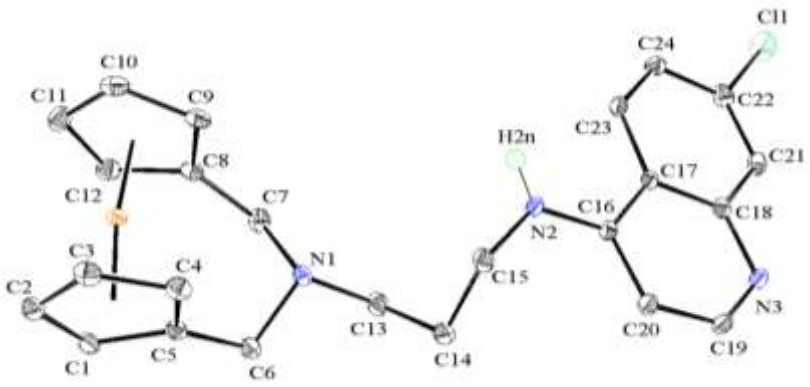

Figure 2.6. ORTEP diagram for compound **5b** with 50% thermal ellipsoid level.

Table 2.4. Selected bond distances (Å) and angles (°) in **5b**.

	5b
C7-N1	1.4808(16)
C6-N1	1.4757(16)
N1-C13	1.4764(14)
C16-N2	1.3514(14)
N2-C15	1.4580(15)
N2-$H2_N$	0.8800
$H2_N$-N2-C16	118.6
C15-N2-C16	122.77(10)
C15-N2-$H2_N$	118.6
C7-N1-C13	109.70(10)
C13-N1-C6	109.03(9)
C6-N1-C7	111.12(10)
C8-C7-N1	113.01(10)
C5-C6-N1	114.36(10)
C13-C14-C15	112.14(10)
N1-C13-C14	112.29(10)
N2-C15-C14	113.98(10)
N1-C7-C8-C9	51.15(17)
C14-C15-N2-C16	-72.96(14)
N1-C13-C14-C15	-69.95(13)

The cyclopentadienyl rings of ferrocene are in an almost eclipsed conformation and the carbon nitrogen bonds of N1 are in the typical range of C-N single bonds. As in **4b** and **4e**, the electronic influence of the quinoline is observed in the shortening of the carbon nitrogen single bond C16-N2 and in the planar sp^2 arrangement around N2 observed by the bond angles.

When compared to the monosubstituted analogue **4b**, **5b** presents significant differences in conformation. In **5b**, the quinoline ring and the ferrocene skeleton are parallel to each other but contained in two distinct planes, connected by a propyl chain that displays a non-staggered arrangement with the quinoline ring almost perpendicular to the propyl chain (Figure 2.6, Table 2.4). As in **4b**, the quinoline ring is perpendicularly oriented to the plane that contains the cyclopentadienyl rings of the ferrocene. No intramolecular hydrogen bonding can be observed for **5b**, but just as for **4b**, an intermolecular hydrogen bond H2N-N3 is seen with a bond distance of 2.14 Å.

Another interesting characteristic of **5b** is that it is an example of a strained ferrocenophane, specifically an aza-[3]ferrocenophane. As expected for a ferrocene with an ansa [3] bridge, the normal geometry of ferrocene has been affected. The parameters used to describe this type of structure are listed in Table 2.5.

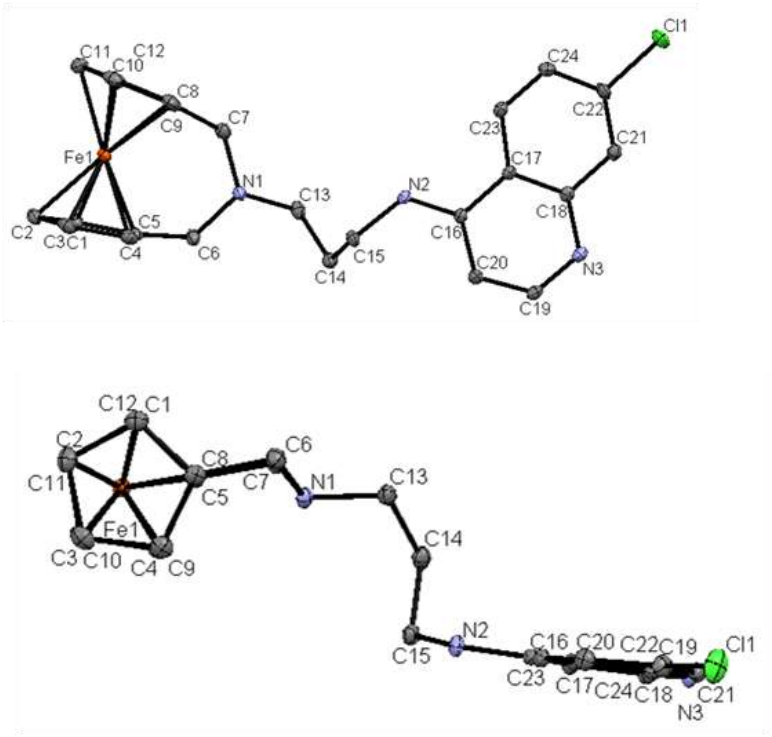

Figure 2.7. Additional ORTEP diagrams of compound **5b** with 50% thermal ellipsoidal level.

Table 2.5. Structural parameters of strained ferrocenophane compound **5b**.

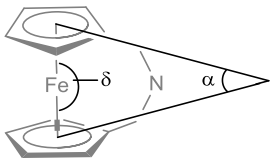

A	12.12°
Δ	171.3(4)°
$Cp_{centroid}$- $Cp_{centroid}$	3.2517(2) Å
N deviation from C5-C6-C7-C8	0.745 Å
C6 deviation from Cp plane	0.138(2) Å
C7 deviation from Cp' plane	0.120(2) Å

The degree of ring tilt is expressed as the tilt angle (α), or the dihedral angle between the two planes that contain each of the Cp rings. The $Cp_{centroid}$-M-$Cp_{centroid}$ angle is denoted as δ and the $Cp_{centroid}$- $Cp_{centroid}$ is the distance between the two Cp rings. The nitrogen lies 0.745

Å out of the plane that contains C5-C6-C7-C8; C6 and C7 have a deviation of 0.138(2) Å and 0.120(2) Å from the plane of their respective Cp rings.

The tilt angle (α) of 12.12° is not considered to induce high strain (tilt angles of up to 32° are considered to induce large amount of strain).[200] This aza-[3]ferrocenophane is structurally similar to a [3]ferrocenophane (a propane chain bridging the two cyclopentadienyl rings) since the latter has tilt angles up to 12.6°.[200]

Strained ferrocenophanes and other strained organometallic rings have been demonstrated to undergo ring-opening reactions such as ring-opening polymerizations.[200] Computational studies indicate that constraining the Cp rings in ferrocene from a value of 0° to 30° leads to strain energy of over 100 $kJmol^{-1}$.[201] This type of species constitutes an interesting source for investigation of the effects of the degree of ring tilting and strain in the behaviour of metallocenophanes.

Ferrocenophanes are in general expected to show unique chemical properties due to the functionality in the side arm. Strain energy can be imbedded in this type of compound (**5a-e**) and that might be a focus of research since this energy and the effects on its conformation can influence the antiplasmodial activity. Alternatively, conjugated groups can be introduced to tune the electronic character of the system. Aza-[n]-ferrocenophanes are known to undergo reversible electron transfer between the Fe and N atoms in the oxidized state.[202]

2.4 Conclusions

A series of 4-aminoquinolines (chloroquine derivatives) with an exocyclic alkyl chain of fours carbons or shorter were functionalized with ferrocene in two different patterns of substitution. A series of disubstituted ferrocene chloroquine derivatives with the terminal nitrogen of the chloroquine derivative bridging the two cyclopentadienyl rings of ferrocene (**5a**-**e**) were synthesized and structurally compared to the mono-substituted terminally-substituted ferrocene chloroquine (**4a**-**e**) analogs. All compounds were characterized by a variety of physical methods.

The structural study and comparison of these two modes of chloroquine substitution was carried out in solution and solid state, by ^{1}H NMR spectroscopy and single crystal X-ray diffraction techniques, respectively. When studied in the solution state, it was observed that, upon derivatization with ferrocene, the biggest deviation was observed for the secondary amine proton at the aromatic heterocycle. The changes in ^{1}H NMR chemical shift upon derivatization could indicate formation or dissolution of hydrogen bonding interactions. It was observed that for the bridged conformation (**5**), an intramolecular hydrogen bond is observed for ethyl chains that is absent in the longer chain analogs. The ^{1}H NMR chemical shift of this hydrogen indicated formation of a hydrogen bond in all members of the mono-substituted ferrocenyl compounds (**4**).

Crystal structures of selected compounds **4** and **5** also demonstrated the structural characterictics of these two forms of derivatization. Compound **4e** displays intramolecular hydrogen bonding interactions in the solid state as well as in solution, as observed by ^{1}H NMR spectroscopy. The orientation of the quinoline in compound **4b** is different and the

latter did not exhibit an intramolecular H-bond in the solid state. Compound **5b** demonstrated a more rigid conformation with the chloroquine-derivative bridging the two Cp rings creating strain in the normally parallel Cp rings of the ferrocene, forming an uncommon species of aza-[3]ferrocenophane.

The presence or absence of hydrogen bonding interactions, the conformation, the degree of rigidity and the lipophilicity of these derivatives are correlated to the biological responses of these compounds against different strains of *P. falciparum* parasites, as described in Chapter 3. These structure-activity relationships are especially important since it is well known that the antimalarial action of ferroquine is strongly structure-dependant, evidenced by the numerous ferroquine analogs that have failed to reproduce the action of ferroquine itself.

CHAPTER 3 BIOLOGICAL ACTIVITY AND STRUCTURE-ACTIVITY RELATIONSHIP STUDY OF CHLOROQUINE-BRIDGED FERROCENYL CONJUGATES

3.1 Introduction

The fact that ferroquine, a close relative of chloroquine, was able to overcome drug resistance[129,130] suggested that the mechanism responsible for resistance is highly selective and structurally specific. The antimalarial activity of ferroquine in chloroquine-resistant parasitic strains could only be due to a specific difference in interaction with the resistance mechanisms of the parasite.

The mechanism of action of ferroquine has been studied in the past, although it is only partially understood. Previous work has focused on the investigation of the physicochemical properties of ferroquine (FQ) in comparison to those of the parent drug chloroquine (CQ).[198] In an effort to explain the activity observed for ferroquine and to gain insight into its mechanism of action, physicochemical properties of FQ have been investigated and compared to those of CQ. [176,198]

Studies of structure-activity relationships (SAR) in CQ and twenty other 4-aminoquinoline analogues revealed the structural elements required for the antiplasmodial activity observed for this class of antimalarial drugs.[191,203] For instance, the 4-aminoquinoline core seems to have a strong unique affinity for Fe(III)PPIX that facilitates the strong

complex formation between the drug and Fe(III)PPIX; the presence of a 7-chloro group in the 4-aminoquinoline ring seems to be a requirement for β-hematin inhibitory activity.[32] While the association with Fe(III)PPIX and the β-hematin inhibitory activity are necessary, they are not sufficient to explain the antiplasmodial activity. This activity seems to be dependent on the presence of the amino alkyl chain attached to the 4-amino-7-chloroquinoline template. Thus, it appears that the basic tertiary amino group in the side chain and the quinoline nitrogen are crucial for drug accumulation in the acidic parasite food vacuole and, therefore, determinant in the elevated antiplasmodial activity.[191] Figure 3.1 presents a summary of the results of structure activity studies on several chloroquine derivatives.[32]

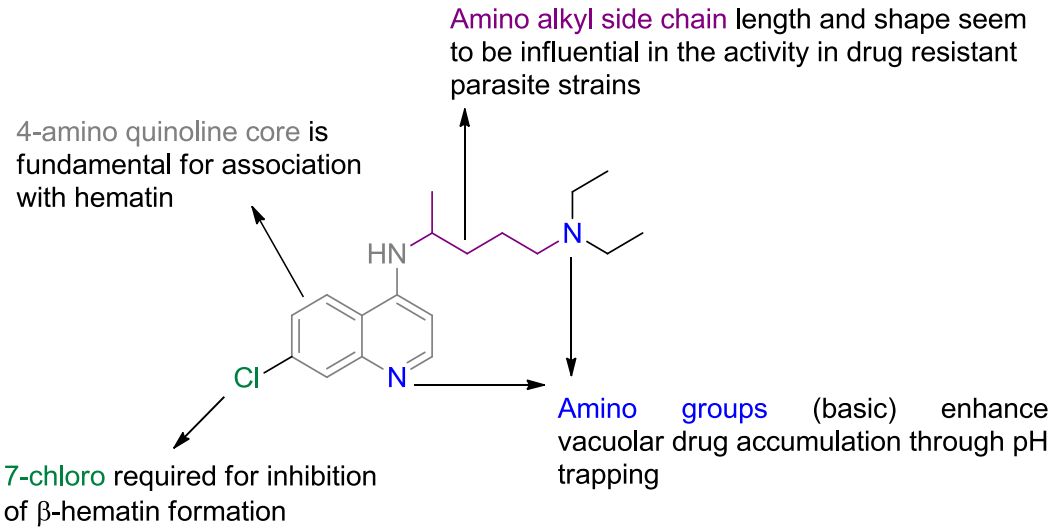

Figure 3.1. Structure-activity relationships proposed for 4-aminochloroquine antimalarial drugs.[32]

Given the close structural relationship between chloroquine and ferroquine, it can be concluded that the remarkable increase of antimalarial activity is caused specifically and exclusively by the introduction of the ferrocene unit. Surprisingly, ferrocene did not improve

the action of any other antimalarial,[149,150,151,152,204] demonstrating the specificity of action of FQ. Compounds of ferrocene with other molecules with suspected antimalarial activity showed at best modest antimalarial activity, with a significant improvement over the parent compounds but usually lower than the control chloroquine.[153,157,205,206,207,208] These observations made apparent that a very structurally-specific set of characteristics in ferroquine gives this compound the specificity necessary to escape the *Pf*CRT resistance mechanisms.

Ferroquine retains the majority of the characteristics of chloroquine identified as necessary for antiplasmodial action. Despite the structural resemblance, the basicity and lipophilicity of ferroquine are significantly different from those of chloroquine.[198] Ferroquine is a weaker base and its lipophilicity at cytosolic pH 7.4 is markedly greater than that of chloroquine. The presence of intramolecular hydrogen bonding, observed in the solid state, was also proposed to be determinant in the activity observed.[198] A flip/flop mechanism between the open conformation of the protonated ferroquine and the folded conformation of the neutral ferroquine was proposed to contribute to the transport from water to the lipophilic membranes (Figure 3.2).[198] Studies replacing the H atom involved in this interaction have shown that this change reduced the activity significantly against both the chloroquine-sensitive and resistant strains even though the physicochemical properties remained almost unchanged.[162,198]

Ferroquine forms complexes with hematin in aqueous solution as effectively as does chloroquine; however, FQ is a stronger inhibitor of β-hematin formation.[198] The rigidity of the molecule is also increased when compared to chloroquine. This is associated with an

increase in entropy that might be related with formation of clusters of ferroquine preferentially in the lipid-water interface regions (where hemozoin formation occurs).[209]

In summary, the therapeutic effectiveness of ferroquine has been attributed to its preferential accumulation in the parasite food vacuole by a factor higher than 50 in comparison to CQ.[209] It has been postulated that ferroquine's weaker basic properties, its higher lipophilicity, and its special conformation, influenced by the intramolecular hydrogen bond, allow this compound better permeation through membranes and, therefore, a higher accumulation at the site of action inside the parasite while targeting the lipophilic site of hemozoin formation more effectively.[162,176,198] It remains to be established which of these factors is the most significant contributor to the antimalarial activity of ferroquine.

The activity of FQ after reaching its site of action can be ascribed to a dual mechanism: firstly, FQ is a strong inhibitor of β-hematin formation, more potent than CQ and, therefore, able to halt more efficiently the detoxification mechanism of the parasite; and second, the redox activation from ferrocene to ferrocenium and consequent generation of reactive oxygen species (ROS) via a Fenton-like reaction under the acidic conditions of the parasite vacuole likely irreversibly damages the parasite.[162,163,209] Figure 3.2 summarizes the results of structural-activity relationship studies on ferroquine.

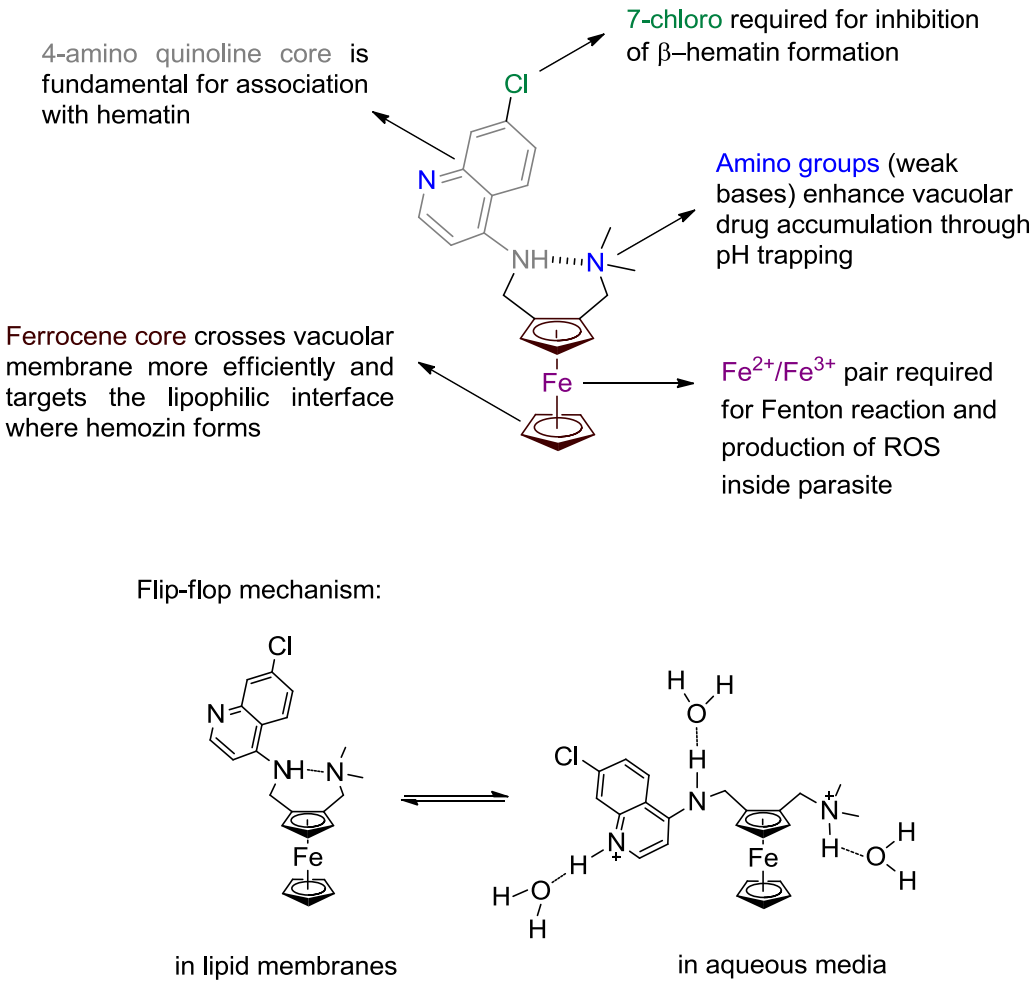

Figure 3.2. Structure-activity relationships proposed for ferroquine.[176,179]

Thus far, the role of the ferrocene moiety in the antimalarial activity of ferroquine remains uncertain. Although it has been shown that ferrocene by itself does have an inherent antiplasmodial action,[141] the ring system has been hypothesised to have a more significant effect on its interaction with *PfCRT* involved in chloroquine resistance.[163,209] The metallocene might act through modification of shape, volume, lipophilicity, basicity and/or electronic profile of the parent molecule, eventually altering its pharmacodynamic behaviour. It is also possible that the ring exerts a unique biological effect not associated with other structural entities.[155]

Thus, properties such as the ability to associate with Fe(III)PPIX, strength of inhibition of β-hematin formation, acid association constant and lipophilicity are intrinsically related to the antimalarial activity. Therefore, an investigation on several of these physicochemical properties is presented here in order to further test this hypothesis and compare the ability of the chloroquine derivatives introduced in the previous chapter to associate to hematin and inhibit β-hematin formation with their ability to inhibit parasite growth in culture.

3.2 Experimental

3.2.1 *In vitro* antiplasmodial activity studies

In vitro antiplasmodial tests were conducted by Dr. Peter J. Smith at the University of Cape Town. The test samples were tested in triplicate on one or two occasions against the chloroquine-sensitive (CQS) D10 strain and the chloroquine-resistant (CQR) Dd2 and K1 strains of *Plasmodium falciparum*. Continuous *in vitro* cultures of asexual 30 erythrocyte stages of *P. falciparum* were maintained using a modified method of Trager and Jensen.[210] Quantitative assessment of antiplasmodial activity *in vitro* was determined via the parasite lactate dehydrogenase assay using a modified method described by Makler.[211] The test samples were prepared as a 2 mg/mL stock solution in 10% DMSO or 20 mg/mL in 100% DMSO and sonicated to enhance solubility. Samples were tested as a suspension if not completely dissolved. Stock solutions were stored at -20 ºC. Further dilutions were prepared on the day of the experiment. Chloroquine (CQ) was used as the reference drug in all

experiments. Test samples were initially tested at three concentrations (10 μg/mL, 5 μg/mL and 2.5 μg/mL). CQ was tested at three concentrations (30 ng/mL, 15 ng/mL and 7.5 ng/mL). A full dose-response was performed for all compounds to determine the concentration inhibiting 50% of parasite growth (IC_{50} value). For D10, test samples were tested at a starting concentration of 100 μg/mL, which was then serially diluted 2-fold in complete medium to give 10 concentrations, with the lowest concentration being 0.2 μg/mL. The same dilution technique was used for all samples. CQ was tested at a starting concentration of 100 ng/mL. Several compounds were retested at a starting concentration of either 1000 ng/mL or 100 ng/mL. For Dd2 and K1, samples were tested at a starting concentration of 1000 ng/mL, which was then serially diluted 2-fold in complete medium to give 10 concentrations, with the lowest concentration being 2 ng/mL. The same dilution technique was used for all samples. CQ was tested at a starting concentration of 1000 ng/mL. The highest concentration of solvent to which the parasites were exposed had no measurable effect on the parasite viability (data not shown). The IC_{50}-values were obtained using a non-linear dose-response curve fitting analysis via Graph Pad Prism v.4.0 software.

3.2.2 *In vitro* antitumor activity and cytotoxicity assay

In vitro antitumor and cytotoxicity tests were conducted in the Biological Services Laboratory of the Department of Chemistry at the University of British Columbia. Human breast cancer cells MDA-MB-435S (HTB-129) were purchased from ATCC. Cells were grown as monolayers in medium (89% *Leibovitz's* L-15 medium with 2 mM L-glutamine, 0.01 mg/mL bovine insulin, 1% penicillin/streptomycin and 10% fetal bovine serum) and

maintained at 37 °C in a humidified atmosphere. Human normal breast epithelial cells MCF-10A (CRL-10317) were purchased from ATCC. Cells were grown as monolayers in medium (93% Dulbecco´s modified *Eagle* Medium F12, 5% fetal bovine serum, 1% penicillin/streptomycin, 1% 2 mM glutamine, 0.01 μg/mL human epidermal growth factor, 0.5 μg/mL hydrocortisone, 10 μg/mL insulin) and maintained at 37 °C in a humidified atmosphere containing 5% CO_2. Cell growth inhibition was assessed using the colorimetric cell proliferation MTT assay.[212] Cells were detached from culture flasks with 0.25% trypsin and 0.03% EDTA (*Sigma*) and resuspended in fresh culture medium at a density of 3 x 10^5 cells/mL (MDA-MB435S) or 1 x 10^5 cells/mL (MCF-10A). Using a Falcon 96-well, flat-bottom plate, 100 μL of the cell suspension was added to each of the wells. The cells were incubated for 24 h after which time the cells were treated with each compound (in triplicate) at concentrations ranging from 0.1 μg/mL to 200 μg/mL. To assist dissolution, the complexes were first dissolved in DMSO to provide stock solutions and then serially diluted with media to give the final concentrations (final concentration of DMSO was 0.5%). A stock solution of chloroquine diphosphate salt was prepared in 0.5% DMSO in medium and serially diluted. Cisplatin was used as positive control and stock solutions were prepared in 0.5% DMSO in medium and serially diluted. After incubation with the compounds for 72 h, 50 μL of a 2.5 mg/mL solution of MTT in PBS was added to each well and further incubated for 3-4 h. The supernatant was removed and the cells were dissolved in 150 μL of DMSO. Cell survival was determined by means of metabolic reduction of MTT. Optical density from the MTT assay was measured at 570 nm on a *Beckman Coulter* DTX 880 Multimode Detector. Absorbance values were corrected to the control and blank. Tests were run in duplicate or triplicate. The IC_{50} values were obtained from plots of cell survival (%) against log of drug

concentration using a non-linear dose-response curve fitting analysis via Graph Pad Prism v.4.0 software.

3.2.3 Association with hematin assay

The association constants of the studied compounds with hematin were measured as described previously in the literature.[213] Hemin (from bovine, ≥ 90.0 %) was obtained from Sigma-Aldrich and a stock solution was prepared by dissolving 6-8 mg of hemin in 10 mL AR grade DMSO and stored in the dark. The working hemin solution (2μM) was prepared freshly from 20 μL of the hemin stock solution diluted to a final volume of 10 ml with the buffered solution (40% v/v DMSO, 0.020 M HEPES, apparent pH 7.5). Hematin-compound interactions were monitored by titrating the hematin solution with each compound and measuring the absorbance of the Soret band at 402 nm. In a UV-vis cell, 2 mL of the 2 μM hematin solution was titrated with a 2 mM solution of the compound in the same buffered solution (40% v/v DMSO, 0.020 M HEPES, apparent pH 7.5). The temperature was maintained at 25 °C using a water circulating bath in a thermostatted cellholder, and absorbance readings were recorded for each addition, after 5 minutes of stabilization, using a Hewlett-Packard 8543 diode array spectrophotometer outfitted with a Fisher Scientific 1016D Isotemp thermostatted water cooling system. Absorbance data were collected using the program Agilent 845x UV-visible Spectroscopy System (Agilent Technologies, Inc. 2003-2008). Different concentrations of compound were analyzed (0/1/3/5/10/15/20/25/30/35/40/50/60/70/80/90/100 equivalents of hematin). A reference cell with the buffered solution (40% v/v DMSO, 0.020 M HEPES, apparent pH 7.5) was also

titrated with the same equivalents of each compound in order to zero the absorbance of the drug. Titrations were repeated in triplicate for each compound and blank. Absorbance data were corrected for dilution, analyzed at 402 nm and fitted to a 1:1 association model using non-linear least squares fitting analysis via Graph Pad Prism v.4.0 software to obtain the association constant (reported as log *K*). Graphs were produced using the OriginPro 7.5 software.

3.2.4 Inhibition of β-hematin formation assay

Qualitative evaluation of inhibition of β-hematin formation.

The inhibition of the formation of β-hematin was assayed as described previously in the literature.[214] A solution of hematin was prepared by dissolving 5 mg hemin (bovine, ≥ 90.0 %, obtained from Sigma-Aldrich) in 1.0 mL of 0.1 M NaOH. This solution was incubated at 60 °C, followed by the addition of previously incubated 0.1 mL 1.0 M HCl and 0.58 mL of 12.9 M acetate (pH 5) at 60 °C. The mixture was incubated at 60 °C for 1 h. After cooling in an ice bath for 5 min, the solid obtained was filtered using a 8μm cellulose acetate/nitrate filter disk Millipore filter and washed thoroughly with water. The solid collected was dried under vacuum for several hours before analysis by infrared spectroscopy in a *Thermo Nicolet* 6700 FT-IR spectrometer. For the study of the compounds, 3 or 5 molar equivalents of the studied compounds were added to the solution prior to the acidification step and continued as specified above.

Quantitative evaluation of inhibition of β-hematin formation.

The inhibition of the formation of β-hematin was assayed as described previously in the literature.[215] A 12.9 M acetate stock solution was prepared using sodium acetate trihydrate,[215] and kept at 70 °C throughout the experiment. The pH of the stock solution was measured as 5.05. A 1.68 mM stock solution of hematin was prepared by dissolving 5.5 mg of hemin (bovine, ≥ 90.0 %, obtained from Sigma-Aldrich) in 5.0 mL 0.1 M NaOH. Stock solutions of each compound were prepared in DMSO in concentrations that ranged from 0.15 to 0.20 M. Hematin stock solution (20.2 μL, 0.035 μmoles) was dispensed to a series of Eppendorf tubes (11 tubes for each compound tested). The 0.1 M NaOH solution was neutralized with 2.02 μL of 1.0 M HCl prior to the addition of the compounds. Pre-determined volumes of the stock solution of the test compounds were added to give 0-10 equivalents relative to hematin in the final solution. After mixing, 11.74 μL of the 12.9 M acetate solution maintained at 70 °C was added to each Eppendorf tube. The final hematin concentration was 1 mM and the final solution pH 4.5. The vortexed solutions were then incubated at 60 °C for 1 h. The solutions were quenched at room temperature with 900 μL of a 5% pyridine solution (200 mM HEPES, pH 8.2), followed by addition of 1100 μL of 5% pyridine solution (20 mM HEPES, pH 7.5). Each tube was vortexed to ensure the complete dissolution of hematin and then allowed to settle for 30 min at room temperature. The supernatant was transferred to a cuvette without disturbing the precipitate. Absorbances were read at 405 nm at a Cary 100 Bio (*Varian*) UV-visible spectrophotometer. Graphs were produced using the OriginPro 7.5 software.

3.2.5 Partition coefficient and molecular shape analysis

Theoretical log *P* values were calculated using the commercially available ACDLABS 11.0 program.[216] Molecular modelling was performed using the Gaussian 09 and GaussView packages (Gaussian, Inc.).[217] Density functional theory (DFT), with the B3LYP functional employing the 6-31+G (d,p) basis set, was used to obtain the optimized geometry and the electron density. Frequency calculations were performed to verify that the optimized structures were a minima, having no imaginary frequencies. The electrostatic potential was mapped onto the calculated electron density surface. Molden package software[218] was used to obtain the topological polar surface area (tPSA) from the optimized structures.

3.3 Results and discussion

3.3.1 *In vitro* antiplasmodial activity studies

The antiplasmodial activity of the compounds **3a-e**, **4a-e** and **5a-e** (Figure 3.3) was evaluated *in vitro* against the chloroquine-sensitive D10 and the chloroquine-resistant Dd2 and K1 strains of *P. falciparum*. An initial three-point concentration screen showed that several compounds have very good activity with less than 10% parasite survival at 2.5 μg/mL (Table 3.1). The activities of these compounds were compared to the reference drug chloroquine diphosphate (CQDP).

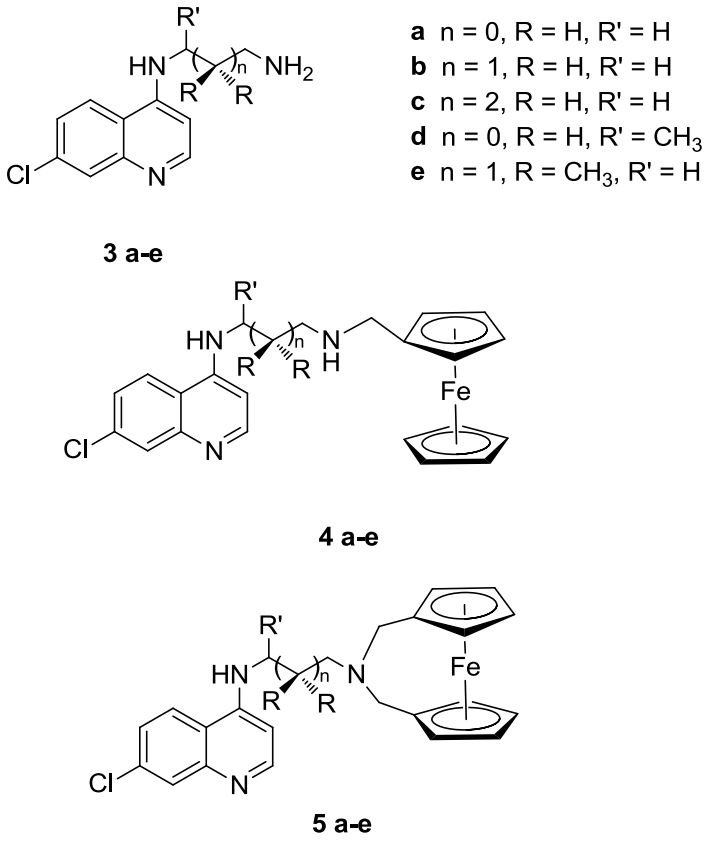

Figure 3.3. Chloroquine derivatives (**3**), monosubstituted chloroquine ferrocenyl compounds (**4**) and 1,1'-disubstituted bridged chloroquine ferrocenyl conjugates (**5**).

Table 3.1. *In vitro* antiplasmodial activity against *P. falciparum* (CQS) D10 strain.

Compound	% parasite survival		
	10 µg/mL	**5 µg/mL**	**2.5 µg/mL**
3a (n=2)	3.70	0.00	1.68
3b (n=2)	0.00	0.00	2.10
3c	0.28	1.38	5.01
3d (n=2)	18.34	8.57	4.56
3e (n=2)	3.85	0.00	1.50
4a	ND	ND	ND
4b	ND	ND	ND
4c	0.00	0.00	0.00
4d (n=2)	0.00	4.25	2.04
4e	ND	ND	ND
5a	0.00	0.00	0.00
5b	5.03	4.04	3.99
5c	0.00	0.00	4.29
5d	0.00	1.22	0.00
5e	0.00	0.77	2.20
	30 ng/mL	**15 ng/mL**	**7.5 ng/mL**
CQDP	15.78	39.06	90.53

ND = not determined, n = number of data sets averaged

A full dose-response was performed for all compounds to determine the concentration inhibiting 50% of parasite growth (IC_{50} value). Chloroquine diphosphate (CQDP) was tested as the positive control. The results are presented in Table 3.2.

Table 3.2. *In vitro* antiplasmodial activity and resistance indices against *P. falciparum* CQS D10, CQR Dd2 and CQR K1 strains.

Compound	IC_{50} - D10 (CQS) (nM)	IC_{50} – Dd2 (CQR) (nM)	RI[a]	IC_{50} – K1 (CQR) (nM)	RI[b]
3a	36.1 (n=2)	261.6	7.3	ND	-
3b	50.9 (n=2)	398.8	7.8	ND	-
3c	76.1	1697.8	22.3	ND	-
3d	29.7 (n=2)	80.6	2.7	158.7	5.3
3e	15.2 (n=2)	30.3	2.0	81.5	5.4
4a	60.8	36.2 (n=2)	0.6	1500	24.7
4b	138.3	297.4	2.2	16.1	0.1
4c	40.2	100.5	2.5	114.1	2.8
4d	43.8 (n=2)	23.1	0.5	260.5	5.9
4e	368.1	1136.8	3.0	90.9	0.3
5a	176.0	129.7	0.7	ND	-
5b	323.0	224.3	0.7	307.3	0.9
5c	91.3	152.2	1.6	ND	-
5d	444.2	269.2	0.6	291.6	0.7
5e	669.0	506.5	0.7	ND	-
CQDP	29.1	180.3	6.2	758.0	26.0

[a] Resistance index (RI^a) = IC_{50} Dd2/ IC_{50} D10
[b] Resistance index (RI^b) = IC_{50} K1/ IC_{50} D10
n = number of data sets averaged
ND = not determined

All disubstituted bridged ferrocenyl compounds **5a-e** demonstrated activity against all the tested parasite strains. The most active compound of this group was **5c** with IC_{50} values of 91.3 nM and 152.2 nM in the parasite strains D10 and Dd2, respectively. In general, compounds **5a-e** were more active in the Dd2 (CQR) strain than in the D10 (CQS) and K1 (CQR) strains, with the exception of **5c**. When compared against control, **5a-e** were less active than chloroquine against D10 (CQS), as expected. However, **5a**, **5b** and **5c**

demonstrated more activity than chloroquine against Dd2 (CQR), as did **5b** and **5d** against K1 (CQR), overcoming the parasitic resistance associated to the quinoline fragment.

The monosubstituted ferrocenyl compounds **4a-e** also demonstrated activity in both chloroquine-sensitive and -resistant strains of *P. falciparum*. The activity of these compounds was sensitive to the level of drug resistance in the parasite strains. The most active compounds against the Dd2 (CQR) strain were **4a** and **4d**, both ethyl-based compounds, with IC_{50} values as low as 36.2 and 23.1 nM, respectively. The most active compounds against the K1 (CQR) strain were **4b** and **4e**, both propyl-based compounds, with IC_{50} values of 16.1 and 90.9 nM, respectively. Unlike **5**, these compounds are generally more active in the chloroquine-sensitive D10 strain than in the chloroquine-resistant Dd2 and K1. When compared to chloroquine, these compounds are less active than the control against both D10 and Dd2 strains with the exception of **4a** and **4d**, but more active than chloroquine against the K1 strain, with the exception of **4a.** The organic component, the chloroquine derivatives **3a-e**, demonstrated a similar profile to chloroquine itself. Like chloroquine, these compounds are active against D10 but lose activity against the chloroquine-resistant Dd2 and K1 strains. The exceptions were the most active compounds **3e** and **3d** with IC_{50} values of 30.3 and 80.6 nM, respectively, against Dd2.

The effects of the substitution on the chloroquine derivatives will be discussed in terms of each set of specific length of the methylene spacer. For the ethyl chain quinoline (**a**), while the ferrocenyl derivatives are less effective than the organic fraction **3a** in the CQS D10 strain, an improvement of 7-fold and 2-fold is observed for the monosubstituted ferrocenyl **4a** and for the bridged ferrocenyl **5a**, respectively, in the CQR Dd2 strain. However, against

the CQR K1 strain, **4a** loses all activity, becoming almost 2-fold less active than chloroquine itself.

A similar situation is observed for the propyl (**b**) and butyl (**c**) chain derivatives. The ferrocenyl derivatives **4b** and **5b** are 1.3- and 2-fold more active than the organic component **3b** in the chloroquine-resistant Dd2 strain, respectively. Even more dramatically, **4c** and **5c** are 17- and 11-times more active than **3c** in the CQR Dd2 strain, respectively.

A different trend is observed for the branched methylene spacer derivatives **d** and **e**. In the case of the isopropyl derivatives (**d**), the activity of the organic component **3d** is superior to the ferrocenyl derivatives against all strains except for **4d** that shows more activity against the CQR Dd2. In the case of the 2,2'-dimethyl-propyl derivatives (**e**), the activity of **3e** is far superior to that of the ferrocenyl derivatives in both D10 and Dd2 strains, but almost equal against K1. **3e** is up to 44 times more active than **5e** in D10 and 38 times more active than **4e** in Dd2.

It was found then that the length of the methylene spacer was not such a strong influence in the activity as is the degree of branching. These results illustrate a different activity trend for the linear and the branched quinoline derivatives: linear derivatives can overcome chloroquine resistance by derivatization with ferrocene; however, the bulkier branched derivatives lose all activity when derivatised with ferrocene.

Even though the benchmark compound ferroquine (FQ) was not used as control during this experiment, IC_{50} values in these parasite strains have been reported in literature.[140] Ferroquine has IC_{50} = 18, 19 and 14 nM in the chloroquine-sensitive strain D10 and the chloroquine-resistant strains Dd2 and K1, respectively.[140] Although, it should be taken into consideration that in the same study an IC_{50} value of 22.9 nM is observed for CQ in the D10

strain, approximately two thirds of the value obtained. In general, values reported from different laboratories can vary greatly; therefore I will abstain from external comparisons and work with the internal control.

The resistance index (RI), defined as the IC_{50} value in the CQR strain divided by the IC_{50} value in the CQS strain, provides a quantitative relationship for how the compound behaves against chloroquine-sensitive and chloroquine-resistant strains. If this variation is small, it indicates that the compound is active regardless of the susceptibility of the parasitic strain. On the contrary, if the difference is large (the compound is much more active in a sensitive strain than in a resistant strain, most likely) it is an indication of loss of activity due to resistance development or likelihood of resistance development. A promising drug lead will have a small resistance index since it is an indication that the drug candidate is not being detected by whatever resistance mechanism. RI values for each compound ranged from 0.5 to 24.7 (Table 3.2). As expected, the quinoline derivatives **3a-e** showed the largest tendency to develop resistance due to their structural similarity to chloroquine. The lowest values of RI were found for the disubstituted bridged ferrocenyl compounds **5a-e** (Table 3.2).

Figure 3.4 illustrates the resistance index calculated for these compounds for the parasite strains D10 and Dd2. The diagonal line represents an equal antiplasmodial potency regardless of the chloroquine susceptibility of the strain (RI=1). Ferroquine (FQ), for example, not only displays low IC_{50} values for both parasite strains but also has an RI value close to 1, which makes this compound very attractive as an antiplasmodial drug lead. Compounds **5a-e** are not as potent as FQ but remain close to the ideal line, unlike compounds **3** and **4** that are more potent, and develop resistance later.

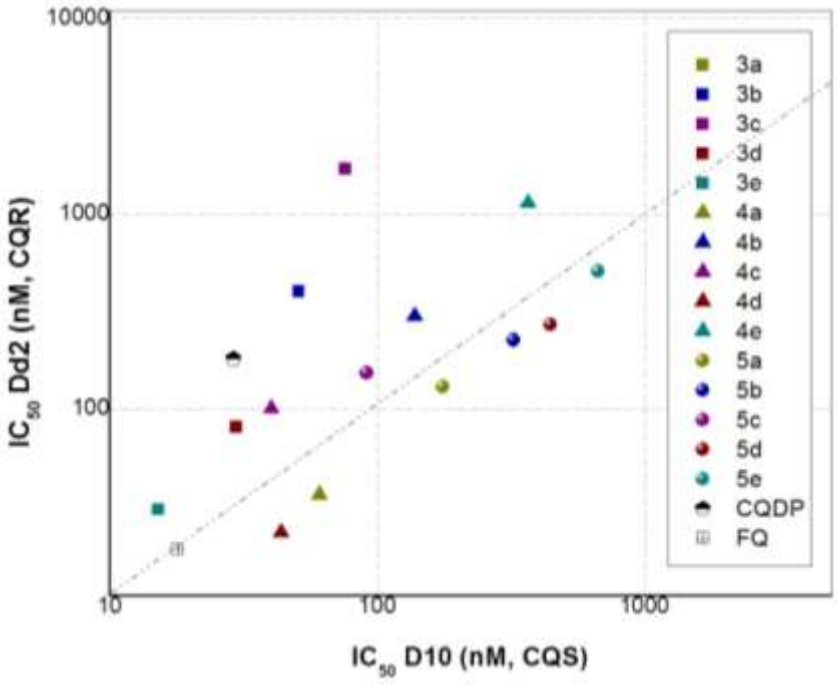

Figure 3.4. Resistance Index (RI) expressed as the correlation of the in vitro antiplasmodial activity against P. falciparum CQS D10 and CQR Dd2 parasite strains.

The fact that some of these compounds are equally or more potent in drug-resistant parasite strains than in drug-sensitive strains indicates that, rather than following the mechanism of accumulation of chloroquine, these are following a different mechanism allowing them not to be detected by the transmembrane proteins responsible for lower accumulation of the drug (origin of resistance). Ferroquine indiscriminative action in parasite strains has been explained in a similar fashion.[176,219]

3.3.2 *In vitro* antitumor activity and cytotoxicity assay

The toxicity of the ferrocenyl chloroquine compounds was assessed *in vitro*. Two human cell lines originally from human breast tissue were employed. The normal breast epithelial cells MCF-10A (CRL-10317) and the breast cancer cells MDA-MB-435S (HTB-129) were used as reference for a healthy and cancerous cell line, respectively. We used these two particular cell lines to compare the cytotoxic and antitumor response of the compounds when cultivated in the presence of healthy cells MCF-10A and breast cancer cells MDA-MB-435S.

In addition, chloroquine and other quinoline-containing drugs, traditionally used as antimalarials, have also been studied as anticancer agents in human breast tissue.[220] Chloroquine and other quinoline compounds have been reported as *in vitro* apoptosis-inducing agents against MCF-7 human breast cancer cells, stimulating cell differentiation by causing DNA damage and reduction in the E2F1 protein.[220]

Antitumor activity and cytotoxicity were assayed using the MTT methodology. The MTT (3-(4,5-dimethylthiazol-2-yl)-2,5-diphenyltetrazolium bromide) assay is a colorimetric test of the viability of cultured cells after exposure to a challenge compound.[212] The assay quantifies the amount of yellow MTT reduced to purple formazan in the mitochondria of living cells; the amount of purple reagent is directly proportional to the percent viability of the cell population.[212] Cisplatin (cis-diamminedichloroplatinum(II)) was used as a positive control for cell death. Chloroquine diphosphate (CQDP) was also used as control.

All tested compounds were found to lower the viability of the test cell cultures, with increasing detrimental effect with increasing compound concentration. Representative survival plots are given in Figure 3.5. Further information on the effect of the compounds in

each cell population is obtained by the means of the IC_{50} value that represents the concentration at which fifty percent of the cell population are non viable (dead). Therefore, the lower the IC_{50} value, the more sensitive is that particular cell line to the compound to which it has been exposed. IC_{50} values calculated for all tested compounds are shown in Table 3.3.

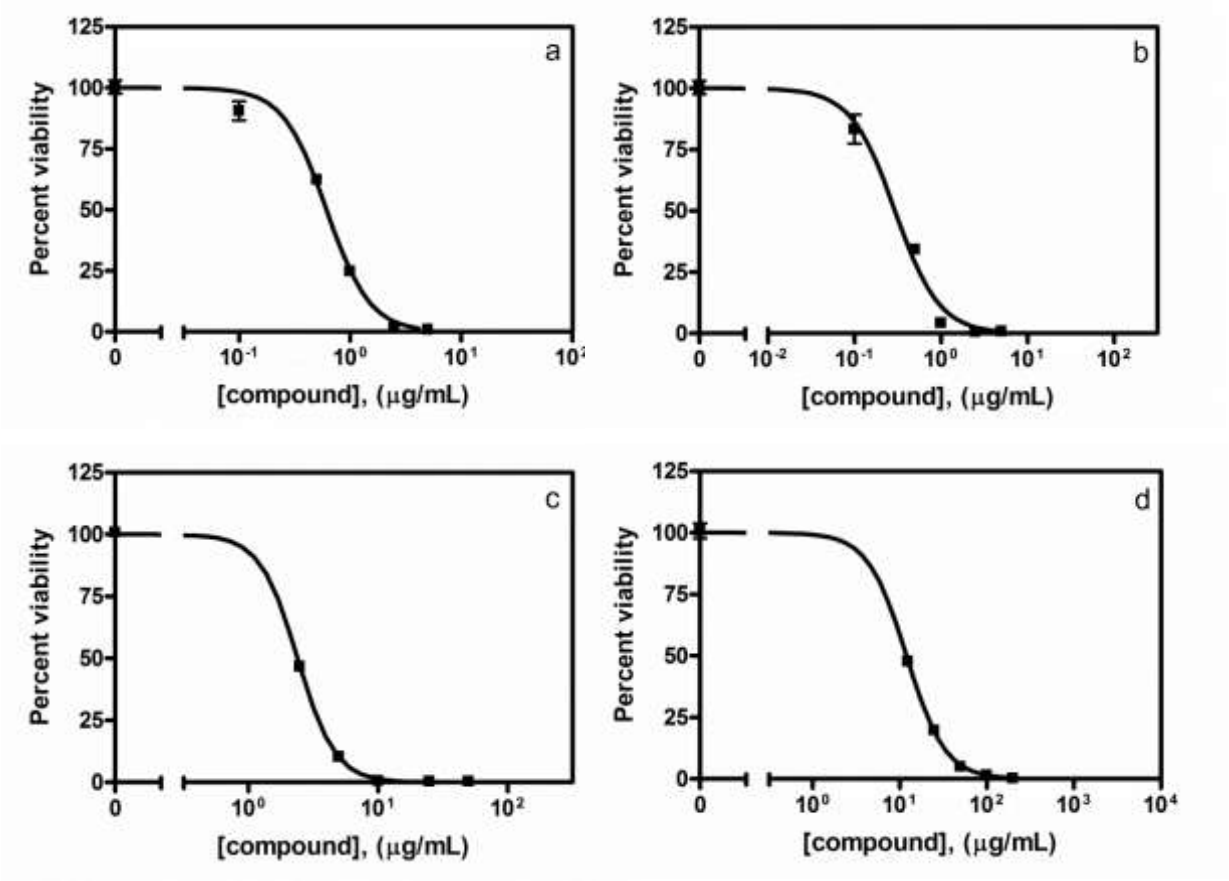

Figure 3.5. Survival plots for (a) **5d** in the MDA-MB-435S cell line, (b) **5e** in the MDA-MB-435S cell line, (c) **4d** in the MCF-10A cell line and (d) **3c** in the MCF-10A cell line.

Table 3.3. Toxicity of the compounds (expressed in IC_{50} values) against the human normal breast epithelial cell line MCF-10A and the human breast cancer cell line MDA-MB-435S.

Compound	IC_{50} - MCF-10A (μM)	IC_{50} - MDA-MB-435 (μM)
3a	74.7 ± 3.7	17.5 ± 1.4
3b	103.0 ± 6.0	21.90 ± 1.3
3c	47.9 ± 1.4	13.56 ± 2.4
3d	107.0 ± 2.1	25.67 ± 0.7
3e	105.3 ± 3.1	22.71 ± 1.2
4a	4.1 ± 0.5	3.1 ± 0.2
4b	2.8 ± 0.3	3.1 ± 0.1
4c	3.8 ± 0.6	3.0 ± 0.2
4d	5.5 ± 0.1	3.2 ± 0.1
4e	5.4 ± 0.1	2.6 ± 0.1
5a	2.4 ± 0.2	1.7 ± 0.1
5b	4.0 ± 1.0	3.1 ± 0.3
5c	4.2 ± 0.9	2.8 ± 0.2
5d	1.4 ± 0.1	1.4 ± 0.1
5e	0.3 ± 0.1	0.6 ± 0.1
Cisplatin	11.1 ± 1.5	92.3 ± 19.8
CQDP	69.7 ± 4.8	20.2 ± 1.2
FQ	26.5 ± 2.0	12.3 ± 0.8

In the normal breast epithelial cell line MCF-10A, the IC_{50} values observed for the organic component, the chloroquine derivatives **3a-e**, range from 50-100 μM indicating mild to non toxicity. These chloroquine derivatives are, in general, less toxic that the parent drug chloroquine diphosphate (CQDP) and ten times less toxic that the drug cisplatin. Once derivatized with ferrocene, the series of compounds **4a-e** and **5a-e** show a noticeable increase in toxicity, an average of 50-fold decrease of IC_{50} values in the MCF-10A cell line.

Against the breast cancer cell line MDA-MB-435S, the chloroquine derivatives **3a-e** are remarkably more active, with IC_{50} values that are roughly a fifth of the values displayed in the normal MCF-10A cell line. These results concur with those of studies of chloroquine and

derivatives as anticancer agents in human breast tissue.[220] These IC_{50} values are similar to those of CQDP and much lower than that of cisplatin, typically used to treat ovarian and testicular cancer, among other types of cancer in combination.[221]

The IC_{50} values obtained for the series of compounds **4a-e** and **5a-e** against the MDA-MB-435S cell line are similar to those obtained for the normal MCF-10A cell line, indicating that any effect is mainly driven by the toxicity associated with the compounds.

In general, the quinoline organic fragment seems to impart some antitumor activity, reflected in how active compounds **3a-e** are against the cancer cell line compared to the normal cell line. The addition of the metallocene fragment increases greatly the toxicity of the compounds, and this is comparable to what has been observed for other ferrocene chloroquine compounds.[222] The mode of substitution, either mono substituted in one ferrocene ring or in the bridged form, does not seem to have a direct influence on the overall activity of the compounds, and neither does the length of the side chain or its degree of branching.

It can be concluded that the organic fragments **3** could have potential as anticancer agents but that the ferrocenyl analogs **4** and **5** seem to lack this potential evinced by their indiscriminate action against both normal and cancer cell lines. The uniform cell death observed in both cell lines after treatment with the ferrocene compounds seems to be caused by necrosis rather that apoptosis (intended form of cell death for cancerous tissues in antitumor therapy) that could be caused by long exposure to toxic compounds. In the future, this test could be run in 24 h exposure intervals instead of 72 h to monitor more effectively the response of the cells to these compounds.

3.3.3 Association with hematin assay

For clarification of some terms used throughout this discussion: the term *heme* will refer to the iron protoporphyrin IX (Fe(II/III)PPIX), the term *hemin* will refer to the ferriprotoporphyrin IX chloride Fe(III)PPIX-Cl, and the term *hematin* will refer to the ferriprotoporphyrin IX hydroxide/aqua Fe(III)PPIX-OH/H_2O. *β-hematin*, as explained in Chapter 1, refers to the crystalline arrangement of heme dimers linked by reciprocal iron-carboxylate bonds to one of the propionate side chains of each porphyrin macrocycle (Figure 3.6).

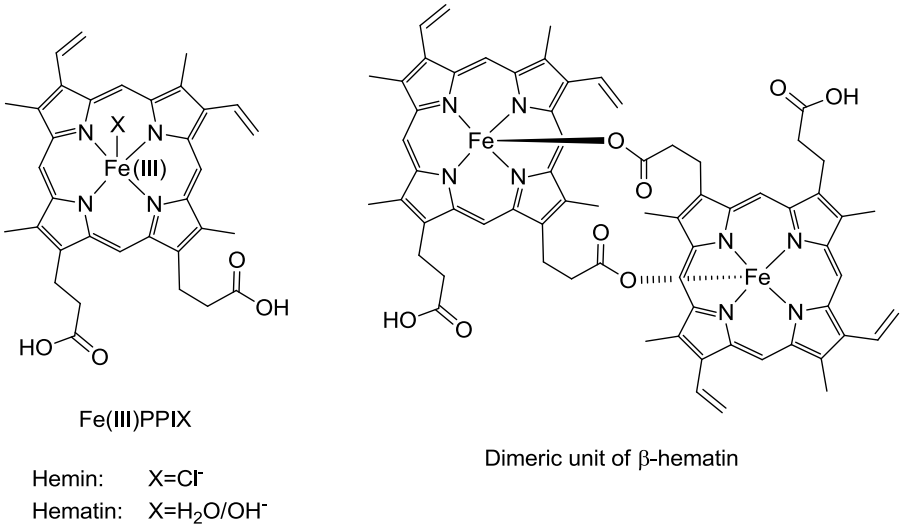

Figure 3.6. Structures of Fe(III)PPIX, hemin, hematin and the dimeric unit of β-hematin.

Extensive evidence supports Fe(III)PPIX as the molecular drug target of quinoline antimalarial drugs.[223] Aminoquinolines act by complexing Fe(III)PPIX thus reducing the availability of monomeric Fe(III)PPIX and its incorporation into hemozoin (β-hematin), hence halting the detoxification process of the parasite.[191,223]

The monomeric Fe(III)PPIX and chloroquine and other 4-amino quinolines and quinoline methanol antimalarials form a π-π complex,[224,225] in neutral or weakly acidic media.[32] The π→π* electronic transitions in the porphyrin give rise to the Soret band at 402 nm.[223] A strong hypochromism is then observed upon complex formation between the Fe(III)PPIX and the quinoline drug. This effect can be quantified and fitted to a model of association to determine the strength of complex formation.

The interaction of the chloroquine ferrocenyl compounds with monomeric hematin was evaluated in a 40% DMSO aqueous buffered medium (apparent pH 7.5, 0.02 M HEPES) at 25 °C. This medium is required to maintain a monomeric unaggregated form of hematin that can interact with the quinoline-containing drug,[226] and mimics the physiological environment (pH 7.5); however, it is an intracellular environment (with acidic pH = 5.2) where the interaction between Fe(III)PPIX and the CQ-derivative is expected to occur. Previous studies have shown that association constants between hematin and quinoline antimalarials in the solvent system mentioned above closely mirror those in acidic aqueous solutions.[227] In this case, one would expect that the association constants determined for these compounds to be a reasonable estimate of the association constant at intracellular conditions.

The alternative, conducting these studies in a purely aqueous medium (which would reflect more closely the biological environment), was discarded several years ago.[213] Studies on enthalpy-entropy compensation in the interaction of quinoline antimalarials with Fe(III)PPIX carried out in the 40% DMSO system and in pure aqueous solution demonstrated that the degree of desolvation and loss of conformational freedom is virtually identical in both systems.[228] This study suggests then that the recognition site on the metalloporphyrin is comparable in both cases, despite the fact that Fe(III)PPIX exists as a

dimer in aqueous solution but is monomeric in 40% DMSO.[228] Studies in aqueous solution give irreproducible and unreliable results,[213,223] hence the 40% DMSO system is employed. It is indicated that electrostatic interactions (ionic strength) do not affect the overall stability of the association of the hematin-complex under the latter conditions,[228] therefore ionic strength was not considered during the experiment.

The formation of the complex between Fe(III)PPIX and the CQ-derivative was monitored as a function of the decrease in absorbance of the Soret band of monomer hematin at 402 nm upon coordination to increasing concentrations of the quinoline moiety. Figure 3.7 shows a set of spectra collected when the hematin solution was titrated with increasing concentrations of the compounds (in this example, compound **4a**). The spectral changes observed show a decrease in the Soret band of Fe(III)PPIX at 402 nm and an increase in the quinoline band at around 338 nm that is explained by the increasing concentration of the quinoline-derivative.

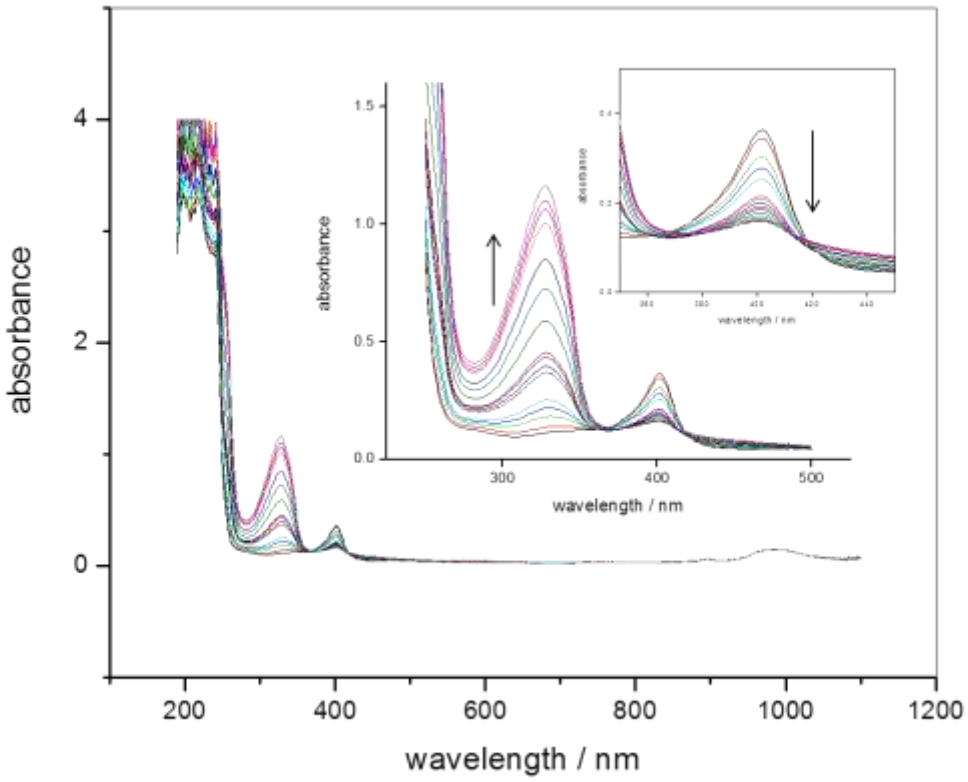

Figure 3.7. Spectroscopic changes observed when Fe(III)PPIX is titrated with compound **4a**. Changes in the Soret band of Fe(III)PPIX can be observed in the insets.

The absorbance values were corrected for the blank and also for dilution. The data obtained were fit to a 1:1 association model to calculate the association constant as log *K*. This 1:1 association model is the best fit model for the parent drug chloroquine under these conditions.[213] The 1:1 complexation model for drug and Fe(III)PPIX was applied using equation 3.1.

$$A = (A_o + A_\infty K[c])/(1 + K[c]) \qquad 3.1$$

A_o is the absorbance of Fe(III)PPIX without drug present, A_∞ is the absorbance of the Fe(III)-quinoline drug complex and K is the conditional association constant.[213] Titration

data for a selection of the compounds are shown in Figure 3.8. The association constants (as log *K*) calculated for the compounds are presented in Table 3.4.

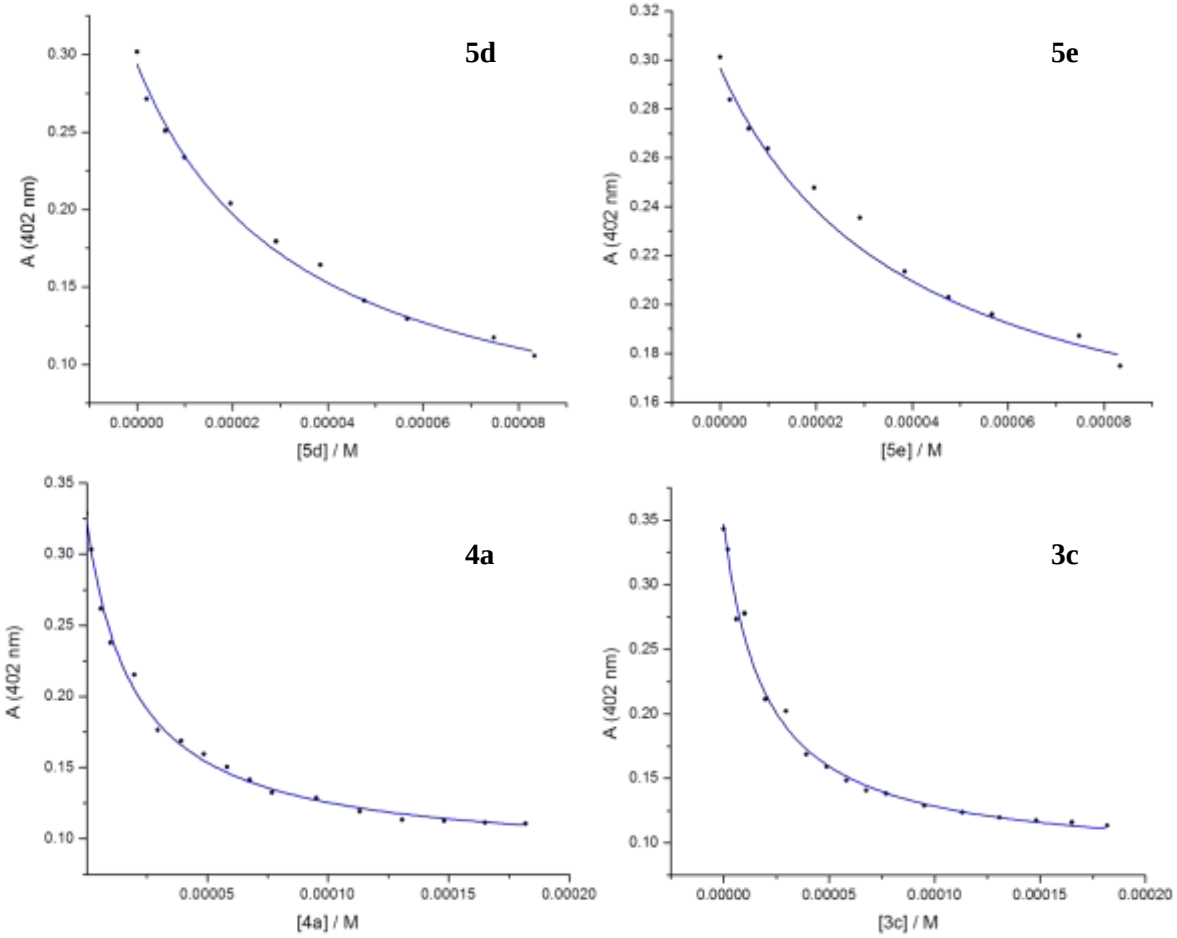

Figure 3.8. Variation in absorbance of Fe(III)PPIX at 402 nm as a function of compound concentration. The solid lines are best fits of the 1:1 association model to the data. Conditions: 40 % DMSO, apparent pH 7.5, 0.020 M HEPES buffer, 25 °C.

Table 3.4. Association constants (log K) obtained from spectrophotometric titrations of Fe(III)PPIX with compounds **3a-e**, **4a-e** and **5a-e** in 40% DMSO, apparent pH 7.5, 0.020 M HEPES buffer at 25 °C.

	3a	**3b**	**3c**	**3d**	**3e**	**4a**	**4b**	**4c**	**4d**	**4e**	**5a**	**5b**	**5c**	**5d**	**5e**
log *K*	4.67 ±0.05	4.85 ±0.02	4.86 ±0.04	4.62 ±0.05	4.80 ±0.03	4.71 ±0.03	4.42 ±0.10	4.13 ±0.05	3.68 ±0.04	ND	4.18 ±0.05	4.23 ±0.15	4.76 ±0.03	4.47 ±0.07	4.41 ±0.13

ND: Not determined

All compounds interacted with Fe(III)PPIX. The association constants (log *K*) obtained for the quinoline fragments (**3a**-**e**) were, as expected, relatively high, with values that ranged from 4.62 to 4.86 regardless of the length or branching of the side alkyl chain. These values are close to the value obtained for chloroquine diphosphate (CQDP) that was used as a control in this study (log K = 5.07 ± 0.05).

The ferrocenyl fragment in the compound series **4a-e** and **5a-e** demonstrated a marked effect in how these compounds interact with the monomeric Fe(III)PPIX under these conditions. The association constants for both types of ferrocenyl substituted series of compounds were on average lower than those observed for the organic fragments. Within the monosubstituted ferrocenyl group of compounds, **4a**, with an unbranched ethyl side alkyl chain, exhibits the highest value for this compound series (log *K* = 4.71). It was observed across this series that a longer and more branched side alkyl chain represented a lower value of log *K*. The association constant of compound **4e** was impossible to calculate due to insolubility.

Unlike compounds **4a-e**, the disubstituted bridged ferrocenyl compounds **5a-e** displayed log *K* values that increased with length and branching of the side alkyl chain. The highest association constant was obtained for compound **5c**, the unbranched butyl side chain (log *K* = 4.76).

The different structural conformations for these two types of ferrocenyl substitution, exemplified in the single crystal X-ray study of **4b** and **5b** (Chapter 2) seem to alter significantly the association of the quinoline fragment in these compounds with Fe(III)PPIX. In the bridged derivative **5b**, the ferrocene fragment is twisted into close proximity to the quinoline fragment, which could sterically hinder the π-π association of the latter and

Fe(III)PPIX, lowering the association constant. In the monosubstituted analog **4b**, the ferrocene is directed further away from the quinoline fragment and hence does not sterically disturb the quinoline fragment association with hematin, which is reflected in a higher value of log *K*. In turn, it is expected that the longer chain in the bridged derivative **5c** (butyl side chain) provides a less sterically hindered interaction between the quinoline fragment and hematin which would explain the elevated log *K* value for **5c** versus the value found for **5b**.

The association constant reported for ferroquine, log $K = 4.95 \pm 0.05$,[198] lower than the value reported for CQ (log $K = 5.52 \pm 0.05$)[191] and found in this study (log $K = 5.07 \pm 0.05$), is still comparable to the values obtained for the association constants of both series of ferrocenyl derivatives.

While bonding to Fe (III)PPIX seems to be a requirement, it is not sufficient for antimalarial activity.[191] Other physicochemical properties such as inhibition of β-hematin formation were also explored.

3.3.4 Inhibition of β-hematin formation assay

The antimalarial properties of these compounds were also explored as a function of their capacity to inhibit the formation of β-hematin. As previously discussed, one of the mechanisms of action known for the quinoline-containing drugs is inhibition of the spontaneous formation of the "malaria pigment" hemozoin. It has been shown that the formation of β-hematin (synthetic analog of hemozoin) is inhibited by chloroquine, quinine and amodiaquine.[214]

The ability of the compounds to inhibit β-hematin formation was evaluated both qualitatively using infrared spectroscopy and quantitatively using the pyridine hemochrome assay by UV-vis spectroscopy.

The qualitative IR assay relies on differences in the infrared spectrum between hematin and β-hematin. β-Hematin can be synthesized in the absence of proteins or enzymes from a solution of hematin.[214] The formation of β-hematin occurs spontaneously at 60 °C in a 12.9 M sodium acetate buffered at pH 4.5.[214] Hematin and β-hematin can be characterized and differentiated by infrared spectroscopy. The IR spectrum of β-hematin presents sharp bands at 1660 and 1207 cm^{-1} that are absent in the IR spectrum of hematin.

This assay was undertaken as described previously in literature.[214] Previously incubated solutions of 0.1 mL 1.0 M HCl and 0.58 mL 12.9 M sodium acetate (pH 5.0) were added to the hematin solution in 1.0 mL of 0.1 M NaOH at 60 °C. The addition of acetate caused the precipitation of hematin and the slurry was incubated for an hour. In other reported procedures, the solution is neutralized first with 1.0 M HCl and then incubated for 10 minutes at 60 °C, followed by the addition of the 12.9 M sodium acetate solution (pH 5) that gives a final solution of pH 4.5.[198] After cooling in an ice bath and filtration onto a cellulose disk, the solid was rinsed thoroughly with water, dried under vacuum and analyzed by infrared spectroscopy.

The tested compounds were added to the assay previous to the acidification step. Three compounds were tested initially, the chloroquine fragment with the propyl side chain **3b**, the mono-substituted ferrocenyl analog **4b** and the bridged substituted ferrocenyl analog **5b**. Solubility issues stalled this stage in the assay. Due to the dark color of the hematin solution, it was unclear if these compounds were insoluble or partially soluble even at the lowest

concentrations recommended for this assay (3 molar equivalents, 13.7 mM). Unfortunately, this assay was designed and has been mainly used[198,214,228] to study antimalarial drugs that were water soluble, whereas the organometallic compounds studied here are not.

The use of other solvents to facilitate the dissolution of the studied products was not tested since the solvent effect on this assay has not been explored and could considerably affect the interactions that cause the formation of β-hematin. The addition of other organic solvents could produce misleading results since, by analogy, increasing the DMSO concentration in the association with hematin assay weakens the interaction of some aminoquinolines with Fe(III)PPIX.[228] Also, the use of fewer molar equivalents is not recommended since barely any inhibition capacity would be observed.[214]

Nonetheless, the tests were carried out indicating that all three compounds were effective β-hematin inhibitors at the lowest concentrations (3 equivalents). The IR spectra obtained for these tests are shown in Figure 3.9. The infrared spectrum of β-hematin has two characteristic sharp peaks at 1660 and 1207 cm^{-1} [214] that are absent in all IR spectra collected, indicating that β-hematin formation was inhibited in the three cases.

Unfortunately, when hematin was treated under the conditions used for the formation of β-hematin, as a control experiment, no β-hematin was obtained as observed in Figure 3.9. Even though the procedure indicated to have worked in several other cases was followed,[203,214,229,230] reliable results for the compounds tested could not be obtained or reproduced.

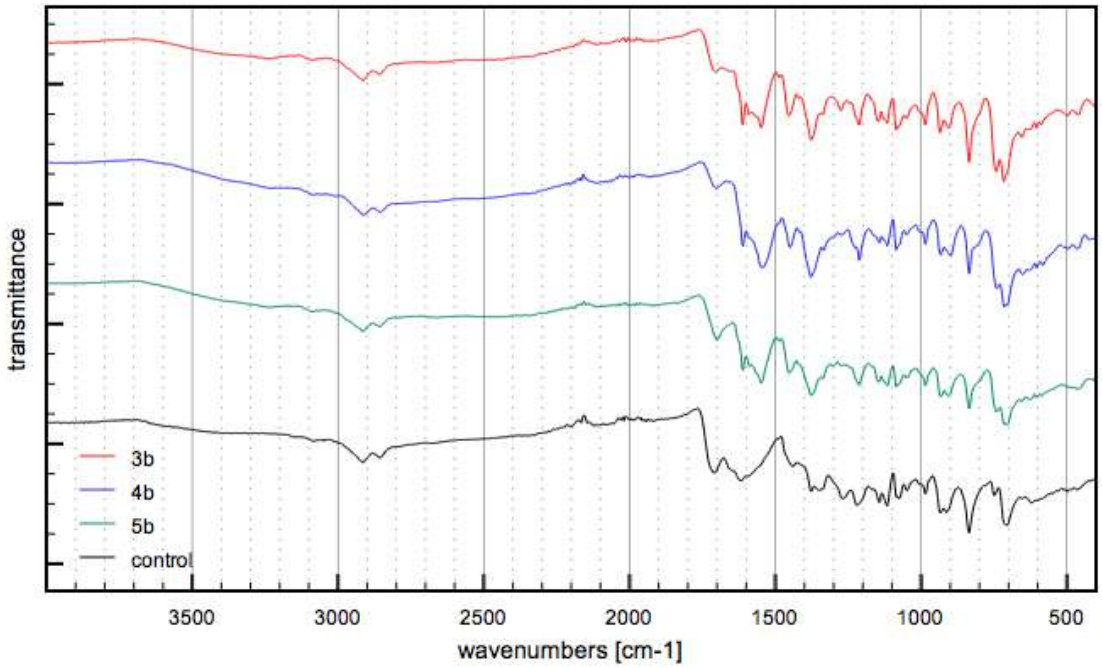

Figure 3.9. Infrared spectra of the hematin/β-hematin mixture obtained after incubation at 60 °C for 1 h in the presence of 3 molar equivalents of compound and no compound (control) in 4.5 M acetate, pH 5. The characteristic very intense β-hematin peaks at 1660 cm^{-1} and 1207 cm^{-1} are absent in all cases.

The ability of these compounds to inhibit β -hematin formation was also studied using the pyridine hemochrome (Phiβ) assay.[215] This method is based on the association between pyridine and free hematin. In aqueous solutions of hematin, formation of the solid β-hematin is stimulated by addition of sodium acetate while in the presence of different concentrations of the studied compounds. The degree of inhibition of β-hematin formation achieved by the test compound is measured after 1 hour by calculating the concentration of free hematin left after this period. This is done by adding pyridine and measuring the absorbance of the complex formed by Fe(III)PPIX and pyridine.

When hematin is present in a purely aqueous medium it exhibits a broad and weak Soret band due to hematin aggregation.[231] Upon titration with pyridine, the latter displaces the

weak field ligand H_2O from the axial position and coordinates Fe(III), causing a red shift in the Soret band (from 389 to ~404 nm) also sharpening and intensifying the band, indicating dissociation of the iron porphyrin dimer.[215]

Also, under pH conditions close to neutral and in low concentrations, the pyridine which displaces the axial aqua ligand in hematin cannot displace the propionate ligand that coordinates iron in the β-hematin dimer.[215] Hence, the measure of the absorbance of the Fe(III)PPIX-pyridine complex formed is directly proportional to the concentration of remaining hematin in solution.[215]

A selection of compounds was screened for their inhibitory activity up to 10 equivalents relative to hematin. Hematin solution in 0.1 M NaOH was incubated in the presence of the studied compounds with increasing numbers of equivalents. The β-hematin formation from this solution of hematin was initiated by the addition of acetate solution to give a final concentration of 4.5 M and pH 4.5. After incubation at 60 °C for 1 hour, the process was quenched by the addition of a 5% (v/v) pyridine solution and buffered at pH 7.5 to give the ideal conditions for the formation of the Fe(III)PPIX-pyridine complex with the hematin remaining in solution.

After stirring briefly to ensure all hematin reacted with the pyridine, the solid β-hematin was allowed to settle. This step separated the crystals of β-hematin from the solution so they do not interfere with the UV-vis reading. The supernatant was then carefully transferred to a cuvette where the UV-vis absorption was read in the 300-700 nm wavelength region. The effect of the addition of pyridine to the hematin/β-hematin mixture is reported in the Soret band of the Fe(III)PPIX-pyridine complex at 405 nm. The relationship between absorbance

and concentration is linear; higher concentrations of hematin in solution indicate the potent effect of the drug to divert the consumption of hematin into the formation of β-hematin.

The set of spectra collected for the drug chloroquine diphosphate is shown in Figure 3.10. Even though each experiment consisted of 0 to 10 drug equivalents of hematin, only the relevant group often formed by 0-5 equivalents is shown. It can be observed in the UV-vis spectra that with no equivalents of the drug, after an hour of incubation, a small amount of hematin is present in solution while the rest presumably forms the crystalline β-hematin left behind. With an increasing number of equivalents of drug, even at one equivalent, the absorbance of the Fe(III)PPIX-pyridine complex increases significantly. In the presence of one equivalent of drug, the concentration of hematin remaining in solution has increased and therefore less β-hematin has been formed.

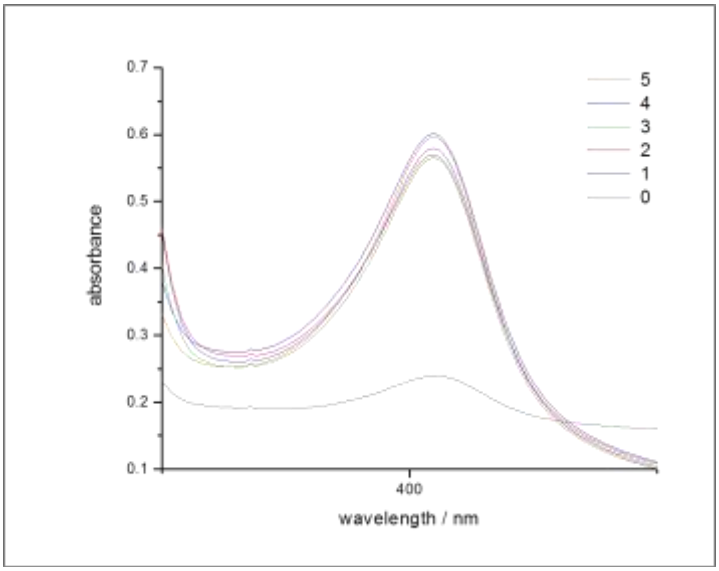

Figure 3.10. Interaction of pyridine and hematin present in solution. The legend indicates the number of equivalents of chloroquine added in each experiment. Increasing amount of the drug chloroquine produced an increased concentration of hematin, judged from the absorbance of the Soret band of the Fe(III)PPIX-pyridine complex at 405 nm. Solvent: 5% pyridine, 100 mM HEPES.

The sets of spectra collected for the mono-substituted ferrocenyl derivative of the ethyl side chain 4-aminoquinoline **4a**, the mono-substituted ferrocenyl derivative of the propyl side chain 4-aminoquinoline **4b** and the disubstituted bridged ferrocenyl analog **5b** are shown in Figure 3.11.

In the spectra for compound **4a**, when no equivalents of the compound are present, a small amount of hematin is observed in solution that is identified by the means of the absorbance of the Fe(III)PPIX-pyridine complex (Figure 3.11). However, at any other number of equivalents, no absorbance is detected for this complex indicating that no free hematin is left in solution.

For compounds **4b** and **5b**, the situation is slightly different. As can be seen from the respective insets in Figure 3.11, respectively, the low absorbance of the Fe(III)PPIX-pyridine complex at 1 or 2 equivalents of the compound quickly decays after the number of equivalents increase. Although this was seen as an improvement, any absorbance detected is well below the level detected for the Fe(III)PPIX-pyridine complex when no compound is present.

These observations could lead to false negative results. If these compounds do not inhibit formation of β-hematin, all spectra obtained would be expected to be identical to the spectra obtained at zero equivalents of the compound. This phenomenon of quenching of the absorbance of the hematin that should remain in solution, even after a large portion of it has been used to form β-hematin is explained by solubility restrictions.

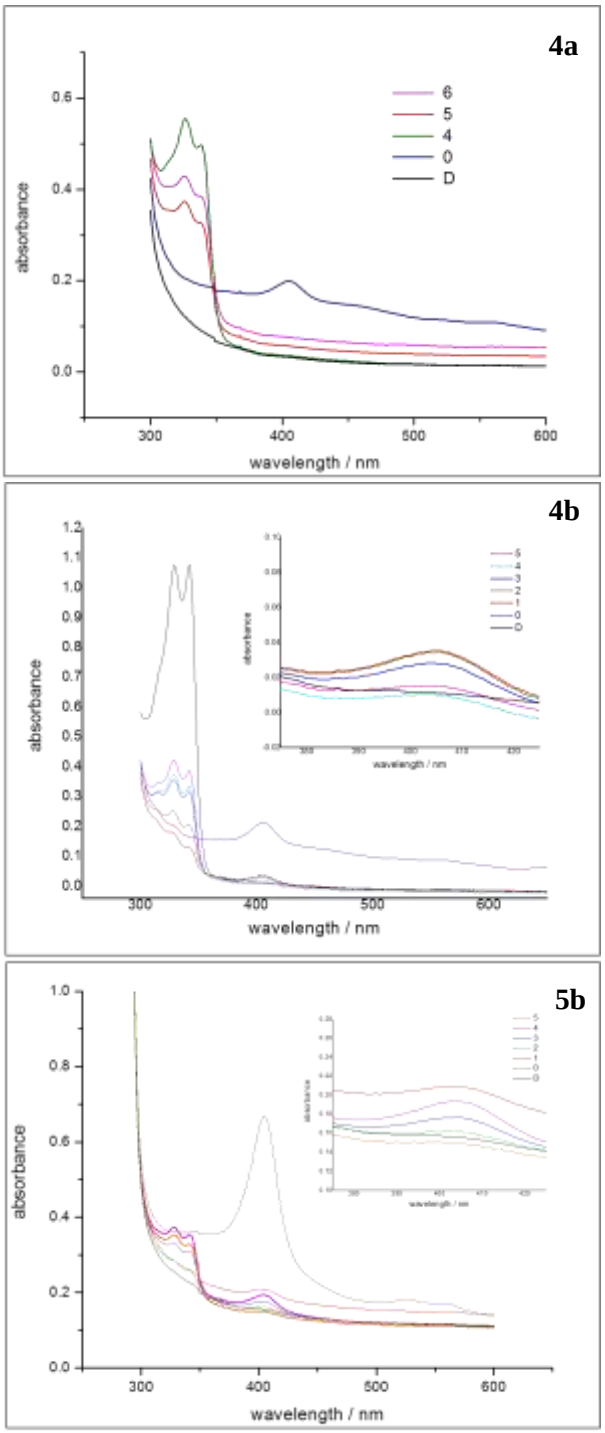

Figure 3.11. Interaction of pyridine and hematin present in solution after incubation for the formation of β-hematin. The sets of spectra correspond to increasing amount of compounds **4a**, **4b** and **5b**. The absorbance of the Soret band of the Fe(III)PPIX-pyridine complex occurs at 405 nm. The legend indicates the number of equivalents of test compound added in each experiment. D indicates drug only, a blank using the maximum concentration of drug in the 5% pyridine aqueous solution.

The weak inhibitory properties are interpreted to be related to the poor solubility of the compounds in aqueous media. The stock solutions of the compounds, completely dissolved in DMSO although some of them required heating, were added to the aqueous media where they could precipitate due to the presence of large amounts of water. It has been noted that poorly water soluble compounds trap unreacted hematin in the solid state.[215] This would explain the absence of the Fe(III)PPIX-pyridine complex absorbance peak. It is known that compounds with very low water solubility, such as the quinoline drug halofantrine, indeed inhibit β-hematin formation and appear to prevent solubilisation of hematin in aqueous pyridine medium giving false negative results.[215] Moreover, the cloudiness arising from partial precipitation of the compounds and/or from the transport of miniparticles of β-hematin can interfere with the measurement of absorbance.

As in the previous assay, adding larger amounts of organic solvents to solubilize the compounds could interfere with the processes occurring for the formation or inhibition of formation of β-hematin; it has not been explored before and thus was not considered as an option to increase the solubility of the compounds.

3.3.5 Partition coefficient

Lipophilicity is a physicochemical characteristic that plays an important role when determining the behaviour of a drug in an *in vivo* system (determining its ADME - absorption, distribution, metabolism and excretion).[232] As was mentioned earlier, accumulation of chloroquine-based compounds in the parasite food vacuole lacks a special transport mechanism and it is determined by physical characteristics that will allow the

crossing of membranes and the retention upon protonation inside the vacuole.[32] Therefore, physical characteristics such as lipophilicity have been suggested to play a determining role in the accumulation of drugs inside the acidic food vacuole of the malaria parasite.[33,39,54]

Log *P* is the partition coefficient that represents the ratio of concentrations of a neutral compound in an octanol-water mixture. Log *P* is used frequently to define the lipophilic character of a drug. For ideal pharmacokinetic and pharmacodynamic properties in a drug, the ideal distribution coefficient is a moderate intermediate between hydrophilic and hydrophobic. Theoretically calculated values of log *P* (Clog *P*) are presented in Table 3.5.

Table 3.5. Theoretical values of log *P* calculated for compounds **3a-e**, **4a-e** and **5a-e**.

$$\log P_A = \log \frac{[\mathrm{A}]_{\mathrm{oct}}}{[\mathrm{A}]_{\mathrm{water}}}$$

Compound	Clog *P*
3a	1.27
3b	1.38
3c	1.83
3d	1.59
3e	2.49
4a	4.48
4b	4.84
4c	4.83
4d	4.79
4e	5.64
5a	6.38
5b	6.74
5c	6.71
5d	6.69
5e	7.54
FQ	5.10

Theoretical log *P (*Clog *P)* values were calculated using the commercially available ACDLABS 11.0 program.[216,233] These values ranged from 1.27 to 2.49 for the organic component **3a-e** and for the ferrocenyl derivatives **4a-e** and **5a-e**, values ranged from 4.48 to 7.54. In general these compounds are all lipophilic (log $P > 0$). The series of chloroquine derivatives **3a-e** experience, as expected, an increase in lipophilicity as the alkyl side chain increases in length and in branching, the 2,2'-dimethyl-propyl side chain derivative (**3e**) being 17 times more lipophilic than the ethyl side chain derivative (**3a**).

The largest change is provided by the incorporation of ferrocene in the structure of the 4-aminoquinoline. The presence of the ferrocenyl entity contributes largely to the lipophilic character and to the electron-donating properties. The predicted value for the log *P* of ferrocene is 3.54,[234] which is strongly lipophilic itself.

The calculated log *P* values show a considerably larger lipophilicity for compounds **4a-e** and **5a-e** compared to **3a-e**. The disubstituted bridged ferrocenyl compounds are 10^5-fold more lipophilic than the parent chloroquine fragment while the mono-substituted ferrocenyl compounds are 10^4 more lipophilic. This approximate 10-fold difference in lipophilicity between series **4a-e** and series **5a-e** arises exclusively from the difference in ferrocene substitution and structural orientation. The more closed conformation of the bridged compounds likely provides a more hydrophobic surface and therefore a higher value of log *P*. The less rotationally restricted monosubstituted analogs show less, but still significant, lipophilicity due to the ferrocene.

Within each of the ferrocenyl series, the lipophilicity of the first four members is relatively similar, but the 2,2'-dimethyl-propyl side chain ferrocenyl derivative (**4e** and **5e**) is the most lipophilic of each group, with an increase of 14-fold in lipophilicity when compared

to the ethyl side chain ferrocenyl derivative (**4a** and **5a**, respectively). These Clog *P* values are similar to those obtained for chloroquine (4.63) and for FQ (5.1).[198] The high lipophilicity of FQ has been postulated to be key in the good absorption and transport properties across cell membranes.[125]

While Clog *P* is useful, a more accurate determination of lipophilicity for ionizable compounds is provided by log *D* or the distribution coefficient that represents the ratio of the sum of the concentrations of all forms of the compound (ionized and un-ionized) in each of the phases of the octanol-water mixture. Another parameter often used in estimation of pharmacological profiles is the vacuolar accumulation ratio (*VAR*) that gives an estimation of the accumulation of compounds in the parasitic vacuole.

Theoretical values of log *D* and *VAR* were attempted by calculation at physiological pH (7.4) and vacuolar pH (5.2) without success. All the programs used for the *in silico* estimation of these pharmacological properties have been developed to work with organic fragments and none of them supports metallic fragments.

Experimental measurements of log *P*, log *D* and *VAR* can be done but they are time consuming and demand large amount of products. So it is a common practice in medicinal chemistry to utilize the product to carry out activity testing when other pharmacological properties are estimated *in silico*. Unfortunately, in inorganic medicinal chemistry that is not yet a possibility.

3.3.6 Molecular shape analysis

Computational methods such as molecular field analysis (MFA) and molecular shape analysis (MSA) are 3D-quantitative structural-activity relationship (3D-QSAR) approaches that compute shape, conformational and electronic properties that can be used to predict important pharmacophoric properties of drug candidates such as the ability of these compounds to permeate biological membranes.[235]

Computational methods have been used in the past to rationalize antimalarial activity.[162,164,198] Specifically, MFA and MSA approaches have been used to predict the antimalarial activity of groups of 4-aminoquinolines showing high correlation between steric and electrostatic field and antimalarial activity, and predictive ability.[236] In the same study, molecular shape analysis revealed the role of spatial properties and conformation in antimalarial activity.[236] Molecular shape analysis demonstrated a better predictive capability than did the molecular field analysis, explained by the fact that MSA takes into consideration an array of conformers, whereas only the minimum-energy conformer is used for MFA.[236]

The generation of the molecular electrostatic potential (MEP) is only one of the many possible outcomes of the MSA process. The overall MSA process has as a goal to generate a quantitative structural-activity relationship that can be useful for activity estimation and evaluation, and therefore for the identification of potential drugs.[235] The molecular electrostatic potential (MEP) surface gives an indication of the charged surface area, its accessibility by polar solvents (giving also an idea of the hydrophilicity of the compounds), and an idea of the importance of the orientation of the molecule for the activity of the drug candidate.

Therefore, the MEP maps of several compounds were generated via the molecular shape analysis approach by computational methods in order to provide insight into key structural features for the compounds such as steric, electrostatic interactions, hydrogen-donor/acceptor properties and lipophilicity. The molecular electrostatic potential (MEP) surfaces, computed at the the DFT-B3LYP level of theory for the neutral state of the studied compounds, are shown in Figures 3.12 and 3.13.

These molecular electrostatic potential (MEP) maps were constructed in a color scale that ranges from more electropositive (blue) to more electronegative (red) surface area in the molecule. All bridged ferrocenyl compounds **5a-e** (Figure 3.12) present similar electrostatic maps. The most electronegative areas in the molecule correspond to the quinoline nitrogen and the Cl-group at the 7- position in the quinoline ring, as expected. Neither the secondary nitrogen at the 4-position in the quinoline ring nor the bridging tertiary nitrogen of the end of the alkyl chain appear to display electronegative character. The only exceptions are the ethyl (**5a**) and butyl (**5c**) side chain derivatives, for which some of the electronegativity of the bridging nitrogen can be detected, indicating that part of the nitrogen lone pair is available. Due to steric hindrance, this charged zone is not observed in the others and the nitrogen lone pair of the bridging nitrogen is thought to be buried in the structure and unavailable for interaction with solvents or other molecules.

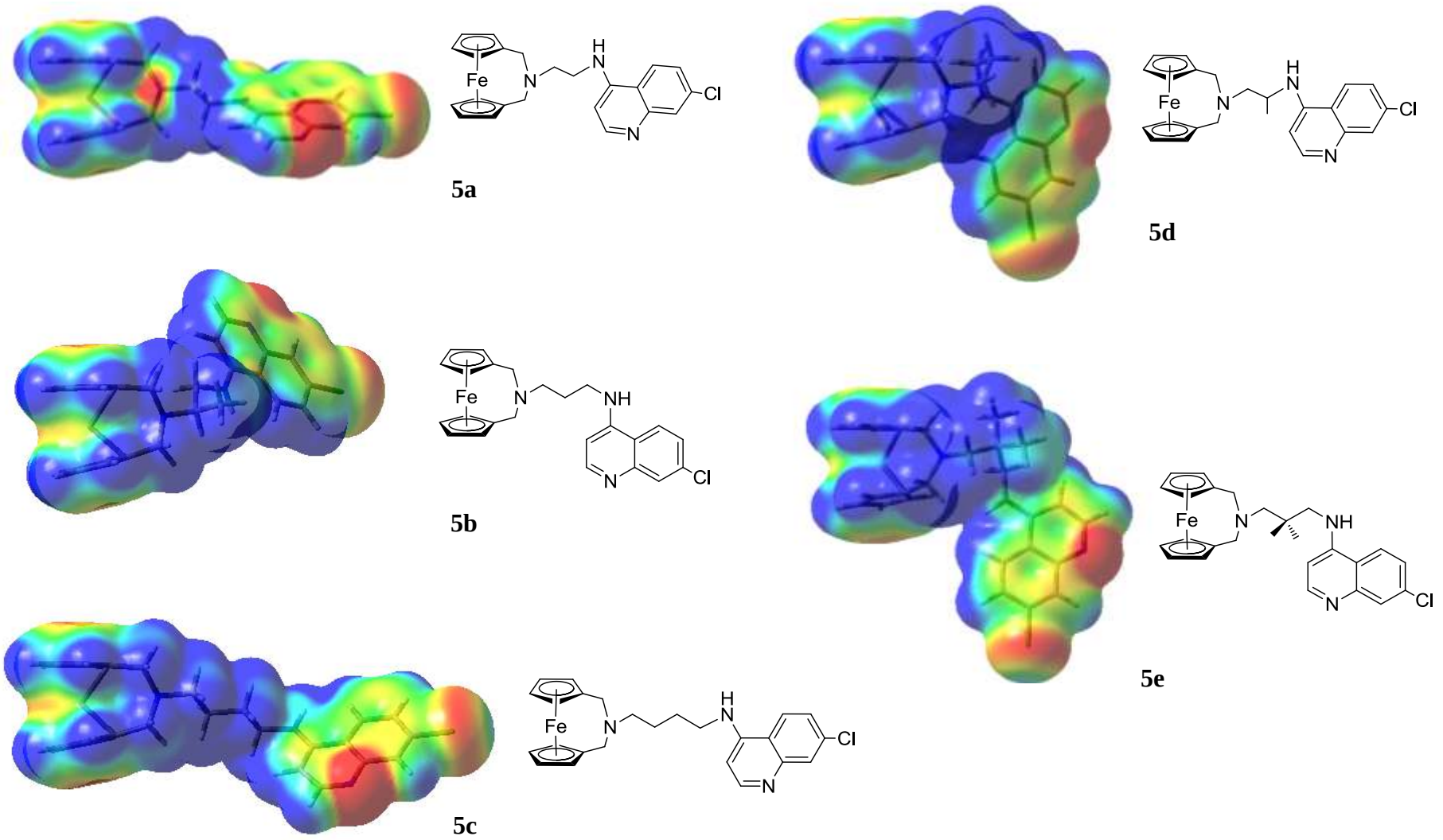

Figure 3.12. Molecular electrostatic potential (MEP) surfaces of the disubstituted bridged ferrocenyl compounds **5a-e** in their neutral state.

Figure 3.13 shows a comparison of the molecular electrostatic potential (MEP) surfaces of a group of relevant compounds discussed in this thesis. When comparing the MEP maps of the two modes of ferrocenyl substitution discussed so far, the disubstituted bridged form (exemplified by **5b**) and the mono-substituted form (exemplified by **4b**), the most noticeable difference comes from the nitrogen that connects the alkyl chain and the ferrocene. In the latter form of substitution, this nitrogen is more electronically available with the lone pair probably oriented towards the outer part of the molecule and therefore more accessible to interactions with the surroundings. In the bridged analog, this electronegative surface area is buried and poorly accessible.

From the MEP surface of the corresponding 4-aminoquinoline fragment **3b**, two more electronegative sites can be observed. As expected, the primary terminal amino group that is unavailable in **5b** and partly available in **4b** is completely available in **3b**, displaying an increased electronegative surface. The most interesting difference stems from the electronegatively charged zone of the nitrogen of the 4-position in the quinoline ring. Absent in both ferrocenyl derivatives, the electron density associated with this nitrogen is thought to be affected by the inductive and electronic changes generated by the attachment of the ferrocene.

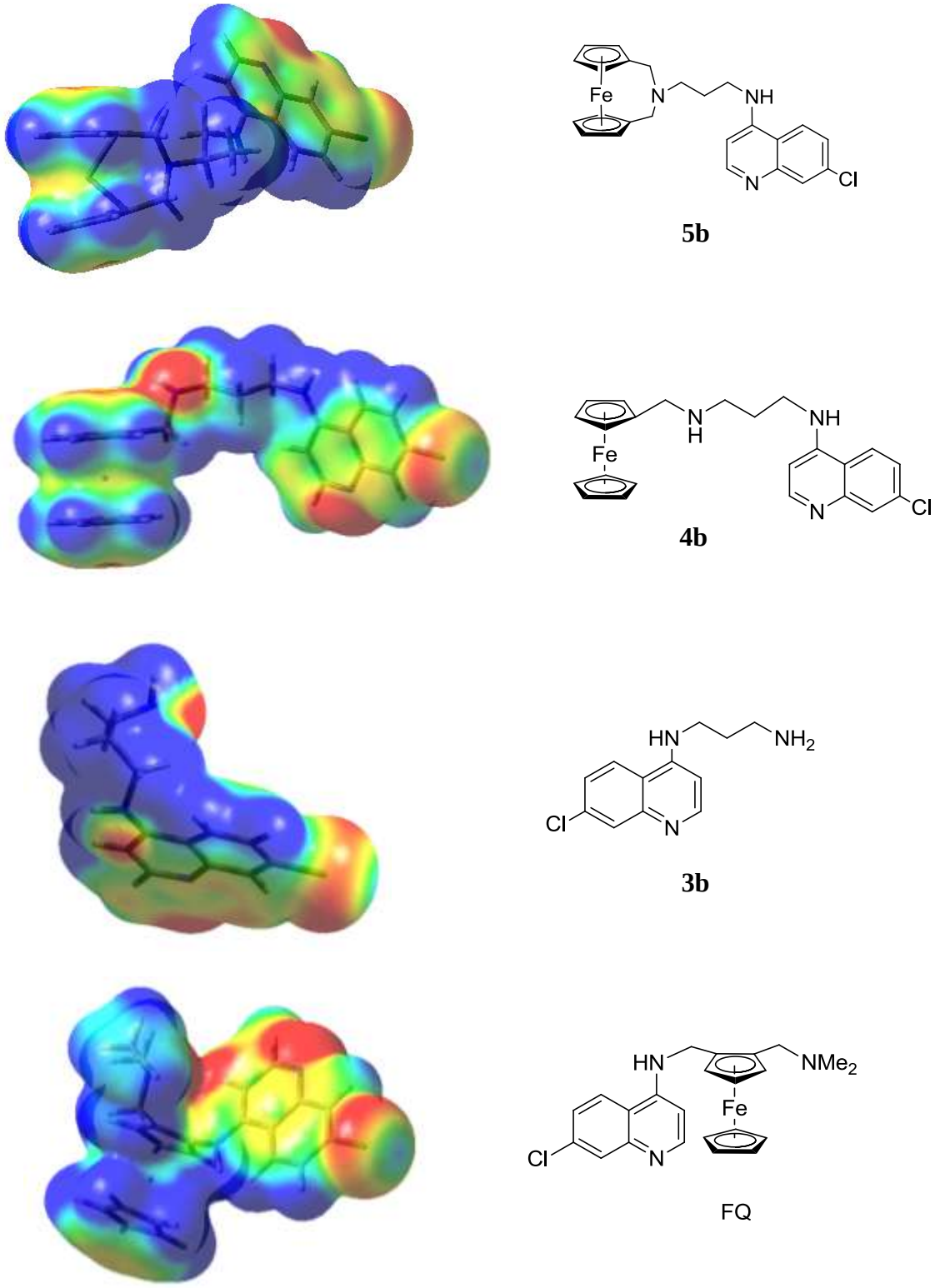

Figure 3.13. A comparison of the molecular electrostatic potential (MEP) surfaces of a selection of compounds from this study.

When compared to the MEP surface of ferroquine, the principal difference noticed with both types of ferrocene derivatives, **5** and **4**, is the availability of the alkyl nitrogen. The conformation and the electrostatic distribution of charge in ferroquine appear to be similar to those observed in the bridged compounds, with the electron density of the tertiary nitrogen partially available and hidden in a pocket of the structure.

In conclusion, ferrocenyl derivatives in general, compared to the organic 4-aminoquinoline fragment have a reduced negative charged surface area, due to a hindered nitrogen (more so in ferroquine and bridged derivatives) and at nitrogen at the 4-position in the quinoline ring. Since, in terms of MEP surface area distribution, the rest of the studied molecules show considerable similarity in the quinoline ring, these changes could be an important factor determining the effect of ferrocene in the accumulation and/or action of chloroquine.

Another physicochemical property that can be estimated from this shape analysis is the polar surface area (PSA) that, along with the partition coefficients, can estimate successfully the capability of compounds to permeate cell membranes, and this is strictly related to an increased accumulation in the cellular organelle.[237,238]

Lipophilicity (expressed as the partition coefficient, log *P*) by itself is insufficient for the estimation of the solute's ability to penetrate a membrane barrier. Therefore, both hydrophobic effects and hydrogen bonding forces should be taken into account when trying to predict the absorption of a compound in biological tissue.[239]

The topological polar surface area (PSA) of a molecule is a measure of the surface rich in oxygen or nitrogen atoms, or hydrogen atoms attached to nitrogen or oxygen atoms. In other words, this is an indication of how heavily hydrated it will be in an aqueous environment.[240]

This parameter estimates the H-bonding ability of a molecule and provides good correlation with experimental transport data, making it an attractive potential predictor of membrane transport.[241]

During the absorption process, a compound must be able to shed its hydration sphere to enter the lipophilic membrane environment. If the compound is heavily solvated, this process is likely to be energetically unfavourable, and so absorption will be hindered.[240] Consequently, compounds with lower PSA values, < 60-140 $Å^2$, are good at permeating cell membranes.[237,240,242]

The influence of the ferrocene in the overall balance between lipophilicity and hydrophilicity of the molecule was explored by examining the calculated lipophilicity with the PSA values and the antimalarial activity observed. This is likely to be relevant in determining in the accumulation of the ferrocenyl drug, considering that the drug must cross a number of membranes to reach the inner part of the parasite food vacuole.

The polar surface area (PSA) values for a selection of compounds in their neutral state are presented in Table 3.6. All studied compounds have PSA < 60-140 $Å^2$ cut-off, indicating they might be good at permeating cell membranes. Compounds with a low PSA value tend to show better permeability/absorption.[240] A non-linear relationship between PSA and permeability has been demonstrated, with permeability declining sigmoidally as PSA increases.[241]

Table 3.6. Polar surface area (PSA) values for a selection of compounds in their neutral state.

Compound	PSA (Å^2)
5a	27.4
5b	25.3
5c	26.0
5d	25.1
5e	21.7
4a	38.7
4b	39.0
4c	38.9
4d	36.0
4e	33.6
3a	51.4
3b	51.0
3c	51.0
3d	51.0
3e	47.5
FQ	26.2

There are, however, certain differences among the group of compounds. All the bridged ferrocenyl compounds seem to have similar relatively low values of PSA ranging from 22 to 27 Å^2, with the lowest value displayed for the 2,2'-dimethyl propyl analog (**5e**). The monosubstituted ferrocenyl compounds **4a-e** display higher PSA values, likely stemming from the alkyl nitrogen availability observable in their MEP surfaces (Figure 3.13). The corresponding quinoline analogs **3a-e**, as expected, have even higher PSA values, almost double those registered for the bridged ferrocenyl group. This is explained by the additional electronic surface provided by the more available alkyl nitrogen and nitrogen in 4-position of the quinoline ring (Figure 3.12).

Interestingly, the PSA value of ferroquine (FQ) falls in the range of values obtained for the bridged ferrocenyl compounds, confirming the similarity observed in the map of

electrostatic potential of these compounds. Although PSA value is not a definite parameter, it indicates that ferroquine and the bridged ferrocenyl compounds should have a similar permeability/absorption profile.

3.4 Structure activity relationship

As mentioned in Chapter 3.1, structural features of these compounds play a remarkable role in their interaction with the parasite transmembrane proteins that allow the accumulation of the drug inside the parasite food vacuole. It has been discussed that specific structural properties of these compounds might influence their ability to accumulate inside the vacuole and therefore overcome drug resistance. Even though the library of compounds contemplated in this thesis is relatively small to develop a proper structural-activity relationship, the observations of this study will contribute to the elucidation of the importance of these physical properties. This discussion was divided into a correlation of each physical property discussed previously with the antiplasmodial activity observed. General conclusions will be given in the following and last subsection of this chapter.

3.4.1 Antiplasmodial activity, hydrogen bonding and conformation

It was discussed earlier in the chapter that the presence of intramolecular hydrogen bonding has been associated with the improved action of ferroquine.[162,198] It is believed that

intramolecular hydrogen bonding will give rise to a closed conformation that can penetrate more efficiently the parasite membranes to reach the drug site of action.[198]

Intramolecular hydrogen bonding between the aromatic NH on the 4-position of the quinoline ring and the nitrogen atom in the β-position of the cyclopentadienyl ring of ferrocene was observed in a low dielectric constant solvent (chloroform) by the means of ^{1}H NMR spectroscopy. All compounds that exhibited shifts in the NH_{Ar} NMR signals towards higher frequencies (indicating the deshielding effect of the formation of intramolecular hydrogen bonding) exhibited also relatively good antimalarial activity. The exception of the group is compound **4e**, the 2,2'-dimethyl propyl alkyl chain derivative which, despite the most pronounced positive shifting, is very inactive, especially in the chloroquine-resistant strain Dd2. This points towards the branching effect of decreasing activity, mentioned previously in the discussion of the antiplasmodial action of these compounds. For these branched quinolines, derivatization with ferrocene seems to be more determinant than the formation of intramolecular bond in the determination of the activity.

Compounds that suffered shifts in the NH_{Ar} NMR signals towards lower frequencies (indicating loss of hydrogen bonding, likely due to conformational restrictions) had mixed results in terms of antiplasmodial activity. Compound **5c**, with a relatively small shifting to lower frequencies, is one of the most active compounds of the group; however, compounds **5b** and **5e**, which shifted -1.68 ppm and -3.35 ppm respectively, were among the least active compounds. These observations confirm that the intramolecular H-bonding observed in solution is associated with an increase in antiplasmodial activity and that the opposite is also true, loss of intramolecular H-bonding is associated with decrease of antiplasmodial action. This correlation is illustrated in Figure 3.14, where it can be seen that the most active

compounds (low IC_{50} values) fall to the right of the diagram corresponding to the shifting of the NH_{Ar} hydrogen towards higher frequencies.

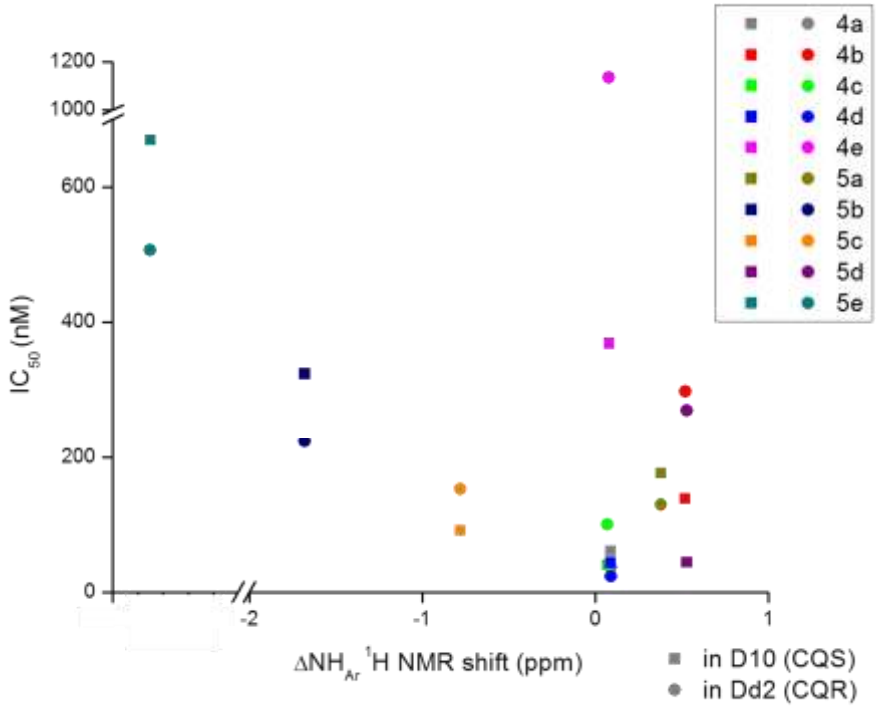

Figure 3.14. Correlation between the ^1H NMR spectroscopic shift of the NH_{Ar} (as indicator of formation/loss of intramolecular hydrogen bond) and the *in vitro* antiplasmodial activity against *P. falciparum* CQS D10 and CQR Dd2 parasite strains.

Intramolecular and intermolecular hydrogen bondings in the solid state were observed in single crystal X-ray structures. Intramolecular hydrogen bonding between the NH on the 4-position of the quinoline ring and the nitrogen atom in the β-position of the cyclopentadienyl ring of ferrocene was observed in the solid state of compound **4e** (Figure 2.5) whereas compounds **4b** and **5b** did not present intramolecular hydrogen bonding but did present intermolecular H-bonding between the NH on the 4-position of the quinoline ring and the quinoline nitrogen of a contiguous molecule (Figures 2.4 and 2.6).

Even though a strong correlation cannot be established between the presence of intramolecular H-bonding in the solid state and antimalarial activity due to the size of the pool of samples, it is relevant to note that **4e**, displaying strong H-bonding, is one of the least active compounds in the group and that **4b** and **5b** surpass its antiplasmodial activity against both parasite strains (Figure 3.14). These observations agree with the previous observations that point to the branching of the side chain as a more important characteristic over the presence or absence of intramolecular H-bonding when determining antiplasmodial activity.

Another characteristic observed in these single crystal X-ray structures was the conformation of the molecules in the solid state that is likely to remain similar in the presence of low dielectric media such as the lipid environment where these compounds accumulate and act. The intramolecular H-bonding and the conformation observed in **4e** is similar to that of ferroquine (Figure 3.2) with the quinoline ring found on top of the ferrocene skeleton. Nonetheless, their antiplasmodial activities are remarkably different.

The interesting and previously unexplored conformation of **5b** (Figures 2.6 and 2.7) is not really similar to the conformation of any ferrocenyl quinoline antimalarial studied before, with the quinoline ring parallel to the ferrocene skeleton but in two distinct planes. The effect of this conformation cannot be elucidated from this unique example; further study will be necessary.

Finally, it has been suggested than a N-quinoline to N-methylene chain distance in the range of 7.52-10.21 Å is required for the formation of a heme-drug complex and, therefore, for antiplasmodial activity.[243] The corresponding distances are 8.912 Å, 6.685 Å and 7.653 Å in compounds **4b**, **4e** and **5b,** respectively. It is worth noting that the only compound in this

group that does not follow this rule is the least active of the three and one of the least active compounds of the complete group (Figure 3.14).

3.4.2 Antiplasmodial activity, association to hematin and inhibition of β-hematin formation

As discussed in Chapter 3.3.3, all compounds exhibited interaction with Fe(III)PPIX. The trend observed was the decrease of association constants (expressed as log *K*) from the purely organic fragments series **3** to the ferrocenyl derivatives, both series **4** and **5,** regardless of length or branching of the methylene side chain. The latter characteristics have different effects in both groups of ferrocenyl derivatives. In the mono-substituted ferrocenyl derivatives, **4**, the shorter and less branched the methylene chain, the higher the value of log *K*. For the bridged disubstituted ferrocenyl derivatives, **5**, the longer and more branched the chain, the higher are the values of log *K* obtained.

Unfortunately, no such clear trend can be observed when correlating these values with those of antiplasmodial activity. In general, large association constants were observed in compounds that were the most active against the chloroquine-sensitive D10 strain. The exceptions are compounds **4d** and **5a** that, with the lowest found values of association constants, log *K* = 3.68 and 4.18, respectively, were among the most active compounds tested. The association constants and the antiplasmodial activity against the chloroquine-resistant Dd2 parasite strain show no clear correlation.

It was confirmed that indeed larger association constants are observed with high antiplasmodial activity (although the opposite was not observed); unfortunately, solubility

requirements made it impossible to prove the β-hematin inhibition property of these compounds.

3.4.3 Antiplasmodial activity, lipophilicity and hydrophilicity

A moderate balance between lipophilicity and hydrophilicity is ideal for the proper absorption of any drug *in vivo*. This is especially true for quinoline-based antimalarial drugs where the delivery, absorption and accumulation of the drug can make the difference between the sensitivity and resistance of the parasite to the drug. Lipophilicity in these test compounds was studied by the means of calculated log *P*.

The trend observed in these compounds was the increase of lipophilicity with the length and branching of the methylene chains. The presence of ferrocene in series **4** and **5** caused a great increase in the lipophilic character, slightly more for compounds **5**. When these values are correlated to their antiplasmodial action in the chloroquine-sensitive D10 strain, the increase of lipophilicity is detrimental since all ferrocene derivatives are less active than their corresponding organic components.

Much more interesting is to correlate these two parameters in the chloroquine-resistant parasite strains since the ultimate goal is to overcome drug resistance. In the organic series **3a-e**, an increase in lipophilicity helped improve the antimalarial action, with the most active compound being **3e**.

In the case of the monosubstituted ferrocenyl compounds **4a-e**, the increase in lipophilicity stemming from the incorporation of ferrocene produced a 4- to 15-fold

improvement in the activity for compounds **4a-d**. For compound **4e**, the most lipophilic of the group (Clog *P* = 5.64), a significant decrease in activity is observed.

Finally, in the case of the bridged ferrocenyl compounds **5a-e**, the closed-conformation represents an increase in lipophilicity of approximately 10 times compared to compound series **4**. This is reflected in a decrease in the antimalarial activity of the first four compounds; however, compound **5e** which has the highest lipophilicity (Clog *P* = 7.54) is 2-fold more active than **4e**.

In conclusion, an increase in lipophilicity was beneficial in improving the activity of the compounds against drug-resistant strains; however, only up to a certain level. When the compounds become too lipophilic, antiplasmodial activity decreases. This would explain the reduced activity observed for the 2,2'-dimethyl propyl ferrocenyl derivatives. The better activity observed for **5e** could be explained by its more rounded conformation that possibly aids in its transportation across membranes with its reduced surface.

Indeed, an intermediate lipophilicity that delivers the best activity seems to be in the range of Clog *P* = 4.5-5.0 which is coincidentally where the lipophilicity of ferroquine falls (log *P* = 5.1).

The hydrophilicity of these compounds was studied by means of the calculation of their molecular electrostatic potential (MEP) surfaces and polar surface values (PSA). The bridged disubstituted ferrocenyl compounds **5a-e** presented MEP surfaces of reduced electronegatively charged area. The methylene nitrogen is described as buried in the structure and mostly inaccessible for interaction with solvents or other molecules, less prone to participate in solvation. Interestingly, the two compounds that showed partial availability of the electronic cloud associated with this nitrogen, **5a** and **5c**, were also the most potent

compounds of this series and those resembling most the MEP surface obtained for ferroquine.

Compounds **4b** and **3b**, representing the series of mono-substituted ferrocenyl derivatives **4a-e** and organic quinoline fragments **3a-e**, respectively, have increased electrostatic potential surface. While this improved the antimalarial action in most but not in all of compounds **4**, the further increase in electronegatively charged area in the purely organic derivatives **3** decreases the antimalarial effectiveness against the drug-resistant strain.

These observations are consistent with the values observed for the polar surface area (PSA). The bridged compounds **5a-e** have relatively low values of PSA, from 21 to 27 $Å^2$. Compound **5e** has, as expected, the lowest value of PSA but that is also accompanied with relatively low activity. The most active compound of this series, **5c**, has a PSA value of 26.0 $Å^2$, very similar to that of ferroquine, 26.2. Higher PSA values for **3b** and **4b** are correlated to lower activity.

Therefore, it seems like more than a trend, a balance, must be reached where the amount of electronegative surface is slightly more than that observed for the bridged compounds **5** but not as much as that observed for compounds **4**, much like what is observed for ferroquine. These ideal hydrophilicity that delivers the best activity seems to be in the approximate range of PSA = 25.9 to 26.2 $Å^2$.

3.4.4 Therapeutic indices

Therapeutic index (TI), therapeutic ratio or selectivity index is a measure of the correlation between the lethal dose and the effective dose of certain compound. In this

particular case, the lethal dose is related to human cell lines and the effective dose is related to the antimalarial activity observed in parasite strains. This value is determined by dividing the IC_{50} value obtained in the cell viability assay for each human cell line, by the IC_{50} value obtained in the antiplasmodial assay for each parasite strain. This ratio is considered a useful tool in the evaluation of the promise of pharmacophores.

Table 3.7. Therapeutic indices.

TI	MCF-10A/D10	MCF-10A/Dd2	MDA-MB-435/D10	MDA-MB-435/Dd2
3a	2069	286	485	67
3b	2024	258	430	55
3c	629	28	178	8
3d	3603	1328	864	318
3e	6928	3475	1494	750
4a	67	113	51	86
4b	20	9	22	10
4c	95	38	75	30
4d	126	238	73	139
4e	15	5	7	2
5a	14	19	10	13
5b	12	18	10	14
5c	46	28	31	18
5d	3	5	3	5
5e	0.4	0.6	0.9	1

It is desirable for a drug to have high therapeutic indices since this indicates low toxicity and high activity. As seen in Table 3.7, the toxicity associated with the ferrocene takes a toll in the therapeutic capacity of compounds **4** and **5**; however, certain compounds remain good prospects, such as **4a** and **4d**. Compounds with the branched 2,2'-dimethyl propyl alkyl chain, **4e** and **5e**, are unattractive or therapeutically undesirable (TI < 1), with little efficacy

as antimalarials and high toxicity for human cells. This correlation should only be taken as a reference point since complete therapeutic profiles must be done in several human cell lines and parasite strains.

3.5 Conclusions

All compounds were active against both chloroquine-sensitive and resistant parasite strains. Purely organic fragments **3a-e** were the most active against the chloroquine-sensitive strain; however they lost activity against the drug-resistant strain. Mono-substituted ferrocenyl compounds **4a-e** were able to overcome this resistance, but remained more active in the sensitive strain, increasing their resistance index and therefore likelihood of developing cross-resistance. Bridged disubstituted ferrocenyl compounds **5a-e** were able to overcome resistance and, in all cases except one (**5e**), were more active in the resistant strain than in the sensitive one, giving them appealing resistance indices < 1. The branching of the methylene spacer was found to be a strong influence in activity, with the derivatives losing efficacy as they grow in branching. The length of this spacer was not a strong influence.

The organic fragments seem to infer some antitumor behavior, judged by the 5-fold more sensitive response from cancer cells than from normal cells. Ferrocenyl compounds were equally toxic against both types of human cell lines, and more toxic than cisplatin. Although this is common for ferroquine compounds, this lowers the therapeutic index and therefore the appeal as pharmacophores.

In terms of hydrogen bonding, mono substituted derivatization with ferrocene (such in **4a-e**) seems to increase the formation of intramolecular H-bonding. On the contrary, formation of the bridged ferrocenyl compounds (such in **5a-e**) seems to cause the loss of the intramolecular H-bond, likely due to conformational restrictions exerted by the bridge structure. The presence of an intramolecular H-bond is associated with the increase of antiplasmodial action and in turn, the loss of this bonding seems to decrease the action. Exceptions to this rule point out that other factors might have a bigger influence in determining the activity. This would suggest that H-bonding is relevant but not determinant for antiplasmodial activity.

Association with hematin was observed for all compounds and it did not seem to determine the activity *in vitro*. This supports the notion that while association with hematin is important, a more important process is the delivery of relevant amounts of the drug to the site of action through the crossing of membranes.

Inhibition of β-hematin formation gave negative results that in light of the demonstrated antimalarial activity could be interpreted as these compounds being antimalarials in a stage other than the erythrocyte antimalarial stage. Judging from their resemblance to chloroquine and strong association with hematin, we discard this option and attribute these results to the solubility issues encountered. Association with hematin and inhibition of β-hematin formation are both phenomena that have been well-studied and well-identified for chloroquine and for most 4-aminoquinoline drugs, thus, we assume that all compounds presented in this thesis will prove positive in the latter assay if given the right conditions for the solubilisation of the compounds.

A balance between the lipophilicity and the hydrophilicity was found to be determinant in the activity displayed by the compounds. The addition of the ferrocenyl unit contributed largely to increase the lipophilicity of the compound and that has been related in the past to improved transport of the drug through membranes.[198] It was found that log *P* values of 4.5-5.0 and PSA values of ~26.0 $Å^2$ give the best balance and that is witnessed in the increase of activity. The values found for both parameters happen to be consistent with what is observed in ferroquine.

It is hypothesized that the closed conformation observed in compounds **5a-e**, that resemble ferroquine, gives the compounds a close to ideal balance where the very lipophilic ferrocene is sticking to the side but parallel to the quinoline ring without disturbing its interaction with hematin. The hydrophobic ferrocene can then establish favourable van der Waals interactions with lipid tissue at the interface with the membranes to be crossed and aid in the accumulation of the drug. This particular conformation, its compact size and lipophilicity/hydrophilicity balance could provide these compounds with the structural characteristics needed to escape the resistance mechanism of the transmembrane proteins and achieve significant accumulation inside the parasite food vacuole. This would explain why their activity is increased in drug-resistant strains.

However, there is room for improvement. These compounds would benefit from being slightly more hydrophilic with more electronegative area available. Also, they could benefit from having an intramolecular hydrogen-bonding interaction that could allow the "flip-flop" mechanism that has been postulated for aiding in the accumulation of ferroquine when crossing membranes.

With these two characteristics in mind and with the parameters observed to be determinant in antiplasmodial activity, *in silico* calculation could aid in the design of improved analogs with tuned lipophilicity/hydrophilicity and intramolecular hydrogen bonding, giving analogs closer to ferroquine in potency.

CHAPTER 4 SYNTHESIS AND CHARACTERIZATION OF OTHER CHLOROQUINE FERROCENYL AND MEFLOQUINE CONJUGATES

4.1 Introduction

In the process of discovering and developing new drugs or improving existing agents, medicinal chemists can make use of multiple approaches in the design of a drug. One of the most recurrent strategies involves the development of structural analogs of current drugs (an approach explored in Chapter 2 and 3). In this and the following chapters two additional drug design strategies will be explored: multiple loading (Chapter 4) and multifunctional therapy strategy (Chapter 5).

The multiple load strategy, often incorporated in imaging and therapy, consists of the multiple loadings of pharmacophore units per molecule of administered imaging/therapeutic agent. This strategy is exemplified in Figure 4.1 where a ferrocene unit could be loaded with more than one pharmacophore (for example, a chloroquine derivative).

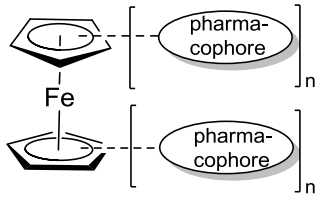

Figure 4.1. Representation of a multiple loading of pharmacophores in a unit of ferrocene.

Even though multiple strategies have been considered for the development of new ferrocenyl antimalarial drugs, only two examples of applied multiple loading therapy were found in the literature.[147] These two examples were briefly mentioned in Chapter 1 and consist of ferrocene quinoline derivatives of triazacyclonane (**50**-**51**, Figure 1.11), containing two units of a chloroquine derivative (**50**) and two units of ferrocene (**51**), respectively.[147] The bischloroquine derivative **50** proved to be more active than the bisferrocenyl derivative **51**, and this was attributed to the favourable lipophilicity and the redox behaviour of **50** while the even higher lipophilicity, high molecular weight and steric hindrance of **51** was proposed to lower its effectiveness.[147]

In an effort to apply this strategy, I set out to develop ferrocene molecules substituted with 4-aminoquinoline derivatives in the 1,1'-fashion, as shown in Figure 4.1, with a maximum of two quinoline units (n =1), derivatives of chloroquine and mefloquine (Figure 4.2). This substitution pattern was selected in order to minimize the steric hinderance and molecular weight, without affecting the therapeutic efficacy. If ferrocene is responsible for the increased accumulation of these drugs, these disubstituted molecules could deliver twice the payload of quinoline derivative to the parasite food vacuole therefore increasing the antimalarial activity.

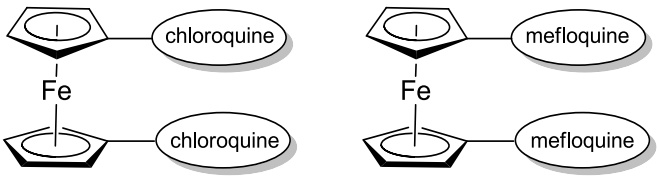

Figure 4.2. 1,1'-Disubstituted ferrocenyl chloroquine and mefloquine derivatives.

4.2 Experimental

4.2.1 Materials and instrumentation

Please refer to Chapter 2.2.1 for general information. For the synthesis of the starting materials 1,1'-bis(*N,N'*-trimethylaminomethyl)ferrocene iodide **2** and 4-aminoquinoline derivatives **3a-e** please refer to Chapter 2.2.2. 2,8-Di(trifluoromethyl)quinolin-4-ol was purchased from Acros Organics and used without further purification. Selected syntheses were carried using an ultrasonic system Branson 5210 (Emerson Industrial Automation).

4.2.2 Synthesis

General procedure for the synthesis of N-Boc protected 4-aminoquinoline derivatives (6a-e).

A mixture of the respective 4-aminoquinoline derivative **3a-e** (0.5 mmol, 1 equiv), di-*tert*-butyl dicarbonate (0.218 g, 1 mmol, 2 equiv) and $NaHCO_3$ (0.336 g, 4 mmol, 8 equiv) in methanol (20 mL) were reacted with sonication in a cleaning bath at room temperature for 2 hours. The undissolved sodium bicarbonate was filtered out and washed with MeOH, then the solvent was removed under reduced pressure. The solid obtained was redissolved in 25 mL of methylene chloride and washed with water (3 x 5 mL, or until it tested pH neutral), and brine solution (1 x 5 mL). The organic layer was dried over anhydrous $MgSO_4$ and the solvent was removed under reduced pressure to yield the product as a solid.

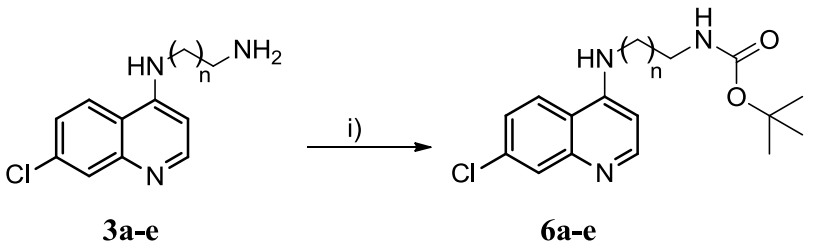

3a-e **6a-e**

Scheme 4.1. General synthetic route for the synthesis of N-Boc protected 4-aminoquinoline derivatives (**6a-e**): i) Boc_2O, $NaHCO_3$, MeOH, 2 h, RT, sonication; **6a** (n=1, ethyl), **6b** (n=2, propyl), **6c** (n=3, butyl), **6d** (2-propyl), **6e** (2,2'-dimethylpropyl).

***tert*-Butyl (2-((7-chloroquinolin-4-yl)amino)ethyl)carbamate (6a).**

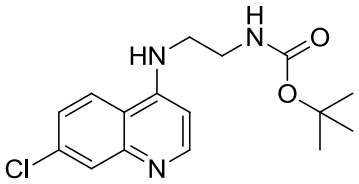

This compound was obtained as a white solid (0.15 g, 0.48 mmol, 96%). ^{1}H NMR (400 MHz, $CDCl_3$): δ (ppm) 8.51 (d, ^3J = 5.1 Hz, 1H), 7.94 (d, ^4J = 2.0 Hz, 1H), 7.80 (d, ^3J = 9.1 Hz, 1H), 7.36 (dd, ^3J = 9.0 Hz, ^4J = 2.2 Hz, 1H), 6.62 (br. s., 1H), 6.30 (d, ^3J = 5.1 Hz, 1H), 5.13 (br. s., 1H), 3.60 (m, 2H), 3.37 (m, 2H), 1.48 (s, 9H). ^{13}C NMR (101 MHz, $CDCl_3$): δ (ppm) 158.7, 152.2, 150.5, 149.3, 135.2, 128.7, 125.6, 122.2, 117.6, 98.5, 80.9, 46.5, 39.8, 28.7. ESI-MS (HR) calculated for $C_{16}H_{21}ClN_3O_2$: 322.1322, found: 322.1324 $[M + H]^+$.

***tert*-Butyl (3-((7-chloroquinolin-4-yl)amino)propyl)carbamate (6b).**

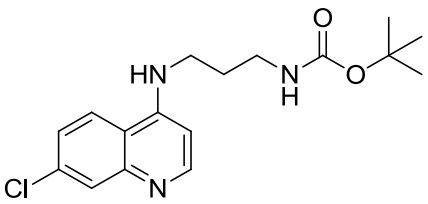

This compound was obtained as a white solid (0.03 g, 0.08 mmol, 16%). ^{1}H NMR (400 MHz, $CDCl_3$): δ (ppm) 8.51 (d, ^3J = 5.5 Hz, 1H), 7.97 (d, ^4J = 2.0 Hz, 1H), 7.89 (d, ^3J = 8.9 Hz, 1H), 7.40 (dd, ^3J = 9.0 Hz, ^4J = 2.2 Hz, 1H), 6.41 (d, ^3J = 5.5 Hz, 1H), 6.34 (br. s., 1H), 4.76 (br. s., 1H), 3.42 (m, 2H), 3.30 (m, 2H), 1.85 (m, 2H), 1.50 (s, 9H). ^{13}C NMR (101 MHz, $CDCl_3$): δ (ppm) 158.8, 152.3, 150.5, 149.3, 137.3, 128.9, 125.3,

122.3, 118.2, 98.6, 80.2, 66.0, 39.5, 29.9, 28.6. ESI-MS (HR) calculated for $C_{17}H_{23}ClN_3O_2$: 336.1479, found: 336.1480 $[M + H]^+$.

***tert*-Butyl (4-((7-chloroquinolin-4-yl)amino)butyl)carbamate (6c).**

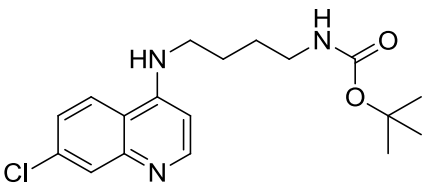

This compound was obtained as a white solid (0.15 g, 0.41 mmol, 85%). ^{1}H NMR (400 MHz, $CDCl_3$): δ (ppm) 8.54 (d, ^3J = 5.2 Hz, 1H), 7.96 (d, ^4J = 1.8 Hz, 1H), 7.82 (d, ^3J = 8.2 Hz, 1H), 7.36 (dd, ^3J = 9.0 Hz, ^4J = 2.0 Hz, 1H), 6.41 (d, ^3J = 5.5 Hz, 1H), 5.46 (br. s., 1H), 4.66 (br. s., 1H), 3.36 (m, 2H), 3.23 (m, 2H), 1.81 (m, 2H), 1.69 (m, 2H), 1.47 (s, 9H). ^{13}C NMR (101 MHz, $CDCl_3$): δ (ppm) 159.8, 155.4, 152.2, 149.5, 133.7, 131.0, 125.4, 121.6, 114.1, 99.2, 53.1, 49.4, 44.4, 43.3, 28.6. ESI-MS (HR) calculated for $C_{18}H_{25}ClN_3O_2$: 350.1635, found: 350.1634 $[M + H]^+$.

***tert*-Butyl (2-((7-chloroquinolin-4-yl)amino)propyl)carbamate (6d).**

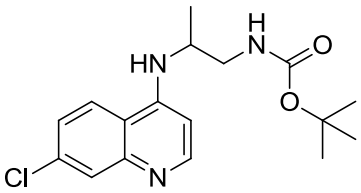

This compound was obtained as a white solid (0.14 g, 0.42 mmol, 84%). ^{1}H NMR (400 MHz, $CDCl_3$): δ (ppm) 8.50 (d, ^3J = 5.5 Hz, 1H), 7.93 (s, 1H), 7.80 (d, ^3J = 8.8 Hz, 1H), 7.35 (d, ^3J = 8.8 Hz, 1H), 6.76 (br. s., 1H), 6.28 (d, ^3J = 4.9 Hz, 1H), 4.70 (br. s., 1H), 4.21 (br. s., 1H), 3.35 (m, 1H), 3.13 (br. s., 1H), 1.76 (br. s., 1H), 1.47 (s, 9H), 1.35 (d, ^3J = 7.0 Hz, 3H). ^{13}C NMR (101 MHz, $CDCl_3$): δ (ppm) 159.1, 152.0, 149.4, 134.8, 128.5, 125.2, 122.0, 117.2, 98.1, 80.6, 61.6, 50.2, 46.0, 28.3, 18.8. ESI-MS (HR) calculated for $C_{17}H_{23}ClN_3O_2$: 336.1479, found: 336.1474 $[M + H]^+$.

***tert*-Butyl (3-((7-chloroquinolin-4-yl)amino)-2,2'-dimethylpropyl)carbamate (6e).**

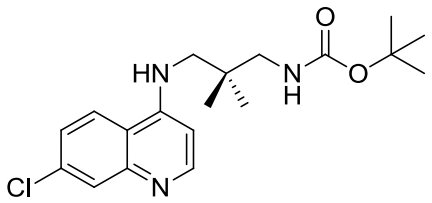

This compound was obtained as a white solid (0.17 g, 0.47 mmol, 94%). ^{1}H NMR (400 MHz, $CDCl_3$): δ (ppm) 8.46 (d, ^{3}J = 5.5 Hz, 1H), 8.02 (d, ^{3}J = 8.8 Hz, 1H), 7.93 (d, ^{4}J = 1.8 Hz, 1H), 7.40 (dd, ^{3}J = 8.8, ^{4}J = 2.1 Hz, 1H), 6.97 (br. s., 1H), 6.43 (d, ^{3}J = 5.5 Hz, 1H), 4.93 (br. s., 1H), 3.09 (m, 4H), 1.49 (s, 9H), 0.95 (s, 6H). ^{13}C NMR (101 MHz, $CDCl_3$): δ (ppm) 157.5, 151.8, 151.1, 149.4, 134.8, 128.3, 125.1, 122.2, 117.6, 98.1, 80.3, 48.6, 48.0, 37.5, 28.3, 23.8. ESI-MS (HR) calculated for $C_{19}H_{27}ClN_3O_2$: 364.1792, found: 364.1788 $[M + H]^+$.

1,1'-Bis{*N*-*tert*-butyl-[N'-[(7-chloroquinolin-4-yl)-butane-1,4-diamine]carbamate]-(*N*-methane-yl)}ferrocene (7).

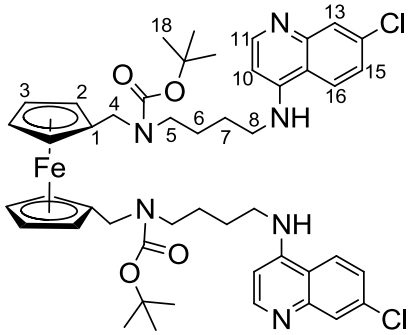

1,1'-Bis(*N,N'*-trimethylaminomethyl)ferrocene iodide **2** (0.10 g, 0.17 mmol, 1 equiv), *tert*-butyl(4-((7-chloroquinolin-4-yl)amino)butyl)carbamate **6c** (0.130 g, 0.37 mmol, 2.2 equiv) and NaOH (0.07 g, 1.7 mmol, 10 equiv) were combined with 20 mL acetonitrile in a 20 mL microwave vial. The reaction was carried out in a microwave reactor for 6 h at 110 °C. The solvent was removed under reduced pressure. Purification of the desired product was done by flash column chromatography on silica with an ethyl acetate /dichloromethane/triethylamine (5:4:1) mixture as eluent to afford the product as a yellow solid (0.02 g, 0.025 mmol, 15 %). ^{1}H NMR (300 MHz, $CDCl_3$): δ (ppm) 8.38 (d, ^{3}J = 5.2 Hz, 2H, H-11), 7.92 (d, ^{4}J =1.8 Hz, 2H, 13-H), 7.85 (d, ^{3}J = 8.3 Hz, 2H, 16-H), 7.40 (dd, ^{3}J = 8.4,

^4J = 2.0 Hz, 2H, 15-H), 6.38 (d, ^3J = 5.2 Hz, 2H, 10-H), 4.26 (m, 4H, 2-H), 4.17 (m, 4H, 3-H), 3.78 (m, 4H, 4-H), 3.33 (br. s., 4H, 5-H), 3.17 (m, 4H, 8-H), 2.21 (s, 4H, 7-H), 1.87 (s, 4H, 6-H), 1.49 (s, 18H, 18-H). ^{13}C NMR (75 MHz, $CDCl_3$): δ (ppm) 158.2 (C11), 154.4 (C9), 153.1 (C12), 149.5 (C17), 133.3 (C14), 127.3 (C13), 123.6 (C15), 120.2 (C16), 111.2 (C10), 92.9 (C1), 77.8 (C2), 75.9 (C3), 58.0 (C5), 51.2 (C8), 49.9 (C7), 44.1 (C6), 28.2 (C18). ESI-MS (+): 909.6 $[M]^{+\cdot}$.

1,1'-Bis{*N*-*tert*-butyl-[N'-[(7-chloroquinolin-4-yl)-2,2-dimethylpropane-1,3-diamine]carbamate]-(*N*-methane-yl)}ferrocene (8).

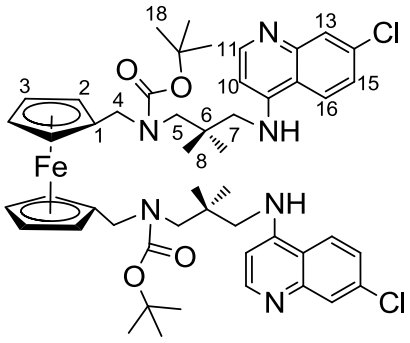

1,1'-Bis(*N,N'*-trimethylaminomethyl)ferrocene iodide **2** (0.10 g, 0.17 mmol, 1 equiv), *tert*-butyl(3-((7-chloroquinolin-4-yl)amino)-2,2'dimethylpropyl)carbamate **6e** (0.135 g, 0.37 mmol, 2.2 equiv) and NaOH (0.07 g, 1.7 mmol, 10 equiv) were combined with 20 mL acetonitrile in a 20 mL microwave vial. The reaction was carried out in a microwave reactor for 6 h at 110 °C. The solvent was removed under reduced pressure. Purification of the desired product was done by preparative TLC on silica with an acetone/dichloromethane/triethylamine (5:4:1) mixture as eluent to afford the product as a yellow solid (0.03 g, 0.035 mmol, 21 %). ^{1}H NMR (300 MHz, $CDCl_3$): δ (ppm) 8.24 (d, ^3J = 5.4 Hz, 2H, H-11), 8.03 (d, ^3J = 8.9 Hz, 2H, 16-H), 7.89 (d, ^4J = 1.8 Hz, 2H, 13-H), 7.46 (dd, ^3J = 8.7, ^4J = 2.0 Hz, 2H, 15-H), 7.03 (br. s., NH), 6.46 (d, ^3J = 5.4 Hz, 2H, 10-H), 4.36 (m, 4H, 2-H), 4.11 (m, 4H, 3-H), 3.59 (m, 4H, 4-H), 3.26 (br. s., 4H, 5-H), 2.68 (s, 4H, 7-H), 1.54 (s, 18H, 18-H), 1.07 (s, 12H, 8-H). ^{13}C NMR (75 MHz, $CDCl_3$): δ (ppm) 155.5 (C11),

151.5 (C9), 151.1 (C12), 149.4 (C17), 134.3 (C14), 126.7 (C13), 124.6 (C15), 122.2 (C16), 106.2 (C10), 88.9 (C1), 74. 7 (C2), 70.9 (C3), 78.3 (C5), 51.6 (C4), 49.3 (C7), 36.1 (C6), 28.2 (C18), 21.9 (C8). ESI-MS (+): 937.6 $[M]^{+\cdot}$.

4-Bromo-2,8-di(trifluoromethyl)quinoline (9).

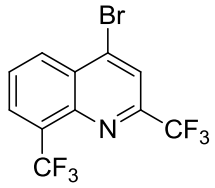

This compound was prepared as previously reported[244] with slight modifications. Phosphorous (V) oxybromide (2.81 g, 10 mmol) was melted at 70 °C in a 50 mL round bottom flask fitted to a condenser under an argon atmosphere. 2,8-Di(trifluoromethyl)quinolin-4-ol (2.87 g, 10 mmol, 1 equiv) was added to the flask under an intense flow of argon and the mixture was heated to 165 °C for 2 hours under continuous stirring. The system was allowed to cool to RT. Water (20 mL) was added to the solidified mixture and stirring was continued overnight. The remaining solid was filtered out on a medium sintered funnel, washed with ice cold water, collected and dried under vacuum to yield a greyish solid (3.00 g, 8.74 mmol, 87%). ^{1}H NMR (300 MHz, $CDCl_3$): δ (ppm) 8.50 (d, ^{3}J = 8.5 Hz, 1H), 8.25 (d, ^{3}J = 7.1 Hz, 1H), 8.13 (s, 1H), 7.84 (t, ^{3}J = 8.0 Hz, 1H). ^{13}C NMR (75 MHz, $CDCl_3$): δ (ppm) 151.3, 148.4, 144.1, 136.1, 131.1, 130.1, 128.9, 128.5, 125.0, 122.0, 121.4.

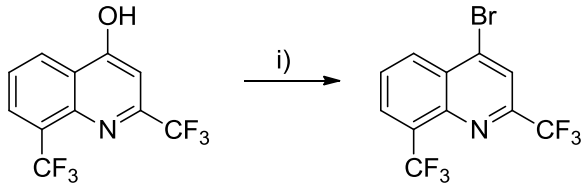

Scheme 4.2. Synthetic route for the synthesis of 4-bromo-2,8-di(trifluoromethyl)quinoline (**9**). i) $POBr_3$, 165 °C, 2 h, neat.

1,1'-Ferrocenedicarboxaldehyde (10).

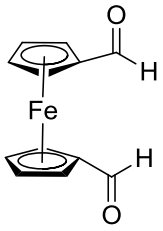

This compound was prepared as previously reported.[245] *n*-Butyllithium (1.6 M in hexanes, 5.3 mL, 8.5 mmol, 1.7 equiv) was added dropwise to a stirred solution of freshly distilled TMEDA (1.8 mL, 12 mmol, 2.4 equiv) and ferrocene (0.93 g, 5 mmol, 1 equiv) in 30 mL of ethyl ether. The reaction mixture was stirred under inert atmosphere at RT for 20 hours, and then cooled to -78 °C in a dry ice bath and dry DMF (1.3 mL, 16.5 mmol, 3.3 equiv) was added dropwise. After 10 minutes, the mixture was allowed to reach room temperature and further stirred under inert atmosphere for 2 hours. To terminate the reaction, a solution of HCl (2.5 M, 50 mL) was added to the yellow-orange suspension. The organic layer was separated and the aqueous layer was extracted with several portions of methylene chloride (4 x 25 mL). The combined organic fractions were washed with saturated $NaHCO_3$ solution and dried over Na_2SO_4. The solvent was removed under reduced pressure to afford a red solid that was purified by flash column chromatography on silica gel. Elution was achieved with hexane/ethyl acetate (3:2) and evaporation of the solvent mixture yielded **10** (0.256 g, 1.06 mmol, 21 %) as a red solid. ^{1}H NMR (300 MHz, $CDCl_3$): δ (ppm) 9.96 (s, 2H), 4.90 (m, 4H), 4.68 (m, 4H). MS-EI (+): 243.3 $[M+H]^+$.

Bis-(4-[(2,8-bistrifluoromethyl)quinolyl)methanol]-1,1'-ferrocene (11).

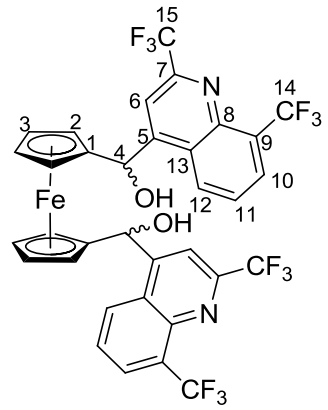

4-Bromo-2,8-di(trifluoromethyl)quinoline **9** (0.729 g, 2.12 mmol, 2 equiv) was dissolved in freshly distilled THF (20 mL) under argon. The solution was cooled to -78 °C in a dry ice bath and *n*-butyllithium (1.6 M in hexanes, 1.4 mL, 2.12 mmol, 2 equiv) was

added dropwise. The reaction mixture was stirred at -78 °C for 30 minutes. A solution of 1,1'-ferrocenedicarboxaldehyde **10** (0.257 g, 1.06 mmol, 1 equiv) in 20 mL of dry THF was added to the reaction mixture and stirring continued for 2 additional hours at -78 °C. The reaction mixture was allowed to warm up to room temperature and water (20 mL) was added to terminate the reaction. The organic layer was separated and the aqueous layer was extracted with diethyl ether (3 x 15 mL). The combined organic fractions were dried over anhydrous Na_2SO_4 and the solvent was removed under pressure to afford an orange oil. Purification of **11** was achieved by flash column chromatography on silica gel with an eluting system of increasing polarity from diethyl ether/hexanes (1:1) to diethyl ether/ethyl acetate (4:1). After removal of the solvent mixture under reduced pressure, compound **11** was obtained as a mixture of diastereomers (0.29 g, 0.37 mmol, 35%).

Diastereomers - set 1: 58%, red solid. ^{1}H NMR (400 MHz, CD_3OD): δ (ppm) 8.74 (d, ^3J = 8.5 Hz, 2H, 12-H), 8.26 (d, ^3J = 7.2 Hz, 2H, 10-H), 8.05 (s, 2H, 6-H), 7.86 (t, ^3J = 7.8 Hz, 2H, 11-H), 6.49 (s, 2H, 4-H), 4.37 (m, 2H, 2-H), 4.34 (m, 2H, 2'-H), 4.30 (m, 2H, 3-H), 4.21 (m, 2H, 3'-H). ^{13}C NMR (101 MHz, CD_3OD): δ (ppm) 157.1 (C8), 155.6 (C7), 152.8 (C5), 132.2 (C12), 130.6 (C10), 128.5 (C11), 126.6 (C9), 124.9 (C13), 122.5 (C14), 120.3 (C15), 116.0 (C6), 93.5 (C1), 70.3 (C2'), 70.1 (C3'), 69.4 (C2), 69.1 (C3), 68.9 (C4). ESI-MS (HR) calculated for $C_{34}H_{20}F_{12}FeN_2NaO_2$: 795.0580, found: 795. 0573 $[M+Na]^+$.

Diastereomers - set 2: 42%, orange solid. ^{1}H NMR (400 MHz, CD_3OD): δ (ppm) 8.70 (d, ^3J = 8.5 Hz, 2H, 12-H), 8.25 (d, ^3J = 6.8 Hz, 2H, 10-H), 8.08 (s, 2H, 6-H), 7.84 (t, ^3J = 7.8 Hz, 2H, 11-H), 6.48 (s, 2H, 4-H), 4.39 (m, 2H, 2-H), 4.26 (m, 2H, 2'-H), 4.20 (m, 2H, 3-H), 4.16 (m, 2H, 3'-H). ^{13}C NMR (101 MHz, CD_3OD): δ (ppm) 155.7 (C8), 150.0 (C7), 147.3 (C5), 130.8 (C12), 130.6 (C10), 128.7 (C11), 126.3 (C9), 124.8 (C13), 124.4 (C14), 119.2 (C15),

116.4 (C6), 93.9 (C1), 70.6 (C2'), 70.0 (C3'), 69.6 (C2), 69.3 (C3), 68.7 (C4). Anal. Calc. for $C_{34}H_{20}F_{12}FeN_2O_2$: C, 52.87, H, 2.61, N, 3.63; found: C, 53.63, H, 2.84, N, 3.44. ESI-MS (HR) calculated for $C_{34}H_{20}F_{12}FeN_2NaO_2$: 795.0580, found: 795.0585 $[M + Na]^+$.

Bis-4-[O-[(2,8-bistrifluoromethyl)quinolyl)]]methyl-1,1'-ferrocene (12).

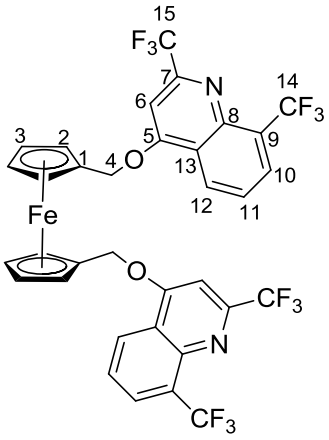

2,8-Di(trifluoromethyl)quinolin-4-ol (0.247 g, 0.88 mmol, 2.2 equiv) was dissolved in 12 mL dry acetonitrile in a 20 mL microwave vial under an excess pressure of argon. Sodium hydride (60% w/w in mineral oil, 0.040 g, 1.00 mmol, 2.5 equiv) was added in one portion to this solution to form a suspension. A solution of 1,1'-bis(N,N'-trimethylaminomethyl)ferrocene iodide **2** (0.234 g, 0.4 mmol, 1 equiv) in 5 mL dry acetonitrile was added dropwise to the suspension and the vial was sealed under argon. The reaction was carried out in a microwave reactor for 6 hours at 110 °C. The solvent was removed under pressure and the red-brown solid obtained was redissolved in ethyl acetate (25 mL) and washed with aqueous NaOH (0.5 M, 10 mL). The organic layer was further washed with water until the aqueous phase was neutral pH, and dried over $MgSO_4$. The solvent was evaporated under reduced pressure. The crude mixture was purified by flash column chromatography on silica using methylene chloride/acetone (1:1) as eluent to afford the product as orange oil (0.034 g, 0.044 mmol, 11 %) after the evaporation of the solvents. ^{1}H NMR (400 MHz, $CDCl_3$): δ (ppm) 8.19 (d, ^3J = 8.2 Hz, 2H, 12-H), 8.08 (d, ^3J = 7.3 Hz, 2H, 10-H), 7.61 (t, ^3J = 7.8 Hz, 2H, 11-H), 6.24 (s, 2H, 6-H), 4.35 (m, 2H, 2-H), 4.20 (m, 2H, 2'-H), 4.06 (m, 2H, 3-H), 3.90 (m, 2H, 3'-H), 3.62 (d, ^3J = 12.96 Hz, 4H, 4-H). ^{13}C NMR (75

MHz, $CDCl_3$): δ (ppm) 163.8 (C5), 155.2 (C8), 154.8 (C7), 150.1 (C15), 130.2 (C14), 129.7 (C10), 128.7 (C12), 126.5 (C11), 124.3 (C9), 122.3 (C13), 102.2 (C6), 96.7 (C1), 69.5 (C2,2'), 67.9 (C3,3'), 62.1 (C4). ESI-MS (+): 795 $[M+Na]^+$.

4.3 Results and discussion

The initial attempts to synthesize of the bischloroquine ferrocenyl derivatives are illustrated in Scheme 4.3,i. The starting material 1,1'-bis(*N,N'*-trimethylaminomethyl)ferrocene iodide (**2**) was reacted with two equivalents of the 4-aminoquinoline derivatives **3a**-**e** in the presence of sodium hydroxide in acetonitrile at 110 °C for six hours, but the expected product was not detected.

Alternative conditions tested included a greater number of equivalents of the 4-aminoquinoline derivatives, greater and lesser quantities of the base sodium hydroxide, and other bases of diverse strength. In all cases, only one product was observed: the bridged ferrocenyl compounds (eg., **5b**) (Scheme 4.3,i), studied in Chapter 2.

Coincidentally, the another research group[197] reported similar outcomes for the synthesis of a bischloroquine ferrocenyl conjugate. When 1,1'-ferrocenedicarboxyaldehyde was reacted with the 4-aminoquinoline derivative **3b**, the only product obtained was the bridged compound **5b**[197] as depicted in Scheme 4.3, ii.

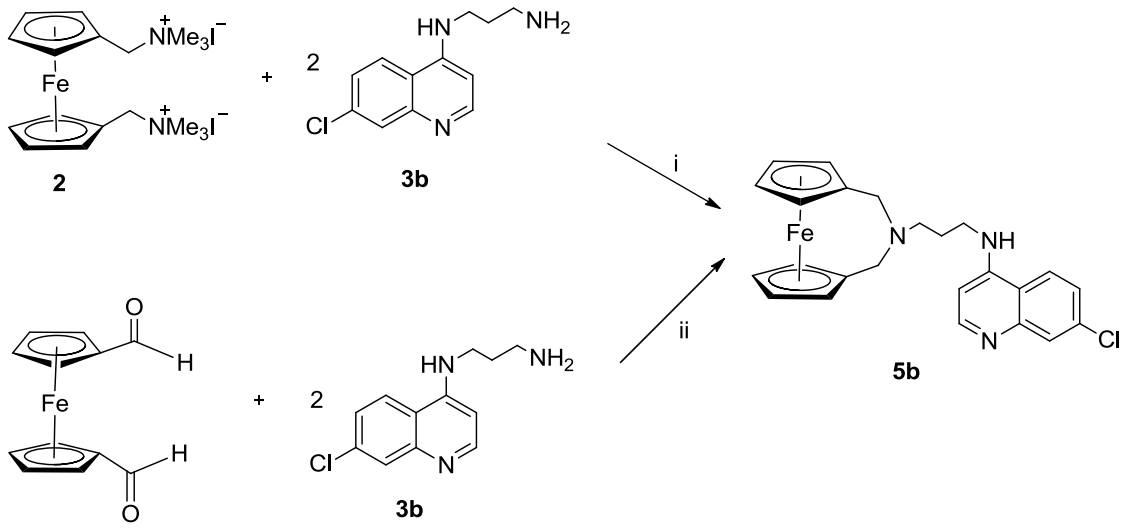

Scheme 4.3. Synthetic routes attempted for the synthesis of the bischloroquine ferrocenyl derivatives that yielded exclusively the bridged ferrocenyl 4-aminoquinoline derivative (**5b**). Route i: NaOH, CH_3CN, 6 h 110 °C. Route ii: MeOH, $NaBH_3CN$, 12 days, 85 °C.

It was then observed that regardless of the method or conditions used, the formation of the bridged ferrocenyl chloroquine compound was favoured over the formation of the bischloroquine ferrocenyl analog when a 1,1'-substituted ferrocenyl starting material was used. It was concluded that the attack of the terminal primary amine functionality in **3** to either the quaternized ammonium groups in **2** or to the aldehyde groups in 1,1'-ferrocenedicarboxyaldehyde occurs in a stepwise fashion. The primary amine loses one of its hydrogen atoms either by condensation with one of the trimethylammonium groups or by reductive amination with one of the aldehyde groups. A second attack of this amine occurs at the remaining trimethylammonium group (i) or aldehyde group (ii) that are very close in proximity, without the need for a second quinoline equivalent, closing the ring to form the bridged ferrocenyl compound.

Therefore, to stop the terminal primary amine in **3** from performing two consecutive attacks, it was decided to convert it to a secondary amine. This was achieved by reacting **3**

with di-*tert*-butyl dicarbonate to form the *N*-*tert*-butoxycarbonyl or N-Boc protected amine. The synthesis of the bischloroquine ferrocenyl derivatives **7**, **8** is described in Scheme 4.4.

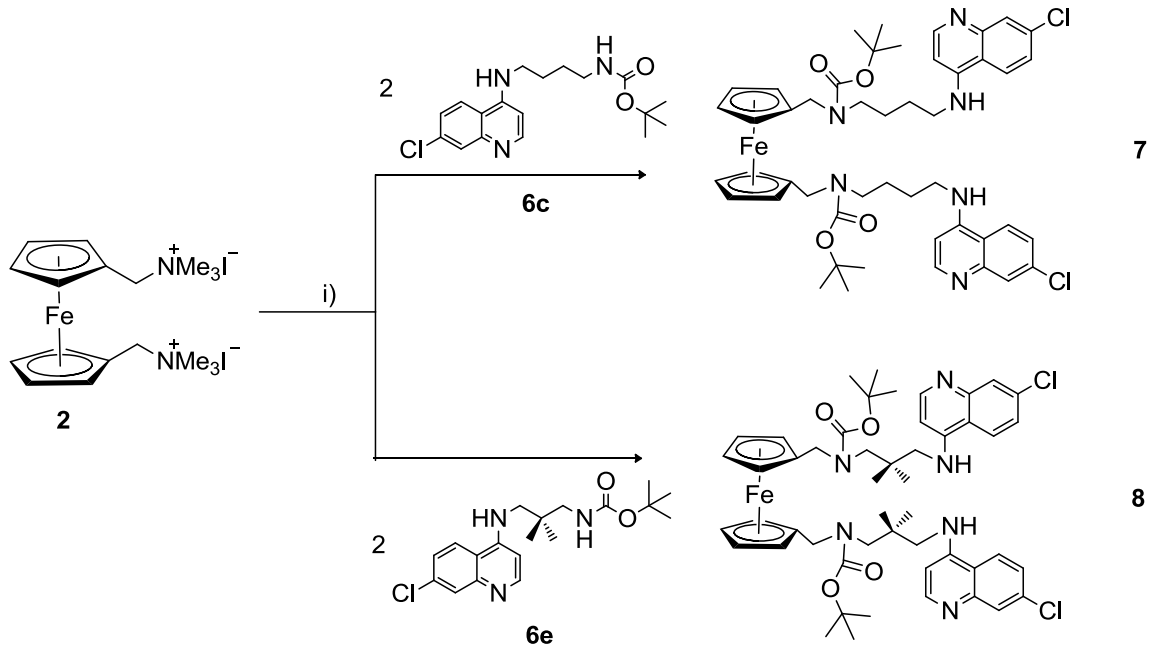

Scheme 4.4. Synthetic route for bis 4-aminoquinoline ferrocenyl derivatives **7** and **8**: i) NaOH, CH_3CN, 6 h, 110 °C.

Compounds **6a-e** were formed by the condensation reaction between the corresponding 4-aminoquinoline derivative **3a-e** and di-*tert*-butyl dicarbonate as shown in Scheme 4.1. The conversion of the primary amine in **3** to a *tert*-butyl carbamate was carried out in a methanolic solution with excess sodium bicarbonate and under sonication over two hours. This rather unconventional method has proven effective for N-Boc protections in ferrocenyl substrates.[246] A typical procedure for N-Boc protection often require dry solvents, heating, greater amounts of di-*tert*-butyl dicarbonate and the aid of catalysts. This procedure was both simpler and effective.

After sonication for two hours, part of the sodium bicarbonate dissolved in methanol. After filtration of the undissolved $NaHCO_3$, the solution was reduced to dryness, then the residue was redissolved in methylene chloride and washed with water repeatedly until all sodium bicarbonate had reacted with the aqueous fraction. Water dissolves efficiently these N-Boc protected 4-aminoquinolines, especially the short chain derivatives such as **6a** and **6b**. Regardless, the compounds are obtained in fairly good yields, with the exception of **6b**. Compound **6b** largely precipitated during the reaction time as it was hardly soluble in the extracting methylene chloride. The pure compounds were characterized by ^{1}H NMR and ^{13}C NMR spectroscopy and HR-MS.

The bis(4-aminoquinoline) ferrocenyl derivatives **7** and **8** were formed by the condensation reaction of 1,1'-bis(*N,N'*-trimethylaminomethyl iodide)ferrocene (**2**) with the corresponding N-Boc-protected 4-aminoquinoline derivatives **6c** and **6e**, respectively (Scheme 4.4). The trimethylamine group of **2** acts as a good leaving group under the nucleophilic attack of the N-Boc-protected 4-aminoquinoline derivative **6**, as it did under the attack of the primary amine of the 4-aminoquinoline derivative **3** when forming the bridged derivative **5**. However, the carbamate nitrogen is less nucleophilic since the ester group attached to it helps delocalize the electron density, therefore **6** is less effective as a nucleophile. In addition, the Boc substituent makes it a bulkier nucleophile creating steric hinderance that impedes the substitution in the ferrocene skeleton.

These difficulties were reflected when tried to synthesize all derivatives corresponding to the series **6a-e**. Lower quantities of base produced only slight amounts of **7** and **8**. When a stronger base such as NaH was employed, no product was obtained. Finally, 10 equivalents of sodium hydroxide (almost double the amount used for **5**) produced **7** and **8** but the

corresponding ferrocenyl bischloroquine analogs for **6a**, **6b** and **6d** were never detected by MS.

The formation of only the ferrocenyl derivatives of the long side chain derivatives **6c** and **6e** is explained by steric hinderance. In these longer alkyl chain derivatives, the attacking nucleophile group is farther away from the quinoline group and therefore slightly less hindered to attack the trimethylamine group of **2**. Compounds **7** and **8** were characterized by ^{1}H NMR and ^{13}C NMR spectroscopy and mass spectrometry.

The bismefloquine ferrocenyl analogs were also synthesized. Two different connectivities were explored for the mefloquine-ferrocene linkage. Compound **11** conserves the secondary alcohol connection observed in the original mefloquine molecule while compound **12** displays an ether connection between the quinoline ring and the ferrocene Cp rings. The synthesis for the bismefloquine ferrocenyl derivative **11** is described in Scheme 4.5.

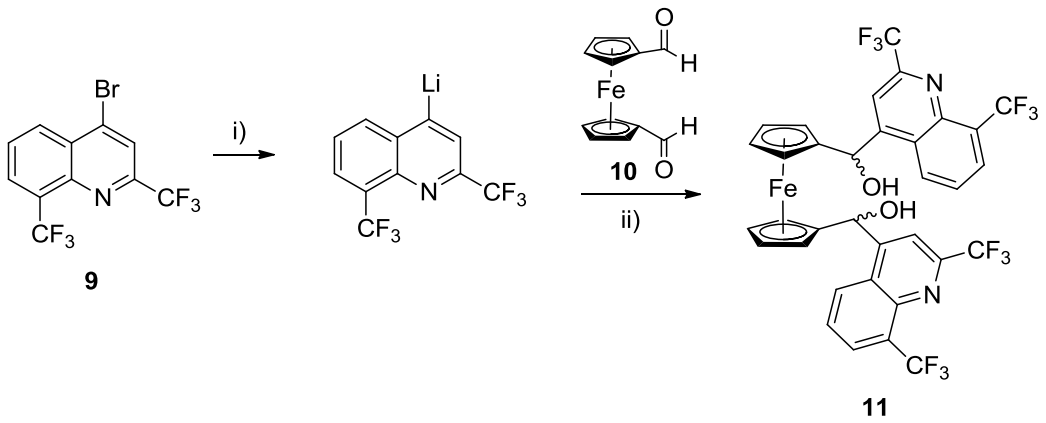

Scheme 4.5. Synthetic route for the bismefloquine ferrocenyl derivative **11** i) nBuLi, THF, 30 min, -78 °C; ii) **10**, THF, 2 h, -78 °C.

4-Bromo-2,8-di(trifluoromethyl)quinoline (**9**) is commercially available, however very expensive. In this work, I followed closely a published procedure for its synthesis from the commercially available 2,8-di(trifluoromethyl)quinolin-4-ol.[244] The latter compound and phosphorous (V) oxybromide were reacted at 150 °C in a neat reaction (Scheme 4.2). Upon cooling, the solidified product was washed thoroughly with water and dried under vacuum to use it in the next step. The structure and purity of **9** was verified by ^{1}H and ^{13}C NMR spectroscopy and LR-MS.

The starting material 1,1'-ferrocenedicarboxaldehyde (**10**) was also prepared as previously reported.[245] Ferrocene was doubly deprotonated at the 1- and 1'-positions by the action of *n*-butyllithium activated by TMEDA. The 1,1'-dilithioferrocene was then reacted with DMF in diethyl ether. The crude product of this reaction contains, as expected, unreacted ferrocene, monosubstituted ferrocenecarboxaldehyde and the disubstituted 1,1'-ferrocenedicarboxaldehyde (**10**). The purification step by column chromatography proved again to be rather complicated, as it is for many 1,1'-ferrocene products that must be separated from the mono and unsubstituted sideproducts. The handling and purification of **10** by column chromatography was further complicated since **10** is light and temperature sensitive, and decomposed rapidly while on the silica column. This compound must be purified immediately and stored in the fridge. The structure and purity of **10** was verified by ^{1}H NMR spectroscopy and LR-MS.

The synthesis of the bismefloquine ferrocenyl compound **11** was inspired by the synthesis of the mefloquine ferrocenyl derivative found in the literature.[152] The bromide ion of the starting material 4-bromo-2,8-di(trifluoromethyl)quinoline (**9**) is replaced with a lithium ion by the action of *n*-butyllithium at low temperatures. In the subsequent addition of the 1,1'-

ferrocenedicarboxaldehyde (**10**), the aldehyde groups act as electrophiles for the attack of the 4-lithio-2,8-di(trifluoromethyl)quinoline, converting them into secondary alcohols after work-up.

The bismefloquine ferrocenyl **11** was isolated as two mixtures of diastereomers. The proposed distribution of these diastereomers is shown in Figure 4.3. The assignment of diastereomers A and B to these two pairs of compounds has been done arbitrarily.

Both groups of enantiomers, A and B, were isolated from flash column chromatography on silica gel. Several ferrocenyl side products and unreacted 2,8-bis(tri-fluoromethyl)quinoline were also obtained, which made the separation rather complicated. Hence, a varying elution system was used, starting from the mixture diethyl ether/hexanes (1:1) and then increasing in polarity. The first group of enantiomers (set 1) elutes with diethyl ether/hexanes (4:1) (Rf = 0.45). The second group of enantiomers (set 2) elutes with diethyl ether/ethyl acetate (4:1) (Rf = 0.24). These two groups of enantiomers present different physical properties; both are solids, but the first set is red and the second set is orange.

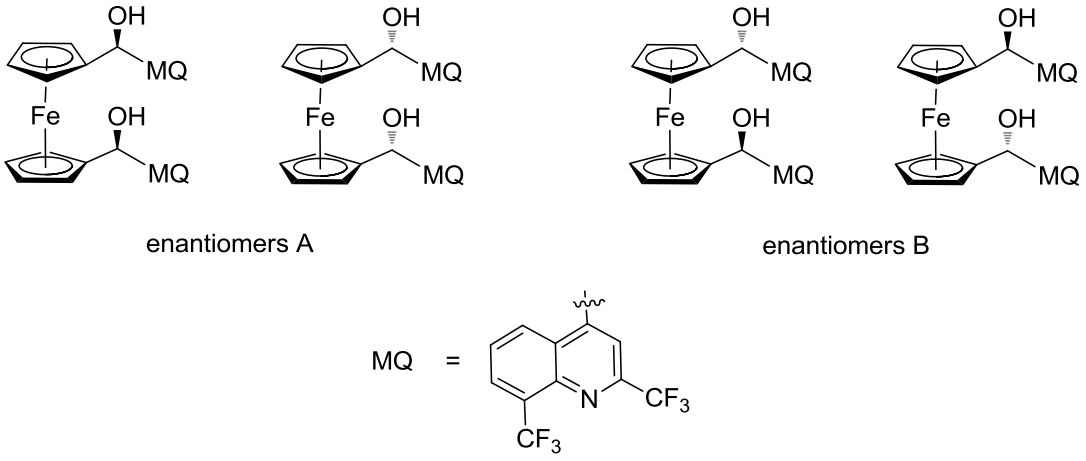

Figure 4.3. Diastereomers of the bismefloquine ferrocenyl derivative **11**.

Each set of diastereomers was characterized by ^{1}H NMR, ^{13}C NMR, 2D NMR spectroscopic techniques (COSY, HMBC, HSQC), HR-MS and elemental analysis. The mass spectrum of both groups is identical, as expected. The ^{1}H NMR and ^{13}C NMR spectra, however, differ in chemical shifts. The set of ^{1}H NMR spectra for both group of diastereomers can be observed in Figure 4.4. The difference in chemical shifts for the quinoline protons is minimal and the ferrocene protons (δ = 4.5-4.0 ppm) are also only slightly affected.

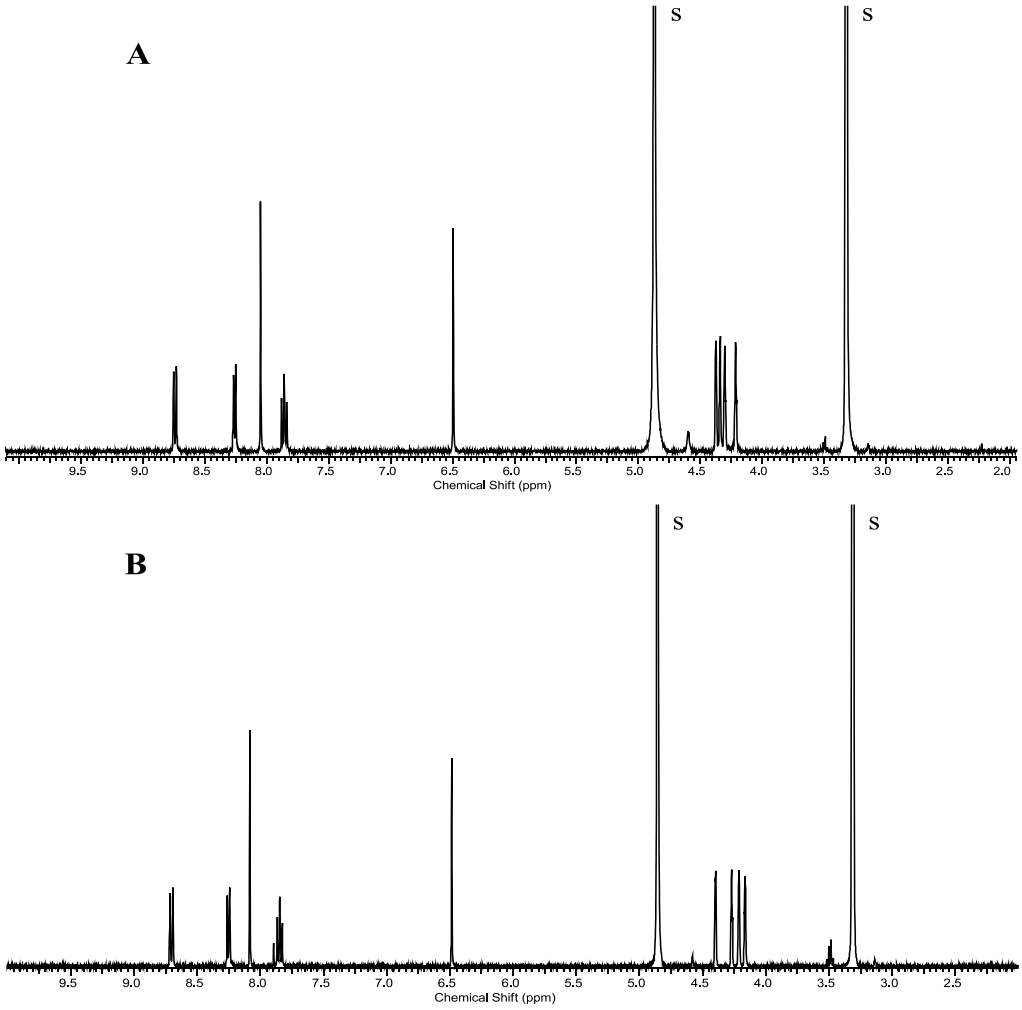

Figure 4.4. ^{1}H NMR (CD_3OD, 400 MHz, RT) spectra of **11** diastereomers A (top) and diastereomers B (bottom); s indicates solvent peaks.

In order to determine the chirality of each set of enantiomers, further studies will be needed that include separation on a chiral column. Finally, the synthesis for the bismefloquine ferrocenyl derivative **12** is described in Scheme 4.6.

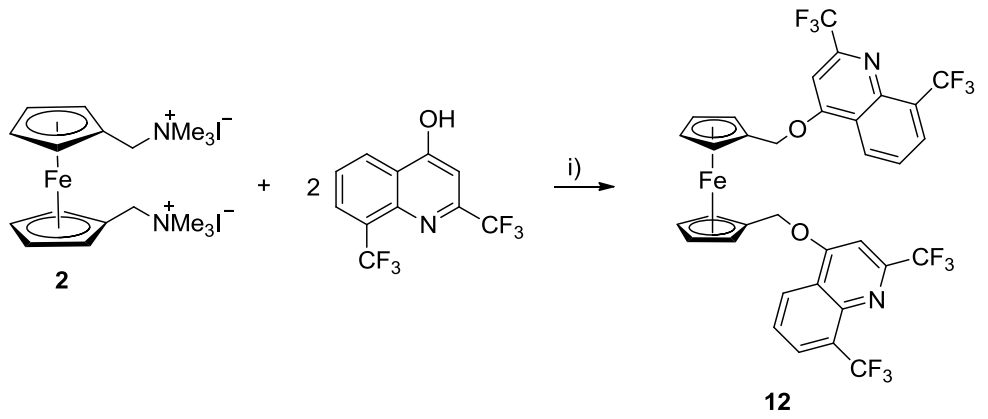

Scheme 4.6. Synthetic route for the bismefloquine ferrocenyl derivative **12**. i) NaH, CH_3CN, 6 h, 110 °C.

The bismefloquine ferrocenyl derivative **12** was synthesized following another condensation reaction between 1,1'-bis(*N,N'*-trimethylaminomethyl)ferrocene iodide (**2**) and the commercially available 2,8-di(trifluoromethyl)quinolin-4-ol. This time, using a stronger base such as NaH, the deprotonated alcohol group in the mefloquine derivative becomes a better nucleophile and is able to displace the trimethylamine groups in **2**. This compound was characterized by ^{1}H NMR, ^{13}C NMR, 2D NMR spectroscopy techniques (COSY, HMBC, HSQC) and mass spectrometry.

4.4 Conclusions

Only one other example of a bischloroquine ferrocenyl derivative[147] and no examples of bismefloquine ferrocenyl derivatives are known in the literature. The compounds reported here represent an important contribution in the library of ferrocenyl quinoline derivatives that have capacity to act as antimalarial drugs.

It would be very interesting to investigate the antimalarial response of these compounds in chloroquine-resistant parasite strains. Their double load of drug could improve their action remarkably if their relatively large size allows them to cross membranes to reach the drug site of action. This delicate balance of increasing the loading while not diminishing their absorption properties needs study *in vitro*.

Furthermore, creation of chiral sites that generate enantiomers (such is the case of **11**) are additional features that would be interesting to study to determine if different diastereomeric groups or even enantiomers (if separation is feasible) exhibit different antiplasmodial activity.

While not many bisquinoline ferrocenyl derivatives exist, possibly because they are synthetically challenging targets, it is offered here relatively simple synthesis that uses a microwave reactor (for some) and could be easily adapted to bench conditions.

CHAPTER 5 SYNTHESIS AND CHARACTERIZATION OF CHLOROQUINE AND MEFLOQUINE FERROCENYL CARBOHYDRATE CONJUGATES

5.1 Introduction

Another strategy pursued in the design of drug candidates presented in this thesis was the multifunctional therapy strategy. Such a strategy, which involves the development of drug agents that incorporate multiple therapeutic targets, is an attractive area in chemotherapeutics, since it reduces the number of agents that have to be administered to the patient without losing effectiveness.

The possibilities of the application of this strategy to antimalarial chemotherapy include the combination of two (or more) antimalarial agents with the same site of action, the combination of an antimalarial drug and an agent that reverses drug resistance, or the combination of an antimalarial drug and an agent that targets the delivery of the antimalarial drug to the drug's site of action.

Successful examples of this strategy include the trioxaferroquines (a series of hybrid compounds consisting of a 1,2,4-trioxane fragment, the main feature of artemisinins, and ferroquine),[145] a 4-aminoquinoline bearing an amino side-chain substituted by an aliphatic Mannich base (whose function is to produce oxidative stress once inside the parasite food

vacuole),[146] and a series of ferroquine analogs conjugated to a gluthatione reductase (GR) inhibitor (also causing oxidative stress).[247]

In this thesis we chose to explore a multifunctional model that includes a conventional antimalarial drug such as chloroquine or mefloquine combined with a targeting agent. This novel entity could improve the targeting of the drug, delivering it more effectively to its site of action and lowering its recognition by the proteins involved in drug resistance.

In addition, the targeting of a drug could reduce the time of drug exposure in general since it will be delivered to the site of action more effectively and spend less time exposed to the parasite, therefore lowering the possibility of developing resistance. The design followed is depicted in Figure 5.1. This approach contemplates the addition of a monosaccharide molecule to the ferrocene chloroquine derivative. The function of the carbohydrate molecule is to target infected red blood cells, delivering more efficiently the antimalarial ferrocene chloroquine derivative.

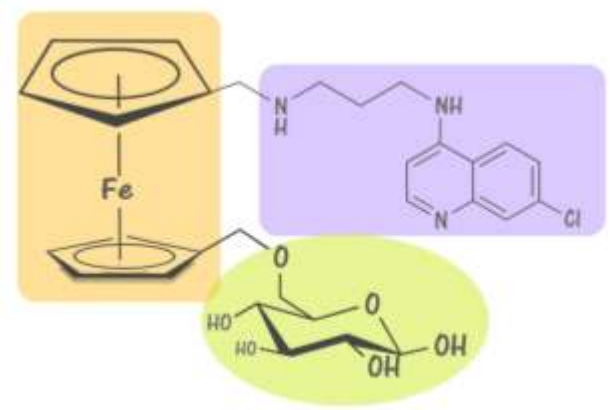

Figure 5.1. Graphic representation of the multifunctional therapeutic approach. The different colors represent the three moieties or functionalities.

In infected erythrocytes, glucose uptake and metabolism are elevated at all stages of the parasite's life cycle: asexual stage parasites require a continuous supply of glucose to survive and multiply.[248] The parasites increase glucose consumption 50-100 fold as compared to uninfected red cells and most of the glucose is metabolized to lactic acid.[249,250,251] Intraerythrocytic stages of *Plasmodium falciparum* are wholly dependent on host glucose for energy.[248]

Glucose consumption has been a target in antimalarial research.[250,252,253] An example consists of the *O*-3-hexose derivatives that inhibit uptake of glucose and fructose by *Pf*HT (glucose uptake is mediated by the parasite-encoded facilitative hexose transporter *Pf*HT)[254] suggesting that the hexose transporter (*Pf*HT) of *P. falciparum* is a potential drug target.[253,255]

Antimalarial activity has even been observed in ferrocenyl carbohydrate compounds with ferrocene substituted with either one or two monosaccharides *via* different linkers, described previously by our group[159] and by Itoh and co-workers.[158] These ferrocenyl carbohydrate derivatives presented a moderate antimalarial activity (in the low micromolar range) against both chloroquine-sensitive and resistant parasite strains.[158,159]

This activity could be potentiated by the activity of a much more active component such as the ferrocenyl chloroquine conjugates. The combined presence of these three moieties (quinoline, carbohydrate and ferrocene) may give these derivatives the potential to retain activity in drug-resistant parasite strains and to increase therapeutic efficacy by targeting infected red blood cells.

Based on the organometallic frameworks of both ferrocenyl quinoline derivatives and ferrocenyl carbohydrates, a carbohydrate moiety and a quinoline moiety (chloroquine and

mefloquine derivatives) were attached at the cyclopentadienyl ring(s) of ferrocene, in a 1,2- and 1,1'- substitution pattern that is illustrated in Figure 5.2.

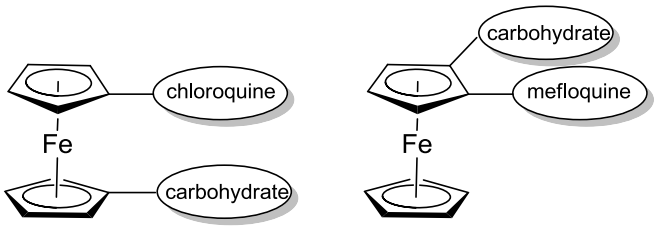

Figure 5.2. Heteroannular ferrocenyl chloroquine carbohydrate conjugate and homoannular ferrocenyl mefloquine carbohydrate conjugate.

5.2 Experimental

5.2.1 Materials and instrumentation

Please refer to Chapter 2.2.1 for general information. All chemicals were purchased from Sigma Aldrich or Acros Organics and used without further purification. TMEDA was freshly distilled from Na under argon, prior to use and stored under argon in the dark. For the synthesis of the starting 4-aminoquinoline derivatives **3a**, **3b** and **3e** please refer to Chapter 2.2.2. For the synthesis of the starting material 4-bromo-2,8-di(trifluoromethyl)quinoline (**9**) please refer to Chapter 4.2.2. Acetyl protected glucosamine was prepared as per literature procedure.[256]

For general information on the *in vitro* antitumor activity and cytotoxicity assay please refer to Chapter 3.2.2. Human colon carcinoma cells Caco-2 (HTB-37) were purchased from

ATCC. Cells were grown as monolayers in medium (89% *Eagle's* Minimum Essential Medium, 10% fetal bovine serum, 1% penicillin/streptomycin) and maintained at 37 °C in a humidified atmosphere containing 5% CO_2. For general information on the X-ray data collection and processing please refer to Chapter 2.2.1.

5.2.2 Synthesis

1,1'-Bis(tri-*n*-butylstannyl)ferrocene (13).

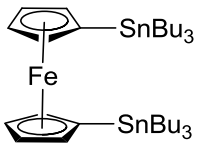

This compound was prepared as previously reported[257] with slight modifications. *n*-Butyllithium (1.6 M in hexanes, 25 mL, 40 mmol, 2.35 equiv) was added dropwise to a stirred solution of freshly distilled TMEDA (6 mL, 40 mmol, 2.35 equiv) in hexanes (7 mL). Ferrocene (3.16 g, 17 mmol, 1.0 equiv) was dissolved in hexanes (100 mL) and added dropwise by syringe over a period of an hour. The reaction mixture was stirred under inert atmosphere at RT for 12 hours. The solution was cooled down to 0 °C in a water/ice bath and tri-*n*-butylstannyl chloride (11.5 mL, 42.5 mmol, 2.50 equiv) was added dropwise. The reaction mixture was allowed to warm to room temperature and stirred under inert atmosphere for 12 hours. Water (20 mL) was added to terminate the reaction. The organic layer was washed with water (3 x 30 mL) and brine (3 x 30 mL) and dried over anhydrous K_2CO_3. The solvent was removed under reduced pressure to afford an orange oil. Purification of the desired product was done by flash column chromatography on neutral alumina Brockman activity I with hexanes as eluent. Product **13** was obtained as an orange-brown oil (9.48 g, 12.4 mmol, 73%). ^{1}H NMR (300 MHz, $CDCl_3$)

δ (ppm) 4.23 (t, ^3J = 5.5 Hz, 4H), 3.96 (t, ^3J = 5.5 Hz, 4H), 1.56 (m, 12H), 1.36 (m, 12H), 1.01 (m, 12H), 0.91 (t, 18H). LR-MS: 764.2 $[M]^{+\cdot}$.

1'-(*N*,*N*-Dimethylaminomethyl)-1-tri-*n*-butylstannyl-ferrocene (14).

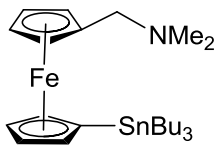

This compound was prepared as previously reported[142] with slight modifications. *n*-Butyllithium (1.6 M in hexanes, 1.7 mL, 2.7 mmol, 1.35 equiv) was added dropwise to a stirred solution of **13** (1.53 g, 2 mmol, 1 equiv) in THF (15 mL) at -78 °C. The reaction mixture was stirred under inert atmosphere at -78 °C for 0.5 h. (*N,N'*-Dimethyl)methyleneammonium iodide (0.56 g, 3.0 mmol, 1.5 equiv) was added in one portion and the mixture was allowed to warm to room temperature and stirred under inert atmosphere for 16 hours. Water (10 mL) was added to terminate the reaction. The organic layer was separated and the aqueous layer was extracted with portions of diethyl ether (3 x 10 mL). The combined organic fractions were dried over anhydrous Na_2SO_4 and the solvent was removed under reduced pressure to afford an orange oil. Purification of the desired product was done by flash column chromatography on neutral alumina Brockman activity V with hexanes/diethyl ether/ triethylamine (70:29:1) as eluent system. Compound **14** was obtained as an orange oil (0.40 g, 0.76 mmol, 38%). ^{1}H NMR (300 MHz, $CDCl_3$) δ (ppm) 4.27 (t, ^3J = 1.8 Hz, 2H), 4.11 (t, ^3J = 1.7 Hz, 2H), 4.04 (t, ^3J = 1.7 Hz, 2H), 3.95 (t, ^3J = 1.5 Hz, 2H), 3.27 (s, 2H), 2.17 (s, NMe_2, 6H), 1.57 (m, 6H), 1.36 (m, 6H), 1.03 (m, 6H), 0.93 (t, 9H).

1'-(Tri-n-butylstannyl)-1-ferrocenecarboxaldehyde (15).

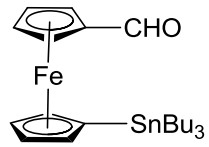

This compound was prepared similarly to **14,** with the following exceptions: N,N-dimethylformamide (0.23 mL, 3.0 mmol, 1.5 equiv) was added instead of (*N,N'*-dimethyl)methyleneammonium iodide and purification of the desired product was done by flash column chromatography on silica gel with hexanes/diethyl ether (1:1) as eluent system. Compound **15** was obtained as an orange oil (0.52 g, 1.10 mmol, 55%). ^{1}H NMR (300 MHz, $CDCl_3$) δ (ppm) 9.95 (s, 1H, CHO), 4.74 (t, ^{3}J = 1.8 Hz, 2H), 4.54 (t, ^{3}J = 1.8 Hz, 2H), 4.48 (t, ^{3}J = 1.6 Hz, 2H), 4.10 (t, ^{3}J = 1.6 Hz, 2H), 1.56 (m, 6H), 1.36 (m, 6H), 1.04 (m, 6H), 0.92 (t, 9H).

1'-(Tri-n-butylstannyl)-1-methyl ferrocenecarboxylate (16).

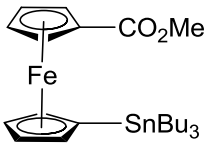

This compound was prepared similarly to **14,** with the following exceptions: methyl chloroformate (0.23 mL, 3.0 mmol, 1.5 equiv) was added instead of (*N,N'*-dimethyl)methyleneammonium iodide, the combined organic fractions were washed with water (2 x 15 mL), saturated NH_4Cl (2 x 15 mL) and brine (2 x 15 mL), and dried over anhydrous Na_2SO_4. The solvent was removed under reduced pressure to afford a red oil. Purification of the desired product was done by flash column chromatography on silica gel with hexanes/diethyl ether (7:3) as eluent system. Compound **16** was obtained as a red oil (0.68 g, 1.28 mmol, 64%). ^{1}H NMR (300 MHz, $CDCl_3$) δ (ppm) 4.77 (t, ^{3}J = 1.8 Hz, 2H), 4.39 (t, ^{3}J = 1.7 Hz, 2H), 4.33 (t, ^{3}J = 1.6 Hz, 2H), 4.04 (t, ^{3}J = 1.7 Hz, 2H), 3.82 (s, 3H), 1.56 (m, 6H), 1.37 (m, 6H), 1.03 (m, 6H), 0.91 (t, 9H).

1'-(*N*,*N*-Dimethylaminomethyl)-1-ferrocenecarboxaldehyde (17).

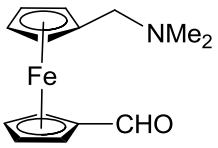

This compound was prepared as previously reported[142] with slight modifications. *n*-Butyllithium (1.6 M in hexanes, 3.2 mL, 5 mmol, 5 equiv) was added dropwise to a stirred solution of **14** (0.53 g, 1 mmol, 1 equiv) in THF (20 mL) at -78 °C. The reaction mixture was stirred under inert atmosphere at -78 °C for 0.5 h. Excess dimethylformamide (3.10 mL, 40.0 mmol, 40 equiv) was added to the mixture which was allowed to warm to room temperature. The reaction was stirred under inert atmosphere for 3 hours. Water (10 mL) was added to terminate the reaction. The organic layer was separated and the aqueous layer was extracted with portions of diethyl ether (3 x 15 mL). The combined organic fractions were dried over anhydrous Na_2SO_4 and the solvent was removed under reduced pressure to afford an orange oil. Purification of the desired product was done by flash column chromatography on neutral alumina Brockman activity V with hexanes/diethyl ether/ triethylamine (70:20:10) as eluent system. Compound **17** was obtained as an orange oil (0.20 g, 0.74 mmol, 74%). ^{1}H NMR (300 MHz, $CDCl_3$) δ (ppm) 9.94 (s, 1H, CHO), 4.74 (t, ^3J = 1.5 Hz, 2H), 4.57 (t, ^3J = 1.7 Hz, 2H), 4.28 (t, ^3J = 1.5 Hz, 2H), 4.24 (t, ^3J = 1.7 Hz, 2H), 3.19 (s, 2H), 2.17 (s, NMe_2, 6H). ESI-MS(+): 272.2 $[M+H]^+$. Anal. Calc. for $C_{14}H_{17}FeNO$: C, 62.02; H, 5.17; N, 6.32. Found: C, 61.89; H, 4.95; N, 6.62.

***N*-(7-Chloro-4-quinolyl)-*N*'-(1-dimethylaminomethylferrocene-1-ylmethyl)-ethane-1,2-diamine (18).**

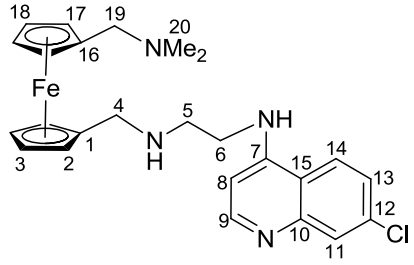

This compound was prepared as previously reported[142] with slight modifications. Compound **17** (0.27 g, 1.0 mmol,

1 equiv) and the 4-aminoquinoline derivative **3a** (0.33 g, 1.5 mmol, 1.5 equiv) were dissolved in dry methanol (20 mL). The mixture was stirred at room temperature overnight. Sodium borohydride (0.115 g, 3.0 mmol, 3 equiv) was added and the resulting mixture was stirred for an additional 2 hours. The reaction mixture was quenched with the addition of 5% $NaHCO_3$ solution (10 mL) and the resulting mixture was extracted with diethyl ether (3 x 25 mL). The combined organic fractions were dried over anhydrous Na_2SO_4 and the solvent was removed under reduced pressure. Purification of the desired product was done by flash column chromatography on silica with a mixture of ethyl acetate/methanol/TEA in increasing polarity 94:4:2 to 75:15:10 ratios. Compound **18** was obtained as an orange oil (0.39 g, 0.82 mmol, 82%). ^{1}H NMR (400 MHz, $CDCl_3$): δ (ppm) 8.54 (d, ^3J = 5.1 Hz, 1H, 9-H), 7.96 (d, ^4J = 2.0 Hz, 1H, 11-H), 7.71 (d, ^3J = 8.9 Hz, 1H, 14-H), 7.37 (dd, ^3J = 9.0 Hz, ^4J = 2.2 Hz, 1H, 13-H), 6.40 (d, ^3J = 5.1 Hz, 1H, 8-H), 5.91 (br. s., 1H, Ar-N*H*-), 4.13 (m, 4H, 2,3-H), 4.10 (m, 4H, 17,18-H), 3.58 (s, 2H, 4-H), 3.34 (m, 2H, 6-H), 3.32 (s, 2H, 19-H), 3.05 (m, 2H, 5-H), 2.18 (s, 6H, 20-H). ^{13}C NMR (101 MHz, $CDCl_3$): δ (ppm) 151.6 (C9), 150.0 (C7), 149.7 (C10), 135.5 (C12), 129.3 (C11), 125.4 (C13), 121.9 (C14), 117.4 (C15), 99.1 (C8), 86.2 (C1), 82.7 (C16), 71.2 (C17), 70.3 (C18), 68.6 (C2), 68.3 (C3), 57.7 (C19), 48.3 (C4), 46.2 (C6), 44.3 (C20), 41.8 (C5). ESI-MS (HR) calculated for $C_{25}H_{30}ClFeN_4^+$: 477.1505, found: 477.1510 $[M + H]^+$.

***N*-(7-Chloro-4-quinolyl)-*N*'-(1-dimethylaminomethylferrocene-1-ylmethyl)-propane-1,3-diamine (19).**

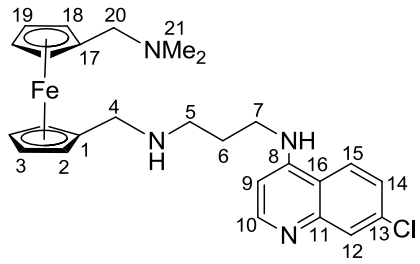

This compound was prepared similarly to **18,** with the corresponding 4-aminoquinoline derivative **3b** (0.355 g, 1.5 mmol, 1.5 equiv). Compound **19** was obtained as an orange oil (0.38 g, 0.77 mmol, 77%). ^{1}H NMR (400 MHz, $CDCl_3$): δ (ppm) 8.46 (d, ^{3}J = 5.4 Hz, 1H, 10-H), 7.93 (br, 1H, Ar-N*H*-), 7.89 (d, ^{4}J = 1.9 Hz, 1H, 12-H), 7.60 (d, ^{3}J = 8.9 Hz, 1H, 15-H), 7.19 (dd, ^{3}J = 8.9 Hz, ^{4}J = 1.9 Hz, 1H, 14-H), 6.26 (d, ^{3}J = 5.4 Hz, 1H, 9-H), 4.15 (br. s., 3H, 18,19-H), 4.14 (m, 2H, 2-H), 4.10 (m, 2H, 3-H), 4.09 (s, 1H, 18-H), 3.59 (s, 2H, 4-H), 3.36 (m, 2H, 7-H), 3.33 (s, 2H, 20-H), 2.97 (m, 2H, 5-H), 2.19 (s, 6H, 21-H), 1.91 (m, 2H, 6-H). ^{13}C NMR (101 MHz, $CDCl_3$): δ (ppm) 151.2 (C10), 150.5 (C8), 149.5 (C11), 136.3 (C13), 129.3 (C12), 125.3 (C14), 122.8 (C15), 117.2 (C16), 98.0 (C9), 84.3 (C1), 79.6 (C17), 71.2 (C18), 69.7 (C19), 69.5 (C3), 69.3 (C2), 57.2 (C20), 48.6 (C4), 48.1 (C7), 43.2 (C5), 42.6 (C21), 26.4 (C6). ESI-MS (HR) calculated for $C_{26}H_{32}ClFeN_4^+$: 491.1661, found: 491.1664 $[M + H]^+$.

***N*-(7-Chloro-4-quinolyl)-*N*'-(1-dimethylaminomethylferrocene-1-ylmethyl)-2,2-dimethyl-propane-1,3-diamine (20).**

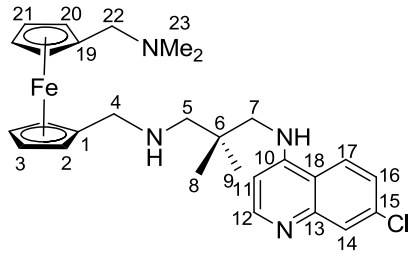

This compound was prepared similarly to **18,** with the corresponding 4-aminoquinoline derivative **3e** (0.40 g, 1.5 mmol, 1.5 equiv). Compound **20** was obtained as an orange oil (0.41 g, 0.79 mmol, 79%). ^{1}H NMR (400 MHz, $CDCl_3$): δ (ppm) 8.55 (br. s., 1H, Ar-N*H*-), 8.46 (d, ^{3}J = 5.1 Hz, 1H, 12-H), 7.90 (d, ^{4}J = 2.0

Hz, 1H, 14-H), 7.57 (d, ^{3}J = 8.9 Hz, 1H, 17-H), 7.18 (dd, ^{3}J = 8.9 Hz, ^{4}J = 2.0 Hz, 1H, 16-H), 6.24 (d, ^{3}J = 5.5 Hz, 1H, 11-H), 4.18 (m, 4H, 2,3-H), 4.14 (m, 2H, 20-H), 4.10 (m, 2H, 21-H), 3.56 (s, 2H, 4-H), 3.29 (s, 2H, 22-H), 3.14 (s, 2H, 7-H), 2.77 (s, 2H, 5-H), 2.18 (s, 6H, 23-H), 1.08 (s, 6H, 8,9-H). ^{13}C NMR (101 MHz, $CDCl_3$): δ (ppm) 152.2 (C12), 150.7 (C10), 149.5 (C13), 135.0 (C15), 128.7 (C14), 125.8 (C16), 122.1 (C17), 116.3 (C18), 98.8 (C11), 86.7 (C1), 81.3 (C19), 73.4 (C20), 72.5 (C21), 69.7 (C3), 69.2 (C2), 59.3 (C7), 56.9 (C22), 56.0 (C4), 48.7 (C5), 44.4 (C23), 32.8 (C6), 24.7 (C8-9). ESI-MS (HR) calculated for $C_{28}H_{36}ClFeN_4^+$: 519.1976, found: 519.1978 $[M + H]^+$.

***N*-(7-Chloro-4-quinolyl)-*N*'-(1-trimethylaminomethyl iodide ferrocene-1-ylmethyl)-ethane-1,2-diamine (21).**

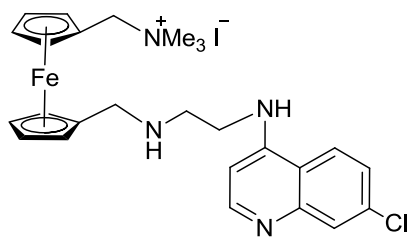

Iodomethane (0.04 mL, 0.6 mmol, 2 equiv) was added slowly to a solution of **18** (0.145 g, 0.3 mmol, 1 equiv) in methanol (10 mL) under inert atmosphere. The reaction mixture was stirred overnight at room temperature. The solvent was removed under pressure. Several portions of methanol and toluene (5 mL) were added to the mixture and the solvent was removed under reduced pressure each time. Compound **21** (0.171 g, 0.28 mmol, 92%), an orange oily solid, was carried to the following step without further purification. ^{1}H NMR (300 MHz, CD_3OD): δ (ppm) 8.52 (d, ^{3}J = 6.2 Hz, 1H), 8.35 (d, ^{3}J = 9.1 Hz, 1H), 7.87 (d, ^{4}J = 2.1 Hz, 1H), 7.59 (dd, ^{3}J = 8.9 Hz, ^{4}J = 2.1 Hz, 1H), 6.91 (d, ^{3}J = 6.2, 1H), 4.94 (s, 1H, -CH_2NMe_3^+), 4.77 (s, 1H, -CH_2NMe_3^+), 4.69 (m, 2H, H_{Cp}), 4.64 (m, 2H, H_{Cp}), 4.55 (m, 2H, H_{Cp}), 4.53 (m, 2H, H_{Cp}), 4.12 (m, 2H), 3.77 (m, 2H), 3.16 (s, 2H), 3.06 (s, 9H, -NMe_3). ESI-MS(+): 491.6 $[M-I]^+$, 432.6 $[M-NMe_3]^+$.

***N*-(7-Chloro-4-quinolyl)-*N*'-(1-trimethylaminomethyl iodide ferrocene-1-ylmethyl)-propane-1,3-diamine (22).**

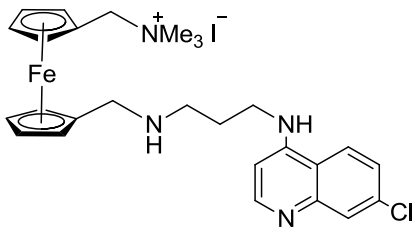

This compound was prepared similarly to **21,** with the corresponding ferrocenyl derivative **19** (0.147 g, 0.3 mmol, 1.0 equiv). Compound **22** (0.163 g, 0.26 mmol, 85%), an orange oily solid, was carried to the following step without further purification. ^{1}H NMR (300 MHz, CD_3OD): δ (ppm) 8.45 (d, ^{3}J = 5.9 Hz, 1H), 8.24 (d, ^{3}J = 8.9 Hz, 1H), 7.81 (dd, ^{3}J = 5.9 Hz, ^{4}J = 2.1 Hz, 1H), 7.48 (dd, ^{3}J = 8.9 Hz, ^{4}J = 2.1 Hz, 1H), 6.77 (d, ^{3}J = 5.9, 1H), 4.78 (s, 1H, -CH_2NMe_3^+), 4.75 (s, 1H, -CH_2NMe_3^+), 4.62 (m, 2H, H_{Cp}), 4.55 (m, 2H, H_{Cp}), 4.49 (m, 2H, H_{Cp}), 4.37 (m, 2H, H_{Cp}), 3.61 (m, 2H), 3.48 (m, 2H), 3.34 (s, 2H), 3.06 (s, 9H, -NMe_3^+), 2.34 (m, 2H). ESI-MS(+): 505.6 $[M\text{-}I]^+$, 446.6 $[M\text{-}NMe_3]^+$.

***N*-(7-Chloro-4-quinolyl)-*N*'-(1-trimethylaminomethyl iodide ferrocene-1-ylmethyl)- 2,2-dimethylpropane -1,3-diamine (23).**

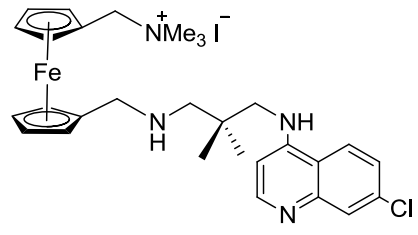

This compound was prepared similarly to **21,** with the corresponding ferrocenyl derivative **20** (0.155 g, 0.3 mmol, 1.0 equiv). Compound **23** (0.192 g, 0.26 mmol, 98%), an orange oily solid, was carried to the following step without further purification. ^{1}H NMR (300 MHz, CD_3OD): δ (ppm) 8.32 (d, ^{3}J = 5.8 Hz, 1H), 7.86 (d, ^{3}J = 8.9 Hz, 1H), 7.75 (dd, ^{3}J = 5.8 Hz, ^{4}J = 2.0 Hz, 1H), 7.35 (dd, ^{3}J = 8.9 Hz, ^{4}J = 2.0 Hz, 1H), 6.54 (d, ^{3}J = 5.8, 1H), 4.56 (s, 1H, -CH_2NMe_3^+), 4.52 (m, 2H, H_{Cp}), 4.41 (m, 2H, H_{Cp}), 4.40 (m, 2H, H_{Cp}), 4.28 (m, 2H, H_{Cp}), 3.77 (s, 1H, -CH_2NMe_3^+), 3.77 (m, 2H), 3.26 (m,

2H), 3.36 (s, 2H), 3.04 (s, 9H, -NMe_3^+), 1.08 (s, 6H). ESI-MS(+): 533.8 $[M-I]^+$, 474.6 $[M-NMe_3]^+$.

_N_-(7-Chloro-4-quinolyl)-_N_'-{[2-_N_-(1,3,4,6-Tetra-_O_-acetyl-α-D-glucopyranose)] ferrocene-1-ylmethyl}-propane-1,3-diamine (24).

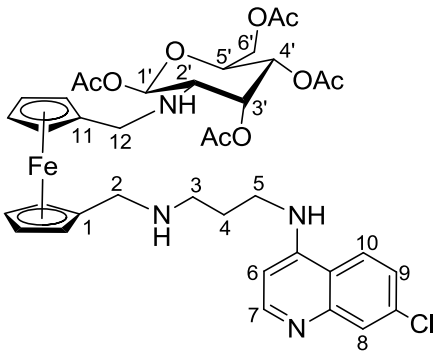

Method A: *N*-(7-Chloro-4-quinolyl)-*N*'-(1-trimethylamino methyl iodide ferrocene-1-ylmethyl)-propane-1,3-diamine (**22**) (0.095 g, 0.15 mmol, 1 equiv), free base glucosamine (0.105 g, 0.3 mmol, 2 equiv) and pyridine (0.06 mL, 0.75 mmol, 5 equiv) were combined with 15 mL of acetonitrile in a 20 mL microwave vial. The reaction was carried out in a microwave reactor for 6 h at 110 °C. The solvent was removed under reduced pressure. Purification of the desired product was done by flash column chromatography on silica with an ethyl acetate 10 % triethylamine mixture as eluent. Method B: *N*-(7-Chloro-4-quinolyl)-*N*'-(1-trimethylamino methyl iodide ferrocene-1-ylmethyl)-propane-1,3-diamine (**22**) (0.095 g, 0.15 mmol, 1 equiv), free base glucosamine (0.105 g, 0.3 mmol, 2 equiv) and pyridine (0.06 mL, 0.75 mmol, 5 equiv) were refluxed in acetonitrile (20 mL) for 48 h. Purification of the desired product proceeded as specified above. Compound **24** was obtained under method A as an orange oil (0.012 g, 0.015 mmol, 10 %). ^{1}H NMR (400 MHz, $CDCl_3$): δ (ppm) 8.55 (d, ^3J = 5.5 Hz, 1H, 7-H), 7.98 (d, ^3J = 2.1 Hz, 1H, 8-H), 7.81 (d, ^3J = 9.1 Hz, 1H, 10-H), 7.40 (dd, ^3J = 8.8 Hz, ^4J = 2.1 Hz, 1H, 9-H), 6.50 (d, ^3J = 5.5, 1H, 6-H), 5.97 (br. s., 1H, N*H*), 5.87 (m, 1H, 1'-H), 5.31 (m, 1H, 3'-H), 5.15 (t, ^3J = 9.8 Hz, 1H, 4'-H), 4.33 (m, 1H, 6'-H), 4.24 (m, 1H, 6'-H), 4.13 (s, 8H, H_{Cp}),

4.12 (m, 1H, 2'-H), 3.52 (m, 2H, 5-H), 2.98 (br. s., 4H, 2,12-H), 2.89 (t, ^{3}J = 6.2 Hz, 2H, 3-H), 2.83 (m, 1H, 5'-H), 2.09 (s, 3H, OAc), 2.05 (s, 3H, OAc), 2.04 (s, 3H, OAc), 2.04 (s, 3H, OAc), 1.97 (s, 2H, 4-H). ^{13}C NMR (101 MHz, $CDCl_3$): δ (ppm) 175.4 (O*C*OCH$_3$), 172.5 (O*C*OCH$_3$), 169.2 (O*C*OCH$_3$), 169.1 (O*C*OCH$_3$), 152.3 (C7), 150.5 (C6), 148.2, 135.1, 128.7 (C8), 125.6 (C9), 123.5 (C10), 116.9, 98.2 (C6), 93.8 (C1'), 85.6 (C11), 80.8 (C1), 74.2 (C_{Cp}), 71.3 (C_{Cp}), 70.8 (C5'), 70.4 (C3'), 69.6 (C_{Cp}), 67.1 (C4'), 62.1 (C6'), 57.2 (C12), 56.9 (C2), 53.4 (C2'), 48.0 (C7), 42.6 (C5), 28.1 (C6), 21.4 (OCO*C*H$_3$), 21.0 (OCO*C*H$_3$), 20.8 (OCO*C*H$_3$), 20.7 (OCO*C*H$_3$). ESI-MS (HR) calculated for $C_{38}H_{46}ClFeN_4O_9^+$: 793.2303, found: 793.2309 $[M + H]^+$.

1'-(*N*,*N*-Dimethylaminomethyl)-2-ferrocenecarboxaldehyde (25).

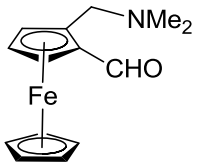

This compound was prepared as previously reported[129] with slight modifications. *n*-Butyllithium (1.6 M in hexanes, 7.0 mL, 11.0 mmol, 1.1 equiv) was added dropwise to a stirred solution of [(dimethylamino)methyl]ferrocene (2.0 mL, 10 mmol, 1 equiv) in anhydrous diethyl ether (30 mL) at room temperature. The reaction mixture was stirred under inert atmosphere at RT for 16 h. N,N-Dimethylformamide (1.15 mL, 15.0 mmol, 1.5 equiv) was added to the mixture and allowed to react for an additional 4 h. Water (10 mL) was added to terminate the reaction. The organic layer was separated and the aqueous layer was extracted with portions of diethyl ether (3 x 20 mL). The combined organic fractions were dried over anhydrous Na_2SO_4 and the solvent was removed under reduced pressure to afford an orange oil. Purification of the desired product was done by flash column chromatography on silica with diethyl ether/hexanes/triethylamine (70:20:10) as eluent system. Compound **25** was obtained

as an orange oil (1.9 g, 7.2 mmol, 72%). ^{1}H NMR (300 MHz, $CDCl_3$) δ (ppm) 10.11 (s, 1H, CHO), 4.78 (t, ^{3}J = 1.5 Hz, 1H), 4.61 (t, ^{3}J = 1.5 Hz, 1H), 4.56 (t, ^{3}J = 1.5 Hz, 1H), 4.23 (s, 5H, H_{Cp}), 3.84 (s, 1H, -CH_2NMe$_2$), 3.34 (s, 1H, -CH_2NMe$_2$), 2.22 (s, 6H, NMe_2). ESI-MS(+): 271.2 $[M]^+$, 227.2 $[M\text{-}NMe_2]^+$.

[2-(N,N-Dimethylaminomethyl)]-{4-[(2,8-bistrifluoromethyl)quinolyl]}ferrocenyl methanol (26).

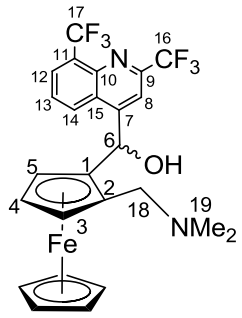

This compound was prepared as previously reported[152] with slight modifications. 4-Bromo-2,8-di(trifluoromethyl)quinoline **9** (1.72 g, 5.0 mmol, 1.5 equiv) was disolved in freshly distilled THF (20 mL) under argon atmosphere. The system was cooled to -78 °C in a dry ice bath and *n*-butyllithium (1.6 M in hexanes, 3.2 mL, 5.0 mmol, 1.5 equiv) was added dropwise. The reaction mixture was stirred at this temperature for 30 minutes. A solution of 2-(N,N-diethylaminomethyl)ferrrocenecarboxaldehyde **25** (0.86 g, 3.33 mmol, 1 equiv) in 20 mL dry THF was added to the system and stirred for an additional 3 hours at -78 °C. The mixture was allowed to warm to room temperature, and water (10 mL) was added to terminate the reaction. The organic layer was separated and the aqueous layer was extracted with portions of diethyl ether (3 x 20 mL). The combined organic fractions were dried over anhydrous Na_2SO_4 and the solvent was removed under reduced pressure to afford an orange oil. Purification of **26** was achieved by flash column chromatography on neutral alumina Brockman activity IV with the eluting system hexanes/ethyl acetate (3:2). Compound **26** was obtained as a mixture of diastereomers (0.87 g, 1.62 mmol, 49%). The two sets of

diastereomers can be separated by preparative TLC on neutral alumina with the eluting system ethyl acetate/hexanes (4:1).

Diastereomers - set 1: 99%, orange oil. ^{1}H NMR (400 MHz, $CDCl_3$): δ (ppm) 8.87 (d, ^{3}J = 8.5 Hz, 1H, 14-H), 8.17 (d, ^{3}J = 7.5 Hz, 1H, 12-H), 7.97 (s, 1H, 8-H), 7.67 (t, ^{3}J = 8.0 Hz, 1H, 13-H), 6.54 (s, 1H, 6-H), 4.22 (m, 1H, 5-H), 4.15 (d, ^{2}J = 12.9 Hz, 1H, 18-H), 4.04 (s, 5H, H_{Cp}), 3.95 (t, ^{3}J = 2.6 Hz, 1H, 4-H), 3.24 (m, 1H, 3-H), 3.00 (d, ^{2}J = 12.63 Hz, 1H, 18-H), 2.32 (s, 6H, 19-H). ^{13}C NMR (101 MHz, $CDCl_3$): δ (ppm) 154.3 (C10), 151.1 (C9), 144.6 (C7), 131.4 (C12), 129.0 (C14), 128.6 (C13), 126.2 (C11), 125.4 (C15), 123.0 (C17), 120.3 (C16), 117.6 (C8), 91.2 (C1), 84.1 (C2), 72.4 (C5), 71.5 (C3), 69.6 (Cp), 69.1 (C4), 66.1 (C6), 58.5 (C18), 44.3 (C19). Anal. Calc. for $C_{25}H_{22}F_6FeN_2O$: C, 55.99, H, 4.13, N, 5.22; found: C, 55.35, H, 4.30, N, 4.96. ESI-MS (HR) calculated for $C_{25}H_{23}F_6FeN_2O^{+}$: 537.1064, found: 537.1069 $[M + H]^{+}$.

Diastereomers - set 2: 1%, orange oil. ^{1}H NMR (400 MHz, $CDCl_3$): δ (ppm) 8.40 (d, ^{3}J = 8.5 Hz, 1H, 14-H), 8.36 (s, 1H, 8-H), 8.18 (d, ^{3}J = 7.2 Hz, 1H, 12-H), 7.72 (t, ^{3}J = 7.9 Hz, 1H, 13-H), 6.25 (s, 1H, 6-H), 4.14 (m, 1H, 5-H), 4.04 (m, 1H, 4-H), 3.92 (d, ^{2}J = 13.3 Hz, 1H, 18-H), 3.81 (s, 5H, H_{Cp}), 3.71 (m, 1H, 3-H), 2.93 (d, ^{2}J = 13.0 Hz, 1H, 18-H), 2.41 (s, 6H, 19-H). ^{13}C NMR (101 MHz, $CDCl_3$): δ (ppm) 155.6 (C10), 150.3 (C9), 148.2 (C7), 137.8 (C12), 132.0 (C14), 133.1 (C13), 128.6 (C11), 124.2 (C15), 122.4 (C17), 120.9 (C16), 117.2 (C8), 92.0 (C1), 87.0 (C2), 73.6 (C5), 71.1 (C3), 70.5 (C4), 69.4 (Cp), 67.0 (C6), 53.5 (C18), 47.3 (C19). ESI-MS (HR) calculated for $C_{25}H_{23}F_6FeN_2O^{+}$: 537.1064, found: 537.1074 $[M + H]^{+}$.

[2-(N,N-Dimethylaminomethyl)]-{3-[(2,8-bistrifluoromethyl-4-bromo)quinolyl]} ferrocenyl methanol (27).

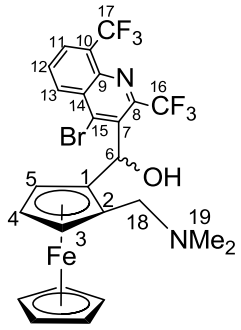

Compound **27** was obtained as a side product from the synthesis of compound **26**. Purification of **27** was achieved by flash column chromatography on silica with an eluting system of increasing polarity from hexanes/ethyl acetate (4:1) to ethyl acetate (100%). Compound **27** was obtained as a mixture of diastereomers (0.102 g, 0.16 mmol, 5%). The two sets of diastereomers produced can be separated by the column chromatography system described above.

Diastereomers - set 1: 84%, orange solid. ^{1}H NMR (400 MHz, $CDCl_3$): δ (ppm) 8.80 (br. s., 1H, O*H*), 8.57 (d, ^{3}J = 7.0 Hz, 1H, H-13), 8.19 (d, ^{3}J = 7.3 Hz, 1H, 11-H), 7.77 (t, ^{3}J = 8.0 Hz, 1H, 12-H), 7.07 (br. s., 1H, 6-H), 4.25 (d, ^{2}J = 11.6 Hz, 1H, 18-H), 4.16 (m, 1H- 5-H), 4.15 (s, 5H, H_{Cp}), 3.94 (t, ^{3}J = 2.4 Hz, 1H, 4-H), 3.48 (m, 1H, 3-H), 2.95 (d, ^{2}J = 12.5 Hz, 1H, 18-H), 2.33 (s, 6H, 19-H). ^{13}C NMR (75 MHz, $CDCl_3$): δ (ppm) 155.4 (C9), 152.8 (C8), 142.0 (C15), 139.0 (C7), 136.3 (C10), 131.4 (C11), 130.7 (C17), 129.5 (C13), 128.4 (C12), 125.1 (C14), 121.5 (C16), 90.8 (C1), 82.8 (C2), 70.4 (C5), 69.9 (Cp), 69.6 (C3), 69.1 (C4), 65.4 (C6), 58.9 (C18), 44.0 (C19). Anal. Calc. for $C_{25}H_{21}BrF_6FeN_2O$: C, 48.81, H, 3.44, N, 4.55; found: C, 49.01, H, 3.48, N, 4.50. ESI-MS (HR) calculated for $C_{25}H_{22}BrF_6FeN_2O^{+}$: 615.0171, found: 615.0179 $[M + H]^{+}$.

Diastereomers - set 2: 16%, orange solid. ^{1}H NMR (400 MHz, $CDCl_3$): δ (ppm) 8.49 (d, ^{3}J = 8.5 Hz, 1H, 13-H), 8.16 (d, ^{3}J = 7.3 Hz, 1H, 11-H), 7.75 (t, ^{3}J = 7.9 Hz, 1H, 12-H), 6.77 (s, 1H, 6-H), 4.65 (s, 1H, 5-H), 4.18 (s, 5H, H_{Cp}), 4.11 (s, 2H, 4,3-H), 3.31 (d, ^{2}J = 12.8 Hz, 1H, 18-H), 2.60 (d, ^{2}J = 12.8 Hz, 1H, 18-H), 1.40 (s, 6H, 19-H). ^{13}C NMR (101 MHz, $CDCl_3$): δ

(ppm) 155.4 (C9), 152.3 (C8), 141.8 (C15), 137.8 (C7), 134.4 (C10), 131.0 (C11), 130.0 (C17), 129.3 (C13), 128.2 (C12), 124.6 (C14), 120.0 (C16), 90.5 (C1), 81.9 (C2), 72.1 (C3), 70.1 (C5), 69.8 (Cp), 69.2 (C4), 65.1 (C6), 57.5 (C18), 44.1 (C19). ESI-MS (HR) calculated for $C_{25}H_{22}BrF_6FeN_2O^+$: 615.0171, found: 615. 0172 $[M + H]^+$.

[2-(N,N,N-Trimethylaminomethyl iodide)]-{4-[(2,8-bistrifluoromethyl) quinolyl]} ferrocenyl methanol (28).

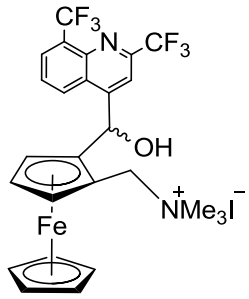

Iodomethane (0.125 mL, 2.0 mmol, 2 equiv) was added slowly to a solution of **26** (0.530 g, 1.0 mmol, 1 equiv) in methanol (20 mL) under inert atmosphere. The reaction mixture was stirred for 24 h at room temperature. The solvent was removed under pressure. Compound **28** (0.54 g, 0.8 mmol, 80%) was recrystallized from methanol to yield orange crystals. ^{1}H NMR (300 MHz, CD_3OD): δ (ppm) 9.17 (d, ^3J = 8.9 Hz, 1H), 8.35 (d, ^3J = 7.3 Hz, 1H), 8.28 (s, 1H), 7.95 (t, ^3J = 7.9 Hz, 1H), 6.61 (s, 1H, C*H*OH), 5.03 (d, ^2J = 13.7 Hz, 1H, -C*H*$_2$NMe$_3^+$), 4.78 (m, 1H, H_{Cp}), 4.74 (d, ^2J = 13.7 Hz, 1H, -C*H*$_2$NMe$_3^+$), 4.50 (t, ^3J = 2.7 Hz, 1H, H_{Cp}), 4.04 (m, 1H, H_{Cp}), 3.90 (s, 5H, H_{Cp}), 3.23 (s, 9H, -NMe_3). ESI-MS(+): 551.2 $[M\text{-}I]^+$, 492.1 $[M\text{-}NMe_3^+]^+$. Anal. Calc. for $C_{26}H_{25}F_6FeIN_2O$: C, 46.04, H, 3.72, N, 4.13; found: C, 45.66, H, 4.00, N, 4.16.

***N*-{[2-*N*-(1,3,4,6-Tetra-*O*-acetyl-α-D-glucopyranose)]-{4-[(2,8-bistrifluoromethyl) quinolyl]} ferrocene-1-ylmethyl-1'-methanol (29).**

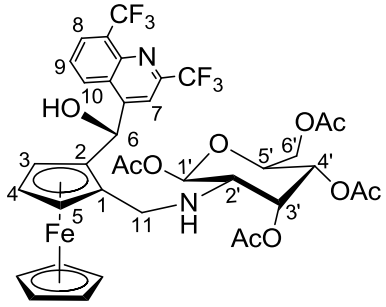

Method A: [2-(N,N,N-Trimethylaminomethyl iodide)]-{4-[(2,8-bistrifluoromethyl) quinolyl]} ferrocenyl methanol (**28**) (0.102 g, 0.15 mmol, 1 equiv) and free base glucosamine (0.105 g, 0.3 mmol, 2 equiv) were combined with 15 mL of acetonitrile in a 20 mL microwave vial. The reaction was carried out in a microwave reactor for 6 h at 110 °C. The solvent was removed under reduced pressure. Purification of the desired product was done by flash column chromatography on silica with a diethyl ether/ethyl acetate (8:1) mixture as eluent. Method B: [2-(N,N,N-Trimethylaminomethyl iodide)]-{4-[(2,8-bistrifluoromethyl) quinolyl]} ferrocenyl methanol (**28**) (0.102 g, 0.15 mmol, 1 equiv) and free base glucosamine (0.105 g, 0.3 mmol, 2 equiv) were refluxed in acetonitrile (20 mL) for 48 h. Purification of the desired product proceeded as specified above. Compound **29** was obtained under method A as an orange oil (0.008 g, 0.01 mmol, 6 %). ^{1}H NMR (400 MHz, $CDCl_3$): δ (ppm) 8.82 (d, ^{3}J = 8.5 Hz, 1H, 10-H), 8.20 (d, ^{3}J = 7.5 Hz, 1H, 8-H), 7.89 (s, 1H, 7-H), 7.72 (t, ^{3}J = 7.9 Hz, 1H, 9-H), 7.02 (s, 1H, C*H*OH), 6.38 (s, 1H, CHO*H*), 5.84 (d, ^{3}J = 8.8 Hz, 1H, 1'-H), 5.42 (dd, ^{3}J = 10.6, 9.2 Hz, 1H, H-3'), 5.14 (t, ^{3}J = 9.6 Hz, 1H, 4'-H), 4.36 (m, 2H, H-5', H-6'), 4.20 (m, 1H, H_{Cp}), 4.15 (m, 1H, 6'-H), 4.08 (s, 5H), 4.05 (d, ^{3}J = 11.6 Hz, 1H, 11-H), 4.04 (m, 1H, H_{Cp}), 3.88 (m, 1H, 2'-H), 3.65 (d, ^{3}J = 11.6 Hz, 1H, 11-H), 3.48 (m, 1H, H_{Cp}), 2.20 (s, 3H, OAc), 2.14 (s, 3H, OAc), 2.11 (s, 3H, OAc), 2.10 (s, 3H, OAc). ^{13}C NMR (101 MHz, CD_3CN): δ (ppm) 172.2 (O*C*OCH_3), 171.4 (O*C*OCH_3), 165.0 (O*C*OCH_3), 163.9 (O*C*OCH_3), 156.2, 153.6, 145.0, 131.7 (C8), 130.7 (C10), 128.6 (C9), 126.1, 125.2, 124.6 (CF_3), 123.8 (CF_3), 115.9

(C7), 97.7 (C1'), 90.3 (C2), 89.1 (C1), 78.5 (C5), 75.6 (C3), 72.8 (C5'), 71.9 (Cp), 71.4 (C3'), 69.8 (C4), 66.7 (C4'), 64.1 (C6), 61.8 (C6'), 59.8 (C11), 55.9 (C2'), 23.4 (OCO*C*H_3), 23.0 (OCO*C*H_3), 22.2 (OCO*C*H_3), 21.7 (OCO*C*H_3). ESI-MS(+): 839.2 $[M+H]^+$, 861.2 $[M+Na]^+$.

5.3 Results and discussion

5.3.1 Heteroannular chloroquine ferrocenyl carbohydrate conjugates

The overall approach followed for the synthesis of the 1,1'-chloroquine ferrocenyl carbohydrate derivatives is shown in Scheme 5.1. The ferrocene skeleton requires two distinct sites of derivatization where the chloroquine and the carbohydrate can be conjugated.

This synthetic pathway started with 1,1'-bis(tri-*n*-butylstannyl)ferrocene (**13**), synthesized following the procedure reported by Wright[257] with slight modifications. Ferrocene was doubly deprotonated at the 1- and 1'-positions by the action of two molar equivalents of *n*-butyllithium, previously activated by a solution of N,N,N',N'-tetramethylethylenediamine (TMEDA) in hexanes. TMEDA fulfills two roles in this synthesis. First, it breaks the clusters of *n*BuLi activating it for a more efficient deprotonation, and second it coordinates the Li atoms at the 1,1' positions, improving the lifetime of this deprotonated intermediate.[258] When this reaction is conducted in the presence of *n*BuLi alone, the 1,2 product is observed almost exclusively. In order for TMEDA to have this effect, it must be distilled prior its use and stored under inert atmosphere in the dark.

A transmetallation reaction occurred when a small excess of two molar equivalents of tri-*n*-butylstannyl chloride was added to the 1,1'-dilithioferrocene intermediate. The purification of the product 1,1'-bis(tri-*n*-butylstannyl)ferrocene(**13**) from the crude mixture also containing unsubstituted ferrocene and 1-(tri-*n*-butylstannyl)ferrocene, was done by column chromatography. This laborious separation was done on an alumina column activity I (Brockman scale) for crude quantities ≤ 1 g. Since the the mono and disubstituted products have similar Rf values, often several consecutive columns were required in order to obtain this product in acceptable yield and purity, confirmed by ^{1}H NMR spectroscopy.

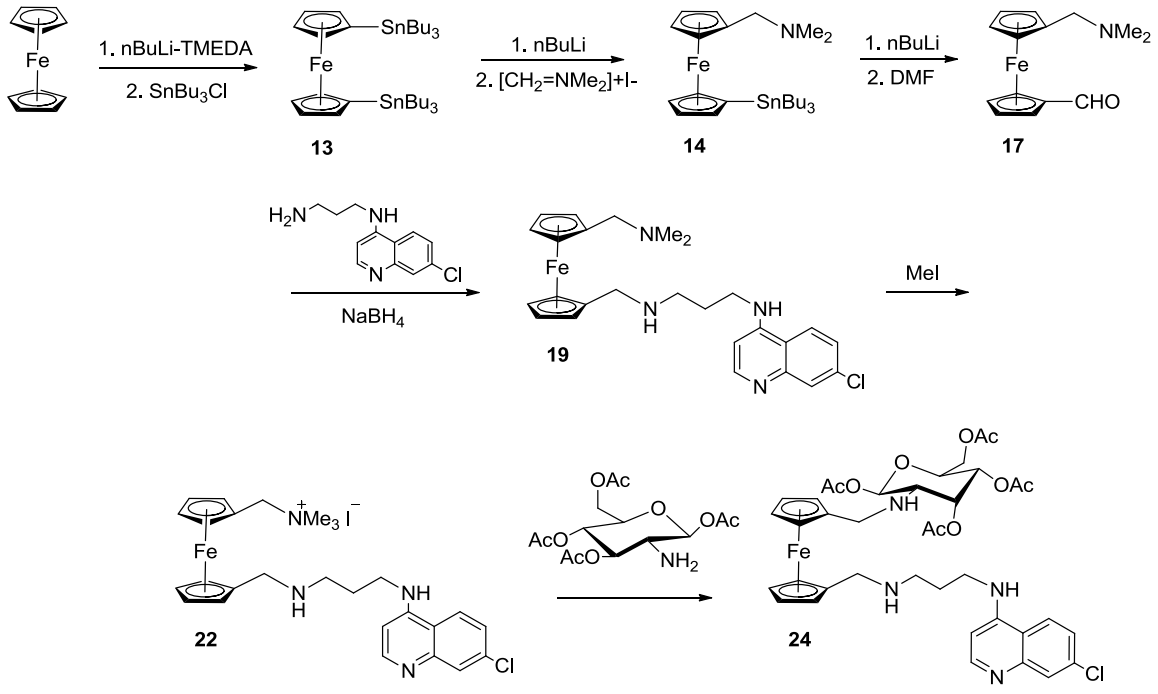

Scheme 5.1. General synthetic route for the synthesis of 1,1'-disubstituted chloroquine ferrocenyl glucosamine **24**.

Other separation systems were tried, such as flash column chromatography on silica gel, and distillation. The compound decomposed on silica gel during the column, and distillation under vacuum was only successful to separate the ferrocene from the mixture leaving the mono and disubstituted products behind. Optimization of this system gave an average yield of 60% with purity of 90%; however, increased yields were observed when the reaction was carried out with freshly sublimed ferrocene (data not reported). The structure and purity of **13** has been verified by ^{1}H NMR spectroscopy and LR-MS. The starting material **13** is relatively stable at room temperature but longer times of exposure to light and heat decomposed it to ferrocene and the monosubstituted product.

The next step in the synthetic route was the stepwise functionalization of the Cp rings of ferrocene. This was achieved by selective transmetallation. Wright demonstrated that 1,1'-bis(tri-n-butylstannyl)ferrocene (**13**) can undergo regioselective and sequential substitution of the tri-*n*-butylstannyl groups.[257] Each ferrocene-Sn bond was cleaved independently with *n*-BuLi and then treated with two different electrophiles to introduce the groups that allowed the coupling of the chloroquine and carbohydrate.

Treatment of **13** with one equivalent of *n*BuLi gave the 1'-tri-*n*-butylstannyl-1-lithioferrocene intermediate which was then reacted with Eschenmoser's salt or (*N,N'*-dimethyl)methyleneammonium iodide to introduce the *N,N*-(dimethylamino)methyl substituent present in **14** by a reaction described previously in the literature.[142] The number of *n*BuLi equivalents used determines the outcome of this reaction. A 1.1 equivalent portion was found to be the ideal amount. If *n*BuLi is used in slightly higher excess (1.5 equivalents, for example), the disubstituted product is largely observed and the yield of **14** decreases to

less than 10%. Titrations of *n*BuLi were necessary to verify the concentration of this reagent prior to use in this reaction.

Very similar reactions were carried with the electrophiles methyl chloroformate (ClCOOMe) and N,N-dimethylformamide (DMF) to give products **15** and **16**, respectively. Products **14**, **15** and **16** were isolated and purified by column chromatography; their structures and purity were verified by ^{1}H NMR spectroscopy.

The next step of the synthesis involved the removal of the second stannyl group, following a procedure similar to that described above, without the restriction of the number of equivalents. Treatment of **14** with one equivalent of N,N-dimethylformamide or methyl chloroformate and treatment of **15** and **16,** separately, with (*N,N'*-dimethyl)methyleneammonium iodide was expected to yield the respective disubstituted product, with both the *N,N*-(dimethylamino)methyl substituent and either the aldehyde or the methyl-protected ester group. This reaction was only effective when the starting material was the intermediate **14**; the carbonyl group of starting materials **15** and **16** seemed to be incompatible with the lithiation step to substitute the second stannyl group.

Based on considerations of yield and purification process, compound **17** was chosen to be the building block which contains both the aldehyde and the dimethyl amino groups that will facilitate the coupling of the quinoline fragment and the carbohydrate. Compound **17** was characterized by ^{1}H NMR spectroscopy, LR-MS and elemental analysis.

The coupling of the chloroquine derivative took place via reductive amination between the aldehyde group present in **17** and the corresponding 4-aminoquinolines **3a**, **3b** and **3e** to afford compounds **18**, **19** and **20**, respectively. These compounds were prepared based on a general methodology reported previously.[142] The process of formation of these derivatives is

similar to that of the monosubstituted ferrocenyl compounds **4a-e**, described in Chapter 2. The desired products were purified by column chromatography and characterized by ^{1}H NMR, ^{13}C NMR, 2D NMR spectroscopy techniques (COSY, HMBC, HSQC) and HR-MS.

The coupling of the carbohydrate molecule was planned to take place by the nucleophilic attack of the carbohydrate at the dimethylamino methyl group. The dimethylamino methyl group is not a good leaving group, thus to help this reaction, this group was quaternized to the trimethylammonium group. This quaternization was inspired in the methylation described in a previously published method,[180] and discussed in detail in Chapter 2 for the synthesis of the starting material 1,1'-bis(*N,N'*-trimethylaminomethyl)ferrocene iodide (**2**).

The formation of the trimethylammonium iodide salts of compounds **18-20**, compounds **21-23**, respectively, was monitored by ^{1}H NMR spectroscopy. The diagnostic signal was the proton signal corresponding to the methyl groups that shifts from δ = 2.17 ppm (6H) to lower field δ = 3.20 (9H). Unlike the starting material **2** that can be isolated by precipitation with the addition of diethyl ether, these products **21-23** could not be precipitated upon addition of diethyl ether or other non-polar solvents, which complicated the purification of these compounds. Column chromatography was not viable since they are salts, and recrystallization attempts failed.

It is estimated that the methylation reaction goes to completion given the high yields obtained. Since these compounds could not be purified by precipitation or recrystallization, the number of equivalents of iodomethane was kept to only a small excess, and when reducing to dryness multiple washes with methanol and toluene were practised to take off the residual iodomethane in the product. The next step was carried out without further

purification of the ferrocenyl salt. Compounds **21-23** were verified by ^{1}H NMR spectroscopy and mass spectrometry.

The formation of the chloroquine ferrocenyl carbohydrate conjugate **24** occurred by a condensation reaction between the *N,N'*-trimethylaminomethyl iodide ferrocene salt **22** and the monosaccharide glucosamine. The nucleophilic displacement of the trimethylammonium group by the amino group of glucosamine in the presence of a base occurs in a similar way to that of the formation of the bridged ferrocenyl 4-aminoquinoline derivatives **5a-e**, described in Chapter 2. The carbohydrate used for this synthesis was glucosamine, a glucose molecule where the hydroxyl group in the 2-position has been replaced by an amino group. To limit the reactivity of this molecule, all other hydroxyls were protected as acetyl groups. This product was purified by column chromatography and characterized by ^{1}H NMR and ^{13}C NMR as well as 2D NMR spectroscopic techniques (COSY, HMBC, HSQC) and HR-MS.

Even though the displacement of the trimethylamino group should afford the desired product in high yields,[195,196] that was not observed for the application of this reaction in the ferrocenyl substrates, such as **24** and the bridged ferrocenyl chloroquine derivatives **5a-e**. The yield of **24** is 10%, whereas the yields of compounds **5a-d** were slightly higher, about 20%. This low yield was explained by the limited availability of the amino group in **24**.

The amino group of glucosamine, which is acting as a nucleophile, is located in the equatorial position of the carbohydrate ring, a position prone to less reactivity. Stronger bases were tested in order to increase the reactivity of the nucleophile but NaH or NaOH had a detrimental impact; mass spectrometric evidence suggests they are incompatible with the acetyl protecting groups of glucosamine which are labile under basic conditions. Only pyridine was compatible with the substrate used. The best efforts for its optimization could

not improve the yields significantly, reporting a large loss of starting material in this last step and decreasing significantly the yield of the synthesis to 1 or 2%.

Thus, the low yields observed for this attack, the low reactivity of the nucleophile group, and possibly impurities present in the starting material, the iodide salt **22**, could contribute to the low yield observed for the chloroquine ferrocenyl carbohydrate conjugate **24**. This low yield complicated the purification of significant amounts of the final product and the number of biological tests possible with it. This low reactivity also limited attempts to synthesize more conjugates via this methodology and reqired improvement of the synthetic path.

5.3.2 Homoannular mefloquine ferrocenyl carbohydrate conjugates

The overall approach followed for the synthesis of the 1,2-mefloquine ferrocenyl carbohydrate derivative is shown in Scheme 5.2. Similar to what was described for the chloroquine ferrocenyl carbohydrate conjugates, this synthetic pathway started with the preparation of the ferrocenyl skeleton that provides two distinct sites of derivatization to which the mefloquine and the carbohydrate can be conjugated.

This is accomplished by starting with the commercially available [(dimethylamino)methyl] ferrocene. The strong directing effect of the dimethylamino group was used as an advantage to synthesize the 1,2-disubstituted ferrocenyl derivative. Direct and simple lithiation of [(dimethylamino)methyl] ferrocene affords **25** without the aid of any catalysts. In this case the dimethylamino group coordinates the lithium atom that holds the position 2 after deprotonation. This allows the formation of **25** without the need for stepwise transmetallation. The condensation of the 1-[(dimethylamino)methyl]-2-lithium ferrocene

intermediate with N,N-dimethylformamide affords the 1,2-disubstituted ferrocenyl 2-[(N,N-dimethylamino)methyl]ferrocenecarboxaldehyde **25**, building block for the formation of the mefloquine ferrocene carbohydrate conjugate.

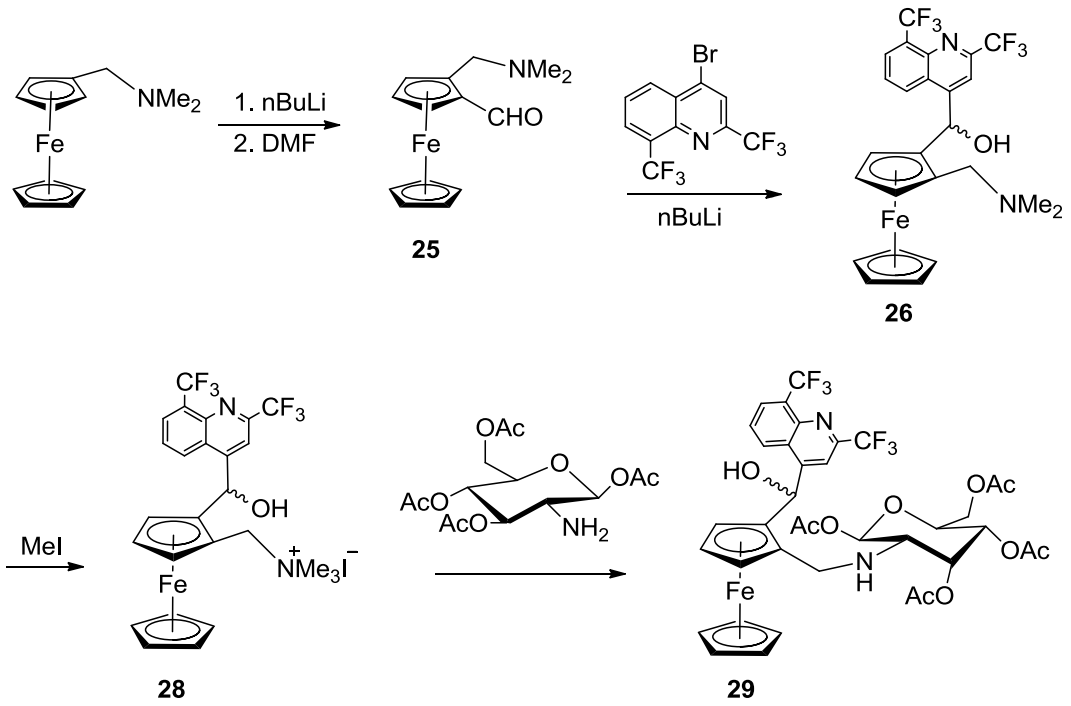

Scheme 5.2. General synthetic route for the synthesis of 1,2-disubstituted mefloquine ferrocenyl glucosamine **29**.

The synthesis of **25** was based on a previously published procedure[129] following slight modifications. [(Dimethylamino)methyl] ferrocene is treated with slightly more than one equivalent of *n*Buli to give the 1-[(dimethylamino)methyl]-2-lithium ferrocene intermediate. The latter is subsequently condensed with N,N-dimethylformamide to afford the crude mixture from which **25** is purified by column chromatography.

It was observed that the addition of greater quantities of *n*BuLi affects the reactivity of the starting material. When *n*BuLi quantities greater than 1.1 equivalents were used, the 1,1'-disubstituted product **17** was detected along with the 1,1',2-trisubstituted product during the purification process. This reduces the yield of the desired product **25** to 25%. The structure and purity of **25** have been verified by ^{1}H NMR spectroscopy and LR-MS.

The coupling of the mefloquine derivative to the ferrocenyl building block in compound **26** was done by following a published procedure.[152] This synthesis occurs by the reaction of the aldehyde group present in **25** and the 4-lithium-2,8-di(trifluoromethyl)quinoline, formed by the reaction of *n*BuLi and 4-bromo-2,8-di(trifluoromethyl)quinoline **9**, in a reaction similar to that described for the synthesis of the bismefloquine ferrocenyl compound **11**, in Chapter 4.

The mefloquine ferrocenyl derivative **26** was isolated as a mixture of diastereomers. In addition to the stereogenic center C6, these molecules display the planar chirality of the substituted ferrocene which gives rise to two sets of diastereomers. Both groups of diastereomers, set 1 (Rf = 0.40) and set 2 (Rf = 0.25), were isolated from preparative TLC on neutral alumina and diastereomers of the first set were much more abundant than the second set of diastereomers. The separation of both sets of diastereomers is based on the different orientation (*R, S*) of the stereogenic center C6, since the planar enantiomers of ferrocene are not likely to be separated by common chromatography techniques. Both sets of diastereomers were characterized by ^{1}H NMR and ^{13}C NMR as well as 2D NMR spectroscopy techniques (COSY, HMBC, HSQC), HR-MS and elemental analysis.

Several ferrocenyl side products were obtained in this reaction. An interesting observation was the formation of a particular set of byproducts in small yield. This product is the

mefloquine ferrocene **27**, the result of the deprotonation and metalation at C7 (Scheme 5.3). The unusual formation of this byproduct can be explained by the acidity of the H connected to C7, located in between the carbons that bear the bromide and the electron withdrawing trifluoromethyl group. In this side reaction, it is hypothesized that the C7 site is deprotonated before there is a metalation that displaces the bromide ion.

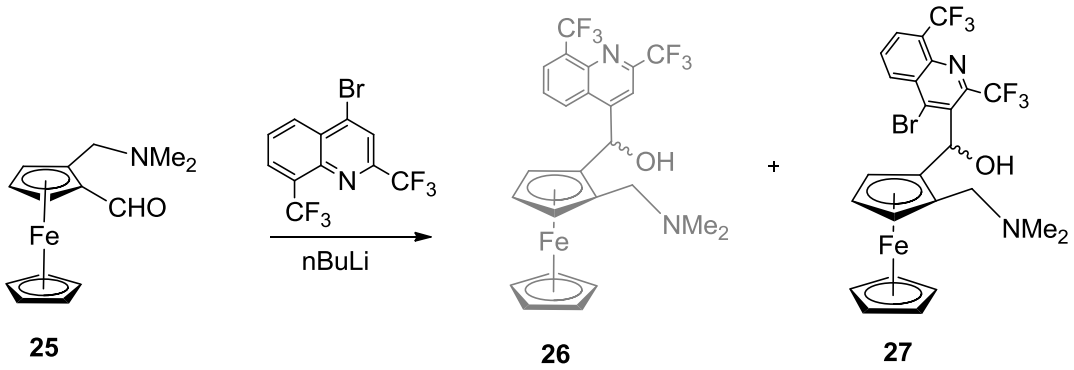

25 26 27

Scheme 5.3. Formation of the sideproduct [2-(N,N-Dimethylaminomethyl)]-{3-[(2,8-bistrifluoromethyl-4-bromo)quinolyl]} ferrocenyl methanol (**27**) during the mefloquine coupling step.

Similar to what was observed for product **26**, the mefloquine ferrocenyl derivative **27** was isolated as mixtures of diastereomers. Both groups of diastereomers, set 1 (Rf = 0.74) and set 2 (Rf = 0.56), were isolated from column chromatography on silica gel and diastereomers A were more abundant that diastereomers B. These diastereomers were not mentioned in the synthesis of the original mefloquine ferrocenyl derivative.[152] Both sets of diastereomers were characterized by ^{1}H NMR, ^{13}C NMR and 2D NMR spectroscopy techniques (COSY, HMBC, HSQC) as well as HR-MS and elemental analysis.

In an approach similar to that used for the synthesis of the chloroquine ferrocenyl carbohydrate derivative, the dimethylamino methyl group on **26** was further methylated to

form the trimethylammonium iodide salt **28**. This reaction was only carried out on the mefloquine ferrocenyl derivative **26**, diastereomer A, since it is the most abundant product afforded from the previous synthetic step.

Compound **28** can be successfully recrystallized from methanol, affording quality crystals described in the following section, and providing a convenient purification method for this compound; this could not be achieved for the chloroquine analogs as described in the previous section. The structure and purity of this compound was verified by ^{1}H NMR spectroscopy, mass spectrometry and elemental analysis.

The coupling of the carbohydrate molecule occurred by the nucleophilic attack of the amino group of glucosamine to the trimethylammonium group of the trimethylaminomethyl iodide ferrocene salt **28** to afford the mefloquine ferrocenyl carbohydrate conjugate **29**. This product was purified by column chromatography and characterized by ^{1}H NMR spectroscopy, ^{13}C NMR, 2D NMR techniques (COSY, HMBC, HSQC) and mass spectrometry.

As discussed for the chloroquine analog **24**, the result of this reaction was affected by the poor performance of this last step on the synthesis, the poor nucleophilic character of the amino group of glucosamine and its inability to work in the presence of stronger bases. The total yield of this synthesis was 2%.

An additional factor was observed during the purification process of **29**. This compound was unstable at room temperature, decomposing on silica gel and possibly in solution. This phenomenon was observed by closely monitoring with ^{1}H NMR spectroscopy and TLC. It is hypothesized that the presence of a large quinoline molecule located at the carbon next to the

glucosamine bound through an equatorial position might create too much steric hinderance causing low yields.

This process complicated the inmediate purification and characterization of the sample due to its short shelf time, obviating any biological test.

5.3.3 X-Ray crystal structure analysis

Single crystals suitable for X-ray diffraction were obtained for compounds **27** and **28**. Characteristic bond lengths and angles for these structures are summarized in Tables 5.1 and Table 5.2.

The crystal structure of compound **27** was the ultimate confirmation of the structure proposed for this byproduct from the reaction of 1'-(*N*,*N*-dimethylaminomethyl)-2-ferrocenecarboxaldehyde (**25**) and 4-bromo-2,8-di(trifluoromethyl)quinoline (**9**) with *n*BuLi. This crystal structure was obtained as two independent units labeled as *a* and *b*; however, both units are identical, they are present in the same asymmetric unit. This crystal structure was obtained from the most abundant set of diastereomers, those designated as A in the experimental section.

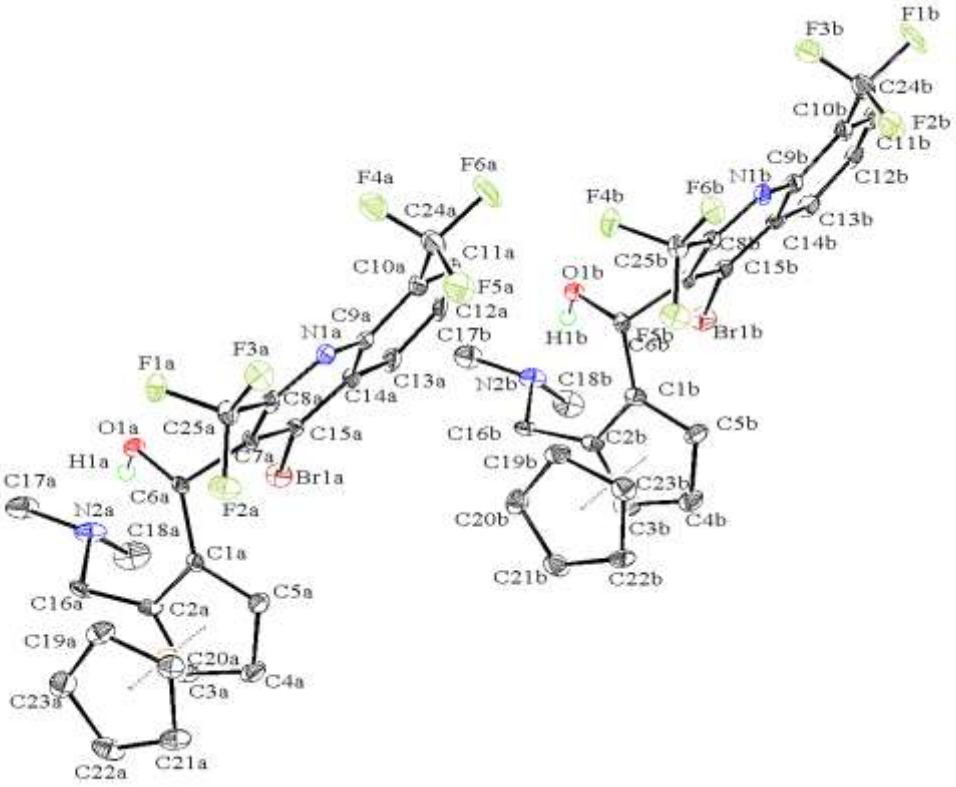

Figure 5.3. ORTEP diagram of the two independent molecules in the unit cell of compound **27** with 50% thermal ellipsoid level.

Table 5.1. Selected bond distances (Å) and angles (°) in **27**.

	27a	**27b**
O1-C6	1.416(6)	1.420(7)
C1-C6	1.518(8)	1.522(8)
C6-C7	1.537(7)	1.540(7)
C15-Br1	1.889(6)	1.889(6)
O1-H1	0.92(13)	0.8400
H1-O1-C6	113(8)	109.5
C1-C6-O1	115.0(4)	113.9(4)
O1-C6-C7	107.4(4)	107.6(4)
Br1-C15-C7	120.4(4)	120.3(4)
C6-C7-C15	122.8(5)	123.8(5)
C2-C16-N2	111.0(5)	110.8(5)
C1-C6-C7-C15	63.8(7)	65.0(7)
C1-C2-C16-N2	64.0(7)	64.3(8)

This crystal structure shows the ferrocene scaffold with eclipsed cyclopentadienyl rings substituted by the mefloquine derivative connected via C7, the 3-position of the quinoline ring, and by the dimethylaminomethyl group. The bond lengths and bond angles (Table 5.1) observed in both independent unit of **27** are as expected, based on other ferrocenyl quinoline derivatives presented in this thesis. Further details and other parameters can be found in Appendix A.

The quinoline ring of **27** is twisted out of the plane of the cyclopentadienyl ring, with C6 as the center, sitting perpendicular to the plane of the cyclopentadienyl ring and parallel to the plane that contains the ferrocene. This orientation brings the hydrogen of the hydroxyl group (H1) in close proximity to the nitrogen of the dimethylamino group (N2). Hydrogen bonding in the solid state is observed for H1-N2. The distance measured between H1-N2 is 1.881 Å, consistent with a hydrogen bonding interaction.[199] A weaker hydrogen bonding interaction is also observed for this hydrogen and the bromide atom Br1. The distance calculated for the interaction is 2.990 Å.

A single crystal structure was obtained for compound **28**, shown in Figure 5.4. The characteristic bond lengths and angles for this structure are summarized in Table 5.2.

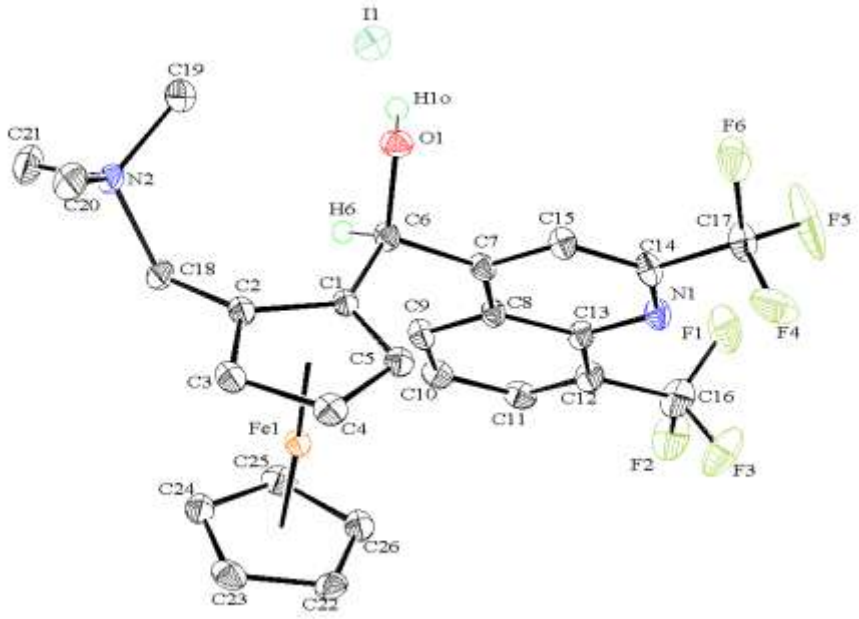

Figure 5.4. ORTEP diagram of compound **28** with 50% thermal ellipsoid level.

Table 5.2. Selected bond distances (Å) and angles (°) in **28**.

	28
O1-C6	1.438(4)
C1-C6	1.512(5)
O1-H1	0.81(5)
H1-O1-C6	104(3)
C1-C6-O1	106.1(2)
O1-C6-C7	108.4(3)
C6-C7-C15	118.2(3)
C2-C18-N2	115.6(3)
C1-C6-C7-C15	-82.4(4)
C1-C2-C18-N2	-101.9(4)
C5-C1-C2-Fe1	-59.6(2)

Similar to what was observed in the crystal structure of compound **27**, the ferrocene scaffold presents eclipsed cyclopentadienyl rings and the quinoline ring is twisted out of the plane of the substituted ring; however, in **28**, the quinoline ring is not sitting close to the Cp

plane but pointing away from it. It is therefore, no surprise to observe no hydrogen bonding interaction between the hydrogen of the hydroxyl group (H1) and the nitrogen of the dimethylamino group N2. Only a weak hydrogen bonding interaction is observed for this hydrogen and the iodide ion located nearby.

5.3.4 *In vitro* antitumor activity and cytotoxicity assay

The toxicity and the antitumor activity of the chloroquine and mefloquine ferrocenyl chloroquine compounds were assessed *in vitro*. Three human cell lines were employed: normal breast epithelial cells MCF-10A (CRL-10317), breast cancer cells MDA-MB-435S (HTB-129) and human colon carcinoma cells Caco-2 (HTB-37).

Since the synthesis and purification of the chloroquine and mefloquine ferrocenyl carbohydrate final product proved to be a challenge, these studies were conducted with the synthetic intermediates. The study of the biological activity of the intermediates of a molecule is a common activity in medicinal chemistry, especially in natural products where the syntheses of the final targets are lengthy and low yielding. It is expected that the activity observed for the fragments reflect the activity of the final product.

This study was performed using the MTT methodology.[212] Cisplatin (cis-diammine-dichloroplatinum(II)) was used as a positive control for cell death. Chloroquine diphosphate (CQdP) and bis{6-*N*-(methyl 2,3,4-tri-*O*-acetyl-6-amino-6-deoxy-α-D-glucopyranoside)}-1,1-ferrrocene carboxamide,[159] a bisglucosamine ferrocenyl derivative represented as Fc(glucosamine)$_2$, were used as internal controls. The results are presented in Table 5.3.

All compounds tested displayed similar good activity against the cancerous cell lines Caco-2 and MDA-MB-435S; however, low IC_{50} values were also observed against the normal breast epithelial cell line MCF-10A, indicating the activity seen for these compounds is likely unspecific toxicity.

The ferrocenyl carbohydrate compound bis{6-*N*-(methyl 2,3,4-tri-*O*-acetyl-6-amino-6-deoxy-α-D-glucopyranoside)}-1,1-ferrrocene carboxamide,[159] $Fc(glucosamine)_2$ was tested to verify that the toxicity was mainly due to the quinoline fragment. As observed in Table 5.3, the values obtained for this building block formed by the carbohydrate-ferrocene combination reflect neither antitumor activity nor relevant toxicity.

Table 5.3. Toxicity of the compounds (expressed in IC_{50} values in μM) against the human normal breast epithelial cell line MCF-10A, the human breast cancer cell line MDA-MB-435S and the human colon carcinoma Caco-2 (HTB-37).

	Antiproliferative activity		**Cytotoxicity**
Compound	**Caco-2**	**MDA-MB-435**	**MCF-10A**
18	15.0 ± 1.2	ND	9.5 ± 0.6
19	10.7 ± 0.5	19.0 ± 0.2	12.2 ± 0.8
20	7.6 ± 0.4	ND	ND
26A	11.4 ± 0.3	16.0 ± 1.2	8.83 ± 0.5
26B	18.1 ± 0.5	ND	23.9 ± 2.7
27A	17.5 ± 1.3	9.7 ± 0.2	10.9 ± 2.0
27B	38.3 ± 1.8	8.5 ± 1.1	20.8 ± 2.3
28A	40.0 ± 0.9	ND	8.13 ± 0.7
$Fc(glucosamine)_2$	≥600	≥300	≥350
Cisplatin	19.8 ± 1.3	117.6 ± 7.4	15.2 ± 1.1
CQdP	111.9 ± 6.9	39.1 ± 2.3	69.6 ± 4.8

ND: Not determined.

These chloroquine and mefloquine ferrocenyl derivatives are, in general, more toxic that cisplatin or the traditional drug chloroquine diphosphate (CQDP). Nevertheless, this toxicity is not a strange observation in metalloantimalarials based on ferrocene, as discussed in Chapter 3. Furthermore, this toxicity is observed in the micromolar range where these compounds are normally active as antiplasmodials in the nanomolar range, leaving a window for their use as therapeutics agents.

For the chloroquine derivatives **18**-**20** no correlation was found with the antiproliferative activity and cytotoxicity and the length of the side chain or its degree of branching. It was interesting to compare the activity of the different diastereomers observed for the mefloquine derivatives **26**, **27** and **28**. An interesting observation was the fact that diastereomers B seemed to be less active/ less toxic than their counterparts by about a factor of two.

5.4 Conclusions

Chloroquine and mefloquine ferrocenyl carbohydrate conjugates were synthesized in an attempt to design a multifunctional therapeutic agent in which the quinoline antimalarial drug chloroquine or mefloquine can improve its antiplasmodial activity in drug-resistant parasite strains by the action of ferrocene, and where the carbohydrate molecule plays a targeting role, ideally increasing the consumption of the drug by the parasite in infected red blood cells.

Two synthetic pathways were designed for the synthesis of these two types of conjugates. Chloroquine and mefloquine were coupled to ferrocene in the 1,1'- and the 1,2-disubstituted

patterns, respectively, relative to the selected carbohydrate molecule glucosamine that was chosen due to its easy accessibility.

The proposed synthetic plans had the potential advantage to offer the final products in a low number of steps, five or six, with no protection necessary. The only protected group, glucosamine, is incorporated as it is. The deprotection of the carbohydrate should occur readily in acid or base catalyzed media as is common for acetyl protecting groups. This should potentially yield an unprotected carbohydrate molecule that could improve the bioavailability of the final product ferrocenyl conjugate by improving its water solubility.

Unfortunately, the low yields obtained in the very last step decreased considerably the total yield of these syntheses and, thus, the applicability of the preparations to produce significant enough amounts for biological tests. Additionally, the 1,2-mefloquine ferrocenyl glucosamine derivative has a short shelf live.

A different synthetic approach is needed to afford these compounds in better quantities. Likely a different coupling reaction is required for the condensation with the carbohydrate, and the carbohydrate to be used should have a more reactive point of attachment, ideally in an axial position.

Further improvements on the synthesis of quinoline ferrocenyl carbohydrate conjugates were undertaken in collaboration with other members of the group in work that is not detailed in this thesis, but that can be found elsewhere.[259,260] These products contain these three basic motifs and, even though they were synthesized in a greater number of steps, the total yields were improved, allowing the testing of antimalarial activity.

The results indicated that 1,1'-disubstituted compounds of chloroquine and protected glucose were slightly more effective than their 1,2-disubstituted analogs, and much more

active than the mefloquine analogs.[259] In some cases, the presence of the carbohydrate improved the activity of the quinoline drug in the drug-resistant parasite strains. It remains to be investigated at what level the monosaccharide contributes to this activity.

CHAPTER 6 CONCLUSIONS AND FUTURE WORK

6.1 Conclusions

A series of ferrocenyl derivatives of traditional antimalarial drugs such as chloroquine and mefloquine were synthesized and studied in their biological properties. These compounds contribute to the library of existing metalloantimalarials drug candidates and we hope they help elucidate the role the structure plays in the action of these quinoline metalloantimalarials, especially those derivatives of chloroquine, against drug-resistant *P. falciparum* strains.

A series of 4-aminoquinolines with short exocyclic alkyl chains were functionalized with ferrocene in two different patterns of substitution: disubstituted ferrocene derivatives with the terminal nitrogen of the chloroquine derivative bridging the two cyclopentadienyl rings of ferrocene **5a**-**e** and monosubstituted ferrocene chloroquine analogs **4a**-**e**. Structural study of these ferrocenyl compounds by ^{1}H NMR spectroscopy and single crystal X-ray diffraction confirmed that these patterns of substitution affect drastically the orientation of the quinoline ring with respect to the ferrocene. While the monosubstituted analogs have more freedom of rotation, the bridging structure limits the rotation of the quinoline ring, making this a much more rigid conformation and compact molecule. The chloroquine-bridged ferrocene derivatives also suffered from absent hydrogen bonding that is present in the majority of the monosubstituted analogs.

The impact of the presence or absence of hydrogen bonding interactions, the conformation, the degree of rigidity and the lipophilicity of these derivatives were correlated

to the biological responses of these compounds against different strains of *P. falciparum* parasites. All compounds tested were active against both chloroquine-sensitive and resistant parasite strains. Compounds **5a-e**, while mildly active, displayed the best resistance indices, indicating that their particular conformation might be of aid to avoid the resistance mechanism in the parasite strains.

While the presence of intramolecular H-bonding is associated with an increase of antiplasmodial action, it was found that other factors have greater influence in determining the activity. A balance between lipophilicity and hydrophilicity was found to be crucial in the activity displayed by the compounds. The closed conformation of **5a-e** provides a balance of lipophilicity/hydrophilicity and a compact size that provides these compounds with the structural characteristics needed to escape the resistance mechanism of the transmembrane proteins and achieve significant accumulation inside the parasite food vacuole.

Some of the few existing examples of bischloroquine and bismefloquine ferrocenyl derivatives are reported here, representing a contribution that fills a gap in the existing library of ferrocenyl quinoline derivatives.

With relatively little success, chloroquine and mefloquine ferrocenyl carbohydrate conjugates were synthesized following the design of a multifunctional therapeutic agent. The synthetic approaches offered the final products in a low number of steps, but were based on a reaction with low yields. Additionally, the 1,2-mefloquine ferrocenyl glucosamine derivative was found to be unstable.

6.2 Future work

Having found that the balance between the hydrophilicity and lipophilicity can be estimated by computational methods, *in silico* calculations could be employed in the design of improved analogs with tuned lipophilicity/hydrophilicity and intramolecular hydrogen bonding.

The investigation of the antiplasmodial activity of the bischloroquine and bismefloquine ferrocenyl derivatives remains outstanding. It remains to be determined if their double load of drug improves their action or if their relatively large size hampers their absorption into the drug site of action.

The development of better synthetic strategies for chloroquine and mefloquine ferrocenyl carbohydrate conjugates is needed. Also, detailed study of the effect of the carbohydrate will help to elucidate its role and if it has a targeting action.

If a remarkable agent were to be found, additional antiplasmodial studies would be undertaken to confirm it as a lead compound. First, this compound will require study against several strains of *P. falciparum* of diverse levels of drug sensitivity. Second, this drug must be tested alongside other antimalarials to find its tendency to develop cross-resistance and finally, complete *in vivo* studies in a malaria mouse model.

As demonstrated by ferroquine, taking an organometallic standpoint for traditional drugs that were sorted out due to resistance might lead to their resurgence in the form of organometallically-derivatized drugs as a next generation approach to pharmacologically active drugs. This could offer a second approach for drug developers in their search for new remedies of disease, benefiting from the previously gathered knowledge base.

Further studies on potential long term accumulation of metal ions in the organism and their metabolism should be undertaken because, in contrast to cancerostatic metal drugs for example, these organometallic antimalarials would require administration over a longer time frame for people residing in malaria-threatened regions of the world. One point to be addressed as well is the intrinsic cost of some of the metals used, which would make a potential drug susceptible to price changes on the market, or unaffordable due to an already high market price. Metals that would be affected by this are (among others) iridium and platinum. Certainly, a focus would have to be on inexpensive and abundant metals such as iron.

In order to continue this battle, synthetic chemistry, physicochemical studies and genomic studies must be carried out in close collaboration to develop candidates that can accurately and effectively fight resistance. These compounds offer diverse scaffolds for the potential exploitation of activity and the study of their properties. Even if not suitable as a stand-alone drug, metalloantimalarials are potential partners for a combination therapy approach with other antimalarials.

Combination therapy is currently used to treat malaria and it is not uncommon in the treatment of diseases that present resistance. Combining natural product chemistry, synthetic chemistry and *in silico* chemistry could possibly lead to the discovery of many more options for the discovery of new antimalarials. This would help optimising lead structures, simulating drug-protein interactions (transmembrane proteins involved in resistance), predicting bioavailability and bioactivity.

For the future, expect to see implementation of genomic information about the resistance originating in transmembrane proteins for the development of more drug candidates. More

details are needed about the role of the metal and how it aids in improved drug accumulation and development of more candidates for malaria therapy.

Malaria control has significantly improved over the last five years, but consistent care must be taken to maintain and further this improvement to prevent a resurgence of the disease, particularly via resistance. Awareness for this disease must be maintained, and a combination of vector control and new therapy approaches is a good way to limit the spread of the parasite. Given the history of the parasite, research on new antimalarials or vaccinations is constantly needed to stop malaria once and for all.

REFERENCES

1. World Health Organization; *World Malaria Report 2011*; WHO Press, Geneva, 2011.
2. Rich, S. M.; Leendertz, F. H.; Xu, G.; LeBreton, M.; Djoko, C. F.; Aminake, M. N.; Takang, E. E.; Diffo, J. L. D.; Pike, B. L.; Rosenthal, B. M.; Formenty, P.; Boesch, C.; Ayala, F. J.; Wolfe, N. D. *Proc. Natl. Acad. Sci. USA* **2009**, *106,* 14902-14907.
3. Carter, R.; Mendis, K. N. *Clin. Microbiol. Rev.* **2002**, *15,* 564-594.
4. *Antimalarial Chemotherapy : Mechanisms of Action, Resistance, and New Directions in Drug Discovery;* Rosenthal, P. J., Ed.; Humana Press: Totowa, NJ, 2001.
5. Malaria: Past and Present. http://www.nobelprize.org/educational/medicine/malaria/readmore/history.html (accessed Oct 15, 2011).
6. Greenwood, B.; Mutabingwa, T. *Nature* **2002**, *415,* 670-672.
7. World Health Organization; *Weekly Epidemiological Record - Malaria, 1982-1997*; Technical Report Number 32; WHO Press, Geneva, 1999.
8. World Health Organization, UNICEF. *The Africa Malaria Report 2003*; WHO Press, Geneva, 2003.
9. Murray, C. J. L.; Rosenfeld, L. C.; Lim, S. S.; Andrews, K. G.; Foreman, K. J.; Haring, D.; Fullman, N.; Naghavi, M.; Lozano, R. Lopez, A. D. *Lancet* **2012,** *379,* 413-431.
10. World Health Organization; *World Malaria Report 2005*; WHO Press, Geneva, 2005.
11. World Health Organization; *World Malaria Report 2010*; WHO Press, Geneva, 2010.
12. *The Global Fund and a new modus operandi* (Editorial) *Lancet* **2011,** *378,* 1896.
13. Donor governments cancel Global Fund Round 11. http://www.healthgap.org/press/gfatm_round11.html (accessed Feb 6, 2012).
14. World Health Organization; *Global Malaria Control and Elimination: Report of a Technical Review;* WHO Press, Geneva, 2008.
15. World Health Organization; *Malaria Vector Control and Personal Protection;* WHO Press, Geneva, 2006.
16. Preventive Treatment for Pregnant Women and Infants. http://www.rbm.who.int/worldmalariaday/ipt.html (accessed Sep 30, 2011).

17. Malaria and Travelers. http://www.cdc.gov/malaria/travelers/ (accessed Sep 12, 2011).
18. Public Health Agency of Canada - Travel Health. http://www.phac-aspc.gc.ca/tmp-pmv/index-eng.php (accessed Feb 3, 2012).
19. Centers for Disease Control and Prevention; *Preventing Malaria in Travellers - A Guide for Travelers to Malaria-Risk Areas*; CDC: Druid Hills, GA, 2011.
20. The PATH Malaria Vaccine Initiative; *Accelerating Progress Toward Malaria Vaccines;* PATH Malaria Vaccine Initiative: Bethesda, MD, 2007.
21. The PATH Malaria Vaccine Initiative; *Strategy for Developing Next-Generation Malaria Vaccines*; PATH Malaria Vaccine Initiative: Bethesda, MD, 2009.
22. World Health Organization. *Guidelines for the Treatment of Malaria*; WHO Press, Geneva, 2006.
23. Malaria. http://www.mdtravelhealth.com/infectious/malaria.html. (accessed Feb 3, 2012).
24. World Health Organization; *Global Report on Antimalarial Drug Efficacy and Drug Resistance: 2000-2010;* WHO Press, Geneva, 2010.
25. World Health Organization. *Guidelines for the Treatment of Malaria*; WHO Press, Geneva, 2006.
26. Enserink, M. *Science* **2010**, *328*, 844-846.
27. World Health Organization; *Global plan for artemisinin resistance containment (GPARC);* WHO Press, Geneva, 2011.
28. Meshnick, S. R.; Dobson, M. J. The History of Antimalarial Drugs. In *Antimalarial Chemotherapy: Mechanisms of Action, Resistance, and New Directions in Drug Discovery;* Rosenthal, P. J., Ed.; Humana Press: Totowa, NJ, 2001; pp 15-28.
29. Rosenthal, P. J.; Miller, L. H. The Need for New Approaches to Antimalarial Chemotherapy. In *Antimalarial Chemotherapy: Mechanisms of Action, Resistance, and New Directions in Drug Discovery;* Rosenthal, P. J., Ed.; Humana Press: Totowa, NJ, 2001; pp 3-13.
30. Rathore, D.; McCutchan, T. F.; Sullivan, M.; Kumar, S. *Expert Opin. Invest. Drugs* **2005**, *14*, 871-883.
31. Rosenthal, P. J. *J. Exp. Biol.* **2003**, *206*, 3735-3744.
32. Egan, T. J. *Expert Opin. Ther. Pat.* **2001**, *11*, 185-209.

33. Olliaro, P. *Pharmacol. Ther.* **2001**, *89*, 207-219.
34. Winstanley, P.; Ward, S. *Adv. Parasitol.* **2006**, *61*, 47-76.
35. Wiesner, J.; Ortmann, R.; Jomaa, H.; Schlitzer, M. *Angew. Chem., Int. Ed.* **2003**, *42*, 5274–5293.
36. Chang, C.; Lin-Hua, T.; Jantanavivat, C. *Trans. R. Soc. Trop. Med. Hyg.* **1992**, *86*, 7-10.
37. Ringwald, P.; Bickii, J.; Basco, L. *Lancet* **1996**, *347*, 24-28.
38. Kain, K. C.; Shanks, G. D.; Keystone, J. S. *Clin. Infect. Dis.***2001**, *33*, 226-234.
39. Tilley, L.; Loria, P.; Foley, M. Chloroquine and other Quinoline Antimalarials. In *Antimalarial Chemotherapy: Mechanisms of Action, Resistance, and New Directions in Drug Discovery;* Rosenthal, P. J., Ed.; Humana Press: Totowa, NJ, 2001; pp 87-121.
40. Shanks, G. D.; Oloo, A. J.; Aleman, G. M.; Ohrt, C.; Klotz, F. W.; Braitman, D.; Horton, J.; Brueckner, R. *Clin. Infect. Dis.* **2001**, *33*, 1968-1974.
41. Zarchin, S.; Krugliak, M.; Ginsburg, H. *Biochem. Pharmacol.* **1986**, *35*, 2435-2442.
42. Krugliak, M.; Zhang, J.; Ginsburg, H. *Mol. Biochem. Parasitol.* **2002**, *119*, 249-256.
43. Francis, S. E.; Sullivan, D. J. Jr.; Goldberg, D. E. *Annu. Rev. Microbiol.* **1997**, *51*, 97-123.
44. Banerjee, R.; Goldberg, D. E. The Plasmodium Food Vacuole. In *Antimalarial Chemotherapy: Mechanisms of Action, Resistance, and New Directions in Drug Discovery;* Rosenthal, P. J., Ed.; Humana Press: Totowa, NJ, 2001; pp 43-63.
45. B Banerjee, R.; Liu, J.; Beatty, W.; Pelosof, L.; Klemba, M.; Goldberg, D. E. *Proc. Natl. Acad. Sci. USA* **2002**, *99*, 990-995.
46. Srivastava, P.; Pandey, V. C. *Int. J. Parasitol.* **1995**, *25*, 1061-1064.
47. Sullivan, A. D.; Meshnick, S. R. *Parasitol. Today* **1996**, *12*, 161-163.
48. Pagola, S.; Stephens, P. W.; Bohle, D. S.; Kosar, A. D.; Madsen, S. K. *Nature* **2000**, *404*, 307-310.
49. Bohle, D. S.; Kosar, A. D.; Madsen, S. K. *Biochem. Biophys. Res. Commun.* **2002**, *294*, 132-135.
50. Bohle, D. S.; Kosar, A. D.; Stephens, P. W. *Acta Crystallogr., Sect. D: Biol. Crystallogr.* **2002**, *D58*, 1752-1756.
51. Hampelmann, E.; Egan, T. J. *Trends Parasitol.* **2002**, *18*, 11.

52. Egan, T. J.; Mavuso, W. W.; Ncokazi, K. K. *Biochemistry* **2001**, *40,* 204-213.
53. Egan, T. J. *Mol. Biochem. Parasitol.* **2008**, *157,* 127-136.
54. Rangarajan, P. N.; Padmanaban, G. *Expert. Opin. Ther. Targets* **2001**, *5,* 423-441.
55. Hyde, J. E., *Microb. Infect.* **2002**, *4,* 165-174.
56. Dorn, A.; Vippagunta, S. R.; Matile, H.; Jaquet, C.; Vennerstrom, J. L.; Ridley, R. G. *Biochem. Pharmacol.* **1998**, *55,* 727-736.
57. Sullivan Jr., D. J.; Matile, H.; Ridley, R. G.; Goldberg, D. E. *J. Biol. Chem.* **1998**, *273,* 31103-31107.
58. Weissbuch, I.; Leiserowitz, L. *Chem. Rev.* **2008**, *108,* 4899-4914.
59. Loria, P.; Miller, S.; Foley, M.; Tilley, L. *Biochem. J.* **1999**, *339,* 363-370.
60. Ginsburg, H.; Famin, O.; Zhang, J.; Krugliak, M. *Biochem. Pharmacol.* **1998**, *56,* 1305-1313.
61. Famin, O.; Krugliak, M.; Ginsburg, H. *Biochem. Pharmacol.* **1999**, *58,* 59-68.
62. Allison, R. G., Hahn, F. E. *Antimicrob. Agents Chemother.* **1977**, *11,* 251-257.
63. Parker, F. S.; Irvin, J. L. *J. Biol. Chem.* **1952**, *199,* 889-895.
64. Cohen, S. N.; Yielding, K. L.. *Proc. Natl. Acad. Sci., USA* **1965**, *54,* 521-527.
65. Sanchez, C. P.; Lanzer, M. *Curr. Opin. Infect. Dis.* **2000**, *13,* 653-658.
66. Egan, T. J.; Hempelmann, E.; Mavuso, W. W. *J. Inorg. Biochem.* **1999**, *73,* 101-107.
67. Wootton, J. C.; Feng, X.; Ferdig, M. T.; Cooper, R. A. ; Mu, J.; Baruch, D. I. ; Magill, A. J.; Su, X.-Z. *Nature* **2002**, *418,* 320-323.
68. Bray, P. G.; Mungthin, M.; Ridley, R. G.; Ward, S. A. *Mol. Pharmacol.* **1998**, *54,* 170-179.
69. Le Bras, J.; Durand, R. *Fundam. Clin. Pharmacol.* **2003**, *17,* 147-153.
70. Krogstad, D. J.; Gluzman, I. Y.; Kyle, D. E.; Oduola, A. M.; Martin, S. K.; Milhous, W. K.; Schlesinger, P. H. *Science* **1987**, *238,* 1283-1285.
71. van Schalkwyk, D. A.; Egan, T. J. *Drug Resist. Updates* **2006**, *9,* 211-226.
72. Henry, M.; Alibert, S.; Orlandi-Pradines, E.; Bogreau, H.; Fusai, T.; Rogier, C.; Barbe, J.; Pradines, B. *Curr. Drug Targets* **2006**, *7,* 935-948.
73. Mita, T.; Tanabe, K.; Kita K. *Parasitol Int.* **2009**, *58,* 201-209.
74. Sanchez, C. P.; Stein, W. D.; Lanzer, M. *Trends Parasitol.* **2007**, *23,* 332-339.

75. Wilson, C. M.; Serrano, A. E.; Wasley, A.; Bogenschutz, M. P.; Shankar, A. H.; Wirth, D. F. *Science* **1989**, *244,* 1184-1186.
76. Foote, S. J.; Kyle, D. E.; Martin, R. K.; Oduola, A. M. J.; Forsyth, K.; Kemp, D.J.; Cowman, A. F. *Nature* **1990**, *345,* 255–258.
77. Fidock, D. A.; Nomura, T.; Talley, A. K.; Cooper, R. A.; Dzekunov, S. M.; Ferdig, M. T.; Ursos, L. M. B.; Singh Sidhu, A. B.; Naude, B.; Deitsch, K. W.; Su, X.-Z.; Wootton, J. C.; Roepe, P. D.; Wellems, T. E. *Mol. Cell* **2000**, *6,* 861-871.
78. Reed, M. B.; Saliba, K. J.; Caruana, S. R.; Kirk, K.; Cowman, A. F. *Nature* **2000**, *403,* 906-909.
79. Wu, X.; Go, M. L. The Use of Iron-based Drugs in Medicine. In *Metallotherapeutic Drugs and Metal-Based Diagnostic Agents: The Use of Metals in Medicine;* Gielen, M., Tiekink, E. R. T., Eds.; Wiley: Chichester, U.K., 2005; pp 179-200.
80. S Farrer, N. J.; Sadler, P. J. Medicinal Inorganic Chemistry: State of the Art, New Trends, and a Vision of the Future. In *Bioinorganic Medicinal Chemistry;* Alessio, E., Ed.; Wiley-VCH: Weinheim, DE., 2011; pp 1-47.
81. Navarro, M.; Gabiani, C.; Messori, L.; Gambino, D. *Drug Discov. Today* **2010**, *15,* 1070-1078.
82. Mabeza, G. F.; Loyevsky, M.; Gordeuk, V. R.; Weiss, G. *Pharmacol. Therap.* **1999**, *81,* 53-75.
83. Weinberg, E. D.; Moon, J. *Drug Metab. Rev.* **2009**, *41,* 644-662.
84. Hershko, C.; Peto, T. E. *J. Exp. Med.* **1988**, *168,* 375-387.
85. Gordeuk, V. R.; Thuma, P. E.; Brittenham, G. M.; Zulu, S.; Simwanza, G.; Mhangu, A.; Flesch, G.; Parry, D. *Blood* **1992**, *79,* 308-312.
86. Gordeuk, V. R.; Thuma, P. E.; McLaren, C.E.; Biemba, G.; Zulu, S.; Poltera, A. A.; Askin, J. E.; Brittenham, G. M. *Blood* **1995**, *85,* 3297-3301.
87. Loyevsky, M.; Lytton, S. D.; Mester, B.; Libman, J.; Shanzer, A.; Cabantchik, Z. I. *J. Clin. Invest.* **1993**, *91,* 218-224.
88. Chevion, M.; Chuang, L.; Golenser, J. *Antimicrob. Agents Chemother.* **1995**, *39,* 1902-1905.

89. Gordeuk, V. R.; Loyevsky, M. Antimalarial Effect of Iron Chelation. In *Iron Chelation Therapy;* Hershko, C., Ed.; Advances in Experimental Medicine and Biology, Vol. 509; Kluwer Academic/Plenum Publishers: New York, 2002; pp 251-272.
90. Pradines, B.; Ramiandrasoa, F.; Basco, L. K.; Bricard, L.; Kunesch, G.; Le Bras, J. *Antimicrob. Agents Chemother.* **1996**, *40*, 2094-2098.
91. Pradines, B.; Rolain, J. M.; Ramiandrasoa, F.; Fusai, T.; Mosnier, J.; Rogier, C.; Daries, W.; Baret, E.; Kunesch, G.; Le Bras, J.; Parzy, D. *J. Antimicrob. Chemother.* **2002**, *50*, 177-187.
92. Pradines, B.; Tall, A.; Ramiandrasoa, F.; Spiegel, A.; Sokhna, C.; Fusai, T.; Mosnier, J.; Daries, W.; Trape, J. F.; Kunesch, G.; Parzy, D.; Rogier, C. *J. Antimicrob. Chemother.* **2006**, *57*, 1093-1099.
93. Loyevsky, M.; John, C.; Zaloujnyi, I.; Gordeuk, V. R. *Biochem. Pharmacol.* **1997**, *54*, 451-458.
94. Hershko, C.; Gordeuk, V. R.; Brittenham, G. M.; Thuma, P. E.; Theanacho, E. N.; Spira, D. T.; Hider, R. C.; Peto T. E. A. *J. Inorg. Biochem.* **1992**, *47*, 267-277.
95. Dehkordi, L. S.; Liu, Z. D.; Hider, R. C. *Eur. J. Med. Chem.* **2008**, *43*, 1035-1047.
96. Nick, H.; Acklin, P.; Lattmann, R.; Buehlmayer, P.; Hauffe, S.; Schupp J.; Alberti, D. *Curr Med. Chem.* **2003**, *10*, 1065-1076.
97. Goudeau, C.; Loyevsky, M.; Kassim, O. O.; Gordeuk, V. R.; Nick, H. *Br. J. Haematol.* **2001**, *115*, 918-923.
98. Tsafack, A.;Loyevsky, M.; Ponka, P.; Ioav Cabantchik, Z. *J. Lab. Clin. Med.* **1996**, *127*, 574-582.
99. Melnyk, P.; Leroux, V.; Sergheraert, C.; Grellier, P. *Bioorg.Med. Chem. Lett.* **2006**, *16*, 31-35.
100. Chibale, K.; Biot, C. *Infect. Disord. Drug Targ.* **2006**, *6*, 173-204.
101. Walcourt, A.; Loyevsky., M.; Lovejoy, D. B.; Gordeuk, V. R.; Richardson. D. R. *Int. J. Biochem Cell Biol.* **2004**, *36*, 401-407.
102. Sánchez-Delgado, R. A.; Anzellotti, A. *Mini-Rev. Med. Chem.* **2004**, *4*, 23-30.
103. Sharma, V.; Piwnica-Worms, D. *Chem. Rev.* **1999**, *99*, 2545-2560.
104. Sharma, V. *Mini-Rev. Med. Chem.* **2005**, *5*, 337-351.

105. Sánchez-Delgado, R. A.; Navarro, M.; Perez, H.; Urbina, J. A. *J. Med. Chem.* **1996**, *39*, 1095-1099.
106. Martínez, A.; Rajapakse, C. S. K.; Naoulou, B.; Kopkalli, Y.; Davenport, L.; Sánchez-Delgado, R. A. *J. Biol. Inorg. Chem.* **2008**, *13*, 703-712.
107. Navarro, M.; Perez, H.; Sánchez-Delgado, R. A. *J. Med. Chem.* **1997**, *40*, 1937-1939.
108. Navarro, M.; Vasquez, F.; Sánchez-Delgado, R. A.; Perez, H.; Sinou, V.; Schrevel, J. *J. Med. Chem.* **2004**, *47*, 5204-5209.
109. Navarro, M.; Castro, W.; Martínez, A.; Sánchez-Delgado, R. A. *J. Inorg. Biochem.* **2011**, *105*, 276-282.
110. Navarro, M. *Coord. Chem. Rev.* **2009**, *253*, 1619-1626.
111. Wasi, N.; Singh, H. B.; Gajanana, A.; Raichowdhary, A. N. *Inorg. Chim. Acta* **1987**, *135*, 133-137.
112. Alesutan, I.; Bobbala, D.; Qadri, S. M.; Estremera, A.; Föller, M.; Lang, F. *Malar. J.* **2010**, *9*, 118-125.
113. Sannella, A. R.; Casini, A.; Gabbiani, C.; Messori, L.; Bilia, A. R.; Vincieri, F. F.; Majori, G.; Severini, C. *FEBS Lett.* **2008**, *582*, 844-847.
114. Gabbiani, C.; Messori, L.; Cinellu, M. A.; Casini, A.; Mura, P.; Sannella, A. R.; Severini, C.; Majori, G.; Bilia, A. R.; Vincieri, F. F. *J. Inorg. Biochem.* **2009**, *103*, 310-312.
115. Goldberg, D. E.; Sharma, V.; Oksman, A.; Gluzman, I. Y.; Wellems, T. E.; Piwnica-Worms, D. *J. Biol. Chem.* **1997**, *272*, 6567-6572.
116. Sharma, V.; Beatty, A.; Goldberg, D. E.; Piwnica-Worms, D. *Chem. Commun.* **1997**, 2223-2224.
117. Ziegler, J.; Schuerle, T.; Pasierb, L.; Kelly, C.; Elamin, A.; Cole, K. A.; Wright, D. W. *Inorg. Chem.* **2000**, *39*, 3731-3733.
118. Ocheskey, J. O.; Polyakov, V. R.; Harpstrite, S. E.; Oksman, A.; Goldberg, D. E.; Piwnica-Worms, D.; Sharma, V. *J. Inorg. Biochem.* **2003**, *93*, 265-270.
119. Ocheskey, J. A.; Harpstrite, S. E.; Oksman, A.; Goldberg, D. E.; Sharma, V. *Chem. Commun.* **2005**, 1622-1624.
120. Gokhale, N. H.; Padhye, S. B.; Billington, D. C.; Rathbone, D. L.; Croft, S. L.; Kendrick, H. D.; Anson, C. E.; Powell, A. K. *Inorg. Chim. Acta* **2003**, *349*, 23-29.

121. Gokhale, N. H.; Padhye, S. B.; Croft, S. L.; Kendrick, H. D.; Davies, W.; Anson, C. E.; Powell, A. K. *J. Inorg. Biochem.* **2003**, *95,* 249-258.
122. Mohapatra, S. C.; Tiwari, H. K.; Singla, M.; Rathi, B.; Sharma, A.; Mahiya, K.; Kumar, M.; Sinha, S.; Chauhan, S. S. *J. Biol. Inorg. Chem.* **2010**, *15,* 373-385.
123. Monti, D.; Vodopivec, B.; Basilico, N.; Olliaro, P.; Taramelli, D. *Biochemistry* **1999**, *38,* 8858-8863.
124. Cole, K. A.; Ziegler, J.; Evans, C. A.; Wright, D. W. *J. Inorg. Biochem.* **2000**, *78,* 109-115.
125. Chavain, N.; Biot, C. *Curr. Med. Chem.* **2010**, *17,* 2729-2745.
126. *Medicinal Organometallic Chemistry;* Jaouen, G., Metzler-Nolte, N., Eds.; Topics in Organometallic Chemistry, Vol. 32, Springer: Berlin, 2010.
127. Top, S.; Tang, J.; Vessieres, A.; Carrez, D.; Provote, C.; Jaouen, G. *Chem. Commun.* **1996**, 955-956.
128. Jaouen, G.; Top, S.; Vessières, A.; Leclercq, G.; McGlinchey, M. J. *Curr. Med. Chem.* **2004**, *11,* 2505-2517.
129. Biot, C.; Glorian, G.; Maciejewski, L. A.; Brocard, J. S.; Domarle, O.; Blampain, G.; Millet, P.; Georges, A. J.; Abessolo, H.; Dive, D.; Lebibi, J. *J. Med. Chem.* **1997**, *40,* 3715-3718.
130. Domarle, O.; Blampain, G.; Agnaniet, H.; Nzadiyabi, T.; Lebibi, J.; Brocard, J.; Maciejewski, L.; Biot, C.; Georges, A. J.; Millet, P. *Antimicrob. Agents Chemother.* **1998**, *42,* 540-544.
131. Biot, C.; Delhaes, L.; Abessolo, H.; Domarle, O.; Maciejewski, L.A.; Mortuaire, M.; Delcourt, P.; Deloron, P.; Camus, D.; Dive, D.; Brocard, J. S. *J. Organomet. Chem.* **1999**, *589,* 59-65.
132. Biot, C.; Daher, W.; Ndiaye, C. M.; Melnyk, P.; Pradines, B.; Chavain, N.; Pellet, A.; Fraisse, L.; Pelinski, L.; Jarry, C.; Brocard, J.; Khalife, J.; Forfar-Bares, I.; Dive, D. *J. Med. Chem.* **2006**, *49,* 4707-4714.
133. Beagley, P.; Blackie, M. A. L.; Chibale, K.; Clarkson, C.; Moss, J. R.; Smith, P. J. *J. Chem. Soc., Dalton Trans.* **2002**, 4426-4433.
134. Pradines, B.; Fusai, T.; Daries, W.; Laloge, V.; Rogier, C.; Millet, P.; Panconi, E.; Kombila, M.; Parzy, D. *J. Antimicrob. Chemother.* **2001**, *48,* 179-184.

135. Delhaes, L.; Abessolo, H.; Biot, C.; Berry, L.; Delcourt, P.; Maciejewski, L.; Brocard, J.; Camus, D.; Dive, D. *Parasitol. Res.* **2001**, *87*, 239-244.
136. Zhou, C. H.; Gan, L.; Zhang, Y.; Zhang, F.; Wang, G.; Jin, L.; Geng, R. *Sci. China, Ser. B: Chem.* **2009**, *52*, 415-458.
137. Pradines, B.; Tall, A.; Rogier, C.; Spiegel, A.; Mosnier, J.; Marrama, L.; Fusai, T.; Millet, P.; Panconi, E.; Trape, J. F.; Parzy, D. *Trop. Med. Int. Health* **2002**, *7*, 265-270.
138. Atteke, C.; Ndong, J. M. M.; Aubouy, A.; Maciejewski, L.; Brocard, J.; Lébibi, J.; Deloron, P. *J. Antimicrob. Chemother.* **2003**, *51*, 1021-1024.
139. *Ferrocenes : Ligands, Materials and Biomolecules;* Štěpnička, P. Ed.; Wiley: Chichester, U.K., 2008.
140. Dive, D.; Biot, C. *ChemMedChem* **2008**, *3*, 383-391.
141. Blackie, M. A. L.; Beagley, P.; Croft, S. L.; Kendrick, H.; Moss, J. R.; Chibale, K. *Bioorg. Med. Chem.* **2007**, *15*, 6510-6516.
142. Beagley, P.; Blackie, M. A. L.; Chibale, K.; Clarkson, C.; Meijboom, R.; Moss, J. R.; Smith, P. J.; Su, H. *Dalton Trans.* **2003**, 3046-3051.
143. Biot, C.; Daher, W.; Chavain, N.; Fandeur, T.; Khalife, J.; Dive, D.; De Clercq, E. *J. Med. Chem.* **2006**, *49*, 2845-2849.
144. Chibale, K.; Moss, J. R.; Blackie, M.; van Schalkwyk, D.; Smith, P. J. *Tetrahedron Lett.* **2000**, *41*, 6231-6235.
145. Bellot, F.; Cosledan, F.; Vendier, L.; Brocard, J.; Meunier, B.; Robert, A. *J. Med. Chem.* **2010**, *53*, 4103-4109.
146. Wenzel, N. I.; Chavain, N.; Wang, Y.; Friebolin, W.; Maes, L.; Pradines, B.; Lanzer, M.; Yardley, V.; Brun, R.; Herold-Mende, C.; Biot, C.; Toth, K. Davioud-Charvet, E. *J. Med. Chem.* **2010**, *53*, 3214-3226.
147. Biot, C.; Dessolin, J.; Ricard, I.; Dive, D. *J. Organomet. Chem.* **2004,** *689*, 4678-4682.
148. Blackie, M. A. L.; Beagley, P.; Chibale, K.; Clarkson, C.; Moss, J. R.; Smith, P. J. *J. Organomet. Chem.* **2003**, *688*, 144-152.
149. Paitayatat, S.; Tarnchompoo, B.; Thebtaranonth, Y.; Yuthavong, Y. *J. Med. Chem.* **1997**, *40*, 633-638.
150. Delhaes, L.; Biot, C.; Berry, L.; Maciejewski, L. A.; Camus, D.; Brocard, J. S.; Dive, D. *Bioorg. Med. Chem.* **2000**, *8*, 2739-2745.

151. Baramee, A.; Coppin, A.; Mortuaire, M.; Pelinski, L.; Tomavo, S.; Brocard, J. *Bioorg. Med. Chem.* **2006**, *14*, 1294-1302.
152. Biot, C.; Delhaes, L.; Maciejewski, L. A.; Mortuaire, M.; Camus, D.; Dive, D.; Brocard, J. S. *Eur. J. Med. Chem.* **2000**, *35*, 707-714.
153. Biot, C.; Pradines, B.; Sergeant, M.-H.; Gut, J.; Rosenthal, P. J.; Chibale, K. *Bioorg. Med. Chem. Lett.* **2007**, *17*, 6434-6438.
154. Khanye, S. D.; Gut, J.; Rosenthal, P. J.; Chibale, K.; Smith, G. S. *J. Organomet. Chem.* **2011**, *696*, 3296-3300.
155. Wu, X.; Wilairat, P.; Go, M.-L. *Bioorg. Med. Chem. Lett.* **2002**, *12*, 2299-2302.
156. Wu, X.; Tiekink, E. R. T.; Kostetski, I.; Kocherginsky, N.; Tan, A. L. C.; Khoo, S. B.; Wilairat, P.; Go, M. *Eur. J. Pharm. Sci.* **2006**, *27*, 175-187.
157. Razafimahefa, D.; Pelinski, L.; Martin, M.; Ramanitrahasimbola, D.; Rasoanaivod, P.; Brocard, J. *Bioorg. Med. Chem. Lett.* **2005**, *15*, 1239-1241.
158. Itoh, T.; Shirakami, S.; Ishida, N.; Yamashita, Y.; Yoshida, T.; Kim, H.; Wataya, Y. *Bioorg. Med. Chem. Lett.* **2000**, *10*, 1657-1659.
159. Ferreira, C. L.; Ewart, C. B.; Barta, C. A.; Little, S.; Yardley, V.; Martins, C.; Polishchuk, E.; Smith, P. J.; Moss, J. R.; Merkel, M.; Adam, M. J.; Orvig, C. *Inorg. Chem.* **2006**, *45*, 8414-8422.
160. Fayolle, M.; Ionita, M.; Krishna, S.; Morin, C.; Patel, A. P. *Bioorg. Med. Chem. Lett.* **2006**, *16*, 1267-1271.
161. Adam, M. J.; Hall, L. D. *Can. J. Chem.* **1980**, *58*, 1188-1197.
162. Dubar, F.; Egan, T. J.; Pradines, B.; Kuter, D.; Ncokazi, K. K.; Forge, D.; Paul, J.-F.; Pierrot, C.; Kalamou, H.; Khalife, J.; Buisine, E.; Rogier, C.; Vezin, H.; Forfar, I.; Slomianny, C.; Trivelli, X.; Kapishnikov, S.; Leiserowitz, L.; Dive, D.; Biot, C. *ACS Chem. Biol.* **2011**, *6*, 275-287.
163. Chavain, N.; Vezin, H.; Dive, D.; Touati, N.; Paul, J.-F.; Buisine, E.; Biot, C. *Mol. Pharmaceutics* **2008**, *5*, 710-716.
164. Rajapakse, C. S. K.; Martínez, A.; Naoulou, B.; Jarzecki, A. A.; Suarez, L.; Deregnaucourt, C.; Sinou, V.; Schrevel, J.; Musi, E.; Ambrosini, G.; Schwartz, G. K.; Sánchez-Delgado, R. A. *Inorg. Chem.* **2009**, *48*, 1122-1131.

165. Martínez, A.; Rajapakse, C. S. K.; Jalloh, D.; Dautriche, C. Sánchez-Delgado, R. A. *J. Biol. Inorg. Chem.* **2009**, *14*, 863-871.
166. Navarro, M.; Pekerar, S.; Perez, H. A. *Polyhedron* **2007**, *26*, 2420-2424.
167. Arancibia, R.; Dubar, F.; Pradines, B.; Forfar, I.; Dive, D.; Klahn, A. H.; Biot, C. *Bioorg. Med. Chem.* **2010**, *18*, 8085-8091.
168. Glans, L.; Taylor, D.; de Kock, C.; Smith, P. J.; Haukka, M.; Moss, J. R.; Nordlander, E. *J. Inorg. Biochem.* **2011**, *105*, 985-990.
169. Chellan, P.; Shunmoogam-Gounden, N.; Hendricks, D. T.; Gut, J.; Rosenthal, P. J.; Lategan, C.; Smith, P. J.; Chibale, K.; Smith, G. S. *Eur. J. Inorg. Chem.* **2010**, *2010*, 3520-3528.
170. Chellan, P.; Nasser, S.; Vivas, L.; Chibale, K.; Smith, G. S. *J. Organomet. Chem.* **2010**, *695*, 2225-2232.
171. van Staveren, D. R.; Metzler-Nolte, N. *Chem. Rev.* **2004**, *104*, 5931-5985.
172. Fouda, M. F. R.; Abd-Elzaher, M. M.; Abdelsamaia, R. A.; Labib, A. A. *Appl. Organomet. Chem.* **2007**, *21*, 613-625.
173. Lipinski, C. A.; Lombardo, F.; Dominy, B. W.; Feeney, P. J. *Adv. Drug Delivery Rev.* **1996,** *46*, 3-26.
174. Henry, M.; Briolant, S.; Fontaine, A.; Mosnier, J.; Baret, E.; Amalvict, R. Fusai, T.; Fraisse, L.; Rogier, C.; Pradines, B. *Antimicrob. Agents Chemother.* **2008**, *52*, 2755-2759.
175. Biot, C. *Curr. Med. Chem.: Anti-Infect. Agents* **2004**, *3*, 135-147.
176. Biot, C.; Dive, D. Bioorganometallic Chemistry and Malaria. In *Medicinal Organometallic Chemistry;* Jaouen, G., Metzler-Nolte, N., Eds.; Topics in Organometallic Chemistry, Vol. 32, Springer: Berlin, 2010; pp 155-193.
177. Daher, W.; Biot, C.; Fandeur, T.; Jouin, H.; Pelinski, L.; Viscogliosi, E.; Fraisse, L.; Pradines, B.; Brocard, J.; Khalife, J.; Dive, D. *Malar. J.* **2006**, *5*:11.
178. Delhaes, L.; Biot, C.; Berry, L.; Delcourt, P.; Maciejewski, L. A.; Camus, D.; Brocard, J. S.; Dive, D. *ChemBioChem* **2002**, *3*, 418-423.
179. Blackie, M. A. L.; Chibale, K. *Met.-Based Drugs* **2008**, *2008*, Article ID 495123, 10 pages.
180. Glidewell, C.; Royles, B. J. L.; Smith, D. M. *J. Organomet. Chem.* **1997,** *527*, 259-261.

181. Musonda, C. C.; Taylor, D.; Lehman, J.; Gut, J.; Rosenthal, P. J.; Chibale, K. *Bioorg. Med. Chem. Lett.* **2004**, *14*, 3901-3905.
182. Solomon, V. R.; Puri, S. K.; Srivastava, K.; Katti, S. B. *Bioorg. Med. Chem.* **2005,** *13*, 2157-2165.
183. Natarajan, J. K.; Alumasa, J. N.; Yearick, K.; Ekoue-Kovi, K. A.; Casabianca, L. B.; de Dios, A. C.; Wolf, C.; Roepe, P. D. *J. Med. Chem.* **2008**, *51*, 3466-3479.
184. Ridley, R. G.; Hofheinz, W.; Matile, H.; Jaquet, C.; Dorn, A.; Masciadri, R.; Jolidon, S.; Richter, W. F.; Guenzi, A.; Girometta, M. A.; Urwyler, H.; Huber, W.; Thaitong, S.; Peters, W. *Antimicrob. Agents Chemother.* **1996**, *40*, 1846-1854.
185. De, D.; Krogstad, F. M.; Cogswell, F. B.; Krogstad, D. J. *Am. J. Trop. Med.* **1996**, *55*, 579-583.
186. Stocks, P. A.; Raynes, K. J.; Bray, P. G.; Park, B. K.; O'Neill, P. M.; Ward, S. A. *J. Med. Chem.* **2002**, *45*, 4975-4983.
187. Madrid, P. B.; Wilson, N. T.; DeRisi, J. L.; Guy, R. K. *J. Comb. Chem.* **2004**, *6*, 437-442.
188. De, D.; Byers, L. D.; Krogstad, D. J. *J. Heterocycl. Chem.* **1997**, *34*, 315-320.
189. Madrid, P. B.; Liou, A. P.; DeRisi, J. L.; Guy, R. K. *J. Med. Chem.* **2006,** *49*, 4535-4543.
190. De, D.; Krogstad, F. M.; Byers, L. D.; Krogstad, D. J. *J. Med. Chem.* **1998**, *41*, 4918-4926.
191. Egan, T. J.; Hunter, R.; Kaschula, C. H.; Marques, H. M.; Misplon, A.; Walden, J. *J. Med. Chem.* **2000**, *43*, 283-291.
192. Bray, P. G.; Hawley, S. R.; Mungthin, M.; Ward, S. A. *Mol. Pharmacol.* **1996**, *50*, 1559-1566.
193. Feng, T.; Guantai, E. M.; Nell, M. J.; van Rensburg, C. E. J.; Hoppe, H. C.; Chibale, K. *Bioorg. Med. Chem. Lett.* **2011**, *21*, 2882-2886.
194. Osgerby, J. M. *J. Chem. Soc.* **1958**, 656-660.
195. Grossel, M. C.; Hamilton, D. G.; Fuller, J. I.; Millan-Barios, E. *J. Chem. Soc., Dalton Trans.* **1997**, *19*, 3471-3477.
196. Bildstein, B; Malaun, M.; Kopacka, H.; Ongania, K.; Wurst, K. *J. Organomet. Chem.* **1998**, *552*, 45-61.

197. N'Diaye, C. M.; Maciejewski, L. A.; Brocard, J. S.; Biot, C. *Tetrahedron Lett.* **2001**, *42*, 7221-7223.
198. Biot, C.; Taramelli, D.; Forfar-Bares, I.; Maciejewski, L. A.; Boyce, M.; Nowogrocki, G.; Brocard, J. S.; Basilico, N.; Olliaro, P.; Egan, T. J. *Mol. Pharmaceutics* **2005**, *2*, 185-193.
199. Emsley, J., *Chem. Soc. Rev.* **1980**, *9*, 91-124.
200. Herbert, D. E.; Ulrich, F.; Mayer, J.; Manners, I. *Angew. Chem. Int. Ed.* **2007**, *46*, 5060-5081.
201. Barlow, S.; Drewitt, M. J.; Dijkstra, T.; Green, J. C.; O'Hare, D.; Whittingham, C.; Wynn, H. H.; Gates, D. P.; Manners, I.; Nelson, J. M.; Pudelski, J. K. *Organometallics* **1998**, *17*, 2113-2120.
202. Horie, M.; Sakano, T.; Osakada, K.; Nakao, H. *Organometallics* **2004**, *23*, 18-20.
203. Kaschula, C. H.; Egan, T. J.; Hunter, R.; Basilico, N.; Parapini, S.; Taramelli, D.; Pasini, E.; Monti, D. *J. Med. Chem.* **2002**, *45*, 3531-3539.
204. Guillon, J.; Moreau, S.; Mouray, E.; Sinou, V.; Forfar, I.; Fabre, S. B.; Desplat, V.; Millet, P.; Parzy, D.; Jarry, C.; Grellier, P. *Bioorg. Med. Chem.* **2008**, *16*, 9133-9144.
205. Molyneaux, C.-A.; Krugliak, M.; Ginsburg, H.; Chibale, K. *Biochem. Pharmacol.* **2005**, *71*, 61-68.
206. Dubar, F.; Anquetin, G.; Pradines, B.; Dive, D.; Khalife, J.; Biot, C. *J. Med. Chem.* **2009**, *52*,7954-7957.
207. Winter, R. W.; Kelly, J. X.; Smilkstein, M. J.; Dodean, R.; Hinrichs, D.; Riscoe, M. K. *Exp. Parasitol.* **2008**, *118*, 487-497.
208. Liu, M.; Wilairat, P.; Go, M. *J. Med. Chem.* **2001,** *44*, 4443-4452.
209. Dubar, F.; Khalife, J.; Brocard, J.; Dive, D.; Biot, C. *Molecules* **2008**, *13*, 2900-2907.
210. Trager, W.; Jensen, J. B. *Science* **1976**, *193*, 673-675.
211. Makler, M. T.; Ries, J.; Williams, J. A.; Bancroft, J. E.; Piper, R. C.; Gibbins, B. L.; Hinrichs, D. J. *Am. J. Trop. Med. Hyg.* **1993**, *48*, 739-741.
212. Mosmann, T. *J. Immunol. Methods* **1983**, *65*, 55-63.
213. Egan, T. J.; Mavuso, W. W.; Ross, D. C.; Marques, H. M. *J. Inorg. Biochem.* **1997**, *68*, 137-145.
214. Egan, T. J.; Ross, D. C.; Adams, P. A. *FEBS Letters* **1994**, *352*, 54-57.

215. Ncokazi, K. K.; Egan, T. J. *Anal. Biochem.* **2005**, *338*, 306-319.
216. ACDLABS. http://www.acdlabs.com/home/. (accessed June 8, 2012).
217. Gaussian. http://www.gaussian.com/. (accessed June 8, 2012).
218. Molden Software. http://www.cmbi.ru.nl/molden/molden.html. (accessed June 8, 2012).
219. Biot, C.; Nosten, F.; Fraisse, L.; Ter-Minassian, D.; Khalife, J.; Dive, D. *Parasite* **2011,** *18*, 207-214.
220. Martirosyan, A. R.; Rahim-Bata, R.; Freeman, A. B.; Clarke, C. D.; Howard, R. L.; Strobl, J. S. *Biochem. Pharmacol.* **2004**, *68*, 1729-1738.
221. Cisplatin. http://www.cancer.gov/cancertopics/druginfo/cisplatin. (accessed May 12, 2012).
222. Herrmann, C.; Salas, P. F.; Patrick, B. O.; de Kock, C.; Smith, P. J.; Adam, M. J.; Orvig, C. *Dalton Trans.* **2012**, *41*, 6431-6442.
223. Egan, T. J. *J. Inorg. Biochem.* **2006**, *100*, 916-926.
224. Moreau, S.; Perly, B.; Chachaty, C.; Deleuze, C. *Biochim. Biophys. Acta* **1985**, *840*, 107.
225. Satterlee, J. D.; Constantinidis, I., *J. Am. Chem. Soc.* **1988,** *110*, 4391-4395.
226. Collier, G. S.; Pratt, J. M.; De Wet, C. R.; Tshabalala, C. F. *Biochem. J.* **1979**, *179*, 281-289.
227. Egan, T. J.; Combrinck, J. M.; Egan, J.; Hearne, G. R.; Marques, H. M.; Ntenteni, S.; Sewell, B. T.; Smith, P. J.; Taylor, D.; van Schalkwyk, D. A.; Walden, J. C. *Biochem. J.* **2002**, *365*, 343-347.
228. Egan, T. J.; Ncokazi, K. K. *J. Inorg. Biochem.* **2004**, *98*, 144-152.
229. Basilico, N.; Monti, D.; Olliaro, P.; Taramellia, D. *FEBS Lett.* **1997**, *409*, 297-299.
230. Egan, T. J.; Koch, K. R.; Swan, P. L.; Clarkson, C.; Van Schalkwyk, D. A.; Smith, P. J. *J. Med. Chem.* **2004**, *47*, 2929-2934.
231. Brown, S.B.; Dean, T. C.; Jones, P. *Biochem. J.* **1970**, *117*, 733-739.
232. Wenlock, M. C.; Austin, R. P.; Barton, P.; Davis, A. M.; Leeson, P. D. *J. Med. Chem.* **2003**, *46*, 1250-1256.
233. Ghose, A. K.; Viswanadhan, V. N.; Wendoloski, J. J. *J. Phys. Chem. A* **1998**, *102*, 3762-3772.

234. Abraham, M. H.; Benjelloun-Dakhama, G. J. M. R.; Acree, Jr., W. E.; Cain, W. S.; Cometto-Muniz, J. E. *New J. Chem.* **2000**, *24,* 825-829.
235. Molecular Simulations, MSI Cerius2, version 4.10. http:// www.msi.com. (accessed May 15, 2012).
236. Sharma, P.; Chhabra, S.; Rai, N.; Ghoshal, N. *J. Chem. Inf. Model.* **2007**, *47,* 1087-1096.
237. Veber, D. F.; Johnson, S. E.; Cheng, Y.-H.; Smith, B. R.; Ward, K. W.; Kopple, K. D. *J.Med. Chem.* **2002**, *45,* 2615-2623.
238. Mannhold, R., *Molecular Drug Properties: Measurement and Prediction.* Wiley-VCH: Chichester, U.K., 2007.
239. Conradi, R. A.; Burton, P.S.; Borchardt, R.T. *Methods Prin. Med. Chem.* **1996**, *4,* 233-252.
240. Clark, D. E.; Grootenhuis, P. D. J. *Curr. Top. Med. Chem.* **2003**, *3,* 1193-1203.
241. Kotecha, J.; Shah, S., Rathod, I.; Subbaiah, G. *Int. J. Pharm.* **2008**, *360,* 96-106.
242. Böcker, A.; Bonneau, P. R.; Hucke, O.; Jakalian, A.; Edwards, P. J. *ChemMedChem* **2010**, *5,* 2102-2113.
243. O'Neill, P. M.; Willock, D. J.; Hawley, S. R.; Bray, P. G.; Storr, R. C.; Ward, S. A.; Park, B. K. *J. Med. Chem.* **1997**, *40,* 437-448.
244. Mao, J.; Wang, Y.; Wan, B.; Kozikowski, A. P.; Franzblau, S. G. *ChemMedChem* **2007**, *2,* 1624-1630.
245. Frohlich, R. F. G.; Zabelinskaja-Mackova, A. A.; Fechter, M. H.; Griengl, H. *Tetrahedron: Asymmetry* **2003**, *14,* 355-362.
246. Catasús, M.; Bueno, A.; Moyano, A.; Maestro, Miguel A.; Mahía, J. *J. Organomet. Chem.* **2002**, *646,* 212-226.
247. Chavain, N.; Davioud-Charvet, E.; Trivelli, X.; Mbeki, L.; Rottmann, M.; Brun, R.; Biot, C. *Bioorg. Med. Chem.* **2009**, *17,* 8048-8059.
248. Kirk, K. *Physiol. Rev.* **2001**, *81,* 495-537.
249. Roth, E. F. Jr. *Blood Cells* **1990**, *16,* 453-460.
250. Roth, E. F. Jr.; Calvin. M. C.; Max-Audit, I.; Rosa, J.; Rosa, R. *Blood* **1988**, *72,* 1922-1925.

251. Sander, B. J.; Osborn, R. L.; Lowery, M. S.; Kruckeberg, W. C. *Exp. Parasitol.* **1982**, *53*, 355-361.
252. Roth, E. F. Jr.; Raventos-Suarez, C.; Rinaldi, A.; Nagel, R. L. *Proc. Natl. Acad. Sci. U. S. A.* **1983**, *80*, 298-299.
253. Lin, A. J.; Li, L.-q.; Andersen, S. L.; Klayman, D. L. *J. Med. Chem.* **1992**, *35*, 1639-1642.
254. Joet, T.; Eckstein-Ludwig, U.; Morin, C.; Krishna, S. *Proc. Natl. Acad. Sci. U. S. A.* **2003**, *100*, 7476-7479.
255. Krishna, S.; Woodrow, C. J.; Burchmore, R. J.; Saliba, K. J.; Kirk, K. *Parasitol. Today* **2000**, *16*, 516-521.
256. Cunha, A. C.; Pereira, L. O. R.; de Souza, M. C. B. V.; Ferreira, V. F. *J. Chem. Educ.* **1999**, *76*, 79-80.
257. Wright, M. E. *Organometallics* **1990**, *9*, 853-856.
258. Astruc, D., *Organometallic Chemistry and Catalysis*. Springer-Verlag: Berlin, 2007.
259. Herrmann, C.; Salas, P. F.; Patrick, B. O.; de Kock, C.; Smith, P. J.; Adam, M. J.; Orvig, C. *Organometallics*, **2012**, *31*, ASAP on line, in press.
260. Herrmann, C.; Salas, P. F.; Cawthray, J.; de Kock, C.; Patrick, B. O.; Smith, P. J.; Adam, M. J.; Orvig, C. *Organometallics*, **2012**, *31*, ASAP on line, in press.

APPENDICES

Appendix A. Crystallographic data

Crystallographic Data for *N*-(7-Chloro-4-quinolyl)-*N*'-ferrocenyl propane-1,3-diamine (4b) (Chapter 2).

Empirical Formula	$C_{23}H_{24}N_3FeCl$
Formula Weight	433.75
Crystal Color, Habit	orange, plate
Crystal Dimensions	0.03 X 0.35 X 0.45 mm
Crystal System	monoclinic
Lattice Type	primitive
Lattice Parameters	a = 16.418(2) Å b = 10.201(1) Å c = 12.6323(1) Å α = 90.0 ^{o} β = 108.828(4) ^{o} γ = 90.0 ^{o} V = 2002.4(3) Å^3
Space Group	*P* $2_1/c$ (#14)
Z value	4
D_{calc}	1.439 g/cm^3
F_{000}	904.00
μ(MoKα)	9.00 cm^{-1}
Residuals (refined on F2, all data): R1; wR2	0.055; 0.089

Crystallographic Data for -(7-Chloro-4-quinolyl)-*N*'-ferrocenyl 2,2-dimethyl-propane-1,3-diamine (4e) (Chapter 2).

Empirical Formula	$C_{32}H_{36}N_3FeCl$
Formula Weight	553.94
Crystal Color, Habit	red, irregular
Crystal Dimensions	0.10 X 0.25 X 0.35 mm
Crystal System	orthorhombic
Lattice Type	primitive
Lattice Parameters	a = 13.1852(5) Å b = 18.4105(7) Å c = 22.4888(9) Å $\alpha = 90^o$ $\beta = 90^o$ $\gamma = 90^o$ V = 5459.1(4) $Å^3$
Space Group	*P bca* (#61)
Z value	8
D_{calc}	1.348 g/cm^3
F_{000}	2336.00
μ(MoKα)	6.77 cm^{-1}
Residuals (refined on F^2, all data): R1; wR2	0.046; 0.096

Crystallographic Data for *N*-{[*N*'-(7-Chloroquinolin-4-yl)]-propane-1,3-diamine}-1,1'-(*N*,*N*-dimethane-yl)ferrocene (5b) (Chapter 2).

Empirical Formula	$C_{24}H_{24}N_3FeCl$
Formula Weight	445.76
Crystal Colour, Habit	yellow, blade
Crystal Dimensions	0.10 X 0.20 X 0.60 mm
Crystal System	monoclinic
Lattice Type	C-centered
Lattice Parameters	a = 9.5407(6) Å b = 20.569(2) Å c = 10.6568(7) Å $\alpha = 90^o$ $\beta = 100.043(1)^o$ $\gamma = 90^o$ V = 993.9(5) Å^3
Space Group	*C c* (#9)
Z value	4
D_{calc}	1.438 g/cm^3
F_{000}	928.00
μ(MoKα)	8.78 cm^{-1}
Residuals (refined on F^2, all data): R1; wR2	0.022; 0.050

Crystallographic Data for [2-(N,N-Dimethylaminomethyl)]-{3-[(2,8-bistrifluoromethyl-4-bromo)quinolyl]} ferrocenyl methanol (27) (Chapter 5).

Empirical Formula	$C_{25}H_{21}N_2OF_6FeBr$
Formula Weight	615.20
Crystal Colour, Habit	orange, irregular
Crystal Dimensions	0.08 X 0.10 X 0.30 mm
Crystal System	monoclinic
Lattice Type	primitive
Lattice Parameters	a = 19.030(2) Å b = 11.286(1) Å c = 23.595(2) Å α = 90 ° β = 110.126(2) ° γ = 90 ° V = 4758.0(8) Å^3
Space Group	*P* $2_1/n$ (#14)
Z value	8
D_{calc}	1.718 g/cm^3
F_{000}	2464.00
μ(MoKα)	23.83 cm^{-1}
Residuals (refined on F^2, all data): R1; wR2	0.095; 0.191

Crystallographic Data for [2-(N,N,N-Trimethylaminomethyl iodide)]-{4-[(2,8-bistrifluoromethyl) quinolyl]} ferrocenyl methanol (28) (Chapter 5).

Empirical Formula	$C_{27}H_{29}N_2O_2F_6FeI$
Formula Weight	710.27
Crystal Colour, Habit	orange, tablet
Crystal Dimensions	0.10 X 0.10 X 0.12 mm
Crystal System	triclinic
Lattice Type	primitive
Lattice Parameters	a = 8.764(2) Å b = 11.724(3) Å c = 13.774(4) Å α = 94.678(6)^o β = 107.370(6)^o γ = 91.325(6)^o V = 1344.5(6) Å^3
Space Group	*P* -1 (#2)
Z value	2
D_{calc}	1.754 g/cm^3
F_{000}	708.00
μ(Mo-Kα)	17.79 cm^{-1}
Residuals (refined on F^2, all data): R1; wR2	0.049; 0.091

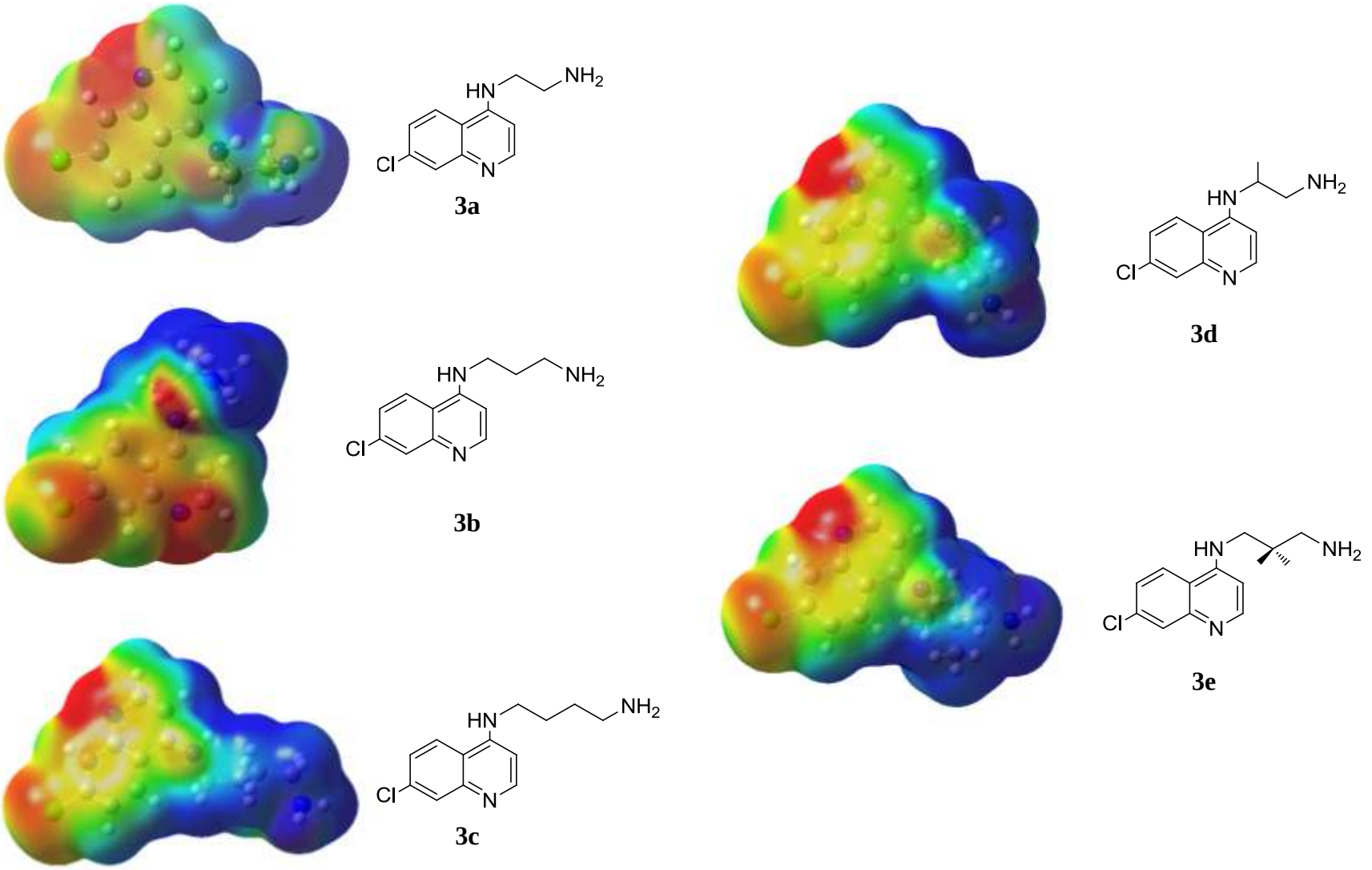

Appendix B. Molecular electrostatic maps.

Figure B.1. Molecular electrostatic potential (MEP) surfaces of the 4-aminoquinoline derivatives **3a-e** in their neutral state.

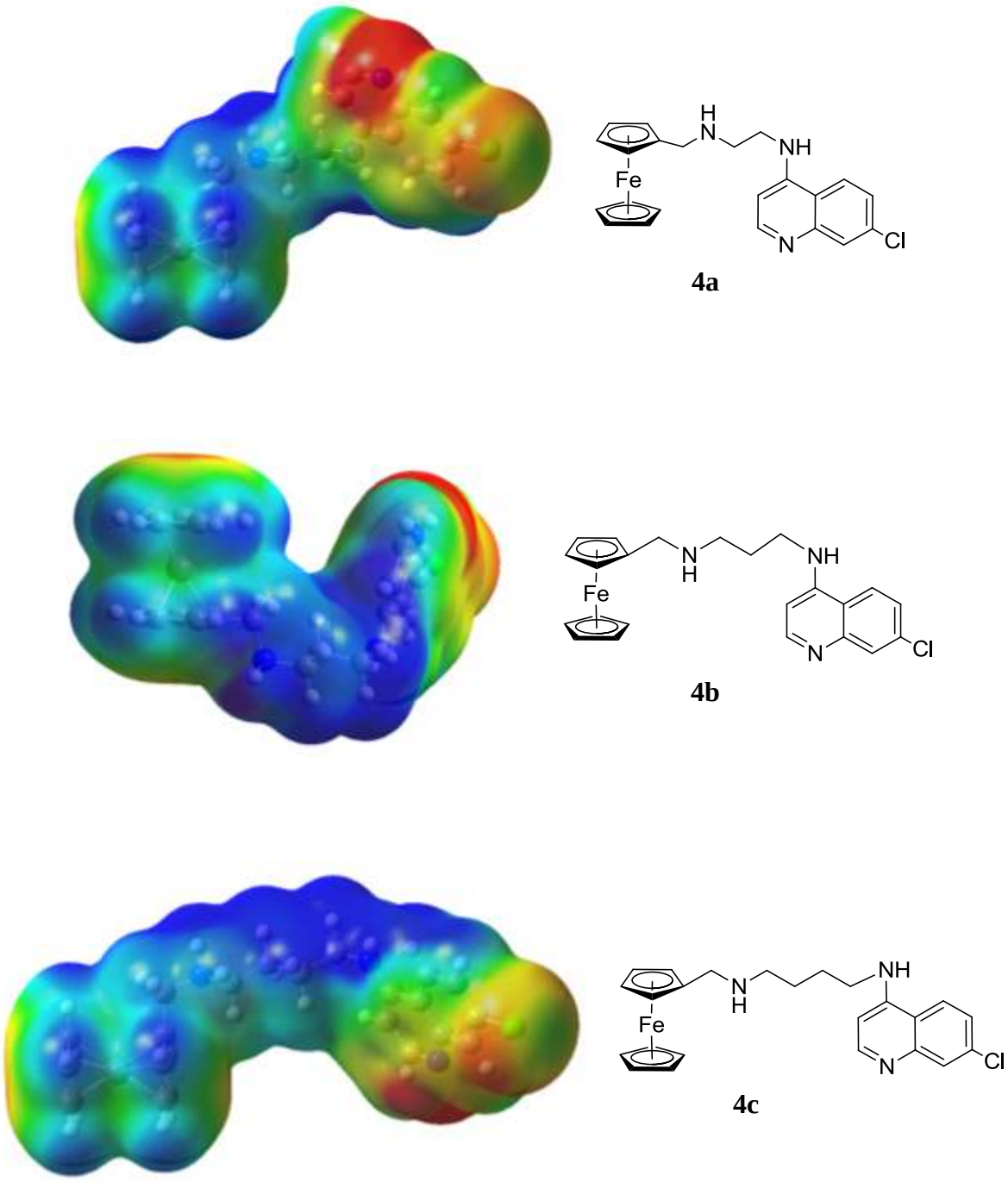

Figure B.2. Molecular electrostatic potential (MEP) surfaces of the ferrocenyl monosubstituted derivatives **4a-e** in their neutral state.

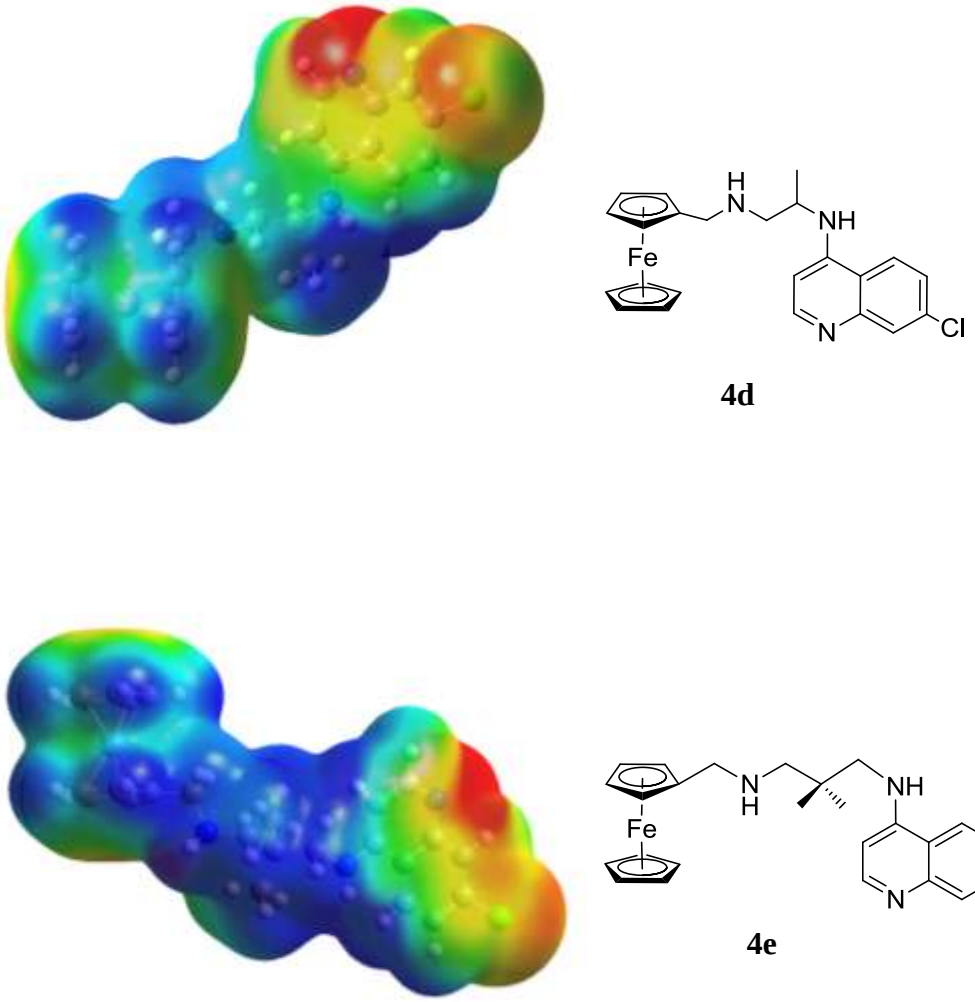

Figure B.2. (cont.) Molecular electrostatic potential (MEP) surfaces of the ferrocenyl monosubstituted derivatives **4a-e** in their neutral state.